

NASA CR-135448
PWA-5512-21



PERFORMANCE DETERIORATION
BASED ON EXISTING (HISTORICAL) DATA
JT9D JET ENGINE DIAGNOSTICS PROGRAM

G. P. Sallee

UNITED TECHNOLOGIES CORPORATION
Pratt & Whitney Aircraft Group
Commercial Products Division

(NASA-CR-135448) PERFORMANCE DETERIORATION N80-22324
BASED ON EXISTING (HISTORICAL) DATA; JT9D
JET ENGINE DIAGNOSTICS PROGRAM (Pratt and
Whitney Aircraft Group) 228 p HC A11/MF A01 Unclas
CSCL 21E 63/07 18053

Prepared for
NATIONAL AERONAUTICS AND SPACE ADMINISTRATION

NASA Lewis Research Center
Cleveland, Ohio 44135

Contract NAS3-20632



PREFACE

The requirements of NASA Policy Directive NPD 2220.4 (September 14, 1970) regarding the use of SI Units have been waived in accordance with the provisions of paragraph 5d of that Directive by the Director of Lewis Research Center.

PRECEDING PAGE BLANK NOT FILMED

TABLE OF CONTENTS

<u>Section</u>	<u>Page</u>
1.0 SUMMARY	1
2.0 INTRODUCTION	5
3.0 HISTORICAL DATA COLLECTION AND ANALYSIS METHODOLOGY	9
3.1 General Approach	9
3.2 Data Collection	12
3.2.1 Engine Performance and Airline Operational Data	12
3.2.2 Part Scrappage and Repair Data	16
3.2.3 Part Condition Data	19
3.3 Performance Data Reduction and Analytical Methodology	19
3.3.1 Overall Approach	19
3.3.2 Analysis of Test Stand Data	22
3.3.3 Analysis of Part Age and Condition Data	27
3.3.4 Validation	33
4.0 PROGRAM RESULTS	37
4.1 Overview	37
4.2 Average Engine Deterioration	38
4.2.1 Production Base Lines	38
4.2.2 Short-Term Performance Deterioration	38
4.2.3 Long-Term Performance Deterioration	41
4.3 Airline Maintenance Practice Variations	57
4.3.1 Parts Repair and Replacement Rates	57
4.3.2 Rebuild Standards	57
4.3.3 Part Repair Practices	60
4.4 Module Deterioration	61
4.4.1 Introduction	61
4.4.2 Fan	62
4.4.3 Low-Pressure Compressor	68
4.4.4 High-Pressure Compressor	82
4.4.5 Combustion System	97
4.4.6 High-Pressure Turbine	99
4.4.7 Low-Pressure Turbine	110
4.5 Verification and Data Enhancement	116
4.5.1 "Top Down" Analysis Procedure	116
4.5.2 "Bottom Up" Analysis Procedure - Long-Term Deterioration	118
4.5.3 Comparison of Top Down and Bottom Up Analysis Results	123
5.0 PRELIMINARY MODELS OF JT9D ENGINE PERFORMANCE DETERIORATION	127
5.1 Module Deterioration Model	127
5.2 Engine Deterioration Model	129

TABLE OF CONTENTS (Cont'd.)

<u>Section</u>	<u>Page</u>
6.0 PRELIMINARY RECOMMENDATIONS	133
6.1 Engine Operating Procedures	133
6.2 Performance Monitoring	134
6.2.1 Performance Trending and Management	134
6.2.2 Test Stand Instrumentation	137
6.2.3 Test Stand Correlation	139
6.3 Maintenance Practices	141
6.3.1 Fan	141
6.3.2 Low-Pressure Compressor	141
6.3.3 High-Pressure Compressor	142
6.3.4 Combustion System	142
6.3.5 High-Pressure Turbine	143
6.3.6 Low-Pressure Turbine	143
6.3.7 Summary	143
6.4 Design Criteria	144
6.4.1 Flight Loads	144
6.4.2 Erosion	145
6.4.3 Thermal Distortion	146
6.4.4 Rebuild Standards	146
6.4.5 Summary	147
6.5 Performance Deterioration Control and Management	147
7.0 CONCLUSIONS	155
7.1 Overall Engine Performance Deterioration	156
7.1.1 Short-Term Performance Deterioration	156
7.1.2 Long-Term Performance Deterioration	157
7.2 Engine Performance Recoverability	157
7.3 Deterioration Models	158
7.3.1 Engine Deterioration	158
7.3.2 Module Deterioration	158
APPENDIX A - AIRLINE VARIATIONS IN OPERATING PROCEDURES AND THRUST USAGE	161
APPENDIX B - USED PARTS CONDITION AND PHOTOGRAPHIC DOCUMENTATION	163
APPENDIX C - PARTS USAGE AND REPAIR RATE ANALYSIS	191
APPENDIX D - REBUILD STANDARDS VARIATIONS	195
APPENDIX E - QUALITY ASSURANCE	211
APPENDIX F - ACRONYMS AND SYMBOLS	213
REFERENCES	217
DISTRIBUTION LIST	219

LIST OF ILLUSTRATIONS

<u>Figure</u>	<u>Title</u>	<u>Page</u>
1	Technical Approach for Historical Data Collection and Analysis	7
2	Engine Performance Deterioration Diagnostic Technique	11
3	Rapid Airfoil Digital Optical Contour (RADOCC) Facility	20
4	Overall Data Analysis Flow Chart	21
5	Initial Steps in Processing Test Stand Data	22
6	Typical Computer Listing of Corrected Test Cell Data	23
7	Typical Computer Plot of Engine Performance Data	24
8	Trend Plot of Typical Engine Parameters	25
9	Absolute Exhaust Gas Temperatures (EGT) for Average Engine as a Function of Engine Age	26
10	Effect of Age on Airfoil Tip Chord	30
11	Different Approaches for Modeling Tip Clearance Effects	33
12	Production TSFC Levels at Take-Off Thrust Versus Time	39
13	Short-Term TSFC Deterioration Trends as a Function of Flight Time	41
14	Short-Term TSFC Deterioration Trends as a Function of Flight Cycles	42
15	Fleet Deterioration for Pan American World Airways	44
16	Fleet Deterioration for Trans World Airlines	44
17	Fleet Deterioration for Northwest Airlines	45
18	Cruise Engine Condition Monitoring Performance for Engine S/N 4190	46
19	Prerepair TSFC Performance Deterioration at Take-Off Thrust for Individual Airline Engines Relative to New Engine Performance Levels	47
20	Prerepair EGT Performance Deterioration at Take-Off Thrust for Individual Airline Engines Relative to New Engine Performance Levels	48

LIST OF ILLUSTRATIONS (Cont'd)

<u>Figure</u>	<u>Title</u>	<u>Page</u>
21	Average Fleet Prerepair TSFC Performance Deterioration at Take-Off Thrust Relative to New Engine Performance Levels	49
22	Average Fleet Prerepair EGT Performance Deterioration at Take-Off Thrust Relative to New Engine Performance Levels	50
23	Postrepair TSFC Performance Deterioration at Take-Off Thrust for Individual Airline Engines Relative to New Engine Performance Levels	51
24	Postrepair EGT Performance Deterioration at Take-Off Thrust for Individual Airline Engines Relative to New Engine Performance Levels	51
25	Average Fleet Postrepair TSFC Performance Deterioration at Take-Off Thrust Relative to New Engine Performance Levels	52
26	Average Fleet Postrepair EGT Performance Deterioration at Take-Off Thrust Relative to New Engine Performance Levels	52
27	Effect of Cold-Section Modifications and Refurbishment on Engine Performance	55
28	Effect of Cold-Section Refurbishment on TSFC	56
29	JT9D Engine Cross Section	61
30	Fan Tip Clearance Effects	62
31	JT9D-7/7F/20 Fan Rub-Strip Rub Depth Growth	63
32	Predicted Fan Clearance Changes from Analytical Studies of the Effects of Flight Loads on Performance Deterioration	64
33	Surface Roughness Measured on Five JT9D Fan Blades	65
34	Effect of Clearance Changes on Fan Flow Capacity and Efficiency	66
35	Effect of Surface Roughness on Fan Efficiency	66
36	Back-to-Back Fan Test Data	67

LIST OF ILLUSTRATIONS (Cont'd)

<u>Figure</u>	<u>Title</u>	<u>Page</u>
37	Sketch of Blade Tip and Rubstrip	69
38	Effect of Trenching on Performance Losses Associated with Blade Tip Clearance	69
39	Definition of Effective Tip Clearance	70
40	Nomenclature for Airfoil Parameters	71
41	Low-Pressure Compressor Blade Length Loss Data for Rotor 3	72
42	Schematic of Low-Pressure Compressor Tip Clearance Wear Mechanisms	73
43	Rub Strip Erosion Data for the Low-Pressure Compressor	73
44	Trench Depth Measurements for the Low-Pressure Compressor	74
45	Effective Change in Blade Tip Clearance for the Low-Pressure Compressor	75
46	Effect of Tip Clearance Increases on Low-Pressure Compressor Performance	75
47	Surface Roughness Data for Second-, Third-, and Fourth-Stage Low-Compressor Rotor Airfoils	76
48	Surface Roughness Data for the Second- and Third-Stage Stator Airfoils	77
49	Average Low-Pressure Compressor Rotor and Stator Roughness Data at 2000 Cycles	77
50	Effect of Low-Pressure Compressor Airfoil Surface Roughness on Efficiency	78
51	Second-Stage Rotor Tip Profile Data	79
52	Estimated Overall Performance Loss for Low-Pressure Compressor	80
53	Low-Pressure Compressor Performance Loss Based on Estimates from Part Condition, Analysis of Historical Data, and Back-to-Back Testing of Service Compressors	81

LIST OF ILLUSTRATIONS (Cont'd)

<u>Figure</u>	<u>Title</u>	<u>Page</u>
54	Schematic of Tip Clearance Wear Mechanism for High-Pressure Compressor	82
55	Blade Length Loss for Sixth-, Ninth-, and Fourteenth-Stage Rotors	84
56	Rup-Strip Errosion Rate for Sixth-, Ninth-, and Fourteenth-Stage Rotors	84
57	Rup-Strip Trench Depth Data for Sixth-, Ninth-, and Fourteenth-Stage Rotors	85
58	Effective Tip Clearance Increases Relative to Production Acceptance	86
59	High-Pressure Compressor Performance Loss Attributed to Blade Tip Clearance Increases	87
60	Surface Roughness Data for JT9D Sixth-, Ninth-, and Fourteenth-Stage Blades	87
61	Surface Rougness Data for JT9D Sixth-, Ninth-, and Fourteen-Stage Stators	88
62	Surface Roughness for JT9D High-Pressure Compressor Blades and Vanes at 2000 Cycles	88
63	Prediction of Effect of Surface Roughness Changes in High-Pressure Compressor on Performance	89
64	JT9D High-Pressure Compressor Blades with High Hourly Usage but Moderate Cycle Usage	90
65	JT9D High-Pressure Compressor Blades with Moderate Hourly Usage but High Cycle Usage	90
66	Chord Erosion Data for Tip Region of Fourteenth-Stage Blade	91
67	Airfoil Geometry Changes for Tip Section of Ninth-Stage Rotor Blade	92
68	Airfoil Contour Changes as a Function of Leading Edge Span (Ninth-Stage Rotor Blades)	93
69	Estimated Effect of Airfoil Contour Changes on Performance	94

LIST OF ILLUSTRATIONS (Cont'd)

<u>Figure</u>	<u>Title</u>	<u>Page</u>
70	Total High-Pressure Compressor Performance Deterioration	95
71	Predicted and Experimentally Measured High-Pressure Compressor Performance Deterioration	96
72	Definition of Combustor Cone Angle	97
73	Combustor Radial Temperature Distributions	99
74	Effect of High-Pressure Turbine Blade Tip Clearance on Turbine Performance	100
75	High-Pressure Turbine First-Stage Vane Leakage Path	101
76	High-Pressure Turbine Second-Stage Vane Leakage Path	101
77	Analytical Estimate of High-Pressure Turbine Vane Leakage Levels as a Percent of Engine Airflow	102
78	Analytical Estimate of High-Pressure Turbine Flow Capacity Change Produced by Vane Bowing	102
79	High-Pressure Turbine Surface Roughness Measurement Results	103
80	Teardown Clearance of High-Pressure Turbine First-Stage Outer Air Seal	104
81	Correlation of High-Pressure Turbine First-Stage Blade Tip Wear With Inferred Initial Clearance	105
82	Predicted High-Pressure Turbine Performance Deterioration	106
83	High-Pressure Turbine Performance Deterioration Resulting from Second-Stage Vane Twisting	106
84	High-Pressure Turbine First- and Second-Stage Flow Capacity	107
85	Estimated High-Pressure Turbine Efficiency Loss Associated with Surface Roughness	108
86	High-Pressure Turbine Overall Performance Deterioration	109

LIST OF ILLUSTRATIONS (Cont'd)

<u>Figure</u>	<u>Title</u>	<u>Page</u>
87	Effect of Blade Tip Clearance on Low-Pressure Turbine Efficiency	110
88	Low-Pressure Turbine Leakage Path Produced by Vane Twisting at Inner Platform	111
89	Estimated Effect of Vane Bow on Low-Pressure Turbine Flow Capacity	111
90	Effect of Vane Inner Platform Misalignment on Low-Pressure Turbine Efficiency	112
91	Low-Pressure Turbine Airfoil Surface Roughness Measurement Data	112
92	Effect of Blade Tip Clearance Changes on Low-Pressure Turbine Efficiency	113
93	Average Loss in Low-Pressure Turbine Flow Capacity Associated With Vane Bow and Twist	114
94	Estimated Average Overall Low-Pressure Turbine Performance Deterioration	115
95	JT9D Fan Module Part Age	120
96	Fan Module Performance vs. Module Age	121
97	Preliminary Model of JT9D Fan Performance Deterioration	127
98	Preliminary Model of JT9D Low-Pressure Compressor Performance Deterioration	128
99	Preliminary Model of JT9D High-Pressure Compressor Performance Deterioration	128
100	Preliminary Model of JT9D High-Pressure Turbine Performance Deterioration	129
101	Preliminary Model of JT9D Low-Pressure Turbine Performance Deterioration	130
102	Preliminary Model of JT9D Prerepair Average Engine and Module Performance Deterioration	131

LIST OF ILLUSTRATIONS (Cont'd)

<u>Figure</u>	<u>Title</u>	<u>Page</u>
103	Preliminary Model of JT9D Prerepair Average Engine Performance Deterioration	131
104	Comparison of Preliminary Model of JT9D Prerepair Average Engine Performance Deterioration and Observed Deterioration	132
105	Hot Rotor/Rub Strip Interaction	135
106	Management Tool Required	136
107	JT9D High-Pressure Compressor Blade Age (Stages 5 through 15)	148
108	JT9D Fan Performance Recovery Potential	150
109	Cost Optimization of Fan Repair Interval	151
110	JT9D Low-Pressure Compressor Performance Recovery Potential	152
111	Cost Optimization of Low-Pressure Compressor Repair Interval	152
112	JT9D High-Pressure Compressor Performance Recovery Potential	153
113	Cost Optimization of High-Pressure Compressor Repair Interval	154
B-1	JT9D Second-Stage Low-Pressure Compressor Blades	B-1
B-2	JT9D Third-Stage Low-Pressure Compressor Blades	B-2
B-3	JT9D Fourth-Stage Low-Pressure Compressor Blades	B-2
B-4	JT9D Low-Pressure Compressor Blades	B-3
B-5	JT9D Low-Pressure Compressor Blades	B-3
B-6	Low-Pressure Compressor Blade Length Loss Data for Rotor 2	B-4
B-7	Low-Pressure Compressor Blade Length Loss Data for Rotor 3	B-5

LIST OF ILLUSTRATIONS (Cont'd)

<u>Figure</u>	<u>Title</u>	<u>Page</u>
B-8	Low-Pressure Compressor Blade Length Loss Data for Rotor 4	B-5
B-9	Second-Stage Rotor Tip Profile Data	B-6
B-10	Second-Stage Rotor Profile Data	B-7
B-11	Third-Stage Rotor Tip Profile Data	B-8
B-12	Third-Stage Rotor Root Profile Data	B-9
B-13	Fourth-Stage Rotor Tip Profile Data	B-10
B-14	Fourth-Stage Rotor Root Profile Data	B-11
B-15	JT9D Fifth-Stage High-Pressure Compressor Blades	B-12
B-16	JT9D Ninth-Stage High-Pressure Compressor Blades	B-13
B-17	JT9D Twelfth-Stage High-Pressure Compressor Blades	B-13
B-18	JT9D Fifteenth-Stage High-Pressure Compressor Blades	B-13
B-19	JT9D High-Pressure Compressor Blades	B-14
B-20	JT9D Sixth-Stage High-Pressure Compressor Blades	B-14
B-21	Geometry Changes for Tip Section of Sixth-Stage Rotor Blade	B-15
B-22	Airfoil Geometry Changes for Root Section of Sixth-Stage Rotor Blade	B-16
B-23	Airfoil Geometry Changes for Tip Section of Ninth-Stage Rotor Blade	B-17
B-24	Airfoil Geometry Changes for Root Section of Ninth-Stage Rotor Blade	B-18
B-25	Airfoil Geometry Changes for Tip Section of Fourteenth-Stage Rotor Blade	B-19
B-26	Airfoil Geometry Changes for Root Section of Fourteenth-Stage Rotor Blade	B-20
B-27	Airfoil Geometry Changes for Span of Sixth-Stage Rotor Blades	B-21

LIST OF ILLUSTRATIONS (Cont'd)

<u>Figure</u>	<u>Title</u>	<u>Page</u>
B-28	Airfoil Geometry Changes for Span of Ninth-Stage Rotor Blades	B-22
B-29	Airfoil Geometry Changes for Span of Fourteenth-Stage Rotor Blades	B-23
B-30	JT9D First-Stage High-Pressure Turbine Vanes	B-24
B-31	JT9D First-Stage High-Pressure Turbine Vanes	B-24
B-32	JT9D First-Stage High-Pressure Turbine Blades	B-25
B-33	JT9D First-Stage High-Pressure Turbine Blades	B-25
B-34	JT9D Second-Stage High-Pressure Turbine Vanes	B-26
B-35	JT9D Second-Stage High-Pressure Turbine Vanes	B-26
B-36	JT9D Second-Stage High-Pressure Turbine Blades	B-27
B-37	JT9D Second-Stage High-Pressure Turbine Blades	B-27
C-1	JT9D Fan Module Part Age	C-2
C-2	JT9D Low-Pressure Compressor Module Part Age	C-2
C-3	JT9D High-Pressure Compressor Blade and Vane Part Age	C-3
C-4	JT9D High-Pressure Compressor Stator and Outer Air Seal Part Age	C-3
C-5	JT9D High-Pressure Turbine Module Part Age	C-4
C-6	JT9D Low-Pressure Turbine Module Part Age	C-4
E-1	Identifying Codes for Compressor Parts	E-2
E-2	Identifying Codes for Turbine Parts	E-2

LIST OF TABLES

<u>Table</u>	<u>Title</u>	<u>Page</u>
I	Summary of Available Engine Calibration Data	13
II	Total Uncertainties for Airlines Test Cells	15
III	Gas-Path Parts Studies	17
IV	Examples of Average Part Ages	29
V	JT9D-7 Sensitivities for a +0.010-Inch Tip Clearance Change	31
VI	JT9D-7 Sensitivity Analysis for a +0.10-Inch Low-Pressure Turbine Clearance Change	32
VII	Engine Simulation for Diagnostic Tracking Top Down Approach	35
VIII	Adjustments to Performance Deterioration Levels by Airline Operator	40
IX	Module Contribution to Short-Term Deterioration	43
X	Airline Deterioration Experience	46
XI	Postrepair Overall Performance Data Relative to Prerepair Performance	53
XII	Postrepair Module Performance Data Relative to Prerepair Performance	54
XIII	Cold Section Refurbishment and Compressor Modification Results	55
XIV	Summary of Differences in Cold Section Maintenance Standards Comparison of Practiced and Written Airline Rebuild Standards	58
XV	Summary of Differences in Hot Section Rebuild Standards	59
XVI	Influence of Rebuild Clearances on TSFC	60
XVII	Total High-Pressure Compressor Efficiency Deterioration	95
XVIII	Average Tip Clearances at Build and Teardown for Airlines A and C	105

LIST OF TABLES (Cont'd)

<u>Table</u>	<u>Title</u>	<u>Page</u>
XXIX	Top Down Analysis for Airline B Postrepair Performance Data at 3500 Cycles Showing the Effect of Low-Pressure Rotor Loss-Split Assumption on Predicted Module Losses	117
XX	Top Down Analysis Results for Airline A Prerepair Performance Data at 3500 Cycles Showing Effects of Test Stand Data Adjustments	119
XXI	Module Average Cyclic Age at 3500 Engine Flight Cycles	121
XXII	Bottom Up Analysis Results for Airline A Prerepair Performance Data at 3500 Cycles	122
XXIII	Results of Top Down and Bottom Up Analysis Results for Airline A Prerepair Performance Data at 3500 Cycles After Appropriate Data Adjustments	123
XXIV	Results of Top Down and Bottom Up Analysis Results for Airline B Prerepair Performance Data at 3500 Cycles After Appropriate Data Adjustments	124
XXV	Results of Top Down and Bottom Up Analysis Results for Airline C Prerepair Performance Data at 3500 Cycles After Appropriate Data Adjustments	125
XXVI	Effect of Recommended Refurbishments	144
XXVII	Comparison of Recommended Repair/Replacement Internals and Associated Average Part Ages with Average Part Ages for Airlines	149
D-I	Variations in Cold Section Rebuild Standards	D-2
D-II	Variations in Hot Section Rebuild Standards	D-10
D-III	Blade Tip Clearance Variation Summary - Airline A	D-12
D-IV	Blade Tip Clearance Variation Summary - Airline B	D-13
D-V	Blade Tip Clearance Variation Summary - Airline C	D-15

SECTION 1.0

SUMMARY

This report presents the results of a study of JT9D engine performance deterioration and its causes. The study was based on historical records and data obtained from five airlines, two airframe manufacturers, and Pratt & Whitney Aircraft (P&WA) covering the period from early 1973 through December 31, 1976. The objectives of this study were to: 1) document the historical trend of JT9D engine performance deterioration with respect to increasing service usage; 2) quantify the levels of performance losses and the distribution of the losses to individual components; and 3) identify the causes or damage mechanisms responsible for these losses. Preliminary models of performance deterioration have been developed at the engine and component/module level to permit an understanding of the role of each causative factor versus increasing service usage (in hours or flights). These preliminary models are to be refined on the basis of new and more controlled data being obtained under other parts of the NASA JT9D Engine Diagnostics Program as it continues. Preliminary recommendations are presented for actions to reduce the levels of deterioration in both the current JT9D engine and future engines. These recommendations will be refined as new knowledge is gained from the continuing elements of the NASA program.

Large quantities of detailed data related to engine performance deterioration, part replacement/repair rates, maintenance practices, and part condition with respect to increasing service usage were collected, documented, and analyzed.

The results of the analyses of these data show that performance deterioration can be broken into two general time frames: (1) that which occurs in the first few hundred flights after entry of an engine into commercial airline service, called short-term deterioration; and (2) that which occurs more gradually as service usage accumulates, called long-term deterioration.

The analysis of historical short term data indicated that the average engine of the JT9D-3A/7/20 family loses 1 percent* in thrust specific fuel consumption (TSFC) on the first flight relative to the level of measured performance at sea-level static take-off conditions of the engine when new. This loss in performance grows to 1.5 percent by the 200th flight. Analysis of these data indicate that 55 percent of the TSFC loss is associated with the performance losses of the low-pressure

* Throughout this report, performance values in thrust specific fuel consumption (TSFC) and exhaust gas temperature (EGT) are referenced to sea level static conditions. Engine condition monitoring (ECM) data in fuel flow (Wf) and EGT are referenced to altitude conditions.

spool (fan, low-pressure compressor, and low-pressure turbine) and 45 percent with the performance losses of the high-pressure spool (high-pressure compressor and high-pressure turbine). This short-term performance loss appears to result from clearance increases caused by rubbing between stationary and rotating parts. This rubbing is caused by deflections of engine cases and rotors produced by aircraft induced flight loads. However, with continuing in-service exposure, the probability of encountering more severe loads becomes greater, causing additional clearance increases, but at a much slower rate.

The long-term performance loss of the engine gradually increases with increased usage. Analyses of prerepair test stand data indicate that the average TSFC performance deterioration of the fleet of JT9D-3A/7/20 family of engines prior to repair is 4.4 ± 0.5 percent at 3500 flights or approximately 12,000 hours of operation relative to new production engine performance levels. The performance losses at this time frame are dominated by the high-pressure spool rather than the low-pressure spool.

The analyses of postrepair test stand data indicate that the fleet average postrepair level of TSFC deterioration is 3.5 ± 0.7 percent at 3500 flights, representing an average recovery of 0.9 percent. The majority of the TSFC recovery results from high-pressure turbine restoration. Historical data indicates that an additional 1.9 percent in TSFC recovery can be realized by refurbishment of the engine cold section (fan, low- and high-pressure compressor). The balance of average unrecovered performance, approximately 1.6 percent in TSFC, is caused by mechanical conditions distributed among all the modules that are not typically refurbished.

Engine performance deterioration results from the degradation of the mechanical condition of engine parts. Four causes of this degradation have been identified: 1) the effects of flight loads that distort the shape of engine cases, produce rubbing, and result in increased clearances; 2) erosion of airfoils and outer air seals resulting in increased roughness and bluntness, loss of camber, loss of blade length, and increased operating clearances; 3) thermal distortion produced by changing turbine inlet temperature patterns resulting in area changes, increased leakages, and changed clearances; and 4) operator repair practices and rebuild standards that have an impact on the cumulative levels of part mechanical damage versus time and the levels of prerepair and postrepair performance. The estimated distribution of the prerepair performance loss at 3500 flights by major causes are 40 percent due to flight loads, 40 percent due to erosion, 20 percent due to thermal distortion with the total level varying by ± 13 percent as a result of differences in maintenance practices.

Module performance loss mechanisms were quantified with respect to usage. The major performance loss mechanism in the fan is estimated to be leading edge bluntness, with airfoil roughness and increased tip clearance being significant, but less important.

The performance loss mechanism of most importance in the low-pressure compressor is estimated to be tip clearance increases, with airfoil roughness being of secondary importance.

The high-pressure compressor performance loss is dominated by the effects of erosion, which cause clearance increases, increased roughness, and airfoil camber loss (with camber loss being the cause of accelerating performance deterioration beyond approximately 3000 flight cycles).

The combustor has no important direct effects but appears to have important indirect effects on turbine performance loss as the result of changes in turbine inlet temperature pattern. Although these temperature pattern changes were not measured during this program, they appear to have occurred based on the examination of the turbine parts. The major portion of high-pressure turbine performance deterioration is increased turbine tip clearance, with vane bow and twisting being of significant but somewhat less importance.

Low-pressure turbine performance deterioration is estimated to be caused by tip clearance increases, with all other mechanisms being of less significance.

Significant progress was achieved in understanding the mechanisms that cause performance deterioration and the role each mechanism plays as the engine ages. Module performance loss estimates which were developed from part inspection data, and correlated with individual airline operator module age, permitted verification of engine and module performance levels determined from analysis of test stand data.

SECTION 2.0

INTRODUCTION

The rapid rise in the cost of oil since the OPEC oil embargo in 1973 has resulted in a national effort to increase the availability of domestic oil, develop alternate sources of energy, and develop near- and long-term means to reduce fuel consumption. To counteract the adverse impact of the world-wide fuel crisis on the aviation industry, NASA has initiated the Aircraft Energy Efficiency (ACEE) program. Included in this program are major propulsion projects which are addressing both near-term and long-term goals. The long-term activities are directed toward developing propulsion technology to reduce fuel consumption of new turbofan engines by at least 12% in the late 1980's and an additional 15% for advanced turboprops in the early 1990's. The near-term activities are a part of the Engine Component Improvement (ECI) Project which is directed toward improving the fuel consumption of current production turbofan engines and their derivatives by 5 percent over the life of these engines. The ECI project is divided into two subprojects: 1) Performance Improvement and 2) Engine Diagnostics. Performance Improvement is directed at developing fuel saving component technology for existing engines to be introduced during the 1980 to 1982 time period.

The NASA JT9D Jet Engine Diagnostics Program has the overall objective of identifying and quantifying the causes and sources of performance deterioration in the JT9D turbofan engine. This document covers the work that has been completed during the first phase of the program, which was the gathering, documentation, and analysis of historical data.

The specific objectives of this effort were to:

- o Collect and document existing historical data on performance deterioration of the JT9D family of engines,
- o Establish the trend of performance deterioration at the overall engine and module level in relation to engine and part usage,
- o Establish the probable causes of performance deterioration, and
- o Identify areas and components where corrective actions could be taken.

The historical data collected during the program was defined as those data which existed prior to January 1, 1977. Included were: new engine baseline data, short-term performance test data, installed engine performance data, instrumentation and test stand calibration records, prerepair and postrepair engine performance test data, parts repair and scrappage rates, and part condition in relation to part usage.

The sources of these data included airline companies, airframe manufacturers, and the Contractor's own historical records. McDonnell Douglas, The Boeing Company, Northwest Airlines, Trans World Airlines, and Pan American World Airways assisted in accomplishing this effort as subcontractors. In addition, American Airlines and United Airlines provided test stand data.

Figure 1 shows the technical approach and related activities involved in completing the study. Large samples of data were obtained from multiple sources to permit averaging and reduction of data scatter through statistical techniques.

Engine performance data (left column of Figure 1) were reduced and averaged to define the overall JT9D engine performance deterioration for an "average" engine. Engine and part utilization data and part condition data (right columns in Figure 1) were used to estimate module performance deterioration as a function of module age. This estimate was then used in an engine simulation to model the overall JT9D engine deterioration. The results were compared with the airline average engine experience determined from the overall engine performance data.

An important part of the analysis was the validation of the performance deterioration models through the use of the "top-down" and "bottom-up" techniques. In brief, this validation process used the engine simulation to model the engine based on each airline's performance data (top down) and on each airline's part condition data (bottom up). Comparison of the two models indicated where reconsideration of the assumptions was required, and, when good agreement was reached, permitted the initial modeling of the module and engine performance deterioration.

The main body of this report has been organized into five sections. Section 3.0 is a detailed discussion of the data gathering and analysis efforts. Section 4.0 present the results of the analysis. Section 5.0 describes the preliminary models of JT9D engine performance deterioration. Section 6.0 presents preliminary recommendations based on the results to date. The conclusions and several issues which could not be resolved from historical data are examined in Section 7.0. Supporting documentation is included in Appendixes A through F.

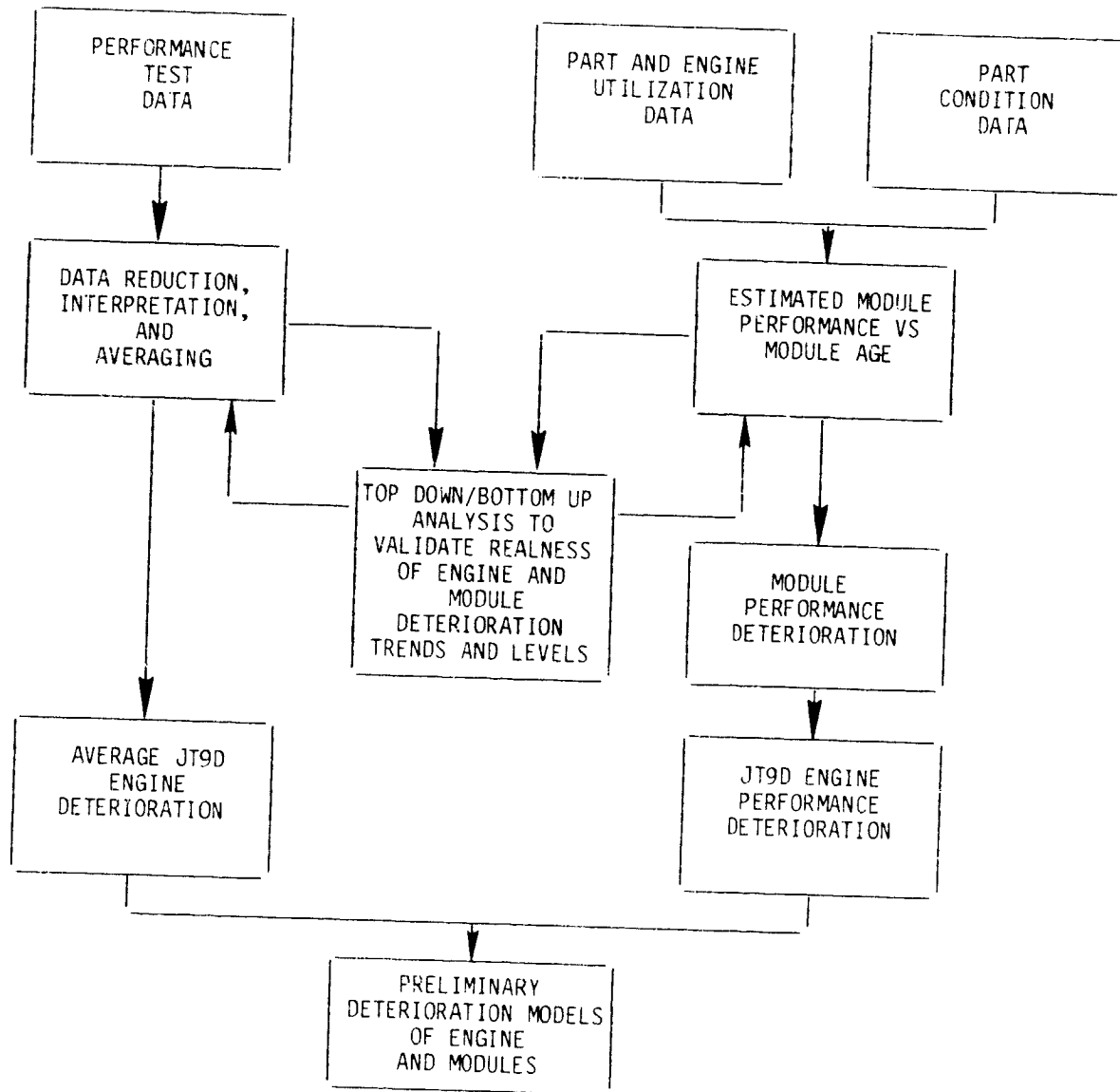


Figure 1 Technical Approach for Historical Data Collection and Analysis - The program was based on combining a "top down" and "bottom up" approach to enhance the data and validate the initial deterioration models.

SECTION 3.0

HISTORICAL DATA COLLECTION AND ANALYSIS METHODOLOGY

3.1 GENERAL APPROACH

The ideal approach for determining the causes of engine deterioration would consist of tracking a large number of individual engines, documenting all their flight and maintenance experience coupled with detailed continuous performance data, and then correlating specific flight or maintenance events with the documented shifts in performance.

Such an approach, however, is unattainable for commercial airline engines. The first problem is that there really is no such thing as an individual engine to track. To minimize maintenance turn-around time, conventional practice is to remove the module requiring maintenance and replace it with an airworthy module. Hence, at any given time, a particular engine might consist of a number of modules with quite different flight and maintenance histories. Maintenance records are available, of course, on a module basis, but the volume of records that would need to be reviewed to construct the full history of any particular module makes such an approach impractical.

The second problem with the ideal approach is that flight histories of power setting and maneuver load events are not kept on a routine basis. The only related data generally available is total operating time and the number of take-off and landing cycles.

The third problem is that the continuous individual engine flight performance data desired are not available since such data normally would serve no useful purpose to airline operation.

The types of data that were available and that provided the basis for the performance deterioration analysis were:

1. Historical airline average engine flight performance and operating data that could be correlated with engine utilization in terms of either hours or cycles;
2. Historical data relating to the engine maintenance practices of individual operators;
3. Test stand data indicating individual engine performance levels (including production performance records); and
4. Inspection results on the condition of parts removed from engines.

A major gap in the desired data spectrum exists in that the first two items relate to overall airline fleet average engine performance while the last two relate to specific parts of specific engines. To meet the objectives of the program, a technique had to be devised to bridge this gap in analyzing the performance of an ill-defined "average" engine and the effects of specific changes on specific engines.

It should be noted that bridging this gap cannot be accomplished by simply summing the individual effects of the deterioration of specific parts. Although individual influence coefficients are well established to define the effects of a single change (such as a one percent loss in compressor efficiency) on the overall engine performance, the complexity of the interaction of the components precludes such an approach where changes occur in virtually all of the engine modules concurrently.

To fill this gap, a novel approach, unique to engine performance analysis, was devised using the Pratt & Whitney Aircraft JT9D engine simulation. This simulation is capable of accounting for the combined effects of concurrent performance shifts in a number of engine modules, thereby avoiding the problems associated with the use of influence coefficients. The process is summarized in Figure 2 and consisted of two basic steps.

The first step involved analyzing the engine data for each airline to define an average engine performance trend as a function of engine cycles and to define the average engine deterioration at selected engine usage levels. Then the engine simulation is used in an iterative fashion to estimate the corresponding levels of individual module performance deterioration. This approach represents a "top down" approach to the module performance level.

The second step involved a "bottom up" approach which consisted of analyzing the part condition and maintenance data to determine the probable effect of the deterioration of individual parts, such as blade contour and clearances, on module performance. The simulation was then used to predict the overall average engine performance deterioration.

These two sets of predictions were compared to guide the interpretation of the data and to estimate module performance losses. This procedure provided confidence in the final result.

Once an acceptable definition of the module performance loss and loss mechanisms had been established in this manner, a preliminary performance deterioration model could be produced through conventional modeling techniques.

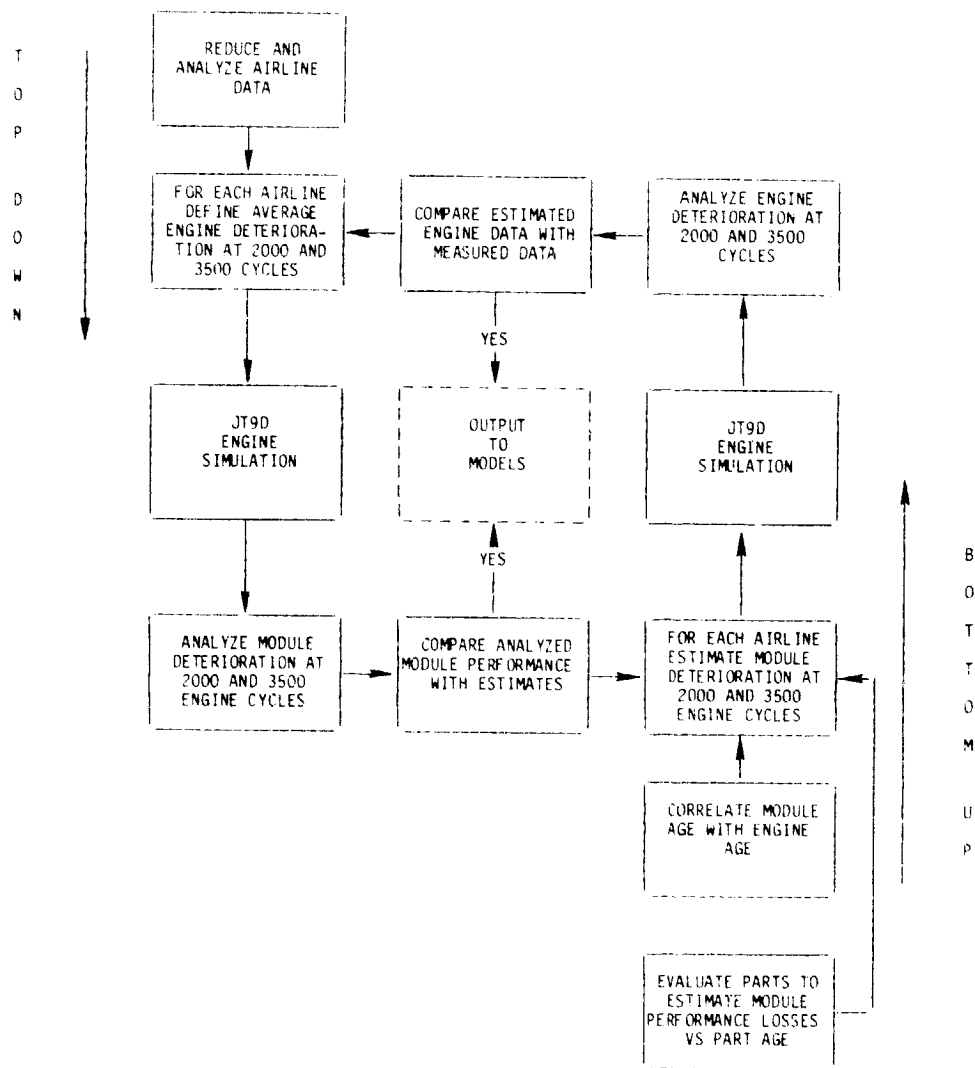


Figure 2 Engine Performance Deterioration Diagnostic Technique - A combination of top down and bottom up analysis utilizing the Pratt & Whitney Aircraft JT9D engine simulation permitted module performance deterioration to be modelled for an average JT9D engine in commercial service.

The following sections describe, in detail, the steps followed in obtaining data, analyzing the data, defining the deterioration mechanisms, and, then, modeling the overall engine and module deterioration.

3.2 DATA COLLECTION

Three major types of data were collected. These types were: 1) engine performance and airline operational data, 2) part scrappage and repair data, and 3) part condition data. The techniques used for collecting each of these sets of data are discussed in detail below.

3.2.1 Engine Performance and Airline Operational Data

Engine performance data were obtained from five airlines (Northwest Airlines, Trans World Airlines, Pan American World Airways, American Airlines, and United Air Lines) and from the Pratt & Whitney Aircraft Service Center. Test stand data were provided by all five airlines and the Service Center while Northwest Airlines, Trans World Airlines, and Pan American World Airways also provided flight and operational data.

Test Stand Data

By far the majority of data contributing to the definition of JT9D engine deterioration characteristics was airline operator prerepair and postrepair data. A considerable volume of postrepair data is available since all engines receiving major repairs are subjected to testing on a test stand to verify compliance with the Overhaul Manual limits. In addition, some engines are tested prior to repair. Table I lists the quantities and types of test stand data obtained for the program. Overall, data were obtained for 1210 individual engine tests. Data was also obtained from special test programs conducted by Pratt & Whitney Aircraft on five service engines.

Data validity was a major concern throughout the program and particularly with respect to the test stand data, since data were to be obtained from a number of sources, and in some cases to detect relatively subtle differences.

It could not be expected that the accuracy of the data obtained from airline test stands would match that of Pratt & Whitney Aircraft

TABLE I
SUMMARY OF AVAILABLE ENGINE CALIBRATION DATA

<u>Operator</u>	<u>JT9D Model</u>	<u>Calibrations Available</u>	<u>Prerepair Calibrations</u>	<u>Engine Hour Range (Thousands)</u>	<u>Approximate Average Engine Hours (Thousands)</u>
PA	D-7 and -7CN	55	18	5-18	14
PA	D-7ACN	69	15	13-18	15
TW	D-3A	169	7	2-13	7
	D-7ACN	107	8	4-16	9
AA	D-3A	299	45	1-13	9
NW	D-7CN	157	20	2-18	8
	D-7	50	1	5-16	8
	D-20	187	5	1-10	5
UA	D-3A	69	0	8-19	12
P&WA	D-7, -7A, -7A(SP)				
Svc. Ctr. Retrofit		48	0	0-11	5

research test stands, since airline test stands are required to provide only sufficient accuracy to verify that their engines comply with the Overhaul Manual limits. Further, all the airlines participating in the study used visual readouts of some data with manual recording. This approach necessarily results in nonsimultaneous recording of data, and any shift in the engine operating point between readings produces an inconsistent data set.

The problem was investigated from two viewpoints: one to establish the inherent accuracy of the data and the second to enhance the accuracy through analytical techniques.

Four sources of information were available for assessing the accuracy of airline test stand data. First, correlation test data were available from calibration engines that were run in a Pratt & Whitney Aircraft stand of known accuracy and subsequently in the airline test stand. Such tests are run periodically and permit the application of corrections for bias errors to the data.

A second source was instrumentation calibration records. However, only limited use of this source was possible since only one of the airlines

retained these records and there still remained the question of the accuracy of the calibration standard.

A third source was the specifications of the instruments themselves. Presumably, with proper care, the instruments would perform within the manufacturer's specifications. This is an assumption, however, and some of the scatter observed in the data may well result from instrumentation operation outside of specifications.

The final source was observations by Pratt & Whitney Aircraft personnel at the airlines' test facilities. These observations provided a basis for evaluating overall confidence in to the various types of data received.

It should be noted that no attempt was made to assess the accuracy of the instrumentation installed in the engine itself. Although premium thermocouple wire is used for all thermocouples in the engine and the rotor speed transmitters are calibrated in accordance with published Pratt & Whitney Aircraft procedures, the specific installation varies from engine to engine and could not reasonably be analyzed for the large number of engines included in the program.

The net result of the determination of inherent data accuracy is shown in Table II for each airline (designated by code letter by agreement with each airline participant) and for each measured parameter.

Data enhancement will be discussed in detail in a following section on data analysis, but, briefly, involved (1) averaging large quantities of data and removing obvious cases of data scatter, and (2) using the top down and bottom up techniques to guide adjustments to the sets of data for bias errors.

Flight Performance and Operational Data

Flight performance and operational data were obtained from Pan American World Airways, Trans World Airlines, and Northwest Airlines. The types of flight performance data were limited to that provided by instrumentation installed in production engines and that data recorded by the Flight Engineer for engine condition monitoring. In most cases, these data consisted of fuel flow, exhaust gas temperature, rotor speeds, and engine pressure ratio. The Flight Engineer also records airplane altitude, air speed, gross weight, and outside air temperature to permit correction of the data to standard conditions. The operational data documented airline procedures such as climb and cruise

TABLE II
TOTAL UNCERTAINTIES FOR AIRLINE
TEST CELLS

<u>Parameter</u>	<u>Airline A</u>	<u>Airline B</u>	<u>Airline C</u>
Thrust (lb)	+109	+152	+75
Fuel Flow (% Reading)	+0.55	+0.79	+0.46
P _{amb} (Barometer)	+0.093	+0.023	+0.04
P _{t2} (inches Hg)	+0.133	+0.053	+0.24
P _{cell} (inches Hg)	--	+0.053	--
P _{t3c} (inches Hg)	+0.48	+0.103	+0.24
P _{s3c} (inches Hg)	+0.24	+0.102	+0.24
P _{s4} (inches Hg)	+0.94	+3.11	+2.4
P _{s5i} (inches Hg)	+1.59	+3.11	+2.4
P _{t7} (inches Hg)	+0.14	+0.062	+0.24
T _{t2} (°F)	+0.30	+1.09	+0.3
T _{t4} (°F)	+1.70	--	+2.0
EGT T _{t6} (°F)	+2.4	+3.0	+2.0
N ₁ (rpm)	+5	+3	+5
N ₂ (rpm)	+10	+5	+10
Vane Angle (Degrees)*	+0.01	+0.01	+0.01

* Resolution of indicator

flight power setting policies and engine derating which might affect the performance trends. These data are presented in Appendix A.

The data available from Pan American World Airways consisted of operational data and fleet average data for the period from 1972 through 1976. Data for individual engines were no longer available.

Trans World Airlines provided the most extensive history of fleet and individual engine data of the three participating operators. Fleet data were available from 1971 through 1976 and individual engine data by engine serial number was available since January 1973. This data was compressed during computerized retrieval to average every ten data points, which suppressed data scatter but still permitted construction of individual engine histories as well as fleet averages. Trans World

Airlines also provided detailed operational data over the time frame for which performance data were available.

The data from Northwest Airlines was of particular interest since it included JT9D engine installations in both Boeing 747 aircraft and Douglas DC-10 aircraft. Unfortunately for the purposes of this program, Northwest Airlines only preserves trend monitoring data for the last 30 flights prior to each engine removal, which results in numerous time gaps. However, all available data was collected and totalled approximately 500 preremoval data sets.

Another source of performance data was the Boeing Company's JT9D-7 and JT9D-7A engine fleet survey data, which Boeing collects on a periodic basis for selected aircraft over a period of thirty days. Unfortunately, these data are correlated against acquisition date rather than engine operating time or cycles, and attempting to convert these data back to engine cycles was well beyond the scope of this program.

3.2.2 Part Scrappage and Repair Data

Part usage data and maintenance experience was collected from visits to maintenance shops for each of the three airlines.

Statistical data collected from each airline consisted of:

1. Number of engine shop visits by year;
2. Number of repairs of each module by year;
3. Number of engine flight hours and cycle by year;
4. Number of gas-path parts scrapped by stage by year;
5. Number of gas-path parts repaired by stage by year;
6. Airline rebuild standards and maintenance philosophy; and
7. Status of incorporation of service bulletins which effect performance.

The selection of parts included in the data for scrappage was limited to those affecting performance. The identification of these parts is shown in Table III.

TABLE III
GAS-PATH PARTS STUDIED

FAN	Blades Outer Duct	COMBUSTOR/FIRST TURBINE VANES Comb. Inner Liner Comb. Outer Liner First-Stage Turbine Vanes
LPC	Blades Stators Inner KE Seals Inner Seal Rings Outer Ducts	HPT Blades Vaness Inner Seal Rings Inner KE Seals Outer Air Seals
HPC	Blades Vaness/Stators Inner Seal Rings Inner KE Seals Outer Ducts	LPT Blades Vaness Inner Seal Rings Inner KE Seals Outer Air Seals
DIFFUSER	HPC Exit Vanes	

The selection of parts included in the data for repair was also limited to those maintenance actions on gas path parts that would be expected to affect performance. Hence, such repairs as filing and blending airfoil nicks, rebrazing stator assemblies, or welding small cracks were excluded from the study. The specific types of repairs that were included were:

Blades

Fan - Reconditioning of leading edges and two-degree root trailing edge uncamber.

Low-Pressure Compressor Third Stage - Recambering to JT9D-7A engine configuration.

High-Pressure Turbine First Stage - Repairing blade tip by machining off tip, welding on new tip, and machining to correct blade length.

Low-Pressure Turbine - Repairing blade tip knife-edge seals and restriking the blade to restore the blade shape.

Stator Vanes

Low-Pressure Compressor Fourth Stage - Restriking the vanes to restore the vane shape.

High-Pressure Compressor Assemblies Stages 8 Through 15 - Replacing defective vanes.

High-Pressure Turbine - Restriking or repairing buttresses.

Low-Pressure Turbine - Restriking and weld-repairing airfoil cracks.

Ducts and Outer Air Seals

Compressor Ducts in Stages 2 Through 7 - Replacing rubber rub strips.

High-Pressure Compressor Ducts in Stages 8 Through 15 - Replacing outer rub strips.

High-Pressure Turbine First-Stage Outer Air Seal - Rotating seal assembly 90 degrees to equalize wear with replacement of seals as required and offset grinding of the complete assembly.

High-Pressure Turbine Second-Stage Outer Air Seal - Replacement of honeycomb rub strips.

Low-Pressure Turbine Third- Through Sixth-Stage Outer Air Seals - Replacement of honeycomb rub strips.

Inner Shrouds

High-Pressure Compressor - Replacement of Seal Land Rub Strips.

High-Pressure Turbine - Replacement of Seal Land Rub Strips.

Low-Pressure Turbine - Replacement of Seal Land Rub Strips.

3.2.3 Part Condition Data

A large sample of airfoils (630 fan and compressor airfoils and 120 turbine airfoils) was collected from engines brought in for repair, representing usage levels up to 5500 cycles. These parts were inspected for geometry and surface finish and the results correlated against operating hours and cycles.

Fan airfoil contours were measured with the Automatic Digital Airfoil Measurement (ADAM) system, which uses mechanical sensors to obtain contour data. The resulting measurements are then digitized for computer analysis. Since this equipment is not capable of accurately defining the leading- and trailing-edge contours, a New England Tracer was used for measurements in these areas.

Airfoil contours for the compressor and turbine blades were made using the Rapid Airfoil Digital Optical Contour (RADOC) equipment which employs a laser optical system to measure the airfoil dimensions. The system converts these measurement to digital form suitable for computer analysis and plotting. The RADOC system is illustrated in Figure 3.

Airfoil contours for the compressor vanes were made using shadowgraph equipment.

Production tooling was used to measure bow and twist of the turbine vanes.

For both compressor and turbine airfoils, surface roughness measurements were made using the Clevite Surfalyzer^(R), and lengths were measured with micrometers.

3.3 PERFORMANCE DATA REDUCTION AND ANALYTICAL METHODOLOGY

3.3.1 Overall Approach

The overall data analysis approach is shown in Figure 4. The process may be divided into two basic efforts. The first, shown in the left column of Figure 4, begins with the test cell performance data, which was reduced and processed to initially develop an estimate of the average engine deterioration experienced by each airline and then an estimate of the overall JT9D engine fleet average deterioration. The second, shown by the remaining columns at the top of Figure 4, deal with the age and condition of individual engine parts (such as blades and vanes). These data were reduced and analyzed to estimate the performance of the engine modules as a function of module age, and then

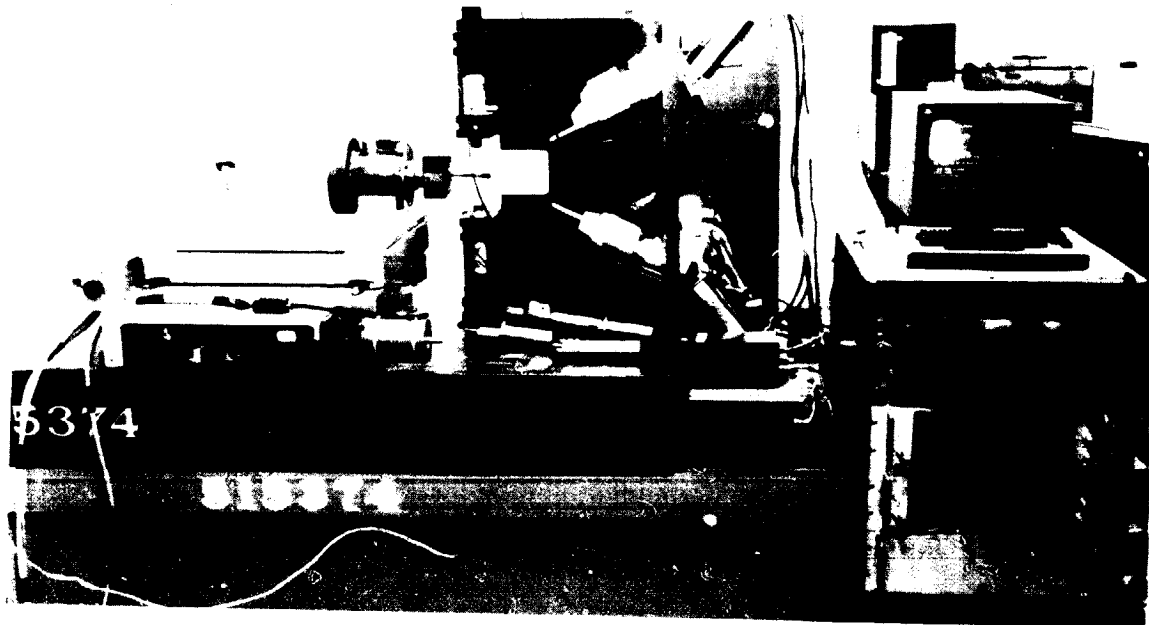


Figure 3 Rapid Airfoil Digital Optical Contour (RADOC) Facility - The RADOC equipment scans the airfoil with a pair of laser beams to measure airfoil contours and then digitizes the data for computer analysis.

analyzed using the JT9D engine simulation to model the deterioration of both the modules and the complete engine.

The validity of these final models was established by two techniques. First, data enhancement was achieved by analyzing the data for individual airlines by a combined top down and bottom up technique for average engines with 2000 and 3500 cycles. In the top down portion of the analysis, average engine data were processed in an iterative fashion to estimate the probable levels of deterioration of each module that would result in the observed overall engine deterioration. Concurrently, the bottom up approach was used to estimate the module performance deterioration on the basis of the condition and age of parts observed for the particular airline, and the engine simulation was then used to estimate the resulting average engine deterioration. Comparison of the module performance deterioration and the overall engine deterioration estimated by each technique indicated the validity of the individual approaches and in some cases suggested areas where additional data reduction and interpretation could improve the data quality.

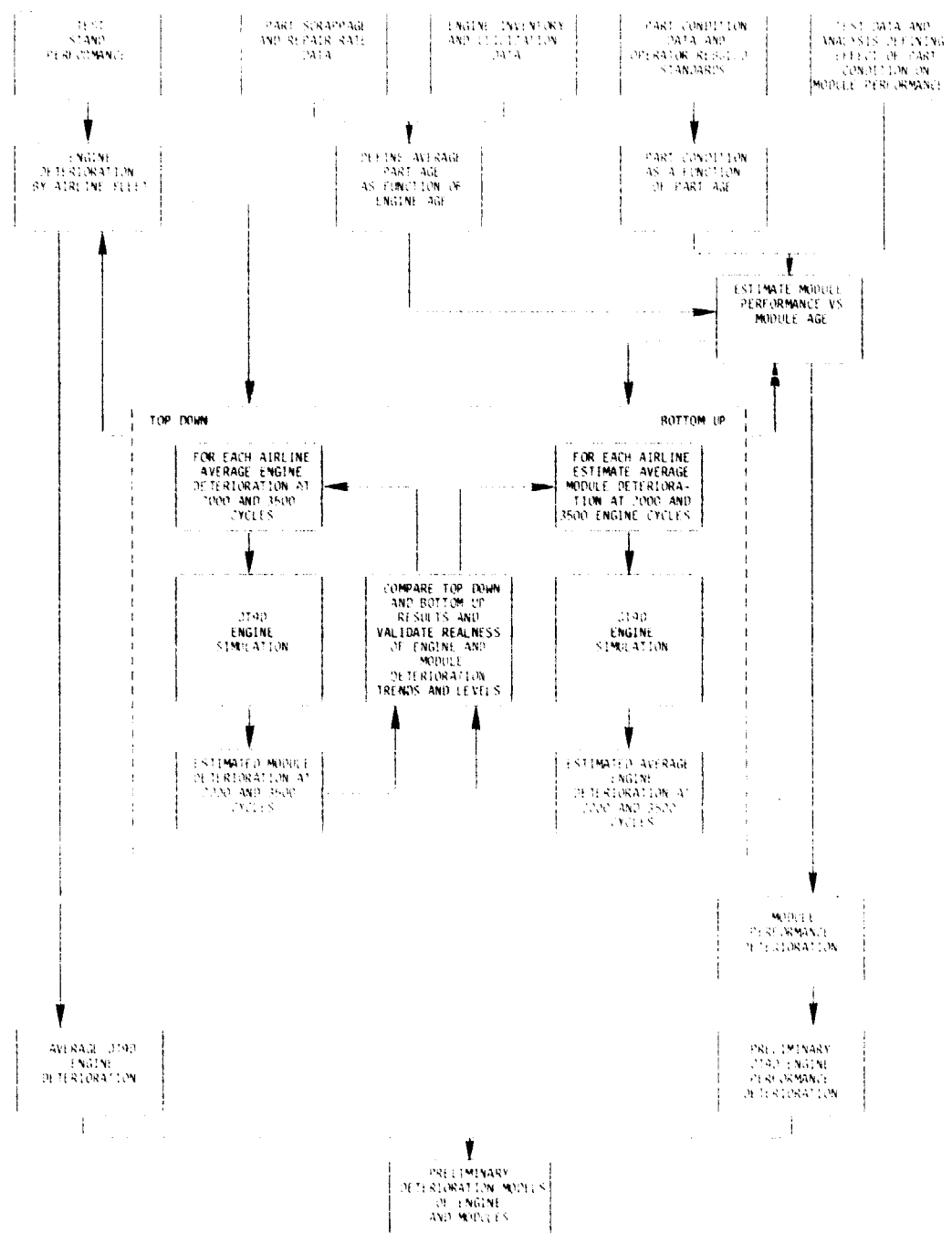


Figure 4 Overall Data Analysis Flow Chart - A "top down/bottom up" approach was used to correlate overall average engine data and the effects of deterioration of individual parts to model engine module deterioration as a function of engine flight cycles.

Secondly, after data enhancement from the use of the top down/bottom up analysis, the preliminary module performance models were developed and then used in conjunction with the JT9D engine simulation to define the preliminary average engine performance model. The performance deterioration trend predicted by this model was then compared with the average engine deterioration trend actually experienced by the airlines. The relative agreement (and, in fact, good agreement was obtained) indicated not only the general validity of the engine deterioration model, but also the validity of the models for the individual modules.

The following sections describe each step of the analytical process in detail.

3.3.2 Analysis of Test Stand Data

The test stand data was received in a variety of forms, including test log sheets, data tapes, and punched cards. These data were sorted by engine serial number, and entered into computer files for reduction and enhancement, as illustrated in Figure 5. The data was then reduced to absolute levels, and pressure ratios and corrected flow rates were calculated. The resulting reduced data were then printed out in tabular form. A typical data sheet is shown in Figure 6.

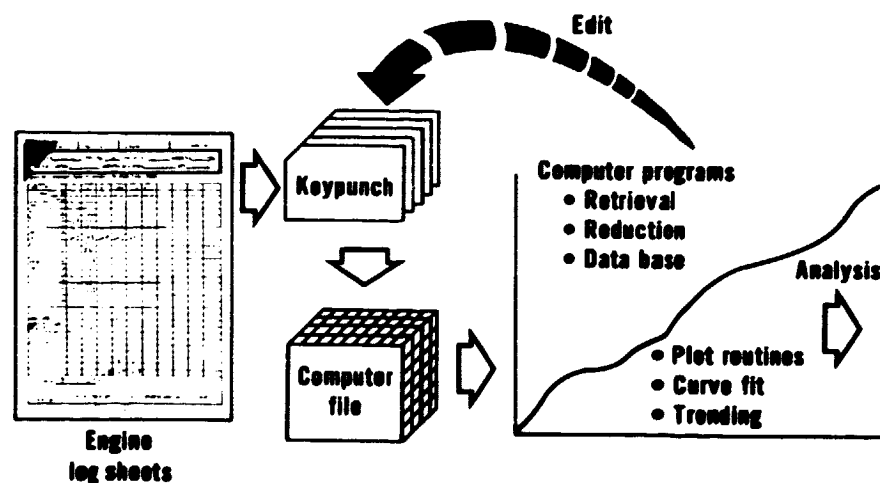


Figure 5 Initial Steps in Processing Test Stand Data - The data was entered into a computer file and plotted to establish trends on an individual engine basis.

OPERATOR: NW ENGINE MODEL: JT9D-20 SERIAL NUMBER: P-686110 DATE: 080274
 CONFIGURATION: -100 PDEC
 INLET: WITHOUT SCREEN

CORRECTED DATA
 SEA LEVEL STATIC STANDARD DAY
 TEST CELL CORRECTIONS NOT INCLUDED

AJP= 6.599 SC.FT. AJP= 19.970 SC.FT. FUEL LEVE 12000. FTU/LH

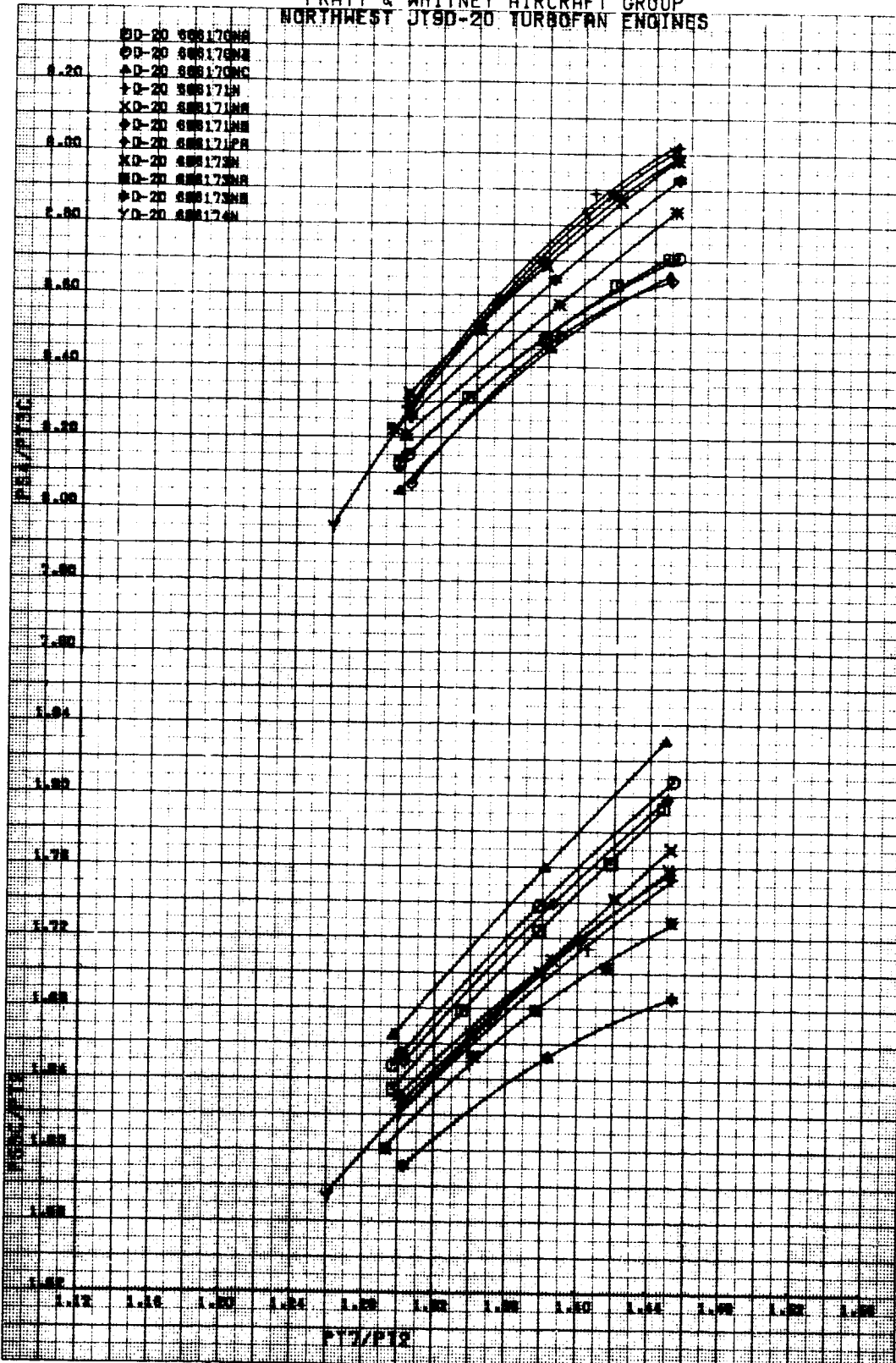
PT NO		1.0000	2.0000	3.0000	4.0000	5.0000
PT7/PT2		1.2637	1.3054	1.3469	1.4093	1.4525
FM/ST2	LBS	28817.	32048.	35181.	39456.	41948.
N1/ROT2	RPM	2805.5	2922.1	3031.5	3166.2	3243.9
N2/ROT2	RPM	7037.8	7125.6	7201.0	7301.2	7334.0
TT6A/(OT2).91	DEGF	1284.7	1341.6	1395.0	1467.5	1510.1
TT6IA/(OT2).91	DEGF	1282.5	1341.8	1397.4	1472.2	1517.4
PT3C/PT2		1.9207	2.0179	2.1084	2.2198	2.2859
PS3C/PT2		1.5649	1.6205	1.6642	1.7132	1.7361
PS4/PT7		12.080	12.667	13.173	12.724	14.012
PS4/PT2		15.266	16.535	17.744	19.341	20.352
PS4/PT3C		7.9479	8.1943	8.4158	8.7131	8.9031
PS51/PT7		8.1564	8.5764	8.9467	9.3380	9.5277
WF/KCST2KH	PPH	10765.	12017.	13297.	15141.	16311.
(PS4-PS51)/PS4		.32482	.32292	.32085	.31647	.29002
(PT3C-PS3C)/PT3C		.18525	.19692	.21066	.22819	.24094
TT6HA-TT6IA	DEGF	2.1667	-1.6650	-2.5000	-4.6665	-7.1665
BETA	AUEG-.40000		.90000	2.5000	3.9000	5.0000

*** PREPARED BY PWA JT9D MODULE ANALYSIS PROGRAM 08/15/77 ***

Figure 6 Typical Computer Listing of Corrected Test Stand Data - Data reduction consisted of calculating absolute values of parameters and then using these absolute values to calculate pressure ratios and corrected flow rates.

The next several steps were designed to remove data scatter and questionable data points. This was achieved by a combination of averaging the data and defining trends. The first step consisted of computer plotting each engine parameter as a function of engine pressure ratio for each engine serial number. Computer generated second-order least squares curve fits were then drawn through the data. A typical computer plot is shown in Figure 7 for several Northwest Airlines engines. These computer-generated least squares fit curves were then read for each engine at an engine pressure ratio of 1.454 and the resulting values plotted on a trend chart by engine serial number and test date, as shown in Figure 8. The computer also generated a constant line at the average of the data and also the two sigma wide band around the data. Data falling outside of the two-sigma band was examined and revised or rejected if it was believed to reflect errors in key punching, data acquisition, etc. This process was then repeated until the trend plot was acceptable.

PRATT & WHITNEY AIRCRAFT GROUP
NORTHWEST JT9D-20 TURBOFAN ENGINES



PSF PERF GROUP ARE/VF 8-29-77

Figure 7 Typical Computer Plot of Engine Performance Data - The data for each engine were plotted as a function of engine pressure ratio and fit with second order curves.

ORIGINAL PAGE IS
OF POOR QUALITY

Northwest JT9D-7 turbofan engine
2 Sigma displayed

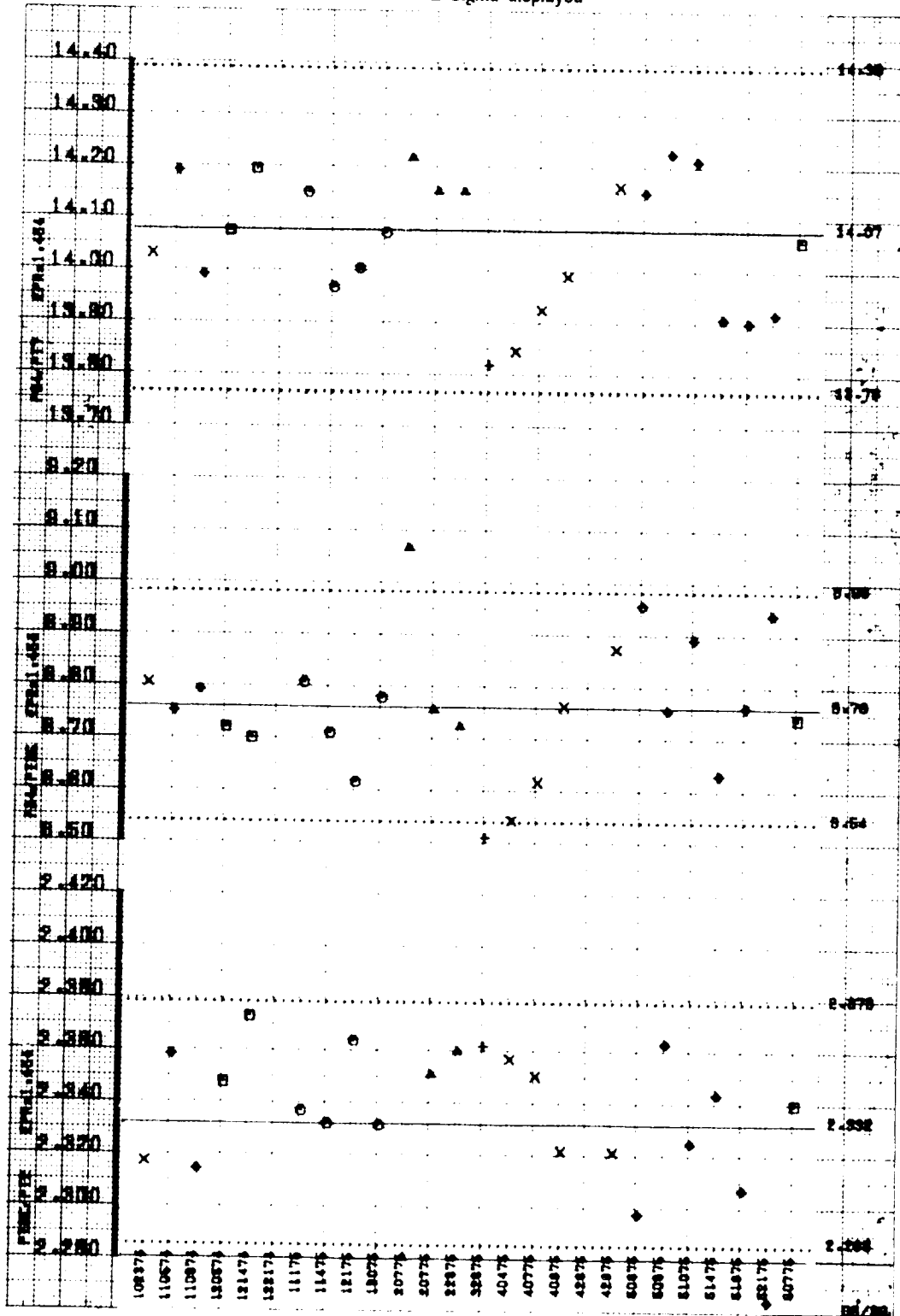


Figure 8 Trend Plot of Typical Engine Parameters - These plots permitted examination of data falling outside of the two-sigma data band for a specific airline.

The resulting corrected data at take-off thrust engine pressure ratio and at take-off thrust were then plotted as functions of engine hours and cycles for each airline. A least squares regression fit of the data was made to define the change in average engine performance data as functions of engine hours and cycles. The result represented the absolute performance levels as functions of engine age (in hours and cycles) for the "average" engine of each airline. A typical set of data is shown in Figure 9.

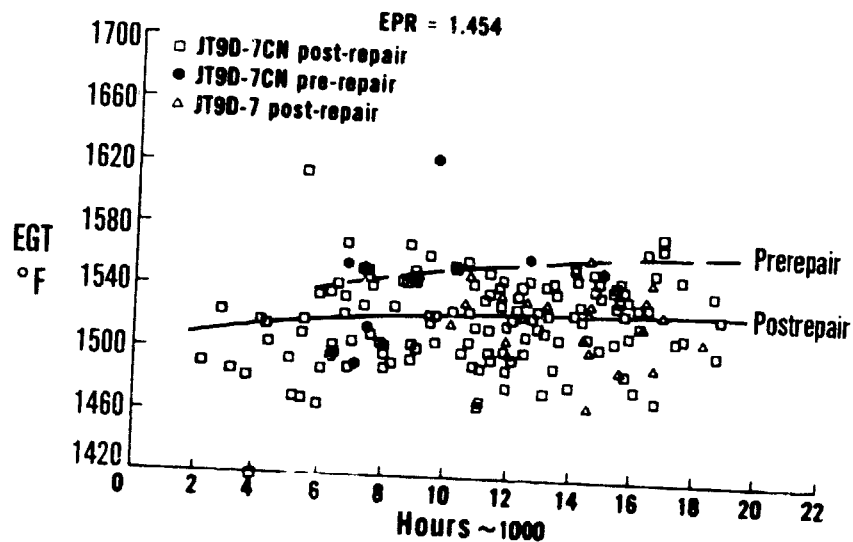


Figure 9 Absolute Exhaust Gas Temperatures (EGT) for Average Engine as a Function of Engine Age - Absolute values were established generally by plotting second-order least squares fits through the corrected data on an airline basis.

Since the absolute levels of performance of the engines from various airlines differed significantly as a result of such fundamental differences as engine model number and Service Bulletin rework, absolute levels could not be used in combining the data from the various airlines to define a JT9D fleet average engine. Rather, the absolute levels had to be reduced to the deterioration relative to the new-engine performance of an identical engine.

Defining an appropriate baseline new-engine performance level required extensive effort, since the service engines for which data was used in the program incorporated a wide range of modifications which would affect performance independent of and usually counter to performance deterioration related to engine age.

The technique used was as follows. First, data on the implementation of performance-related modifications were analyzed to define the average level of performance improvement resulting from modifications for each airline as a function of calendar time. Based on engine utilization, a calendar time period was then assigned for each age level (cycles or operating hours) for the average engine for each airline. This technique permitted a definition of the configuration for the average engine as a function of engine age. Baseline performance was then established by averaging the new-engine performance for a block of engines with configurations equivalent to that defined for the average engine, and then correcting this performance to the test conditions and biases of the airline test stand.

With the base-line performance levels established for the average engine for each of the airlines, the absolute values could be reduced to performance changes. The results for each airline were then averaged to define the performance deterioration of a JT9D fleet average engine.

3.3.3 Analysis of Part Age and Condition Data

Five major steps were involved in estimating engine performance on the basis of the condition of the individual parts:

1. Define the age of the parts as a function of engine age;
2. Define the condition of the parts as a function of part age;
3. Determine the effect of part condition and operator rebuild standards on module performance;
4. Estimate the module performance as a function of engine age; and
5. Estimate the engine performance as a function of engine age.

Estimate of Part Age as a Function of Engine Age

Average part age for the average engine for any given calendar time period was estimated on the basis of airline part scrappage and repair rate data and on engine utilization and inventory data. Part age records normally are not maintained by operators and statistical methods were employed to estimate the age of parts in the average engine as a function of time.

By definition, the average age of a particular type of part in an engine equals the sum of the ages of the individual parts divided by the number of parts. However, if some of the parts were replaced, but no parts were replaced more than once, the average part age equals the age of the engine minus the ages of the parts replaced. That is:

Average Age =

$$\frac{(\text{Total Parts})(\text{Engine Age}) - \text{Sum of (Replaced Parts X Age at Replacement)}}{\text{Total Number of Parts}}$$

This reduces to:

$$\text{Average Age} = \text{Engine Age} - \text{Sum of (Replacement Rate) X Age at Replacement}$$

In integral form this equation becomes:

$$T_a = T_e - \int_0^{T_e} r t dt$$

where:

T_a = Average part age

T_e = Engine age

r = Part replacement rate per hour

t = Time

If r is constant, then

$$T_a = T_e - r(T_e)^2/2$$

An example of the calculation for the combustor inner liner for Airline A would be as follows:

The total flight hours for the fleet was 1,785,000 hours on 171 engines. Therefore, the average engine age was 1,785,000/171 or 10,438 hours. The part replacement rate for the period was 5.3 percent per 1000 hours or 0.000053 per hour. Evaluating the equation for average age then yields:

$$T_a = 10,438 - 0.000053(10,438)^2/2$$

$$T_a = 10,438 - 2,887$$

$$T_a = 7,551$$

In actual practice, the replacement rate, r , was not always constant throughout the life of the engine. As a result, a four-year moving average value of r was used and applied to a statistical discrete summation form of the equation to facilitate calculation.

Serialized part number records were available for Airline A. These records provided the total part time for selected components and permitted calculation of actual average part ages for these selected components. These calculations were made and compared with the estimated average part ages developed using the part utilization rate formula described above. The results from both approaches are shown in Table IV. As shown, the estimated age tends to be within about 15 percent of the actual average part age.

TABLE IV
EXAMPLES OF AVERAGE PART AGES

<u>Component</u>	<u>Engine Age (Hours)</u>	<u>Replacement Rate (Percent per Thousand Hours)</u>	<u>Estimated Average Age (Hours)</u>	<u>Actual Average Age (Hours)</u>
Fan Blade	10,438	0.52	10,155	9,100
Combustor:				
Outer Liner	10,438	5.3	7,551	6,500
Inner Liner	10,438	5.1	7,660	6,500

Definition of Condition of Parts as a Function of Part Age

The inspection data from parts collected and observations made during the airline shop visits were plotted against part age. Plotted were such parameters as rub strip depths, blade length loss, blade tip clearance, roughness, and airfoil profile data.

These plots were analyzed to produce a continuous curve representing condition as a function of age. A typical plot is shown in Figure 10. Considerable engineering judgement was exercised in fitting curves through the data. Although a very large number of parts was inspected, relatively little data were available for some engine stages and time

frames. However, the resulting trends are believed to represent real absolute levels of deterioration and generally reflect the deterioration trend accurately on an overall average basis.

Determination of Effect of Part Condition and Operator Build Standards on Module Performance

The effects of changes in the condition of parts on module performance were assessed analytically as follows: (1) the effects of increased airfoil roughness on performance were determined using correlations of airfoil loss as a function of Reynolds number and roughness-to-chord length ratio; (2) the effects of chord loss and camber changes in compressors were determined using radial stream tube compressor performance computer models; (3) the effects of changes in turbine nozzle areas were assessed based on correlations of physical and effective area developed from engine testing; and (4) the effects of clearance changes were determined on the basis of analysis of component rig data and back-to-back engine test data.

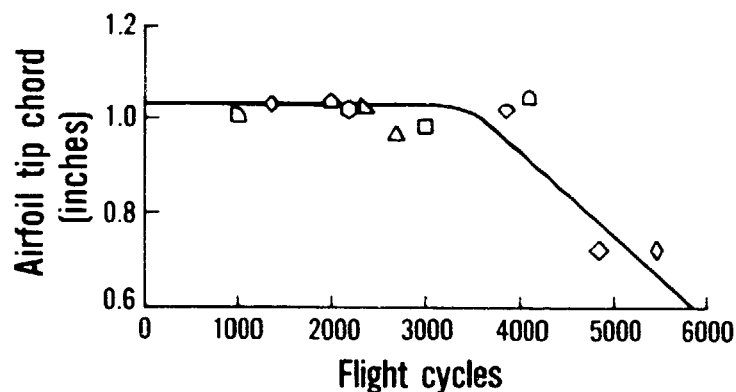


Figure 10 Effect of Age on Airfoil Tip Chord - Plots such as this example reflect Pratt & Whitney Aircraft's best engineering judgement on individual part deterioration trends.

These clearance data provided definition of the change in flow capacity and change in efficiency resulting from a given tip clearance change for each module of the engine. Typical results are shown in Table V for each engine module in response to a 0.01-inch increase in tip clearance. Table

VI defines the individual effects of the outer and inner air seal clearances in the low-pressure turbine.

Part age affects the level of performance but even with new parts differences from recommended clearances can have a major impact on performance deterioration.

The then current written rebuild standards of Airlines A, B, and C relating to clearances and blending limits were examined and compared with the Pratt & Whitney Aircraft recommendations. This analysis permitted determination of the probable average clearances in the engine of each operator as well as the maximum allowable clearances, defined in terms of the "repair if over" limit.

TABLE V
JT9D-7 SENSITIVITIES FOR A +0.010-INCH
TIP CLEARANCE CHANGE

	<u>Percent Change in Efficiency</u>	<u>Percent Change in Flow Capacity</u>
Fan	-0.1	-0.15
Low-Pressure Compressor	-0.5	-0.83
High-Pressure Compressor	-1.2	-1.60
High-Pressure Turbine Outer Air Seals:		
1	-0.5	+0.27
2	-0.38	+0.03
Low-Pressure Turbine Outer and Inner Air Seals:		
3	-0.13	+0.2
4	-0.16	+0.07
5	-0.1	+0.01
6	-0.06	--

Estimation of Module Performance as a Function of Engine Age

The determination of the performance of each module as a function of average engine age was a straightforward task of cross plotting the data for part age as a function of engine age and module performance as a

function of part age. Estimates were made for component flow capacity and efficiency changes for each average module for each airline at 2000 and 3500 cycles as a function of engine cycles.

TABLE VI
 JT9D-7 SENSITIVITY ANALYSIS FOR A +0.010-INCH
 LOW-PRESSURE TURBINE CLEARANCE CHANGE

	<u>Percent Change in Efficiency</u>	<u>Percent Change in A6</u>
Outer Air Seals		
3	-0.11	+0.10
4	-0.08	+0.03
5	-0.05	+0.01
6	-0.03	0
Inner Air Seals		
3	-0.02	+0.10
4	-0.08	+0.04
5	-0.05	0
6	-0.03	0

Estimation of Engine Performance as a Function of Engine Age

Average engine performance deterioration was predicted on the basis of the module performance data as a function of engine age by using the Pratt & Whitney Aircraft JT9D engine simulation.

A new method of modeling changes in flow capacity of the fan, low-pressure compressor, and high-pressure compressor was developed that provides substantially higher accuracy than previously used techniques. Traditionally, flow capacity losses (primarily resulting from tip clearance increases) have been modeled either by "flow scaling", which results in shifting the entire component performance map horizontally to the left, or by "speed scaling", which results in renaming the corrected speed lines. In effect, the speed lines (and only the speed lines) are shifted down and to the left. However,

existing compressor rig data obtained with a heated inlet (which has the effect of increasing tip clearance and decreasing flow capacity), indicated that neither approach was strictly correct. These data indicated that the entire component map shifts down and to the left, along a typical operating line slope, as tip clearance is increased and flow capacity is reduced. These effects are shown in Figure 11. On the basis of these results, the fan, low-pressure compressor, and high-pressure compressor component maps in the computer engine simulation were modified to simulate heated inlet rig results through changing map scaling constants.

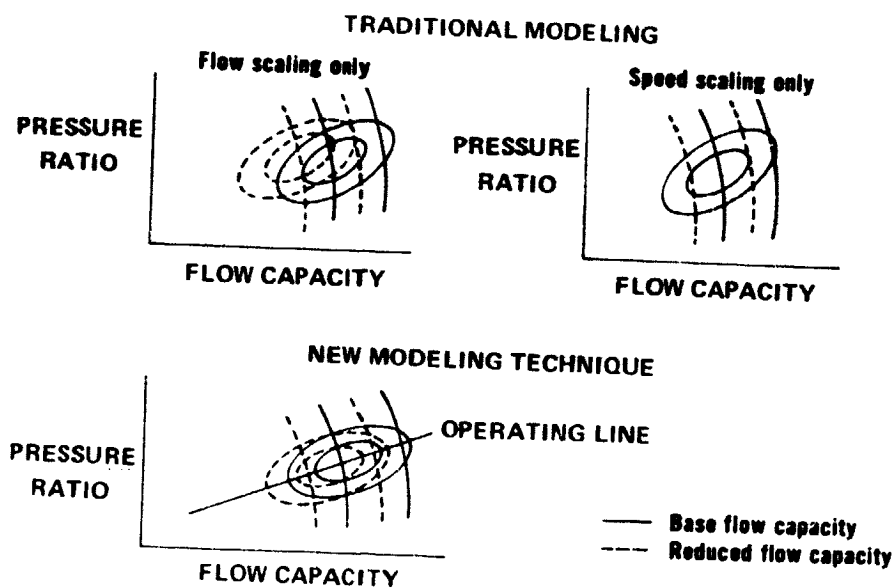


Figure 11 Different Approaches for Modeling Tip Clearance Effects - Traditional approaches modeled through either speed line shifts of flow shifts, whereas data indicate that the real effect is a shift approximately along the operating line.

3.3.4 Validation

Because the data analysis necessarily incorporated a number of assumptions due to the limited amount of data for any particular engine stage and age and because of the large number of variables that could not be accounted for, a unique iterative technique was developed for making adjustments to these assumptions and enhance the effective quality of the data.

This technique has been identified as the "top down/bottom up" technique and is shown in the center of Figure 2. In essence, the technique involved detailed analysis of data obtained for the average engine of each airline at 2000 and 3500 cycles. The overall engine performance data were processed by the Pratt & Whitney Aircraft JT9D engine simulation to estimate the module performance data, and, inversely, the estimated module performance based on part condition and age was used to predict overall engine performance. Comparison of the two estimates of module performance and the measured and predicted overall engine performance data provided a guide for adjusting the data reduction assumptions and correlation factors. The process was then repeated until good agreement was achieved for each airline data set. The resulting, much enhanced, data were then used to define the preliminary average JT9D engine performance deterioration trends on both an overall engine and a module basis.

The top down analysis posed a particularly difficult problem because of the relatively small number of engine performance variables measured in the test cells. In fact, the number of unknowns (flow capacity and efficiency of each module) exceeded the number of performance parameter measurements made, precluding a closed solution to the module performance loss definition without an additional relationship.

Such a relationship was found in studying the data from the bottom up analysis. It was noted in the data obtained for effects of tip clearance on fan and low-pressure compressor efficiency and flow capacity that a given change in flow capacity is accompanied by a definable corresponding change in efficiency. This relationship is clearly evident in the data presented previously in Table V. By "coupling" these two variables in the engine simulation program, two unknowns were eliminated, and sufficient measured variables were now available.

The possibility of coupling other variables was explored in the hopes of further enhancing the data, but no suitable parameters were found. Flow capacity and efficiency in the high-pressure compressor could not be coupled because of the variable vanes. The vane scheduling is periodically trimmed as a part of maintenance work, with the result that the flow capacity changes without the same loss in efficiency that would occur from performance deterioration mechanisms. Individual vane indexing errors also cause uncoupled shifts in flow capacity and efficiency. Sufficient parameters were available in the turbines to define both efficiency and flow capacity providing T_{t4} data were available.

With the coupled relationships incorporated into the engine simulation, the simulation was used in an iterative manner (with computerized iteration logic) to find the combination of module performance losses that provided the measured levels of engine performance. The primary component variable iterated to match the observed parameter shift are outlined in Table VII.

TABLE VII
ENGINE SIMULATION FOR DIAGNOSTIC TRACKING
TOP DOWN APPROACH

<u>Observed Parameter Shifts</u>	<u>Component Variable Iterated</u>
Percent Change in N_1	Percent Change in Fan Flow Capacity (Coupled to Fan Efficiency)
Percent Change in N_2	Percent Change in High-Pressure Compressor Flow Capacity
Percent Change in P_{t3}/P_{t2}	Percent Change in Low-Pressure Compressor Flow Capacity (Coupled to Low-Pressure Compressor Efficiency)
Percent Change in P_{s4}/P_{t7}	Percent Change in A_5
Change in T_{t4}	Change in High-Pressure Compressor Efficiency
Change in T_{t6}	Percent Change in A_6
Percent Change in W_f	Change in Low-Pressure Turbine Efficiency
Percent Change in F_n	Change in High-Pressure Turbine Efficiency

It should be pointed out that the module performance parameters which have been selected for the iteration balances are those which have a strong effect on the corresponding observed parameter. For example, fan flow capacity has been selected for iteration to modify low-pressure rotor speed. However, with a change in fan flow capacity, the simulation then simultaneously computes changes in low-pressure rotor speed and all other observed parameters. Hence, the simulation always finds a self-consistent solution, and the individual iteration balances simply represent the mechanics of instructing the computer how to proceed in the direction of a solution.

The bottom up calculation is much more straightforward and is essentially as described in Section 3.3.3, since the computer simulation calculates overall engine performance directly from module performance levels. For the data validation and enhancement, therefore, all that was required was to read the module performance levels from the module deterioration curves for each airline at the appropriate module age for an average engine age of 2000 and 3500 cycles and enter the values into the computer simulation.

SECTION 4.0

PROGRAM RESULTS

4.1 OVERVIEW

The results of the analyses described in Section 3 show that performance deterioration can be broken into two general time frames: 1) that which occurs rapidly in the first few hundred flights after entry of an engine into commercial airline service, called short-term deterioration; and 2) that which occurs more gradually as service usage accumulates, called long-term deterioration.

The analysis of historical short term data indicated that the average engine of the JT9D-3A/7/20 family loses 1 percent in thrust specific fuel consumption (TSFC) on the first flight relative to the level of measured performance at sea-level static take-off conditions of the engine when new. This loss in performance grows to 1.5 percent by the 200th flight. Analysis of these data indicate that 55 percent of the TSFC loss is associated with the performance losses of the low-pressure spool (fan, low-pressure compressor, and low-pressure turbine) and 45 percent with the performance losses of the high-pressure spool (high-pressure compressor and high-pressure turbine).

The long-term performance loss of the engine gradually increases with increased usage. Analyses of prerepair test stand data indicate that the average TSFC performance deterioration of the fleet of JT9D-3A/7/20 family of engines prior to repair is 4.4 ± 0.5 percent at 3500 flights or approximately 12,000 hours of operation relative to new production engine performance levels. The performance losses at this time frame are dominated by the high-pressure spool rather than the low-pressure spool.

The analyses of postrepair test stand data indicate that the fleet average postrepair level of TSFC deterioration is 3.5 ± 0.7 percent at 3500 flights, representing an average recovery of 0.9 percent. The majority of the TSFC recovery results from high-pressure turbine restoration. Historical data indicates that an additional 1.9 percent in TSFC recovery can be realized by refurbishment of the engine cold section (fan, low-, and high-pressure compressor). The balance of average unrecovered performance, approximately 1.6 percent in TSFC, is caused by mechanical conditions distributed among all the modules that are not typically refurbished.

Engine performance deterioration results from the gradual degradation of the mechanical condition of engine parts. Four causes of this degradation have been identified: 1) flight loads that distort the shape of engine cases, produce rubbing, and result in increased clearances; 2) erosion of airfoils and outer air seals resulting in increased roughness and bluntness, loss of camber, loss of blade

length, and increased operating clearances; 3) thermal distortion due to changing turbine inlet temperature patterns resulting in area changes, increased leakages, and changed clearances; and 4) airline operator repair practices and rebuild standards that have an impact on the cumulative levels of part mechanical damage versus time and the levels of prerepair and postrepair performance. The estimated distribution of the prerepair performance loss at 3500 flights by major causes are 40 percent due to flight loads, 40 percent due to erosion, 20 percent due to thermal distortion with the total level varying by ± 13 percent as a result of differences in maintenance practices.

4.2 AVERAGE ENGINE DETERIORATION

The following discussion presents the results of the analytical studies of short- and long-term performance deterioration directed toward quantifying the level and trends of performance loss with usage based on overall engine performance data.

The first section discusses production baselines. This is followed by a discussion of short-term deterioration, including the average performance loss versus usage and estimated distribution of the overall engine loss among modules. The subsequent section deals with longer term performance deterioration. Individual airline trends as well as average trends for the fleet of engines are presented. The performance recovered for typical hot section and cold section refurbishment are discussed.

4.2.1 Production Base Lines

As discussed in Section 3, a production base line equivalent to each airline operator's engine configuration versus calendar time was constructed based on engine model changes and Service Bulletin incorporation status data obtained during airline visits. These base lines were derived on the basis of performance improvements obtained when the modifications were incorporated into production engines. Figure 12 shows the effect of incorporating these modifications on the production engine performance trends. The base-line performance data for each airline was then used to adjust the engine performance deterioration levels to establish a common level for comparison among all airlines. The estimated adjustments to performance deterioration levels at the specific time frame varied from -0.3 to +0.8 percent in TSFC among operators as shown in Table VIII. These adjustments are included in the individual airline trends but had no effect on the fleet average prerepair or postrepair deterioration levels.

4.2.2 Short-Term Performance Deterioration

Data were collected on engines returned to Pratt & Whitney Aircraft and calibrated in a production test cell prior to any restoration of seal clearances. These data were then compared to each engine's original

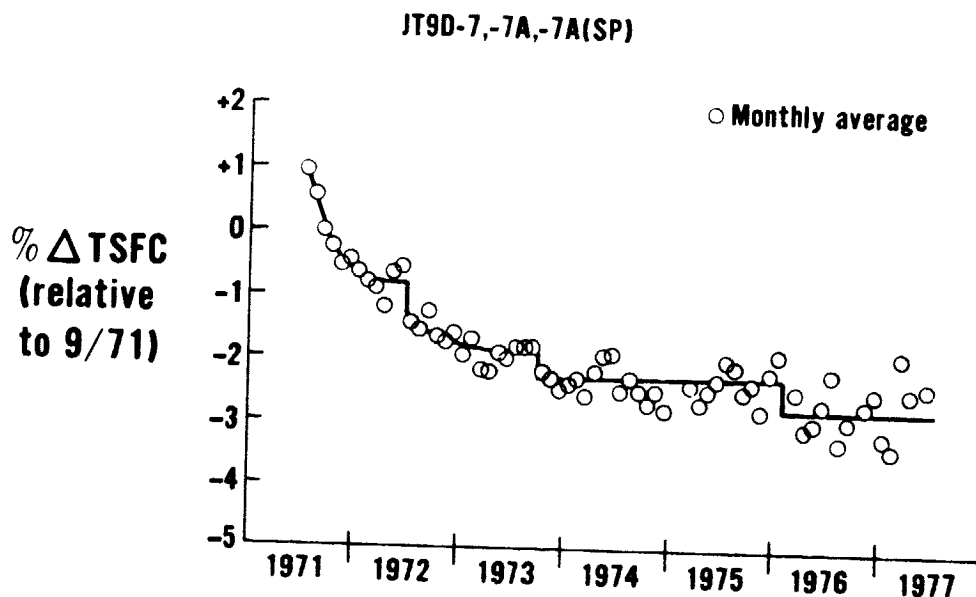


Figure 12 Production TSFC Levels at Take-off Thrust versus Time - The production TSFC trend shows the effect of various modifications incorporated in production engine take-off thrust TSFC levels at sea-level static conditions.

production test results to determine its performance loss. Most of the engine data recovered from historical files were involved in aircraft certification testing at either the Boeing Commercial Airplane Company or Douglas Aircraft Company and therefore represented engines with low numbers of hours per flight or cycle.

Figure 13 shows the percent change in thrust specific fuel consumption (TSFC) data from the engines plotted against flight hours. Also shown on the figure is the two-sigma deviation range. A slightly better correlation is obtained by plotting the deterioration against flight cycles and is shown in Figure 14. Typical airline delivery occurs at about 12 hours or after four cycles. It can be seen that a significant loss in performance occurs over the first few cycles or hours followed by a gradual, but continuing deterioration over approximately the first 250 flights.

Also shown in Figure 14 is data obtained from engine P-695743. This engine was specifically selected for removal from revenue service on a Pan Am 747 SP after 141 flights. More detailed information concerning the results of testing and analytical teardown of this short term

TABLE VIII
ADJUSTMENTS TO PERFORMANCE DETERIORATION
LEVELS BY AIRLINE OPERATOR

<u>Operator</u>	<u>Engine Model</u>	<u>Engine Hours</u>	<u>Baseline Change in TSFC</u>
A	D-7	16000	-0.2
B	D-3A	16000	0
B	D-7ACN	16000	-0.3
C	D-7/7ACN	16000	0.8
D	D-3A	16000	0
E	D-3A	9000	0

Note: The adjustments for baseline shifts due to modifications and engine conversions are shown for the engine hour time frame indicated.

engine are reported in NASA CR-135431 (Reference 1). It should be noted that the level of deterioration measured in engine P-695743 is typical of that for the other engines for which data are shown in Figure 14.

To determine the contribution of the individual modules to short-term performance deterioration, an analysis was conducted on the "average" of the fifteen JT9D-7A/SP engines for which data is shown in Figures 13 and 14. This "average" engine had accumulated 174 hours of operation and 149 cycles. The results of this analysis are shown in Table IX. It should be noted that the estimated contribution of the individual components to the overall performance losses may be somewhat inaccurate because of the lack of detailed instrumentation for a more complete analysis. However, the instrumentation is adequate to determine the breakdown between the high- and low-pressure spool performance losses with reasonable accuracy. As shown, this analysis indicates that the low-pressure spool contributes 55 percent to the overall engine deterioration while the high-pressure spool contributes 45 percent.

On the basis of the above data and analysis, the average short-term performance deterioration is 1 percent in TSFC on the first flight, followed by additional deterioration up to approximately 1.5 percent by the 200th flight. It is important to remember, however, that individual engines may show higher or lower losses. The cause for the differences

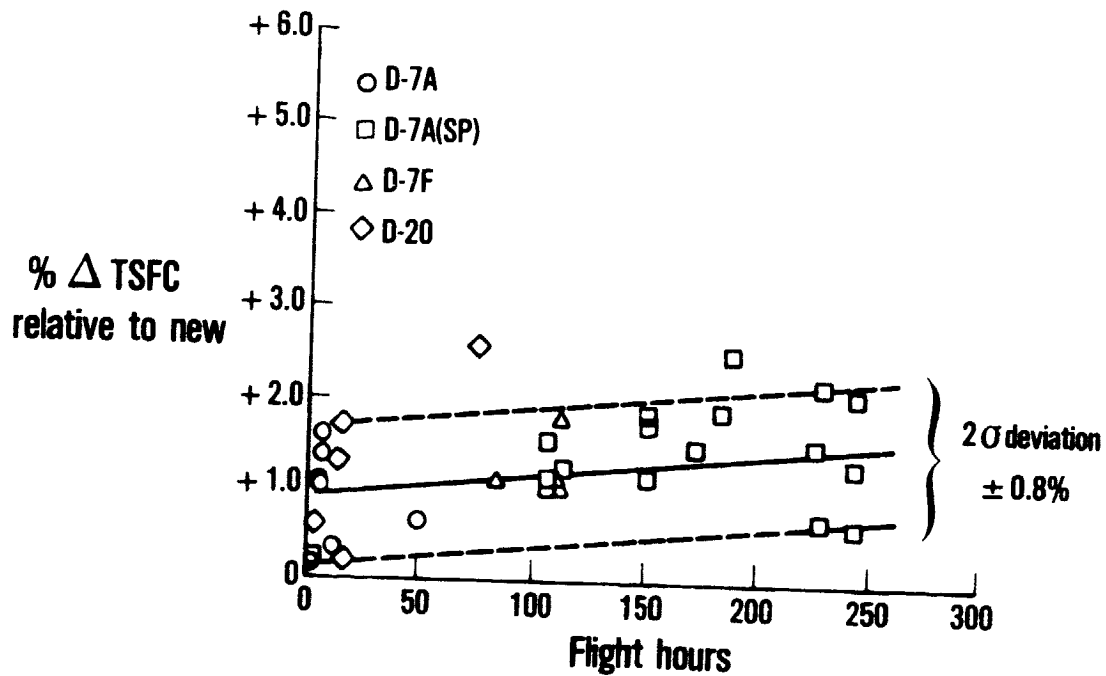


Figure 13 Short-Term TSFC Deterioration Trends as a Function of Flight Time - A significant loss in performance occurs very early followed by a more gradual, but continuing deterioration.

among engines cannot be determined at this time from the available historical data. Overall, the early loss in performance is believed to be caused by clearance increases associated with structural loading changes such as occur during take off rotation, flight maneuvers, and landing and thrust reversal. Engine power transients during these flight events may also contribute to rotor/case interferences that produce increases in clearances.

4.2.3 Long-Term Performance Deterioration

Much more historical data were available for evaluating long-term deterioration than short term. These long-term data consisted of engine condition monitoring data taken during cruise flight conditions and engine prerepair and postrepair test stand data.

The historical flight performance data collected was found to be unsatisfactory for analyzing long-term performance deterioration. The

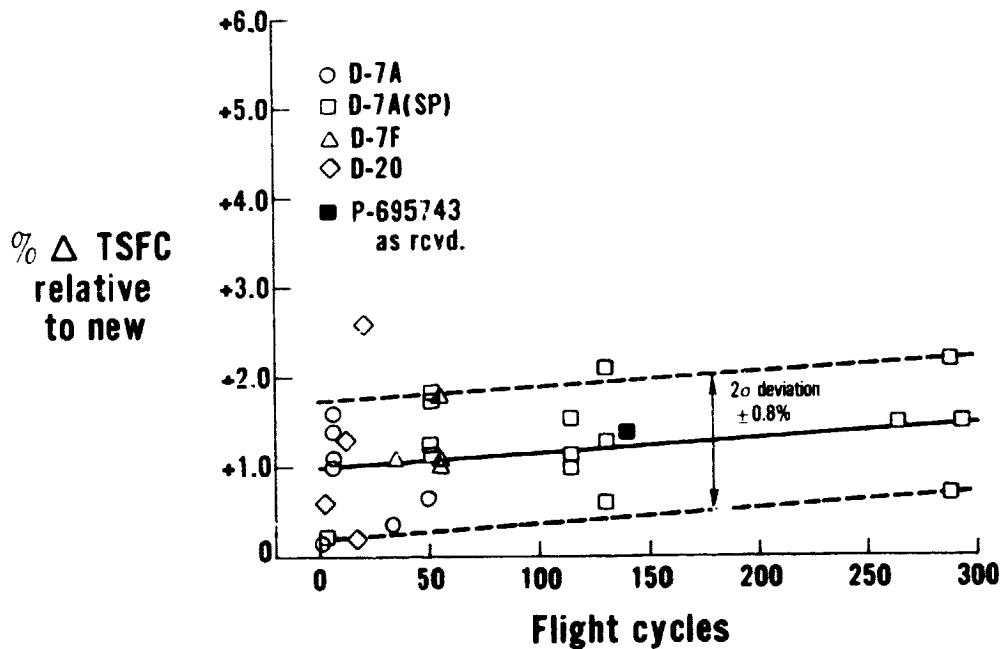


Figure 14 Short-Term TSFC Deterioration Trends as a Function of Flight Cycles - Short-term performance deterioration correlates better with flight cycles than flight time, indicating that this type of deterioration is probably related to structural loading.

engine parameters recorded for engine condition monitoring are not of sufficient number to permit analysis of module deterioration. Further, the absence of thrust as a measured parameter requires an assumption to be made concerning thrust changes, if any, to analyze changes in thrust specific fuel consumption from fuel flow trends. The individual engine data obtained tended to show changes in fuel flow with time which were not always consistent with expected deterioration trends, suggesting that either instrumentation problems or variations in bleed flow were influencing data quality. The quality of the individual engine data was therefore limited in its usefulness. The average-engine airline fleet trends were more consistent and a summary of these data on an airline-by-airline fleet basis is presented in the following section.

It should be noted that the actual in-flight fleet average engine performance level would be expected to be between the levels of prerepair and postrepair performance, since the engines in use can be presumed to be somewhere between the maximum performance obtained

TABLE IX
MODULE CONTRIBUTION TO SHORT-TERM DETERIORATION

	<u>Efficiency Change (%)</u>	<u>Flow Capacity Change (%)</u>	<u>TSFC Change (%)</u>
Fan	-0.25	-0.25	+0.15
Low-Pressure Compressor	-0.5	-0.5	+0.15
High-Pressure Compressor	-0.5	-1.25	+0.3
High-Pressure Turbine	-0.5	+0.25	+0.35
Low-Pressure Turbine	-0.5	0.0	<u>+0.5</u>
	Total		+1.45
	Low-Pressure Spool		+0.8
	High-Pressure Spool		+0.65

immediately following repair and the lower performance of an engine just prior to repair.

Test stand data, therefore, provided the primary source for long-term performance deterioration analysis. The bulk of these data were obtained from postrepair engine testing. While prerepair testing is not usually conducted, at least a limited amount of prerepair test data were available for all but one airline. The results of the analysis of these test-stand data are presented following the discussion, below, of the flight performance data.

Flight Performance Data

Fleet deterioration trends for the participating airlines are shown on Figure 15, Figure 16, and Figure 17. The overall deterioration for each airline is tabulated in Table X. Summaries of the operational data are presented in Appendix A.

The large differences in the experiences of the operators clearly illustrate the difficulty in using such data to generalize long-term performance deterioration trends. The data really serve only to indicate average fuel flow changes versus time from operator to operator.

JT9D-3A/-7/-7CN (747-100)

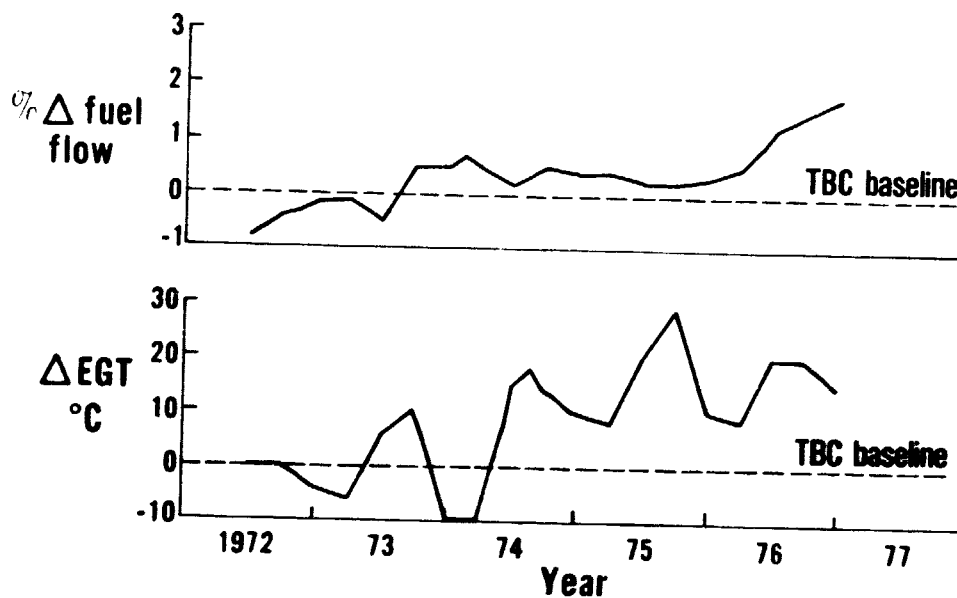


Figure 15 Fleet Deterioration for Pan American World Airways - Pan American engines exhibited gradual, continuing deterioration in fuel consumption with relatively large variations in exhaust gas temperature.

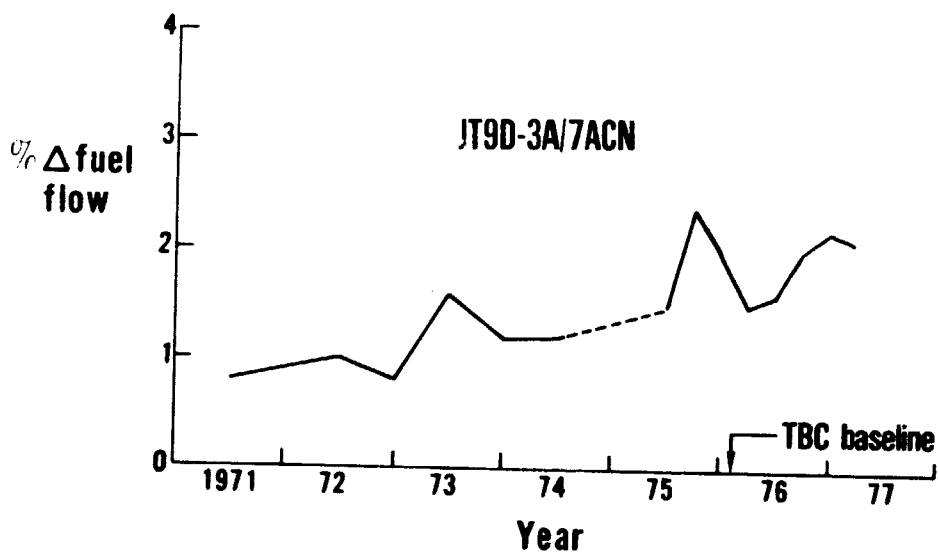


Figure 16 Fleet Deterioration for Trans World Airlines - Trans World Airlines experienced substantial variations in fuel consumption with a level higher than that of Pan American but a deterioration rate that was slower.

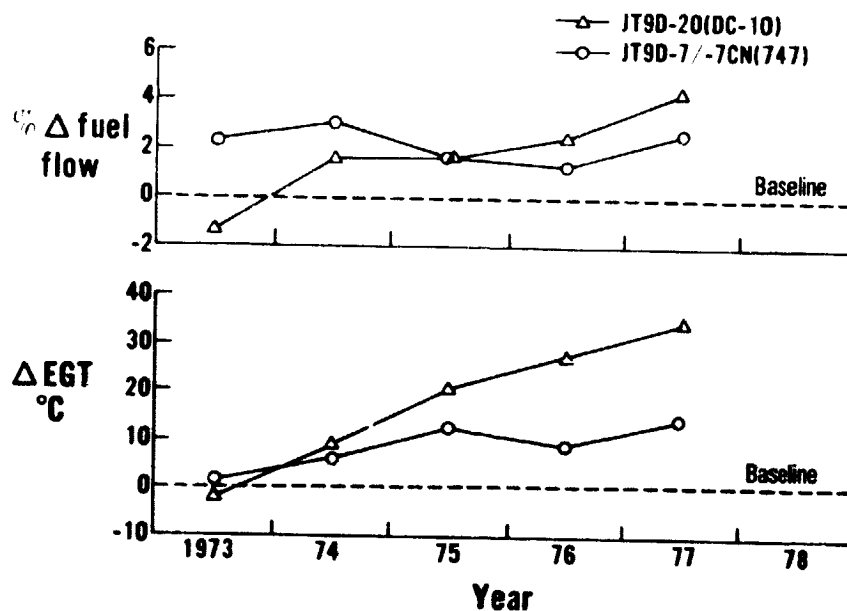


Figure 17 Fleet Deterioration for Northwest Airlines - The JT9D-2 trends are referenced to the Douglas DC-10 base line while the JT9D-7/7CN trends are referenced to the Boeing 747 base line.

Data for individual engines are potentially far more useful, and data for one such engine is shown in Figure 18. These data illustrate on-the-wing deterioration trends and performance improvements achieved by individual shop visits. However, few engines will reflect as obvious a trend as shown in Figure 18. Further, in-flight data acquisition is the least accurate means of evaluating engine performance. It is subject to instrument inaccuracies, gage reading inaccuracies, parameter drift during data acquisition, human error, variations in flight conditions, infrequent gage calibration, etc.

Overall, the in-flight historical data collected were not sufficient to identify and correlate factors that cause some engines to deteriorate slowly while others deteriorate rapidly. The time lapse between the present and the historical 1973-to-1976 data has lost an accurate definition of shop activity for each build of each engine.

TABLE X
AIRLINE DETERIORATION EXPERIENCE

Airline	Starting Level Relative to Baseline	Final Level Relative to Baseline	Change Relative to Start of Trend	Absolute Change From Baseline
Pan American				
Δ Fuel Flow (%)	-0.8	+1.8	+2.6	+1.8
Δ EGT (°C)	0	0	+20	+18
Trans World				
Δ Fuel Flow (%)	+0.8	+2.2	+1.4	+2.2
Δ EGT (°C)			Not Available	
Northwest				
JT9D-7				
Δ Fuel Flow (%)	+2.3	+2.6	+0.3	+2.6
Δ EGT (°C)	+2	+14	+12	+14
JT9D-20				
Δ Fuel Flow (%)	-1.4	+4.3	+5.7	+4.3
Δ EGT (°C)	-2	+34	+36	+34

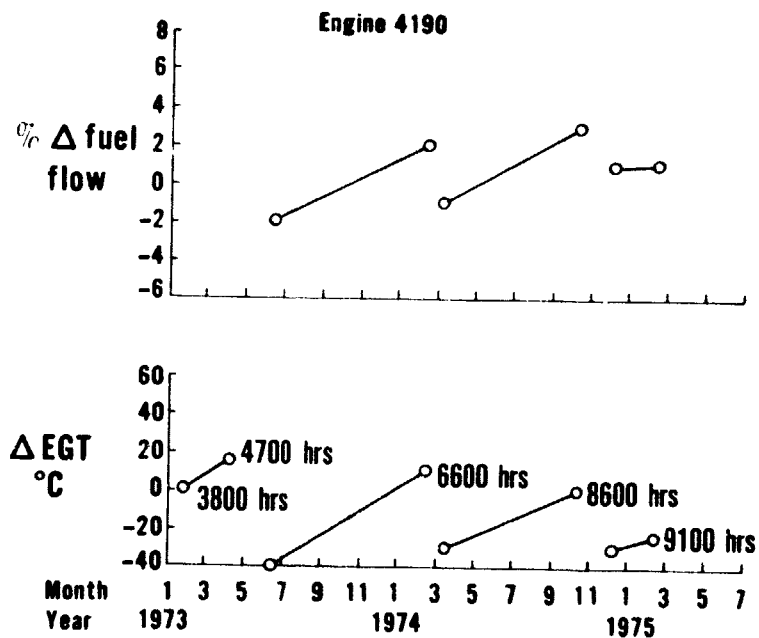


Figure 18 Cruise Engine Condition Monitoring Performance for Engine S/N 4190 - This engine demonstrated classical performance characteristics with a series of deterioration and recovery steps.

Test Stand Data

Prerepair Engine Performance

Prerepair engine performance deterioration in terms of fuel consumption and exhaust gas temperature is presented as a function of flight cycles in Figure 19 and Figure 20. The data are shown relative to a new production engine, and the airline operators and engine models are indicated. Adjustments have been made to the data for incorporation of Service Bulletin changes and, in some cases, for exhaust gas temperature errors due to temperature profile changes. With these adjustments, Figures 19 and 20 indicate similar performance deterioration trends for the JT9D-3A, JT9D-7, and JT9D-7A series of engines. The data are presented as a function of flight cycles rather than flight hours because many of the performance deterioration mechanisms correlated better with the number of flights rather than number of flight hours..

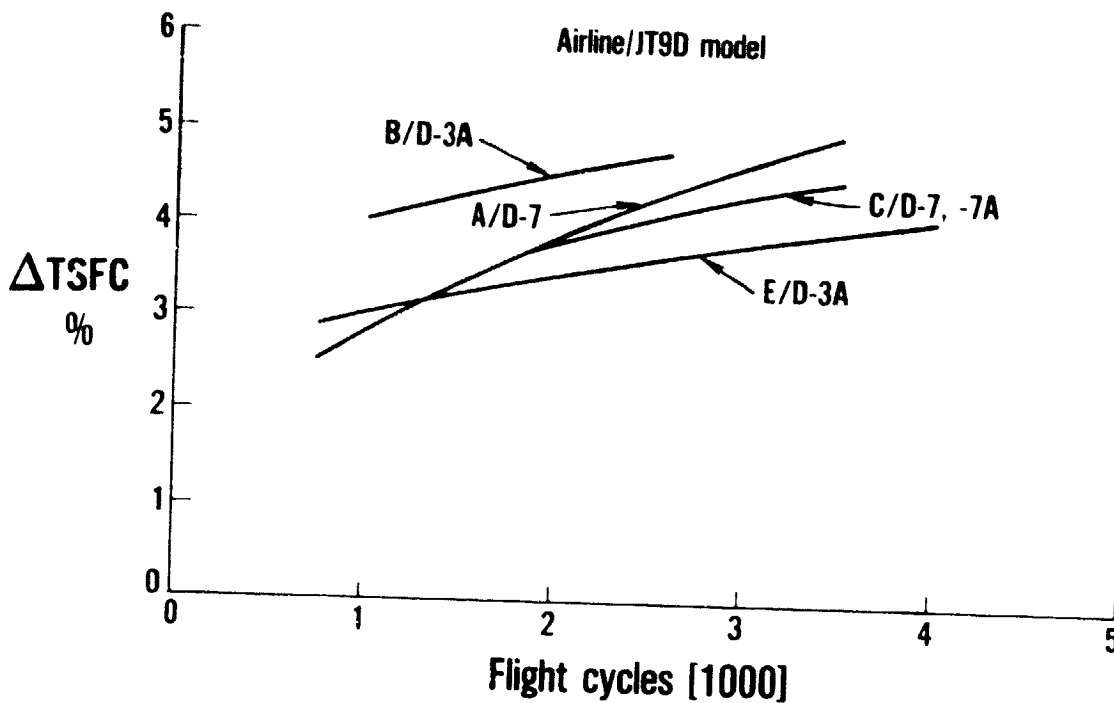


Figure 19 Prerepair TSFC Performance Deterioration at Take-Off Thrust for Individual Airline Engines Relative to New Engine Performance Levels - The data indicate significant variations among airline operators.

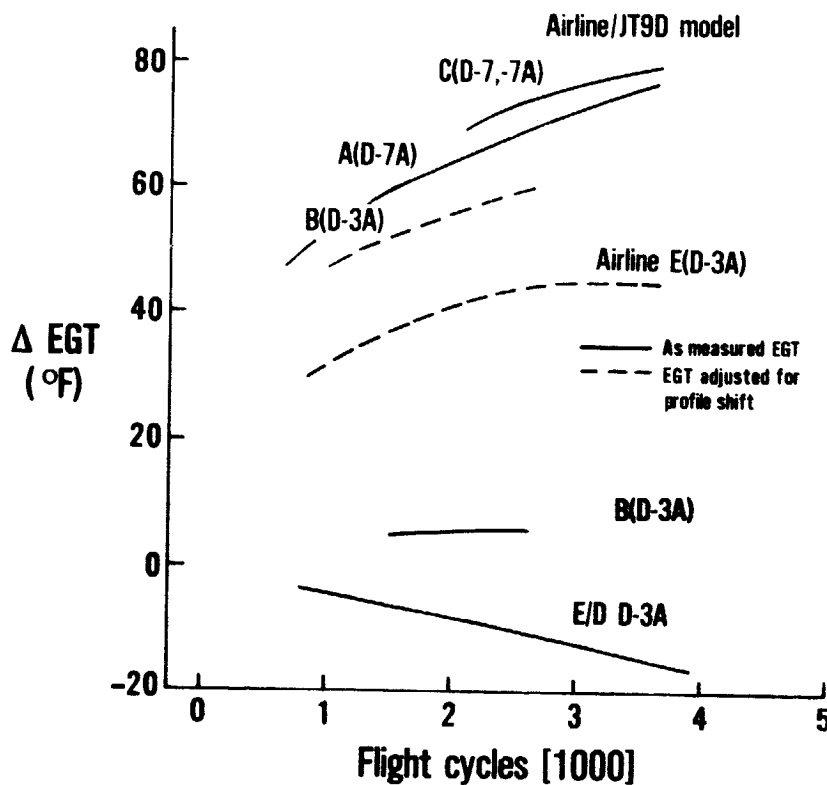


Figure 20 Prerepair EGT Performance Deterioration at Take-Off Thrust for Individual Airline Engines Relative to New Engine Performance Levels - The EGT data also shows large variations among airline operators.

As shown in the figures, the curves indicate significant airline operator-to-operator differences in deterioration trends. For example, at 3500 engine flight cycles, the TSFC changes range from +3.9 to +4.9 percent and the exhaust gas temperature changes range from approximately 45°F to 80°F.

The individual airline data for each engine model were combined to develop "average" JT9D prerepair performance deterioration trends. These trends are shown in Figure 21 and Figure 22. As shown, the average increase in thrust specific fuel consumption ranges from 3.2 percent at 1000 cycles to 4.4 percent at 3500 cycles while the average increase in exhaust gas temperature ranges from 43°F at 1000 cycles to 63°F at 3500 cycles.

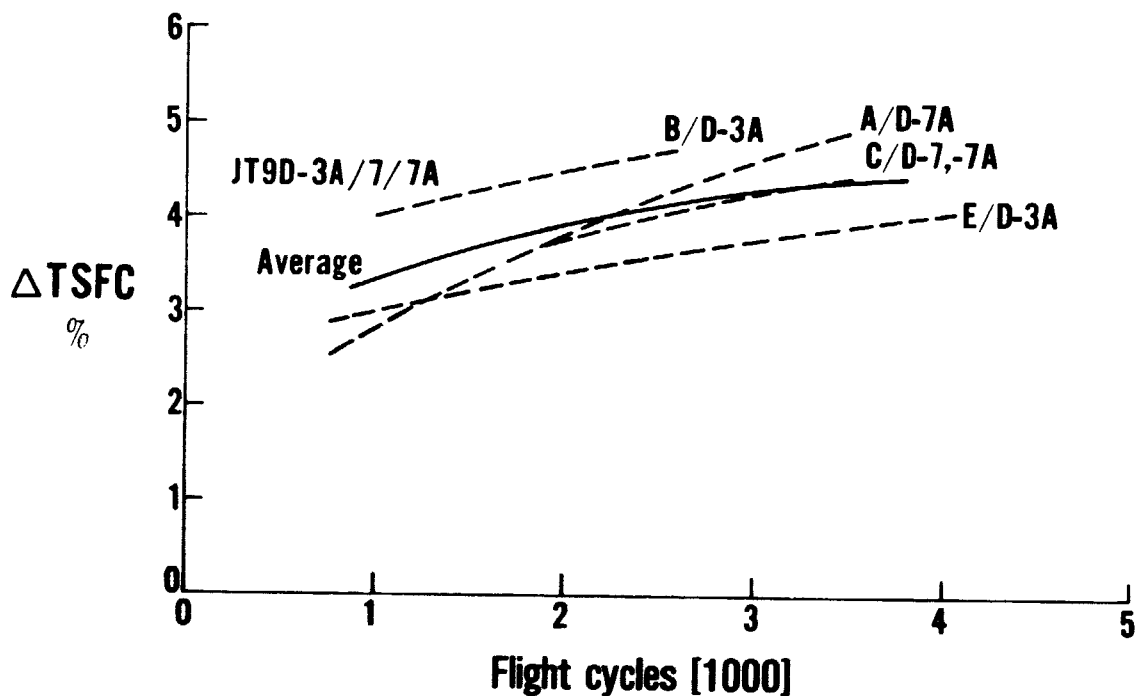


Figure 21 Average Fleet Prerepair TSFC Performance Deterioration at Take-Off Thrust Relative to New Engine Performance Levels - Average engine TSFC deterioration ranges from 3.2 to 4.4 percent between 1000 and 3500 flight cycles.

These data indicate the magnitude of deterioration experienced by average high-time JT9D engines. In applying these average trend curves, it should be noted that significant variations were observed from engine to engine. The average one-sigma distribution for the change in thrust specific fuel consumption is +1.1 percent.

Postrepair Engine Performance

Figure 23 and Figure 24 present postrepair TSFC and EGT changes relative to a new production engine base line for all five airline operators. Again, the data are presented as functions of flight cycles rather than flight hours because of the better correlation developed for many performance deterioration mechanisms with flight cycles. The most significant feature of these curves is the extremely wide variation existing from operator to operator. At 3500 engine cycles, the TSFC changes range from +2.8 to +4.2 percent. Similarly, at 3500 cycles, the change in EGT ranges from 32°F to 75°F. These variations appear to be related to variations in specific engine maintenance and repair practices.

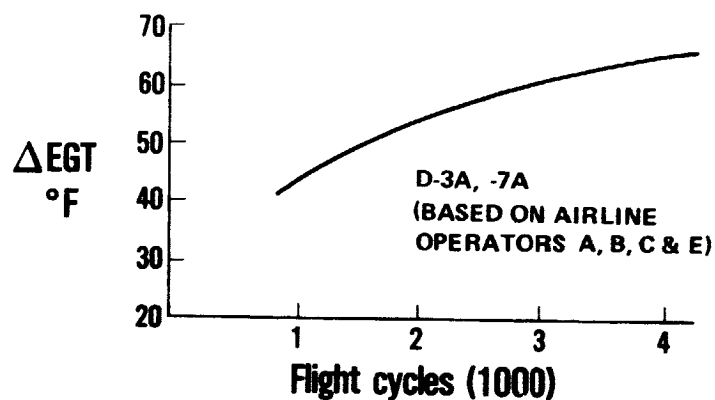


Figure 22 Average Fleet Prerepair EGT Performance Deterioration at Take-Off Thrust Relative to New Engine Performance Levels - Temperature increases up to 63°F are experienced by high-time JT9D engines.

It should be noted that data from Airline B indicates an improvement in TSFC with time, contrary to the trend shown for the other operators. However, this apparent anomaly was traced to Airline B's engine maintenance program which included model conversion and extensive compressor refurbishment for many of the higher time engines, which was sufficient to provide an improvement in Airline B's fleet performance.

As with the prerepair data, the postrepair data for the individual airlines for each engine model were combined to develop "average" JT9D postrepair performance deterioration trends. These trends are shown in Figures 25 and 26. Similar to the prerepair data for thrust specific fuel consumption, the average one-sigma distribution for the change in postrepair TSFC is ± 1.5 percent indicating significant engine-to-engine variation; however, on an average basis, the curves represent the postrepair performance deterioration trend for high-time engines.

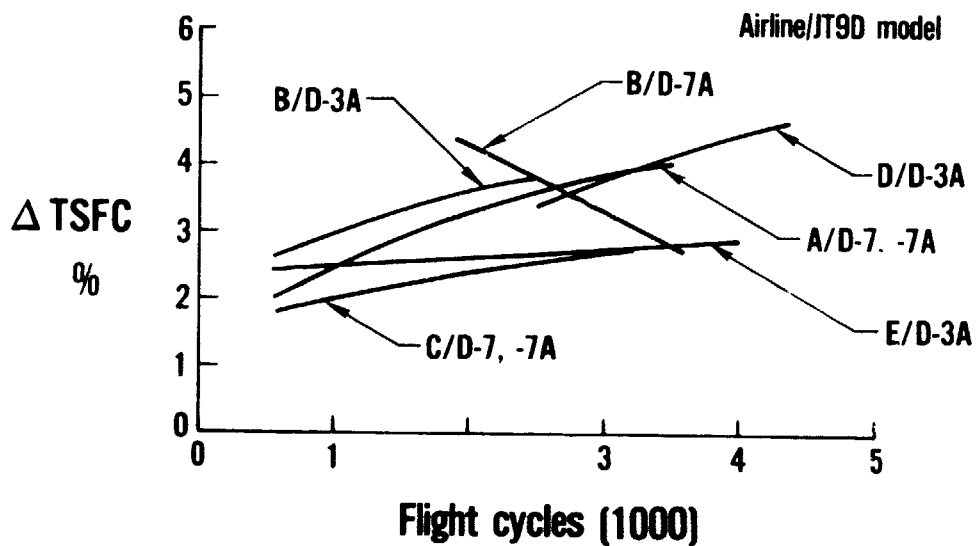


Figure 23 Postrepair TSFC Performance Deterioration at Take-Off Thrust for Individual Airline Engines Relative to New Engine Performance Levels - Similar to the prerepair data, the postrepair data indicate significant variations among airline operators, with one operator actually achieving an improvement in performance as a result of an extensive refurbishment program.

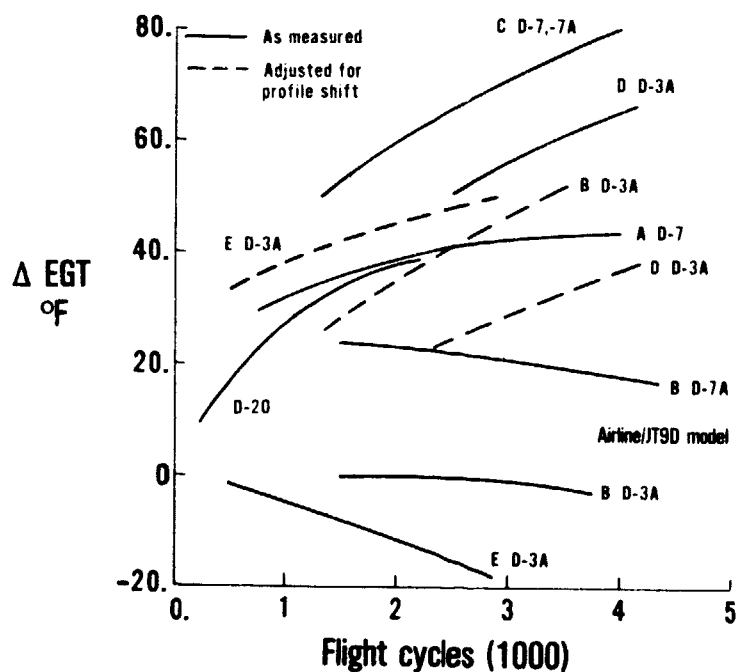


Figure 24 Postrepair EGT Performance Deterioration at Take-Off Thrust for Individual Airline Engines Relative to New Engine Performance Levels - Similar to the prerepair data, the postrepair data indicate significant variations among airline operators.

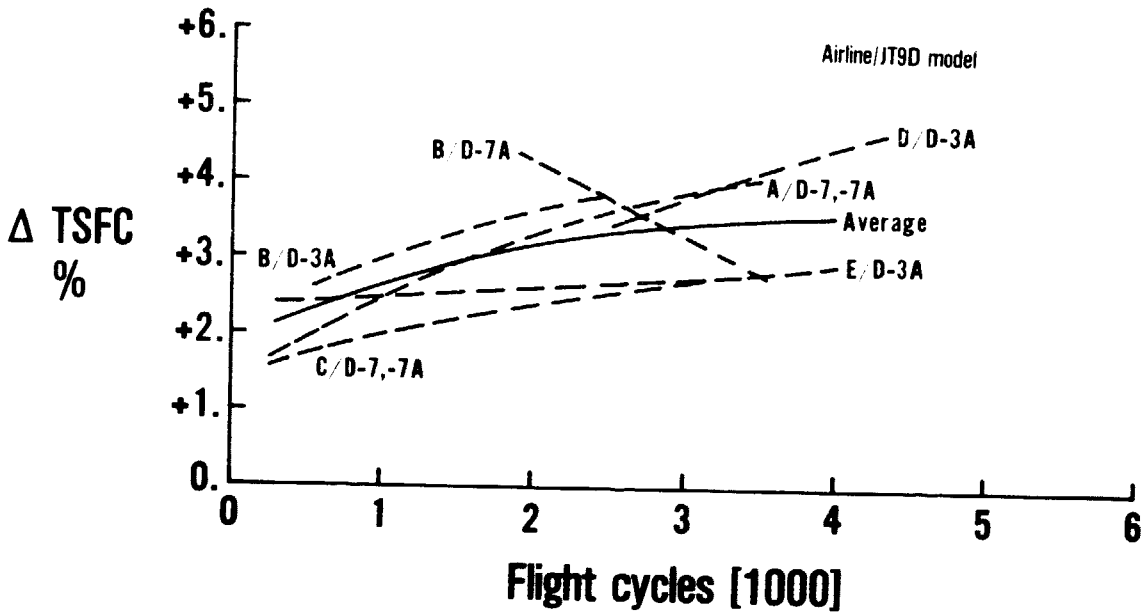


Figure 25 Average Fleet Postrepair TSFC Performance Deterioration at Take-Off Thrust Relative to New Engine Performance Levels - Average engine TSFC deterioration following repair ranges from 2.1 to 3.6 percent.

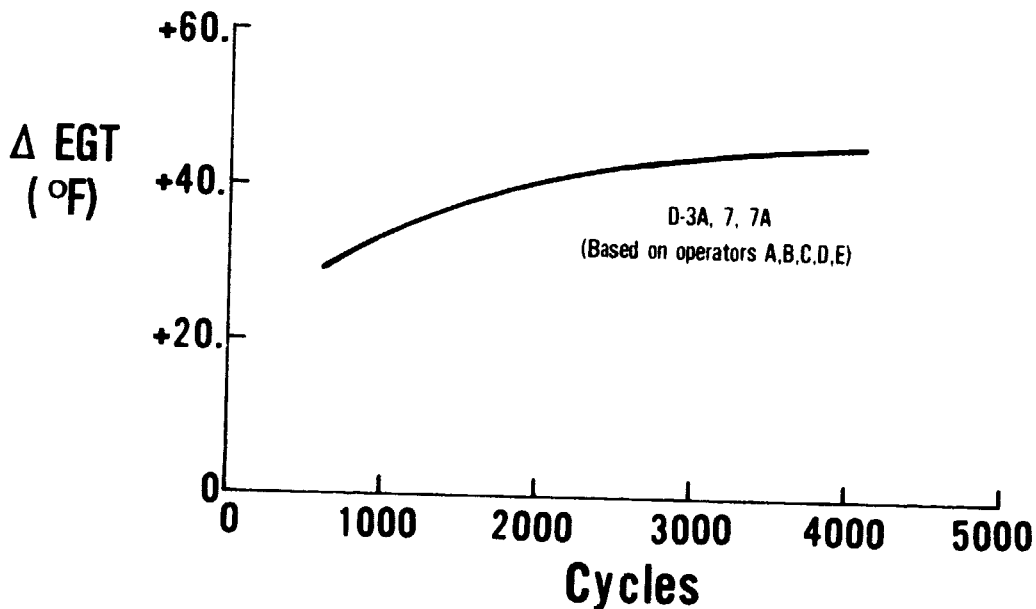


Figure 26 Average Fleet Postrepair EGT Performance Deterioration at Take-Off Thrust Relative to New Engine Performance Levels - Average temperature increases up to 40°F are experienced by high-time JT9D engines following repair.

Postrepair Data Relative to Prerepair Data

Study of the prerepair and postrepair data (Table XI) shows the engine performance recovery realized by repair. These data indicate an average recovery of 1 percent in TSFC with an average EGT reduction of 23°F.

TABLE XI
POSTREPAIR OVERALL PERFORMANCE DATA
RELATIVE TO PREPREPAIR PERFORMANCE

	Airline Operator				Average
	A	B	C	E	
JT9D Model	D-7, -7(CN)	D-3A	D-7A(CN)	D-3A	
Flight Hours	16000	12000	16000	9000	
Average Flight Cycles	4700	2140	3800	3200	
Engine Pressure Ratio	1.454	1.422	1.454	1.422	
Change in Performance					
Low-Pressure Rotor Speed, N1, (%)	-0.2	0	0	0.3	
High-Pressure Rotor Speed, N2, (%)	0	0	0	0.1	
Low-Pressure Compressor Exit Temperature (°F)	+7	---	---	---	
High-Pressure Turbine Exit Temperature, Tt6, (°F)					
As Measured	-35	-64	-9.0	-40	
Adjusted for Profile (°F)	-23	-38	9.0	-40	-23
Low-Pressure Compressor Pressure Ratio, Pt3/Pt2, (%)	-0.7	-0.7	0.4	-0.3	
Turbine Expansion Ratio, Ps4/Pt7, (%)	0.8	2.1	1.7	1.2	
TSFC at Constant Thrust (%)	-1.1	-0.8	-1.2	-0.9	-1.0

Table XII shows the performance recovery obtained during repair on an engine module basis. These results indicate that the major portion of the recovery resulted from an increase in the high-pressure turbine efficiency, as was expected, since this area receives the major portion of the repair effort.

Cold Section Refurbishment

During the historical time period covered in these studies, several operators experienced significant increases in engine problems associated with engine stall. As a consequence, a number of operators began a program to refurbish the cold section of the engine. The cold section refurbishment program included cleaning the vanes and blades and replacing those with chord lengths that were out of recommended limits along with restoration of tip clearances to new engine levels. In addition, compressor modifications were incorporated to improve basic performance. These modifications included a restagger of the stage 7 and 8 vanes and a change to the variable vane control schedule.

TABLE XII
 POSTREPAIR MODULE PERFORMANCE DATA RELATIVE
 TO PREPAIR PERFORMANCE

	Airline Operator			
	A	B	C	E
JT9D Model	D-7, -7(CN)	D-3A	D-7A(CN)	D-3A
Engine Hours	16000	12000	16000	9000
Change in:				
Fan				
Efficiency (Points)	0	0.1	0.6	-0.3
Flow Capacity (%)	0	0.2	0.8	-0.4
Low-Pressure Compressor				
Efficiency (Points)	0.4	0.5	0.6	0.2
Flow Capacity (%)	0.6	0.8	0.9	0.3
High-Pressure Compressor				
Efficiency (Points)	-0.2	---	---	---
Flow Capacity (%)	0.9	1.5	0	0.8
High-Pressure Turbine				
Efficiency (Points)	1.3	1.2*	1.1*	1.0*
Effective Inlet Area, A5, (%)	-0.3	-0.3	-0.3	-0.3
Low-Pressure Turbine				
Efficiency (Points)	0	0.1	0.9	0.2
Effective Inlet Area, A6, (%)	0	0.1	-0.6	0.1

* High-pressure spool efficiency split not performed where high-pressure compressor temperature not measured. Number provided represents total high-pressure rotor efficiency change.

As a result, data became available relating the effects of cold section refurbishment on engine performance. These data are presented in Figure 27 and show that the combination of compressor modifications, cold section refurbishment, and "normal" maintenance in the hot section provides a 2.1 percent recovery in TSFC. Based on back-to-back tests, the compressor modifications contribute a 0.8 percent improvement, and, therefore, the compressor refurbishment is responsible for a recovery of approximately 1.3 percent.

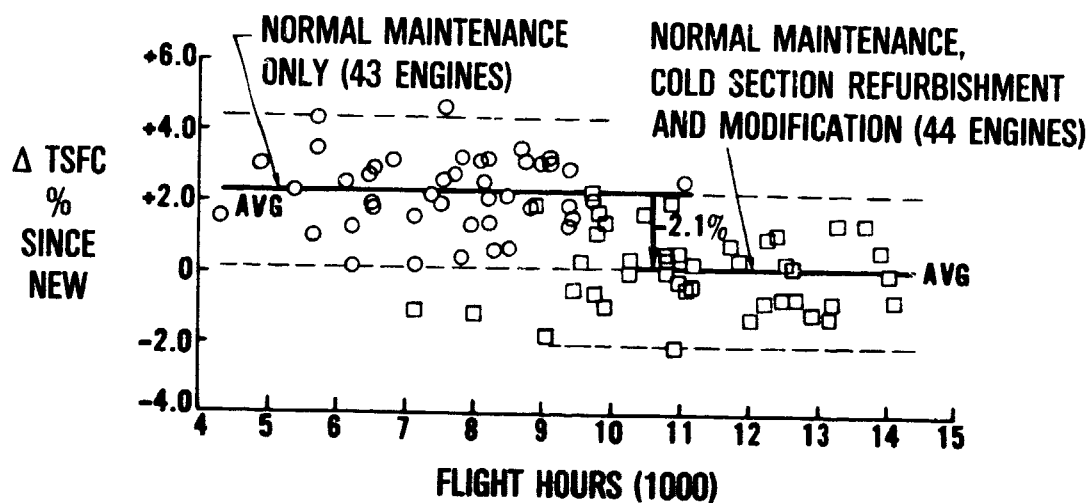


Figure 27 Effect of Cold-Section Modifications and Refurbishment on Engine Performance - A 2.1-percent recovery in TSFC was achieved, with 0.8 percent attributed to the modifications and 1.3 percent attributed to the refurbishment.

Additional analysis of these data covering postrepair performance recovery with and without compressor modification and refurbishment indicate that the performance recovery obtained from modification and refurbishment was equally divided between the fan/low-pressure compressor and the high-pressure compressor. These data are shown in Table XIII.

TABLE XIII
COLD SECTION REFURBISHMENT AND COMPRESSOR MODIFICATION RESULTS

	Percent Change in TSFC		Total
	Low-Pressure Rotor (Fan and Low-Pressure Compressor)	High-Pressure Rotor (High-Pressure Compressor)	
Overall Recovery	-1.0	-1.1	-2.1
Performance Improvement			
Fan	-0.4		-0.8
High-Pressure Compressor		-0.4	
Net Recovery for Refurbishment	-0.6	-0.7	-1.3

Since these initial cold-section refurbishment programs, more airline operators have refurbished the cold sections of their engine fleets. At this writing, the average of the results from all operators has been a 1.9 percent recovery in TSFC performance and an exhaust gas temperature reduction of 27°F.

Airline D provided considerable data on both engines with and without compressor refurbishment. The data are summarized in Figure 28 and indicate an average TSFC recovery of 2.2 percent.

The deterioration of cold section components is discussed in Section 4.4 of this report and provide a basis for understanding the kind of recoveries achieved through refurbishment. The fact that TSFC recovery levels ranging from 1.3 to 2.1 percent were obtained by the various operators provides an indication of the level of deterioration in the cold section modules that existed on engines before refurbishment.

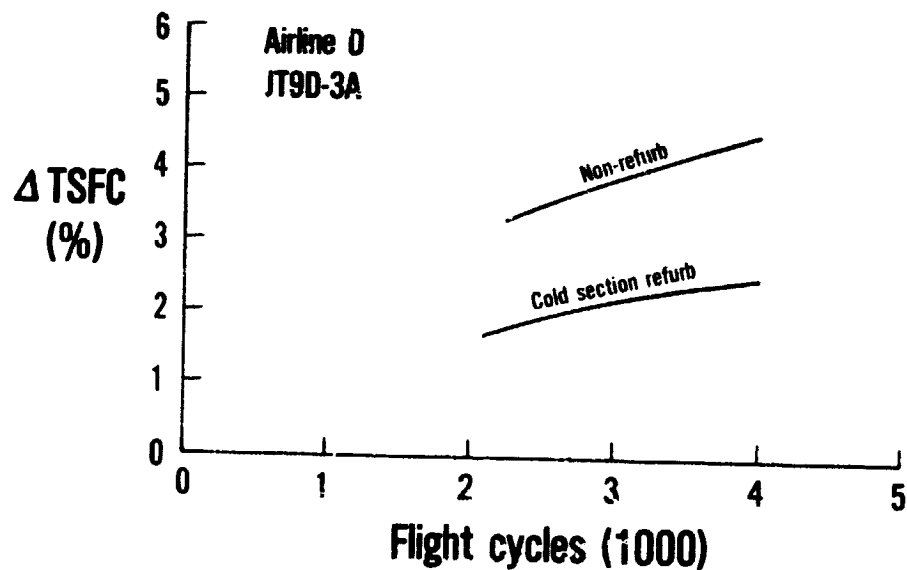


Figure 28 Effect of Cold-Section Refurbishment on TSFC - Airline D demonstrated a 2.2 percent recovery in TSFC through cold-section refurbishment. The changes in TSFC are all shown relative to new production engines performance levels.

These data demonstrate that airline maintenance practices play a significant role in determining an operator's deterioration level.

4.3 AIRLINE MAINTENANCE PRACTICE VARIATIONS

Differences in the maintenance practices among airline operators are a major cause for differences in the performance deterioration experience of each operator relative to the fleet average. Maintenance practices are reflected in (1) parts repair and replacement rates which determine the average performance age of parts in the average engine, and (2) rebuild standards which impact the condition of parts and modules with respect to limits on clearance, blends, and erosion.

4.3.1 Parts Repair and Replacement Rates

The relationship between average engine performance and the condition of the parts can generally be defined on the basis of the correlations developed to date in this program. Maintenance actions which restore the mechanical condition of parts such as seal replacement also recover performance and must be included when estimating the performance of seal parts. Similarly, the repair of airfoils which restore leading edge shape also recover performance loss due to bluntness (if the work is performed correctly) and must be accounted for in estimating the performance age of airfoils.

However, in estimating the average performance age of parts, it must be recognized that repair practices vary and any conclusions drawn from calculated average part performance age must be tempered by information on repair practices.

The results of the part age analysis for each of the airlines is provided in Appendix C. Briefly, these results showed that, of the three operators, Airline A generally exhibited the highest part age since performance recovery. Airline B consistently showed, since 1973, lower parts age since performance recovery than the other airlines studied. The age of parts for Airline C since performance recovery on most parts was between the values exhibited by Airlines A and B.

4.3.2 Rebuild Standards

Generally, the airlines' Overhaul and Repair (O&R) Manual show differences in rebuild standards from those recommended in the Pratt & Whitney Aircraft Overhaul Manual, and actual practices vary from both of these manuals. For cold-section maintenance, the differences between observed practices, the airline manuals, and the Pratt & Whitney Aircraft Overhaul Manual recommendations for Airlines A, B, and C are summarized in Table XIV. For the hot section, the differences between the airline manuals and the Pratt & Whitney Aircraft Overhaul Manual for these airlines are summarized in Table XV. These differences are presented in detail in Appendix D.

TABLE XIV

**SUMMARY OF DIFFERENCES IN COLD SECTION MAINTENANCE STANDARDS
COMPARISON OF PRACTICED AND WRITTEN AIRLINE REBUILD STANDARDS**

Module	Airline A			Airline B			Airline C		
	Practiced Airline Limits	Airline Manual Limits	Practiced Airline Limits	Airline Manual Limits	Practiced Airline Limits	Airline Manual Limits			
Fan	Inspected and blended to P&WA Manual limits. Repair by qualified vendors. Some LE bluntness seen. LE not being chamfered at this time due to manpower limitation.	Tip blending limits more liberal than P&WA. ASG rubstrip rub depth limits 0.055 tighter than P&WA but rub may occur anywhere on circumference. Blade tip clearance strip case opened 0.020. For 0.085 offset honeycomb, opened 0.020.	LE is supposed to be chamfered but some were found blunt. Pitting also seen on airfoil.	Blade blending limits generally tighter than P&WA Manual. Fan blade tip clearances for offset honeycomb opened 0.020.	Blades are being chamfered and LE is not blunt.	Blend to P&WA Manual limits. Allow 0.010 more rub on honeycomb rubstrip. Tip clearances set to P&WA limits.			
LPC	Airfoils blended per P&WA Manual except number allowed per stage is more limited. Ducts are regularly replaced at O/H. Tip clearances and blade length not checked. Some blade airfoil thinness seen. Chord dimension not checked.	Number of blended airfoils allowed per stage same as P&WA Manual. Limits on rubstrip rub depth and erosion recommended in lieu of P&WA recommendation of full replacement of rubstrip at disassembly. LPC tip clearances measured, but no RIO limits in manual.	Blended airfoils not more limited than manual. No obvious erosion.	Number of blended airfoils per stage same as P&WA but certain types of blends not counted. Limits on rubstrip rub depth and erosion recommended in lieu of P&WA recommendations of full replacement of rubstrip at total disassembly. LPC tip clearances same as P&WA.	Blended airfoils not more limited than manual. Ducts sometimes reused and tip clearance said to be in limits. No serious erosion.	Blade lengths measured. Tip clearances checked at assembly. No RIO limits given in manual.			
HPC	Airfoils blended per P&WA Manual but number limited to less than manual. Ducts and air seals replaced at overhaul. Blade airfoil tip wear limit allows 0.006 greater wear than P&WA manual but erosion limit is 0.020 tighter and limits Pad blades. Fixed vanes are replaced at 8-10K hours.	Number of blended airfoils allowed per stage same as P&WA Manual. Allowable duct wear 0.010 - 0.015 greater than P&WA Manual. Min. blade length 0.005 less than P&WA Manual. Erosion limits same as P&WA Manual. Tip clearances same as P&WA full restoration clearances.	Number of blends same as manual. Some evidence of excessive vane blending. Fixed vanes not replaced on a schedule. Blade airfoil length measured per P&WA manual. Blade erosion not measured but all blades are being replaced. Inner airseals usually	Number of blended airfoils per stage same as P&WA but certain types of blends not counted. 8th and 11th-15th duct abrasion limit 0.010-0.015 more liberal than P&WA manual. Tip clearances same as P&WA Manual. Tip clearances same as P&WA Manual.	Blade blend limits same as manual. Blade airfoil length limit allows wear 0.004" beyond manual. Ducts sometimes reused but tip clearances are said to be in limits. Blade chord is said to be checked but some erosion seen on front stages. Rear stage blades being replaced. 6th, 9th, and 10th stator vanes replaced if more than 1500 hours.	Blade blend limits same as P&WA Manual. Blade airfoil length same as P&WA limit. Tip clearances checked at assembly, but no RIO limits given. Generally, build standards for CN engines are looser than for non-CN engines.			

TABLE XV

SUMMARY OF DIFFERENCES IN
HOT SECTION REBUILD STANDARDS

AIRLINE A

High-Pressure Turbine

Decrease first-stage turbine blade tip clearance RIO limit from 0.095" to 0.080".

Low-Pressure Turbine

Increase third, fourth, fifth, and sixth blade knife edge maximum clearance by 0.020".

AIRLINE B

High-Pressure Turbine

Increase vertical offset grind by 0.005" on both first- and second-stage outer air seal and increase first-stage outer air-seal diameter by 0.010". Increase clearance on first-stage turbine inner air seal by 0.020".

AIRLINE C

High-Pressure Turbine

Trailing edge blend to first row of pedestals on first- and second-stage turbine blades limited to one per blade. First-stage blade maximum tip clearance increased by 0.006".

Low-Pressure Turbine

Third-stage blade knife edge minimum/maximum tip clearance increased by 0.003"/0.005" for honeycomb outer air seal.

Fourth-stage blade knife edge maximum tip clearance increased by 0.010".

Fourth-stage turbine inner air-seal RIO limit decreased by 0.040".

The differences in rebuild standards from the Pratt & Whitney Aircraft recommended standards have a potential influence on postrepair engine performance. Table XVI shows the impact of these differences on the "average" or nominal engine for each airline as well as the maximum influence for an engine operating at maximum (repair if over) clearances.

TABLE XVI
INFLUENCE OF REBUILD CLEARANCES ON TSFC

<u>Airline</u>	<u>Percent Change in TSFC Due to Tip Clearance Change</u>	
	<u>Nominal</u>	<u>RI0*</u>
A	+0.5	+2.7
B:		
Overhaul	+0.7	+3.3
Maintenance	+1.1	+4.1
C	+0.4	+3.3

*Repair if over

4.3.3 Part Repair Practices

Considerable variation in the aerodynamic quality of repaired parts was observed as a result of differences in repair practices. Typical examples of these practices are presented below.

Practices regarding fan blade leading edge rework and limitations on the number of blended fan blades in the fan rotor were significantly different. These variations in repair process and resulting airfoil quality affect fan performance.

Cleaning processes for compressor airfoils also varied. For example, grit blasting was used by one airline to remove surface dirt accumulation on airfoils. This approach could increase the surface roughness, producing performance losses and reducing the life of the parts.

Turbine airfoil repair practices were much more uniform. However, turbine blade tip wear varied considerably as a result of different rebuild clearance standards or other factors such as operating practices, case out-of-roundness, or combustor temperature profiles.

4.4 MODULE DETERIORATION

This section presents the results of the analysis conducted on module deterioration based on the inspection of engines at airlines facilities and the analysis of the condition of parts with various usage times were returned to Pratt & Whitney Aircraft for inspection.

The approach used allowed quantification of the damage mechanisms responsible for module performance deterioration and how the level of each type of damage changed with increased usage. Historical data and engineering experience were used in the analysis of the performance effects of each type of part damage on module performance.

The following sections deal with the results of the module performance analysis beginning with the fan and proceeding through the engine. Figure 29 shows a cross section of the JT9D engine and defines the location of each module of the engine.

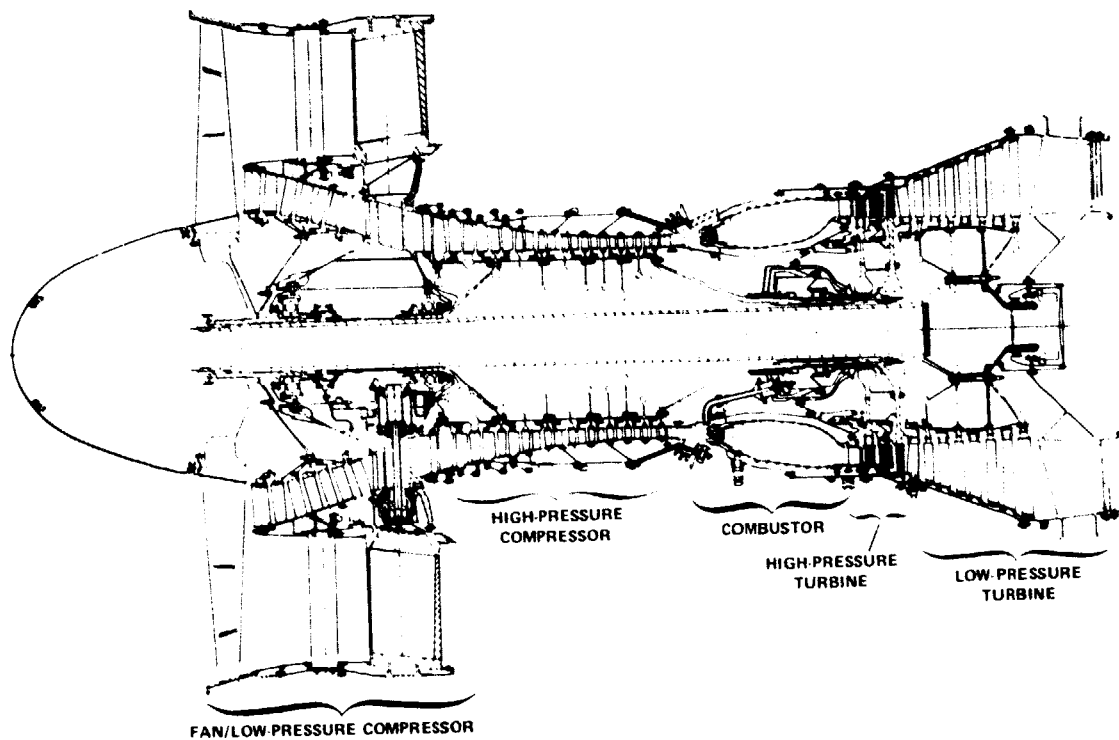


Figure 29 JT9D Engine Cross Section - The modules identified correspond to the breakdown used for module performance deterioration analysis.

As a final step in establishing a level of confidence in the analytical prediction of module deterioration levels as a function of usage, the analytically estimated module deterioration was compared with module performance deterioration data measured during back-to-back testing of service engines at Pratt & Whitney Aircraft.

4.4.1 Fan

Performance Loss Mechanisms

Fan performance deterioration is caused by increasing tip clearance, airfoil surface roughness, and airfoil leading edge contour changes (bluntness).

Engine testing has established the effect of fan tip clearance on performance, and the results are shown in Figure 30.

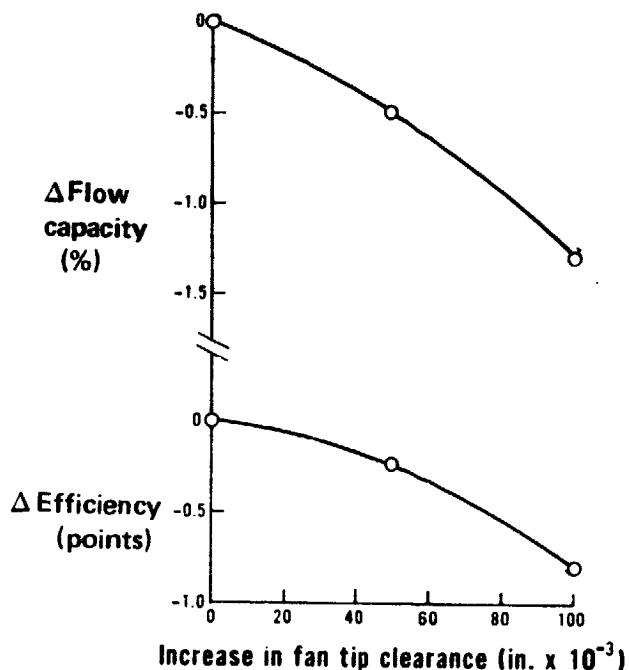


Figure 30 Fan Tip Clearance Effects - Engine test data show that increases in fan tip clearance result in reduced efficiency and reduced flow capacity.

Surface roughness caused by dirt accumulation and metal loss (pitting) also affects fan performance. The effect of surface roughness was evaluated by use of existing correlations of airfoil loss coefficient as a function of Reynolds number and roughness. These correlations indicate that a 10-percent increase in airfoil-roughness loss coefficient will result in a 1.0 point loss in fan efficiency.

Airfoil leading edge contour changes also influence fan efficiency and are tentatively estimated to be the major contributor to fan performance deterioration at high cyclic part age. Visual inspection of service fan blades has shown that the fan blade leading edge becomes eroded, blunt, and pitted with increasing usage. Quantitative analysis of this phenomenon from parts inspection has not been completed at this time because of difficulty in obtaining an adequate number of fan blades with known usage times. The problem has been that very few airlines maintain usage records on individual fan blades. Preliminary estimates of the losses caused by contour changes have been included, however, in the component loss versus usage curves. The estimates have been based on service fan back-to-back test results and by assigning the residual unaccounted for loss in fan performance to this damage mechanism.

Representative Performance Deterioration

Tip Clearance Changes - Tip clearances will increase as a result of blade length loss, blade rub strip trenching during engine transients and aircraft maneuvers, and rub strip erosion. Fan blade length loss, however, was judged to be insignificant based on visual inspection of the parts. Erosion does not occur in this area because the blade tip is thick and little centrifuging of dirt particles has occurred in the fan. In addition, visual inspection shows that blade length loss due to rubbing is negligible.

Rub strip trenching due to engine transients in combination with aircraft flight maneuvers is significant. Historical rub depth data for JT9D-20 engines on DC-10 aircraft, limited data from four JT9D-7F/747 certification flight-test engines, and a data band representing rub strip measurements on ten JT9D-7 engines from 747 aircraft are shown in Figure 31. Although there were no hour or cycle data available for the

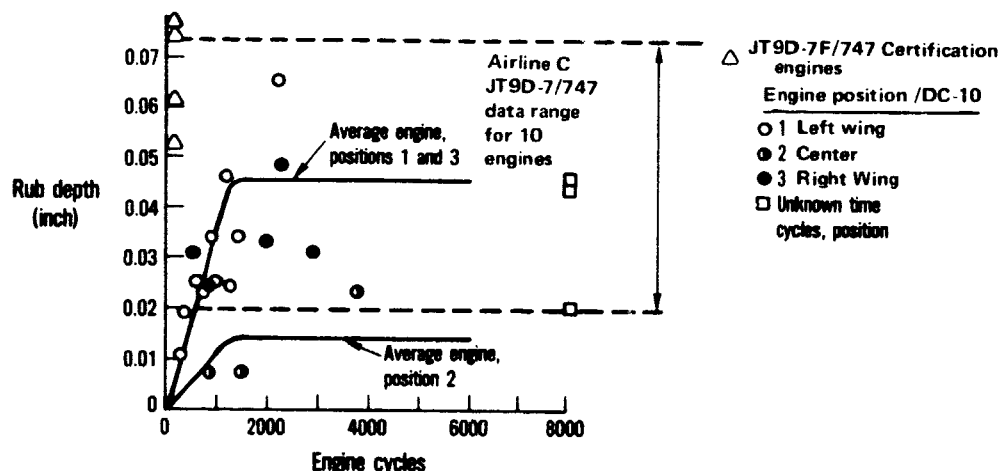


Figure 31 JT9D-7/7F/20 Fan Rub-Strip Rub Depth Growth - The trench is fully established within 1000 flight cycles.

JT9D-7 engines, the range of data was consistent with the JT9D-7F and JT9D-20 data shown. The DC-10 center engine enjoys an advantage because inlet cowl air loads are not imposed on the fan case as with the wing engines on both the DC-10 and 747 aircraft. However, engineering experience and analytical studies on the effects of flight loads on fan tip clearances (Reference 2) suggest that the trench is established early in the life of the engine and then tends to remain constant. Figure 32 shows the predicted fan clearance changes from the Reference 2 study. Comparison of the historical data and the predicted data shows good agreement for DC-10 and 747 wing engine positions.

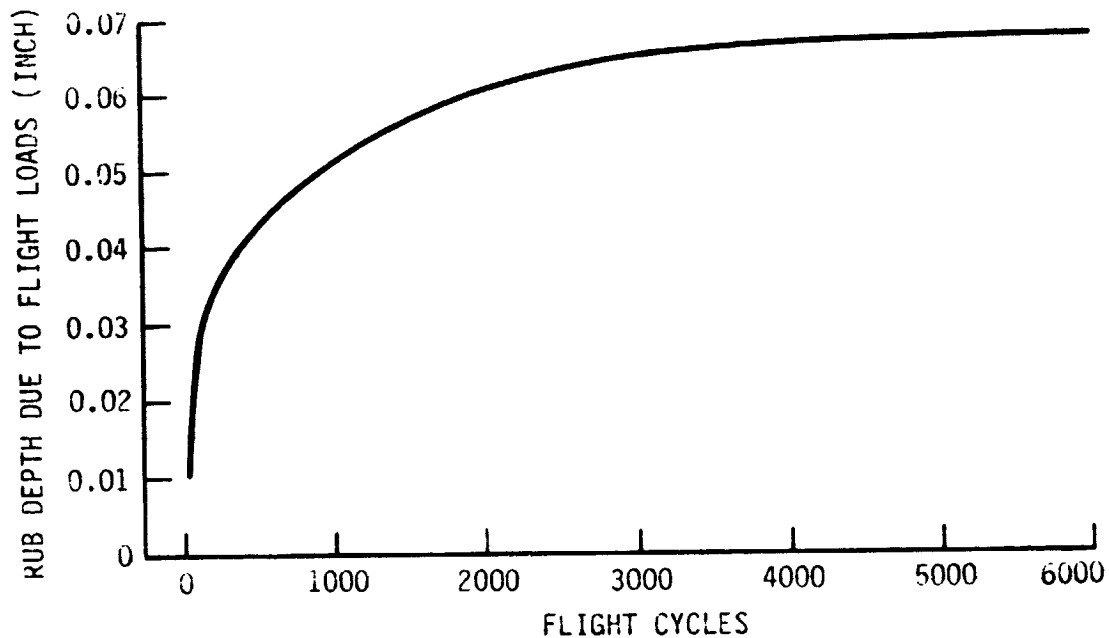


Figure 32 Predicted Fan Clearance Changes from Analytical Studies of the Effects of Flight Loads on Performance Deterioration - The clearance changes are predicted to occur most rapidly within the first 1000 flights.

Visual inspection of fan rub strips at the airline maintenance facilities showed that negligible erosion had occurred. Trench corners were sharp, and no erosion pitting was evident.

Airfoil Roughness - The surface roughness measured on five blades for which time was known is shown in Figure 33. The data at zero cycles is the roughness level of production fan blades. The fairing between production levels of roughness and 1000 cycles and the constant level of roughness beyond 1000 cycles is based on observations of many parts and engineering experience. These observations suggest that roughness builds up rapidly and then remains constant.

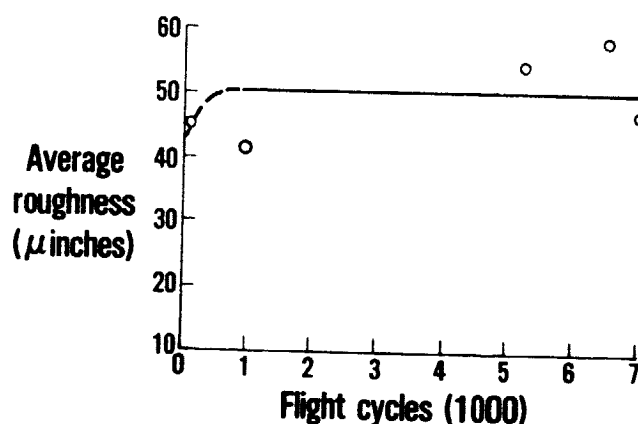


Figure 33 Surface Roughness Measured on Five JT9D Fan Blades - Engineering experience suggests that surface roughness builds up within about 1000 cycles and then remains constant.

Overall Deterioration - Based on the hardware conditions described above and engineering experience, the effects of fan blade tip clearance and surface roughness on fan efficiency and flow capacity were predicted. The results are illustrated in Figures 34 and 35 for clearance and surface roughness, respectively. The effect of surface roughness on fan flow capacity could not be established and consequently is not shown. As expected, the fan performance deterioration trends with flight cycles followed the rub strip depth and surface roughness trends previously shown, that is, a rapid loss during the early flight cycles followed by no further deterioration due to tip clearance effects or surface roughness.

These predicted results along with the results of several back-to-back fan tests previously conducted by Pratt & Whitney Aircraft are shown on Figure 36. As can be readily observed, the test data exhibits greater losses than the predicted results. This is particularly true as the number of flight cycles is increased. The difference between the predicted data and the test data is believed to be associated with leading-edge contour changes brought about by erosion and the repairs to local foreign object damage. These data were used to establish overall fan performance loss levels versus usage.

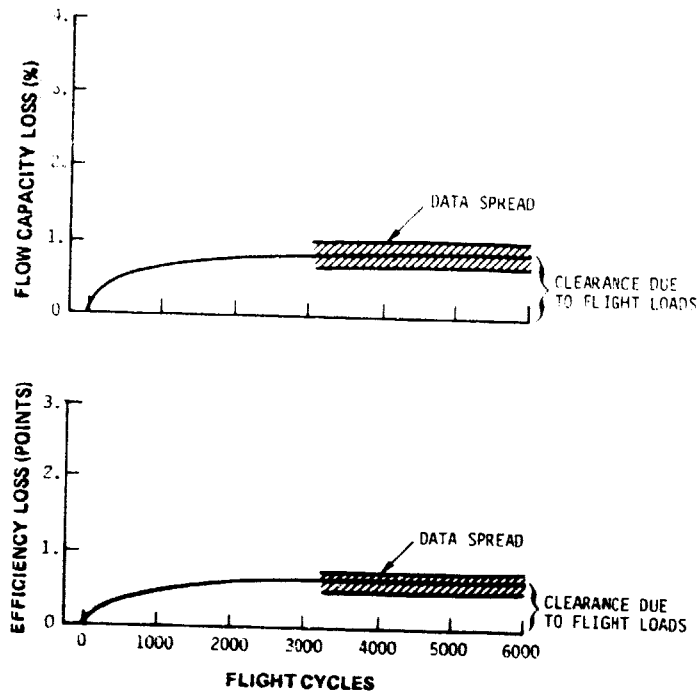


Figure 34 Effect of Clearance Changes on Fan Flow Capacity and Efficiency - Changes in flow capacity and efficiency were predicted based on the observed condition of service parts.

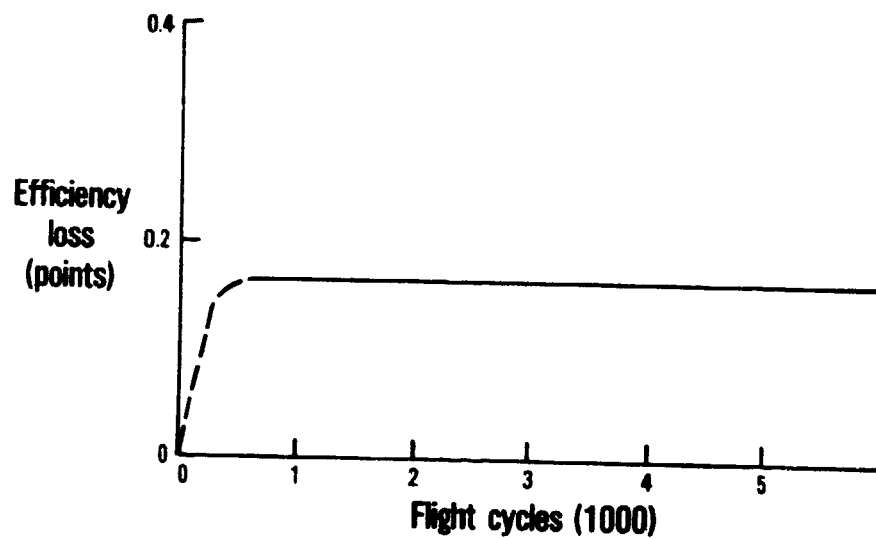


Figure 35 Effect of Surface Roughness on Fan Efficiency - Predictions based on observed parts condition indicate that surface roughness produces a small change in fan efficiency.

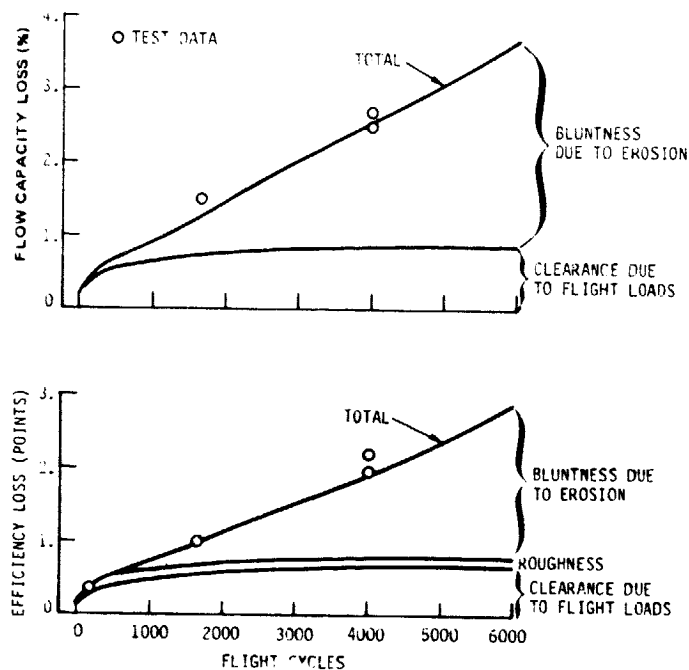


Figure 36 Back-to-Back Fan Test Data - The data establishes the level of deterioration being experienced by the average fan module.

Performance Recovery Approach

Fan blade tip clearance is governed by rub strip trenching due to engine transients and aircraft maneuver. Figure 31 showed that the trench is fully established early in the life of the engine. The only means of recovering this increment in performance loss is by replacement of the rub strips. The difference between the DC-10 center engine and the wing engines suggests that structural design changes could reduce trenching in future engines by reducing the engine bending from inlet cowl air loads.

The fan deterioration increment due to surface roughness is recoverable by cleaning the blades. The blades must, however, be cleaned at frequent intervals.

The performance loss due to leading edge contour should be recoverable by leading edge rework. Based on the overall fan performance deterioration trend, this rework should be performed approximately every 3000 flight cycles.

Concerns

The collection and documentation of fan blade leading edge contour changes did not show discernable bluntness on JT9D-7A(SP) fan blades up to 2100 cycles relative to new blades. Test data from engines with high-time fans with, and without, restored leading edges (by chamfer cutting) show significant engine performance improvements for fan with restored blade leading edges (about 0.5 percent in sea level TSFC). However, data are not currently available to determine the rate of performance loss for the restored leading edge blades. The majority of airlines have not maintained records of part times.

In measuring service fan blade roughness the stylus of the Clevite Surfalyzer penetrated through the surface layer of dirt and therefore did not measure the roughness of the aerodynamic surface. Hence, the measured roughness levels are probably less than the true level. No means is currently available to inspect roughness that would leave the dirt undisturbed.

4.4.2 Low-Pressure Compressor

Performance Loss Mechanisms

Low-pressure compressor performance deterioration is caused by blade tip clearance and airfoil surface roughness increases. Airfoil contour changes are another potential cause of long-term deterioration.

In estimating the performance loss caused by tip clearance changes, consideration must be given to the condition of the rub strip upstream, underneath, and downstream of the blade (see Figure 37). In production acceptance testing, the rub strip is trenched. It has been found that blade tip-to-trench bottom clearance resulted in less loss than an equal clearance to a hard wall without the trench. This difference is indicated in the upper part of Figure 38 which shows compressor efficiency as a function of tip clearance (ϵ) for these two configurations based on compressor testing. To correlate the data, an effective tip clearance parameter was developed. Effective tip clearance is defined as the main stream flow path clearance (α) plus one-half of the trench depth (D). Utilizing this correlation, the data generalizes as shown in the lower part of Figure 38.

The analysis of low-pressure compressor deterioration conducted during the program recognized this difference plus the change in clearance that would occur from rub strip erosion and blade length loss. An expanded definition of effective tip clearance was defined to account for these additional potential changes to effective tip clearance. Effective tip clearance, as shown in Figure 39, is defined as including original running clearance, blade length loss, rub strip erosion, plus one-half of trench depth measured from the rub strip surface immediately ahead of the blade to the bottom of the trench.

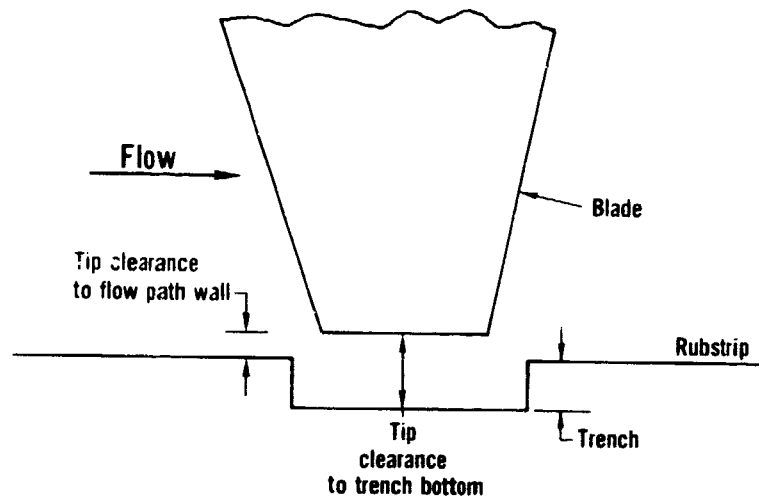


Figure 37 Sketch of Blade Tip and Rub Strip - In evaluating performance effects of clearance changes, consideration must be given to the condition of the rub strip ustream, underneath, and downstream of the blade.

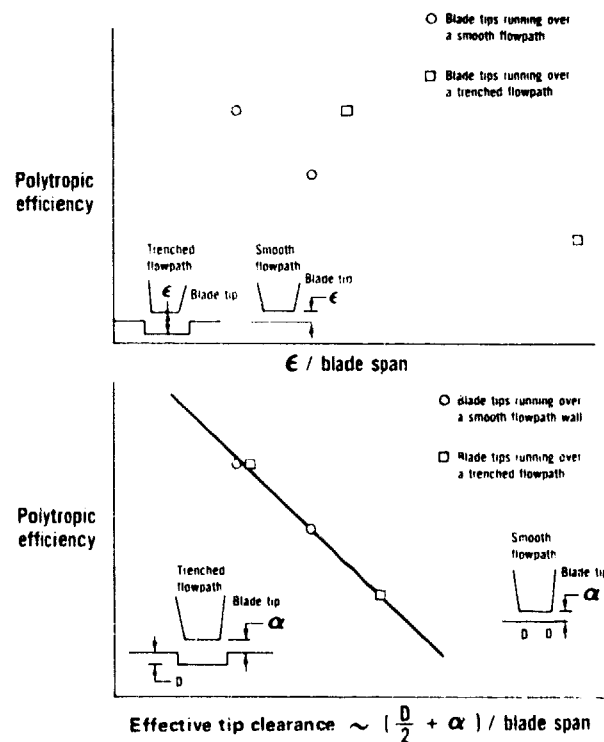


Figure 38 Effect of Trenching on Performance Losses Associated with Blade Tip Clearance - Test data shows that the clearance in the trench produces one-half the loss associated with the clearance in the mainstream.

- Original running clearance (A)
- Blade length loss (B)
- Rotor rubstrip erosion (C)
- Rub (trench) depth (D)

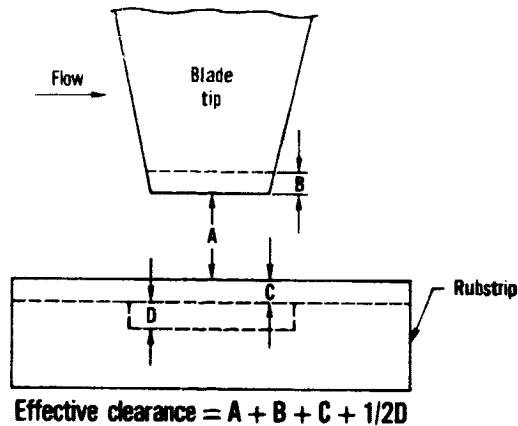


Figure 39 Definition of Effective Tip Clearance - Because of the effect of trenching, an effective tip clearance parameter was obtained to correlate the measured clearance data with performance.

Engineering experience based on systematic tests conducted in a low speed rig and a multi-stage high-pressure compressor estimates that a 0.010 inch increase in low-pressure compressor effective tip clearance will result in a loss of 0.5 point in adiabatic efficiency and a 0.83 percent decrease in flow capacity.

Surface roughness, caused by pitting and accumulation of dirt, negatively affects the performance of the low pressure compressor. As with the fan blades, the effect of airfoil surface roughness was evaluated with existing correlations of airfoil loss coefficient as a function of Reynolds number and roughness.

Erosion of the airfoil contour will affect performance through changes to the leading-edge shape, and airfoil camber.

The performance deterioration for airfoil contour changes caused by erosion were estimated using a radial streamtube compressor performance computer model. This model consists of the equations of motion combined with cascade loss and turning correlations.

The geometrical airfoil properties which govern cascade performance are leading edge angle (β_1^*), trailing edge angle (β_2^*), gap to chord ratio (τ/b), and thickness to chord ratio (t/b), as shown in Figure 40. Changes to these parameters due to erosion were determined from the inspection of used parts. In the case of the low-pressure compressor, the airfoils collected with usage levels up to 5500 cycles indicated negligible changes to these airfoil properties as discussed in the following section.

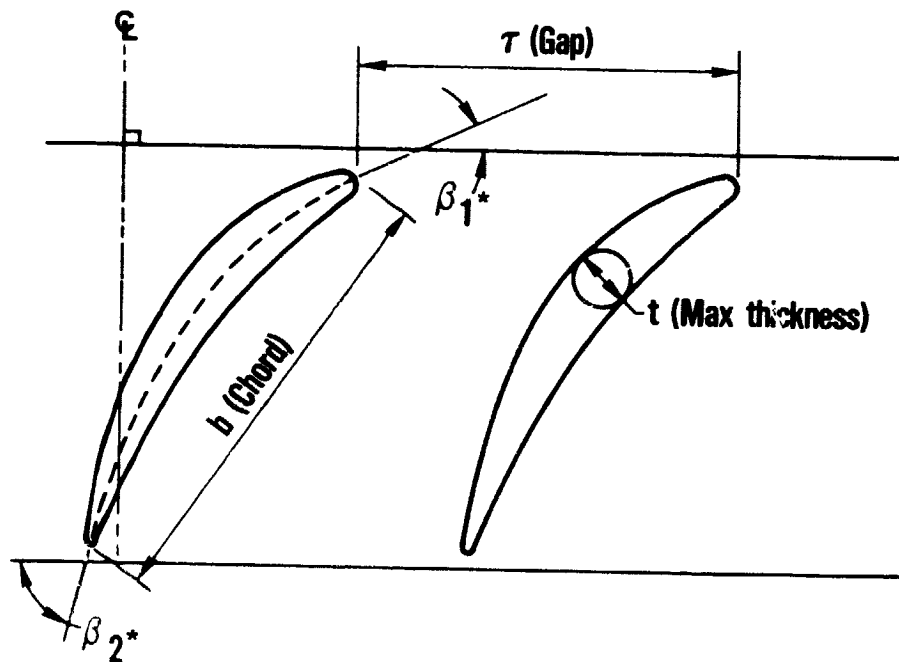


Figure 40 Nomenclature for Airfoil Parameters - The parameters shown are the significant parameters with respect to the effects of erosion on airfoil performance.

Representative Performance Deterioration

Tip Clearance Changes - Tip clearances can be affected by loss of blade length, by rub strip trenching due to rubs during engine transients and aircraft maneuvers, and by rub strip erosion. Of these, the rub strip trenching and erosion were found to be significant. Results of measurements taken on service parts indicated that blade length losses were insignificant for the three stages of the low-pressure compressor. For example, the third-stage blade length loss data compared to

production tolerances is presented in Figure 41. (All stages are shown in Appendix B.) The lack of significant losses in blade length is attributed to the soft rubber rubstrip, the size of the airfoils, and the low tip-speed operation.

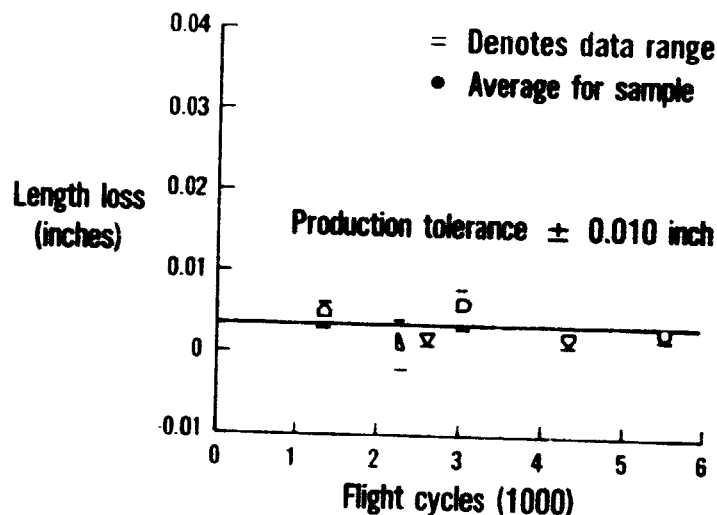


Figure 41 Low-Pressure Compressor Blade Length Loss Data for Rotor 3 - The blade length loss in the third stage is negligible as a result of the soft rubber rub strip and apparent lack of significant blade tip erosion.

Rub Strip Trenching and Erosion - Typically, a low time part with less than 1000 cycles will have no erosion but a trench will already be formed as a result of rubbing. After about 1000 cycles, some erosion will have occurred ahead of and behind the blade, but none will have occurred in the bottom of the trench over the blade tip. However, the erosion continues with increasing usage and ultimately penetrates to the bottom of the trench, producing a trough contour over the blade tips as shown in Figure 42.

Historical rub-strip erosion and trench depth data were combined to determine the effective tip clearances and the resulting effect on performance. Rub-strip erosion data, summarized in Figure 43, were used to develop erosion rates for each stage. As can be seen, the erosion rate increases with each low pressure compressor stage. Trench depth data for each stage, as measured from the rubstrip surface just ahead of the blade to the bottom of the trench are shown in Figure 44. As

described above, the deep trench depth (0.012 to 0.030 inches) formed by rubbing within the first 350 cycles gradually decreases as a function of the rub-strip erosion rate until a trough (zero trench depth) is produced.

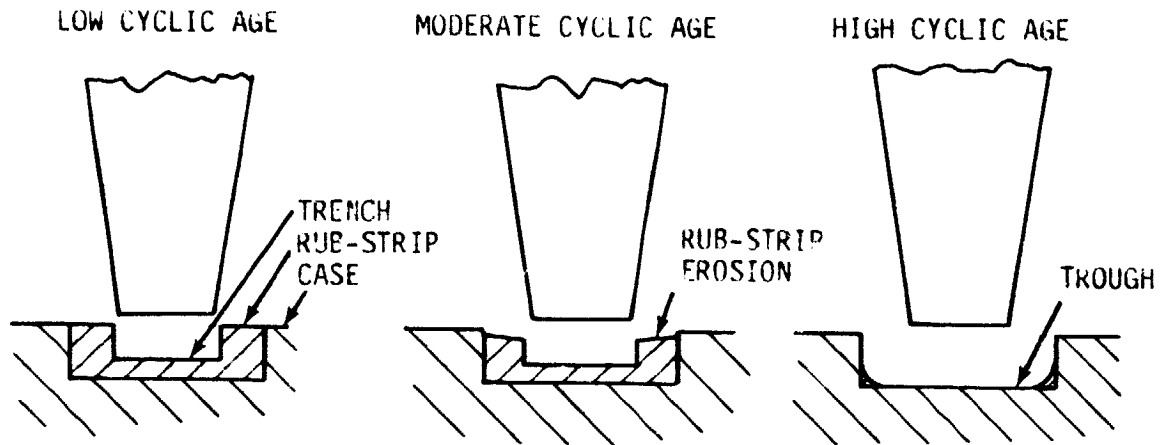


Figure 42 Schematic of Low-Pressure Compressor Tip Clearance Wear Mechanisms - Trenching occurs early followed by erosion of the rub strip until it is virtually eroded away.

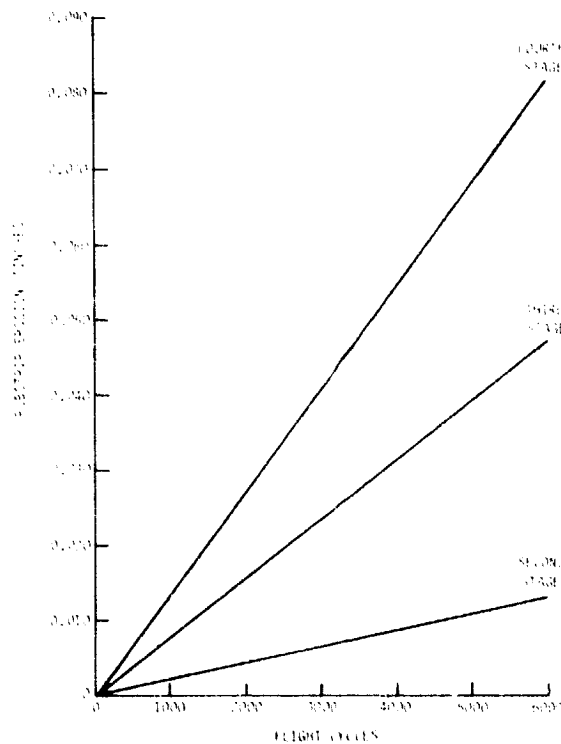


Figure 43 Rub Strip Erosion Data for the Low-Pressure Compressor - The erosion rate increases with each successive stage.

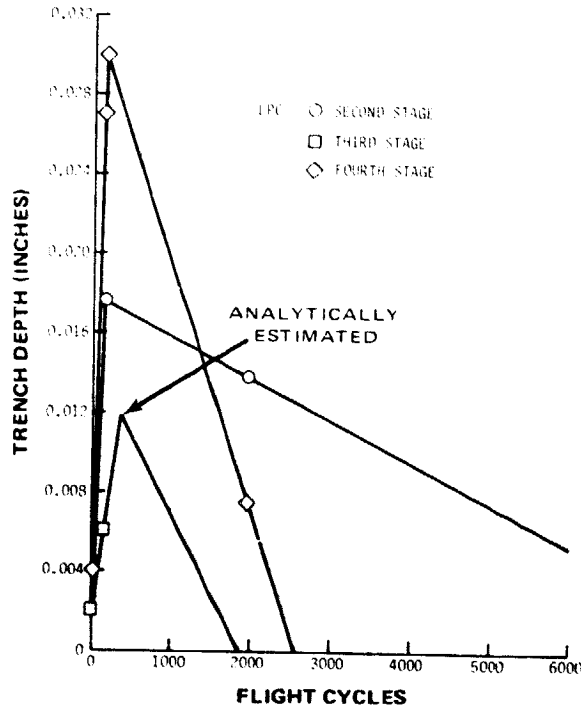


Figure 44 Trench Depth Measurements for the Low-Pressure Compressor - The trench becomes well established in the first several hundred cycles and then erodes to a trough with additional cycles.

These data in conjunction with rub predictions based on analysis of the effects of flight loads on performance deterioration (Reference 2) were used to determine the effective tip clearance increase relative to production acceptance tip clearances. The results are presented in Figure 45. The overall average effective tip clearance increase due to flight loads and erosion are indicated.

The estimated effect of tip clearance increases on low-pressure compressor performance is shown in Figure 46 and indicates a loss of two points in efficiency and 3.3 percent decrease in airflow capacity after 5000 cycles.

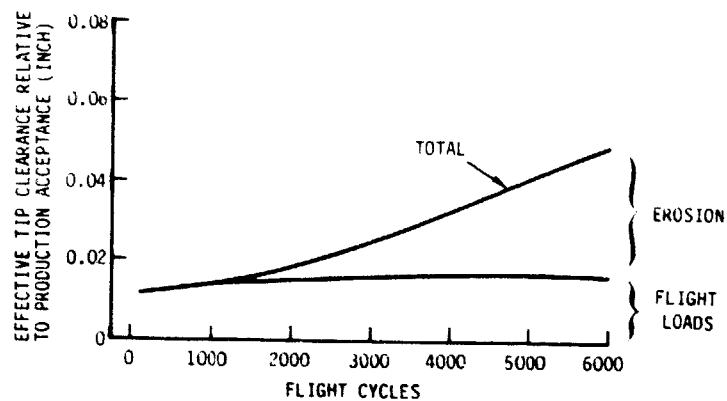


Figure 45 Effective Change in Blade Tip Clearance for the Low-Pressure Compressor - The average effective clearance reaches 0.04 inch in 5000 flights.

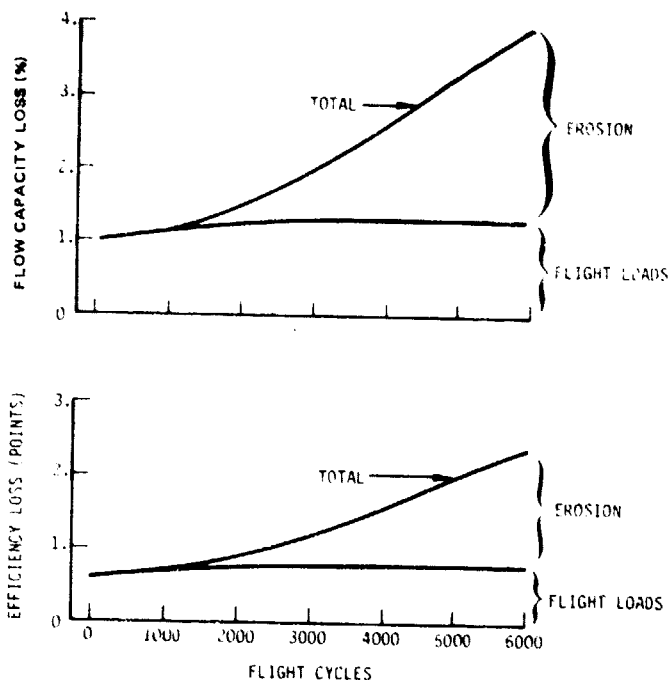


Figure 46 Effect of Tip Clearance Increases on Low-Pressure Compressor Performance - The increases in tip clearance produced by trenching and erosion will produce a loss of two points in efficiency after 5000 cycles.

Airfoil Roughness - Airfoil surface roughness changes were also documented from inspection of parts. The data taken on the low-pressure compressor airfoils are shown in Figure 47 for blades and Figure 48 for stators. The intersection at zero cycles indicate the production level of roughness. Based on engineering experience and visual observation, it is estimated that the roughness builds up within about 400 cycles and then remains constant. The fairing between production levels of roughness and 1200 cycles is based on observations of many parts and engineering experience. The two portions of the curves have not been faired together because the real nature of the change in roughness in this area is unknown. It is estimated that the largest increases in roughness occur on the stators. These data were then used to estimate the average roughness for the rotor and stator blades, and the results are shown in Figure 49. As with the fan, the effect of surface roughness on flow capacity was not determined.

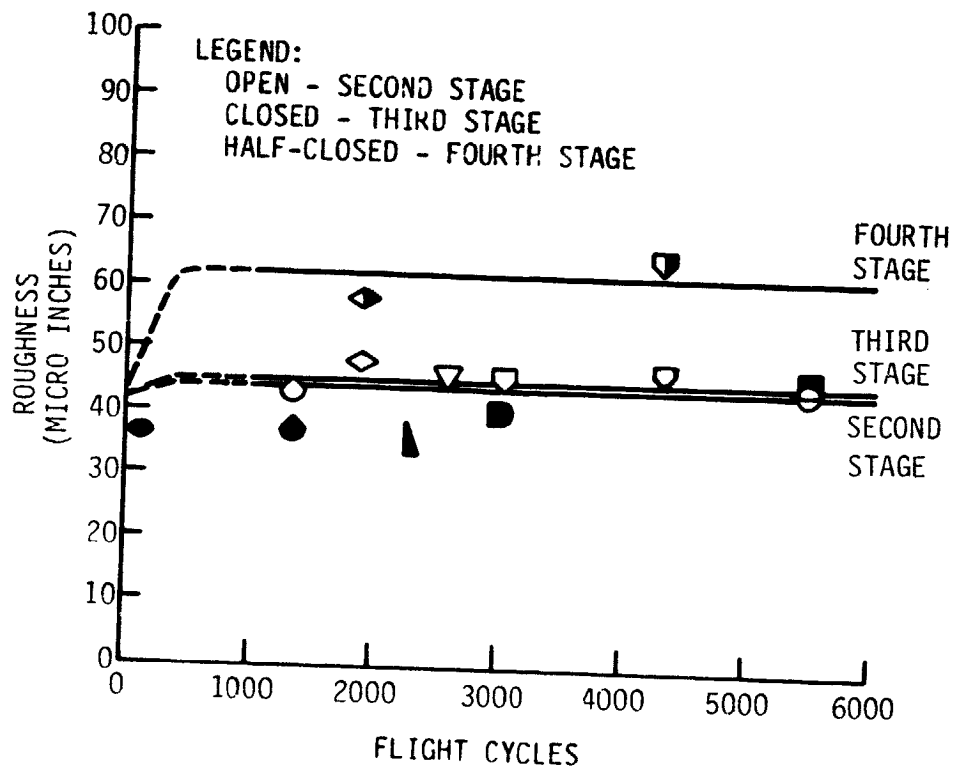


Figure 47 Surface Roughness Data for Second-, Third-, and Fourth-Stage Low-Compressor Rotor Airfoils - The surface roughness is estimated to increase rapidly and then remains constant.

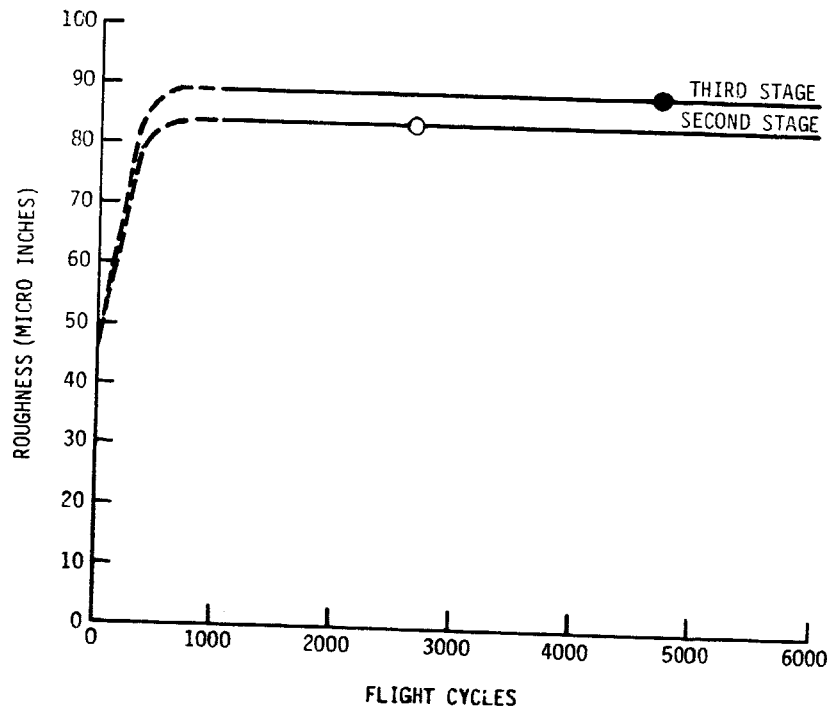


Figure 48 Surface Roughness Data for the Second- and Third-Stage Stator Airfoils - Surface roughness is estimated to increase rapidly and then remain constant.

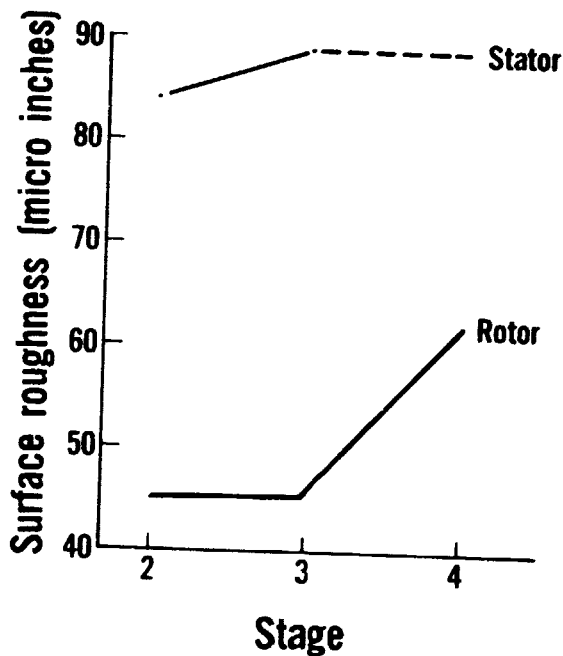


Figure 49 Average Low-Pressure Compressor Rotor and Stator Roughness Data At 2000 Cycles - Roughness is highest in the stators and in the rear stages.

The effect of roughness at sea level on low-pressure compressor efficiency was estimated. The result is shown in Figure 50. As shown, surface roughness increases cause an efficiency loss of approximately 0.2 percentage points. The effect of surface roughness on compressor flow capacity was not determined.

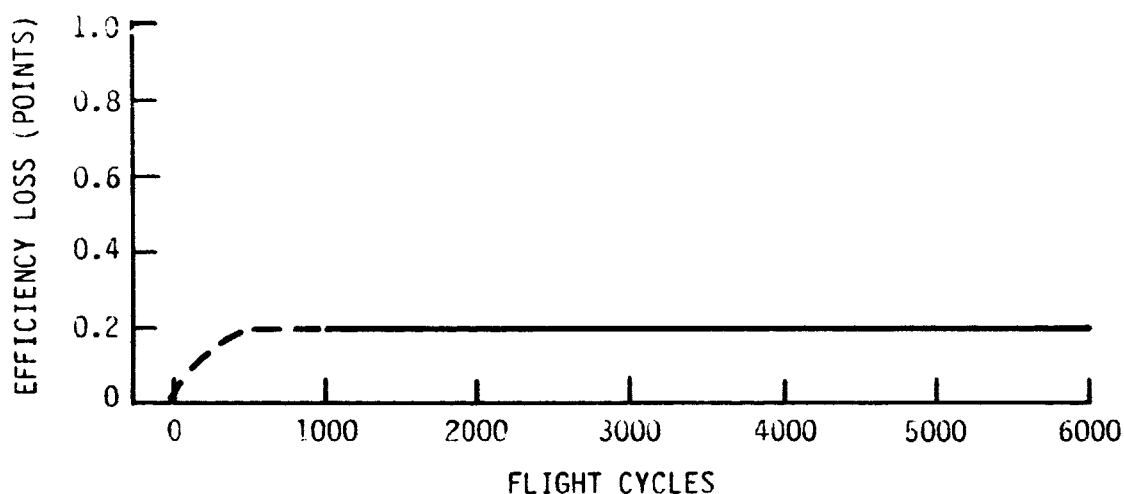
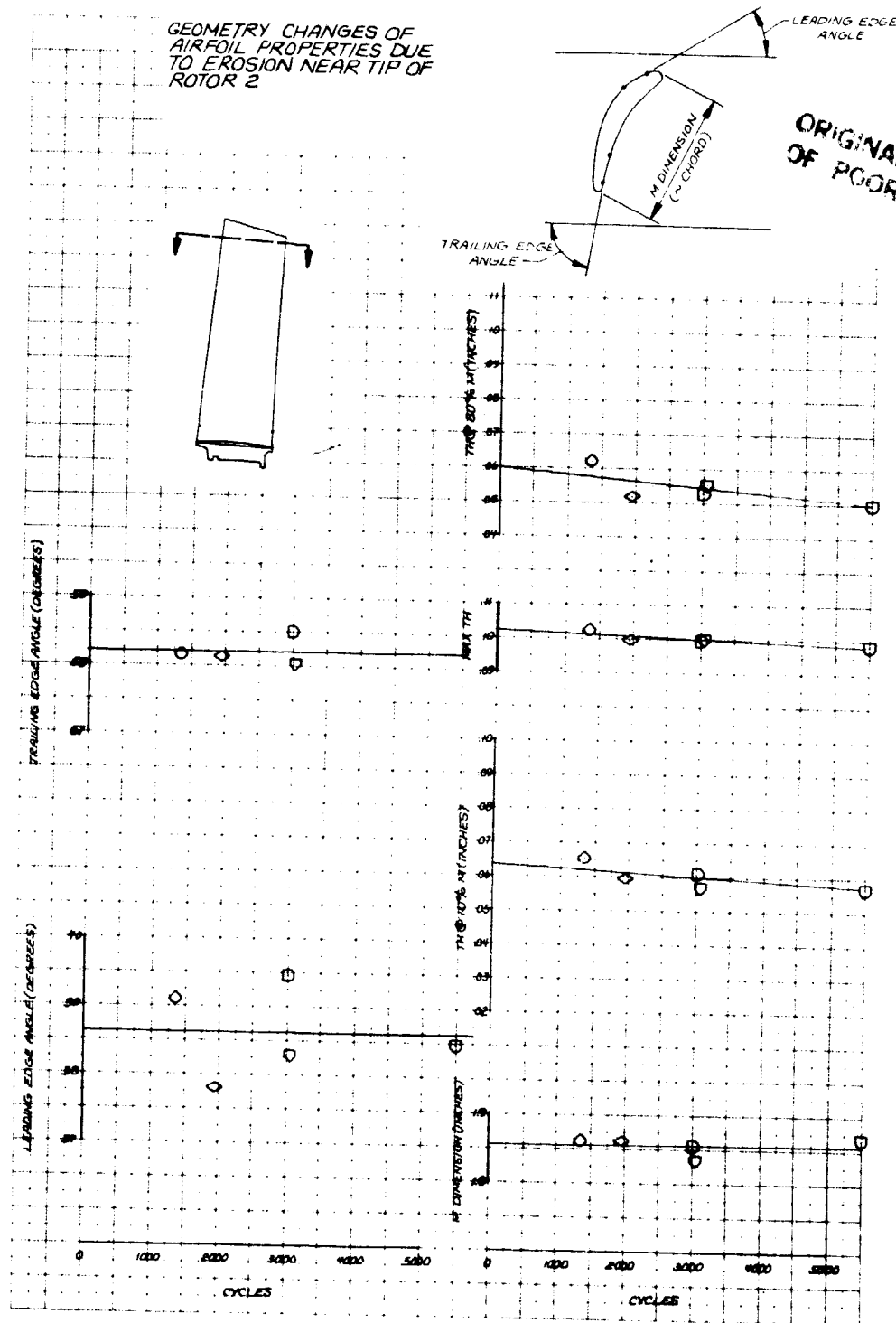


Figure 50 Effect of Low-Pressure Compressor Airfoil Surface Roughness on Efficiency - The increase in surface roughness causes a loss of 0.2 percentage point in low-pressure compressor efficiency.

Airfoil Contour Changes - Typical data for airfoil profile changes versus cycles for the tip section of stage 2 are shown in Figure 51 as an example. All stages are shown in Appendix B. Shown on these figures are the changes in: 1) leading edge angle; 2) trailing edge angle; 3) chord length (M dimension); 4) thickness at the 10-percent chord position (measured from the leading edge); 5) maximum thickness; 6) and thickness at the 80-percent chord position. Examination of these data for all stages indicate that the airfoil parameters have not changed significantly over the time frame of usage available from the parts collected. The performance penalty due to airfoil contour changes is therefore judged to be negligible.

Overall Deterioration - In summary, the overall performance deterioration of the low-pressure compressor is dominated by rub-strip trenching due to flight loads, rub-strip erosion, and airfoil surface roughness. The estimated performance loss as a function of engine flight cycles is shown in Figure 52. As can be seen for both efficiency and airflow, the losses due to rub-strip erosion continue to increase with flight cycles. The efficiency loss resulting from airfoil surface roughness is estimated to remain constant after the initial 400 cycles.



ORIGINAL PAGE IS OF POOR QUALITY

Figure 51 Second-Stage Rotor Tip Profile Data - Typical of the rotor tip profile data, these data show only a minor decrease in airfoil thickness with increasing flight cycles.

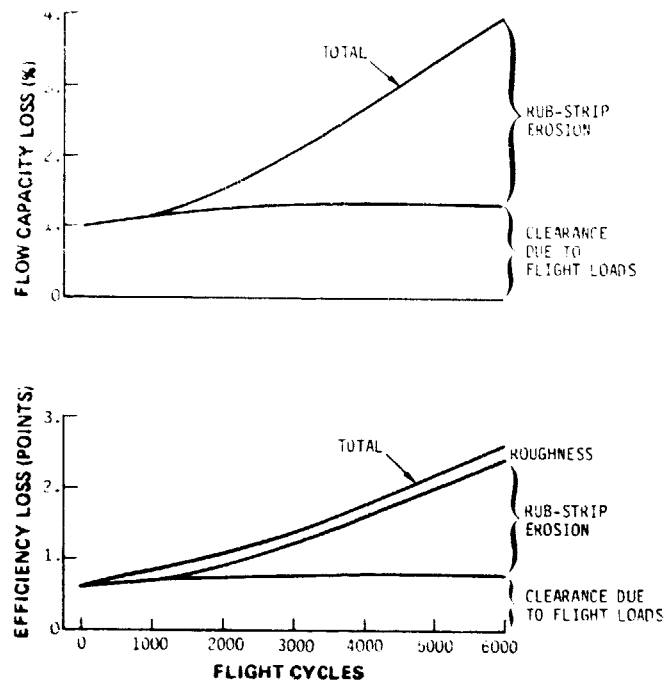


Figure 52 Estimated Overall Performance Loss for Low-Pressure Compressor - The analysis, based on used part inspection, indicates an efficiency loss of 2.2 percentage points after 5000 cycles.

Figure 53 shows the estimated performance data presented in Figure 52 together with the measured low-pressure compressor performance changes determined from back-to-back testing of service engines at Pratt & Whitney Aircraft. The results of analyses of prerepair historical data for Airlines A and C are also shown at the appropriate low-pressure compressor ages for average 2000 and 3500 flight cycle engines. Comparison of these sets of data reveals that the analysis does not account for all of the flow losses. Since the analysis did not indicate a flow capacity loss associated with surface roughness, it is possible that the observed flow loss differences in some engines may result from variations in surface roughness. The estimated flow loss line in Figure 53 is based on engineering experience. This experience indicates that somewhat higher losses would be anticipated as a result of the first-stage stator trunion popping into the airstream, which was observed during trips to the airlines, coupled with the very high relative Mach number into the vane. Additionally, there is uncertainty in the measured value of low-pressure compressor flow capacity loss because of the limited instrumentation. It seems reasonable to establish the overall flow capacity loss at a somewhat high level for conservatism for the preliminary model.

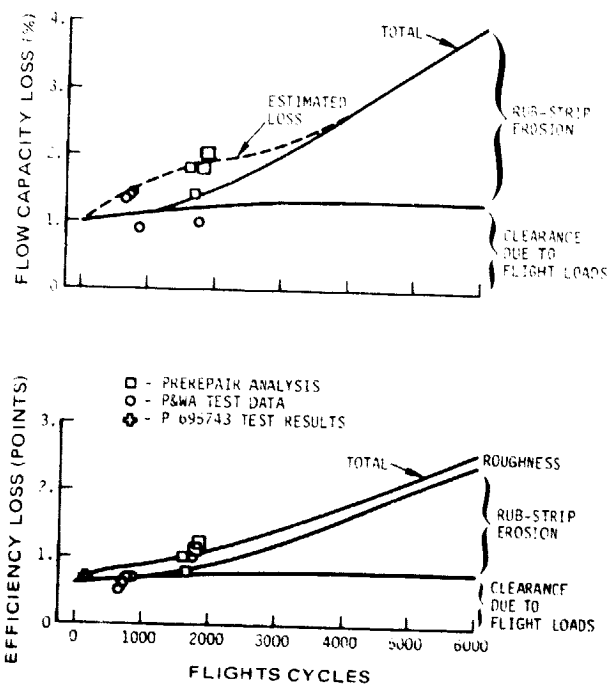


Figure 53 Low-Pressure Compressor Performance Loss Based on Estimates from Part Condition, Analysis of Historical Data, and Back-to-Back Testing of Service Compressors - The estimated flow loss line is based on engineering judgement.

Performance Recovery Approach

Low-pressure compressor blade tip clearance was shown to be governed by trenching due to rubs and by rub strip erosion. The increment due to erosion is recoverable by replacing rub strips.

The surface roughness induced increment is theoretically recoverable. The roughness, however, was found to build up quickly. Therefore, frequent cleaning would be required. An improved method for practical on-wing cleaning needs to be developed.

Concerns

As discussed for the fan modules, the equipment used to measure surface roughness disturbed the surface contamination. As a result, the performance loss increment analytically estimated for roughness may be understated. The analysis did not indicate an effect of roughness on flow capacity loss, although such an effect might be expected. Testing of airfoils with various roughness levels would be required to establish any such effect.

4.4.3 High-Pressure Compressor

Performance Loss Mechanisms

High-pressure compressor performance deterioration is caused by three factors: changes in blade tip clearance, airfoil surface roughness, and airfoil contour.

Tip Clearance - The tip clearance wear in the JT9D high-pressure compressor is made up of three parts: 1) the trench dug in the rub strip during engine transients and aircraft maneuvers, 2) erosion of the rub strip, and 3) loss of blade length. All three wear mechanisms produce significant effects on performance.

A schematic of the tip clearance wear mechanism for several ages is shown in Figure 54. At low cyclic age, no erosion has taken place on the blade and the rub strip. However, a trench has been formed due to rubbing. At moderate cyclic age, some erosion has taken place on the blade and on the flow-path wall ahead of and behind the blade tip. At high cyclic age, additional erosion has foreshortened the blade, and the flow-path wall has been eroded to the extent that the trench is no longer visible.

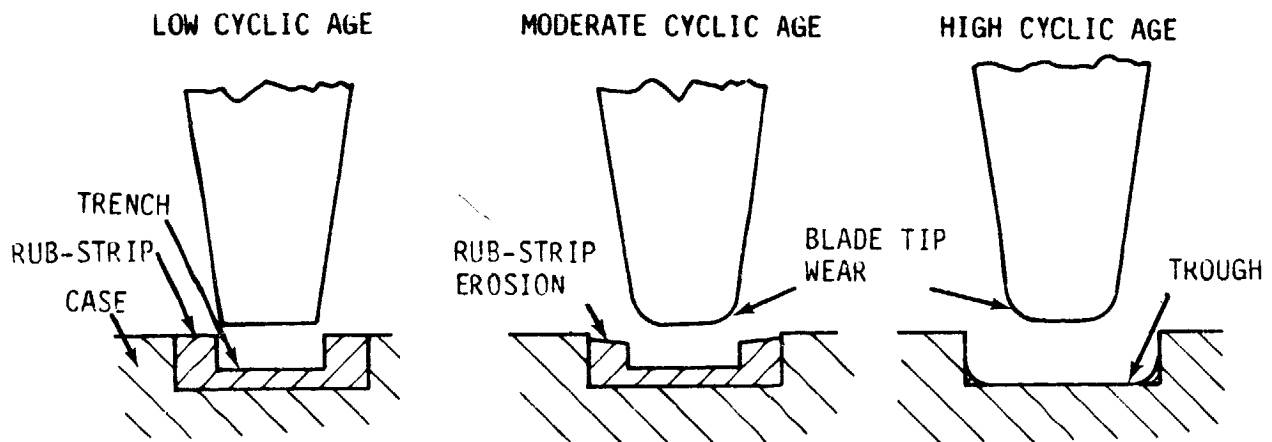


Figure 54 Schematic of Tip Clearance Wear Mechanism for High-Pressure Compressor - Erosion and trenching occur early in the compressor life, but continued usage results in erosion that virtually eliminates all evidence of trenching.

The effect of tip clearance on compressor performance deterioration must consider the radial clearance between the blades and the rub strip with consideration given to the condition of the rub strip upstream and downstream of the blade as discussed for the low-pressure compressor, and shown in Figures 37 through 39.

Similar to the analysis for the low-pressure compressor, separate records were kept for the tip clearance relative to the mainstream wall and the trench depth to calculate an effective tip clearance with due accounting for the effects of the trench.

The effect of tip clearance changes on performance was estimated based on a correlation of data from many compressors. An increase in blade effective tip clearance of 0.010 inch will result in an estimated loss of 1.2 points in adiabatic efficiency and 1.6 percent loss in airflow.

Surface Roughness - The effect of surface roughness was evaluated by use of correlations of airfoil loss as a function of Reynolds number and roughness as described for the fan.

Contour Changes - The performance deterioration prediction for airfoil contour change caused by erosion was accomplished using a radial stream-tube compressor performance computer model. This model consists of the equations of motion combined with cascade loss and turning correlations as discussed for the low-pressure compressor.

Representative Performance Deterioration

Tip Clearance - Tip clearance changes caused by blade length loss, erosion, and trenching were measured for all stages of selected compressors. Data from the sixth, ninth, and fourteenth stages are used for the discussion to show the variation in blade length loss from an early stage to a rear stage of the compressor.

Blade length loss data are shown in Figure 55. The data indicate higher blade length losses in the forward stages than in the rear stages. Data for the fourteenth stage showed a negligible loss, in part because the blades in this stage are fabricated from a nickel-steel alloy while the other stage blades are fabricated from titanium.

Rub-strip erosion rates are shown in Figure 56. The erosion rate in the sixth stage is high because of the soft rubber rub-strip material. Less erosion occurs in the rear stages since these stages use a Feltmetal rub strip.

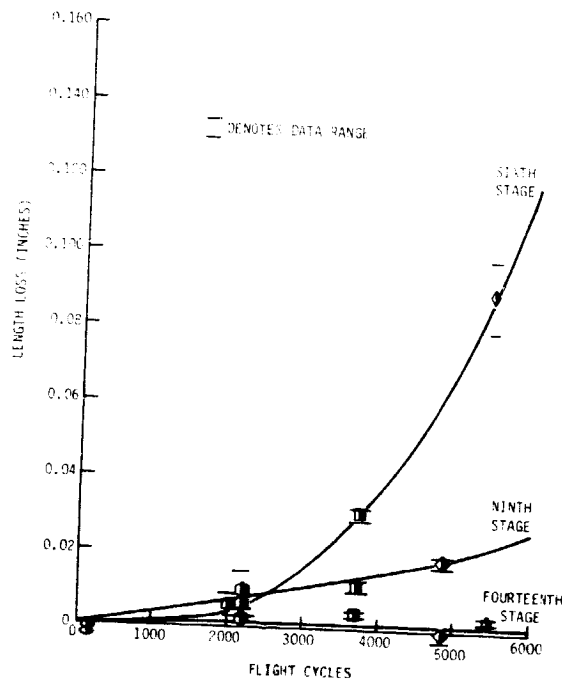


Figure 55 Blade Length Loss for Sixth-, Ninth-, and Fourteenth- Stage Rotors - Blade length loss is primarily of major importance in the front stages.

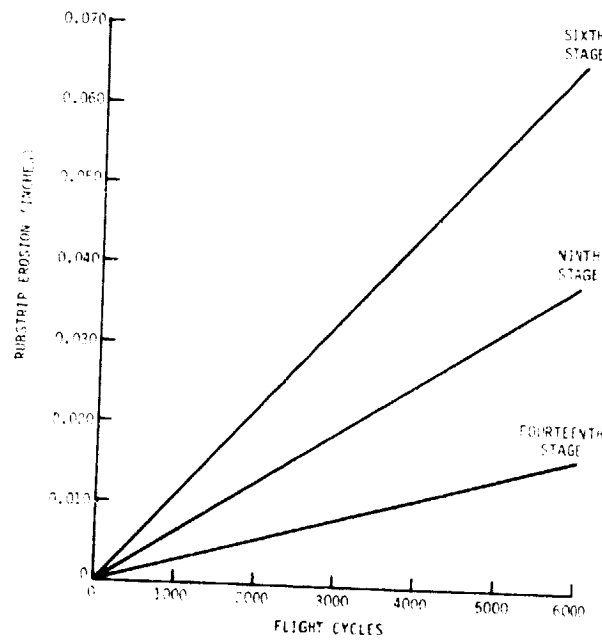


Figure 56 Rub-strip Erosion Rate for Sixth-, Ninth-, and Fourteenth-Stage Rotors - The rate of erosion diminishes progressively towards the rear stages of the high-pressure compressor.

Trench depth data measured from the rubstrip surface just ahead of the blade to the bottom of the trench are shown in Figure 57. As discussed earlier for the low-pressure compressor, some erosion will have occurred ahead of and behind the blade, but none will have occurred in the bottom of the trench over the blade tip. However, the erosion continues with increasing usage and ultimately penetrates the bottom of the trench, producing a trough contour over the blade tips.

An average effective tip clearance was calculated for the high-pressure compressor including those portions due to trenching, blade length loss, and rub-strip erosion. The portion due to trenching was based on data from engine P-695743 (Reference 1), analytical studies of the effect of flight loads (Reference 2), and the data presented in Figure 57. The results are shown in Figure 58.

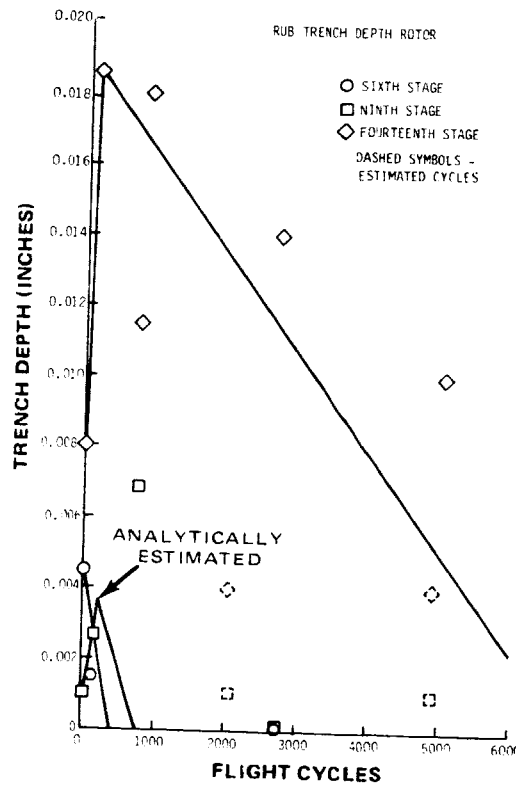


Figure 57 Rub-strip Trench Depth Data for Sixth-, Ninth-, and Fourteenth-Stage Rotors - Trenches are rapidly eroded away in all stages.

The resulting high-pressure compressor performance loss estimates are shown in Figure 59. Rub-strip wear and blade length loss due to erosion cause the majority of the deterioration induced by tip clearance changes.

C-2

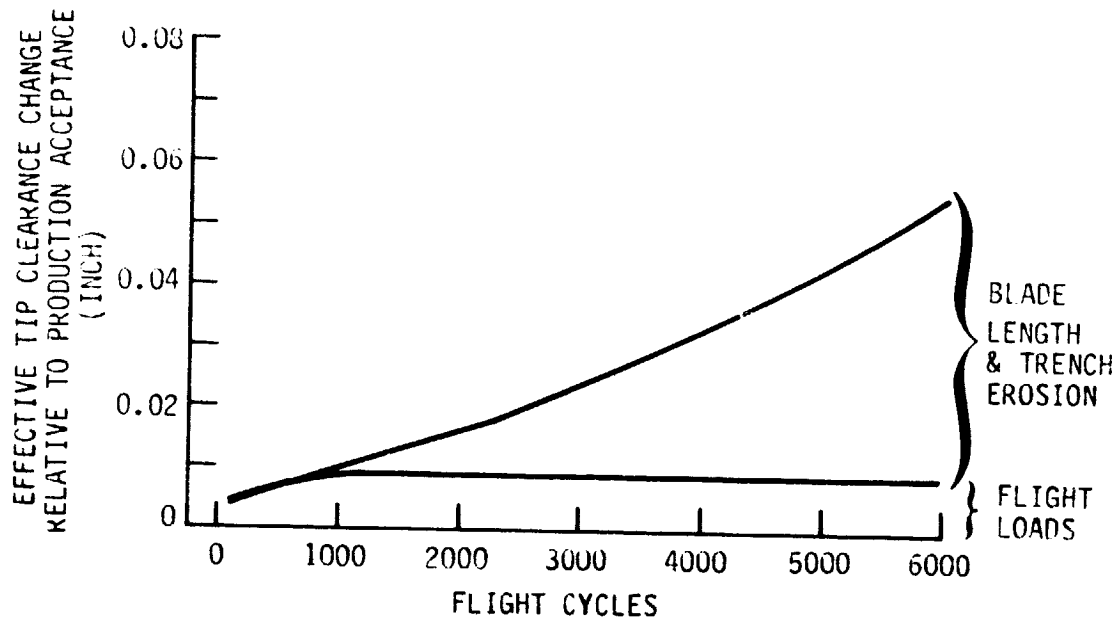


Figure 58 Effective Tip Clearance Increases Relative to Production Acceptance - Blade length loss and trench erosion are the major causes for clearance changes.

Surface Roughness - Base-line surface roughness for new hardware was determined by measurements made on available new parts. The data were averaged for parts produced using the same materials and processes. Roughness measurement data for stages six, nine, and fourteen are presented in Figures 60 and 61 for the blades and stators, respectively. Similar to the low-pressure compressor, inspection of used parts and engineering experience indicate that roughness builds up quickly in about 1000 flight cycles and then remains constant. The zero cycle data represent average production levels of roughness measured on new parts. A crossplot of roughness at 2000 flight cycles by stage number is shown in Figure 62.

The effect of surface roughness on the high-pressure compressor efficiency was predicted and the results are presented in Figure 63. The observed change in surface roughness would result in a loss of 0.23 point in efficiency for both sea level and cruise conditions. The analysis did not predict a change in flow capacity for roughness.

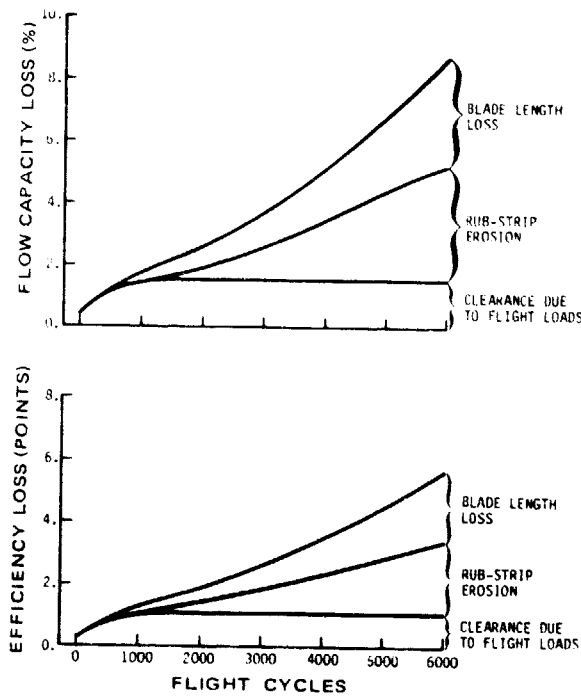


Figure 59 High-Pressure Compressor Performance Loss Attributed to Blade Tip Clearance Increases - Rub-strip erosion and blade length loss cause the majority of the deterioration induced by tip clearance changes.

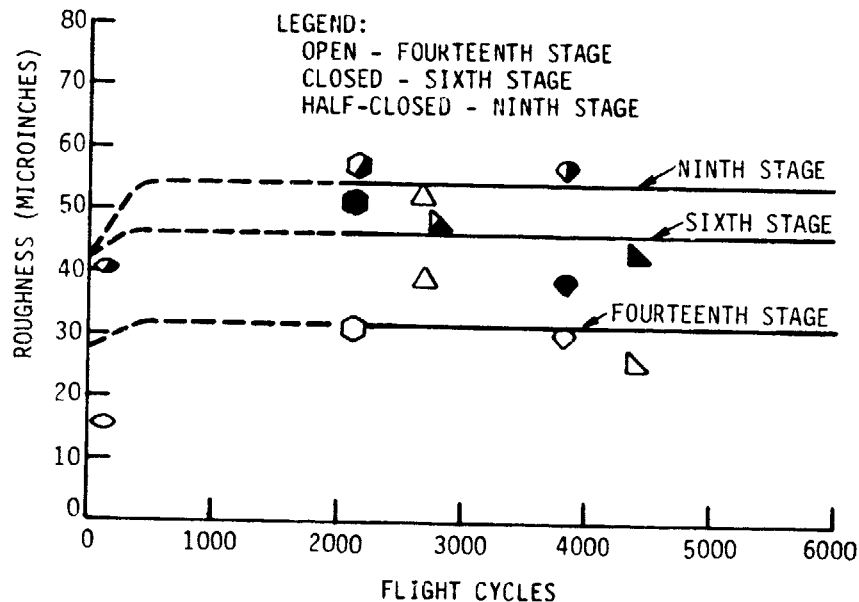


Figure 60 Surface Roughness Data for JT9D Sixth-, Ninth-, and Fourteenth-Stage Blades - Surface roughness increases slightly during the first 500 cycles and then remains constant.

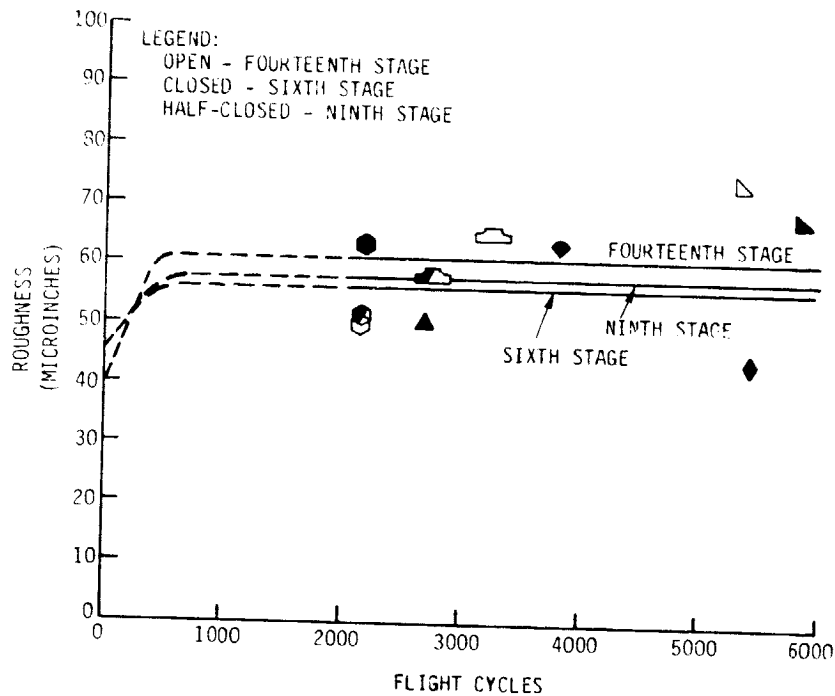


Figure 61 Surface Roughness Data for JT9D Sixth-, Ninth-, and Fourteenth-Stage Stators - The trend for surface roughness for stators is similar to that for the blades with an initial increase followed by no further change.

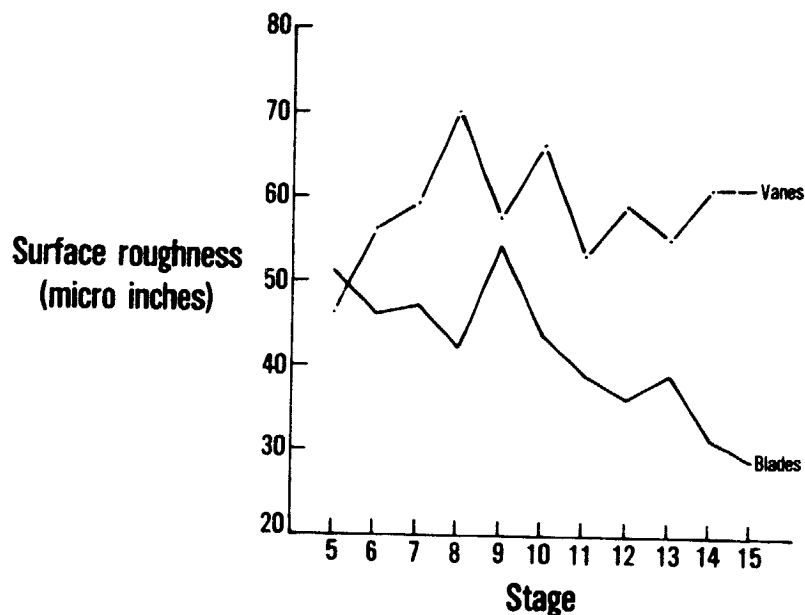


Figure 62 Surface Roughness for JT9D High-Pressure Compressor Blades and Vanes at 2000 Cycles - Surface roughness increases are greater for the vanes than for the blades, with the least change occurring in the rear stage blades.

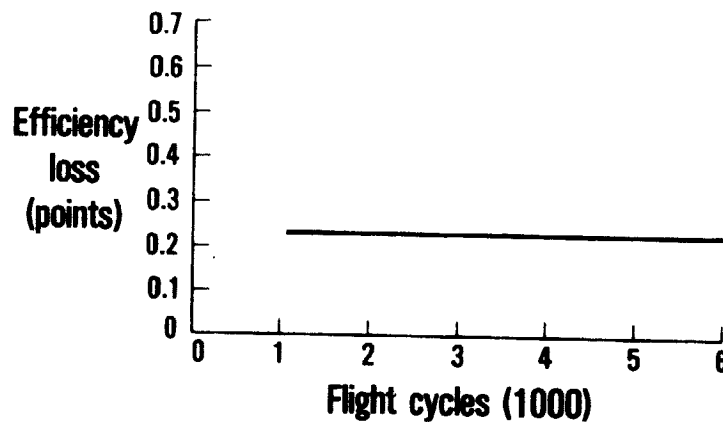


Figure 63 Prediction of Effect of Surface Roughness Changes in High-Pressure Compressor on Performance - The observed change in surface roughness would result in a loss of 0.23 point in efficiency.

Airfoil Contour Changes - The changes to airfoil contours were determined to be a function of flight cycles rather than hours. This is evident from inspection of the airfoils shown in Figures 64 and 65 which show a set of blades with high hourly usage but with moderate cycles and a set with moderate hourly usage and high cycles, respectively. The parts set with the higher cycle time, shown in Figure 65, is much more eroded than the parts shown in Figure 64, although the eroded set had lower hourly age. Severe erosion in Figure 65 is indicated by the rounded blade tips.

This flight cycle dependency is also evident from the data shown in Figure 66 where airfoil tip chord is presented as a function of flight hours and flight cycles. The different symbols shown represent data from different engines and were used for data quality assurance reasons. The data for all stages is shown in Appendix B. As can be seen, only slight changes are indicated when plotted as a function of hours, whereas more significant changes are indicated when plotted as a function of cycles.

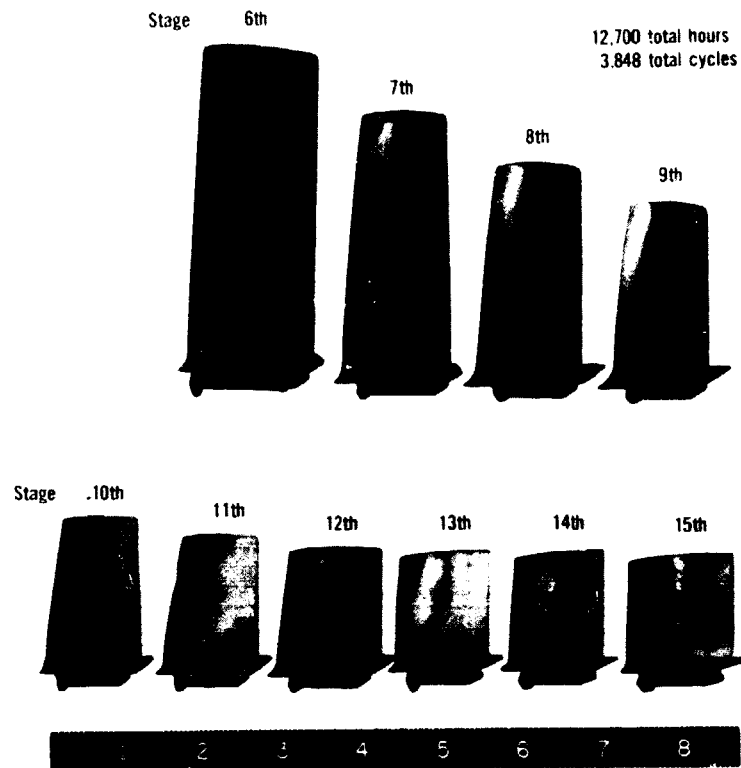


Figure 64 JT9D High-Pressure Compressor Blades with High Hourly Usage but Moderate Cycle Usage - These blades show relatively little wear.

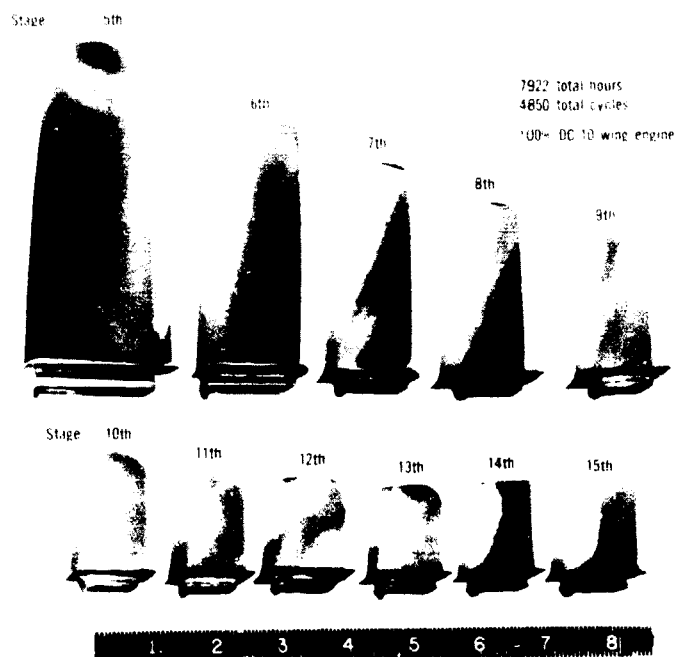


Figure 65 JT9D High-Pressure Compressor Blades with Moderate Hourly Usage but High Cycle Usage - These blades show severe wear

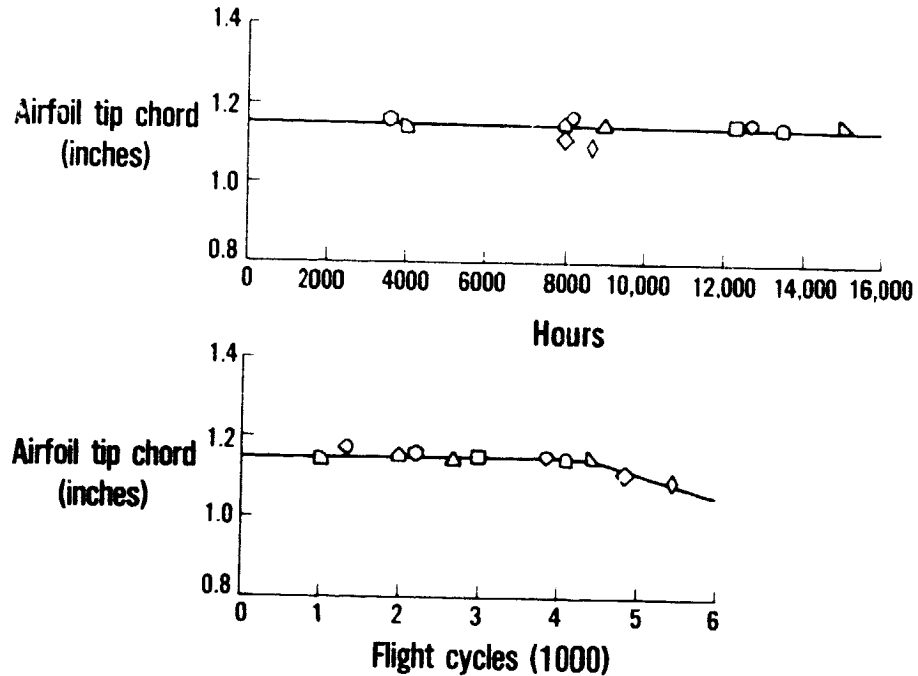


Figure 66 Chord Erosion Data for Tip Region of Fourteenth-Stage Blade - These data show that erosion is a function of cycles, not hours.

As for the low-pressure compressor, changes in the geometric airfoil properties due to erosion were determined from used part inspection. Figure 67 shows typical airfoil geometry changes due to erosion at a tip section for Rotor 9. Changes in root cross-section contour were found to be negligible for all stages. Further inspection of the blades showed that the erosion occurred primarily in the outer (tip) 50 percent of the span, shown in Figure 68, which shows a crossplot of the ninth stage blade contour changes as a function of blade span from root to tip. Visual inspection of high pressure compressor stators showed that no contour loss was evident until approximately 5400 flight cycles. Therefore, for the range of this study, stator contour changes are considered negligible.

GEOMETRICAL CHANGES OF AIRFOIL PROPERTIES DUE TO EROSION NEAR TIP OF ROTOR 9

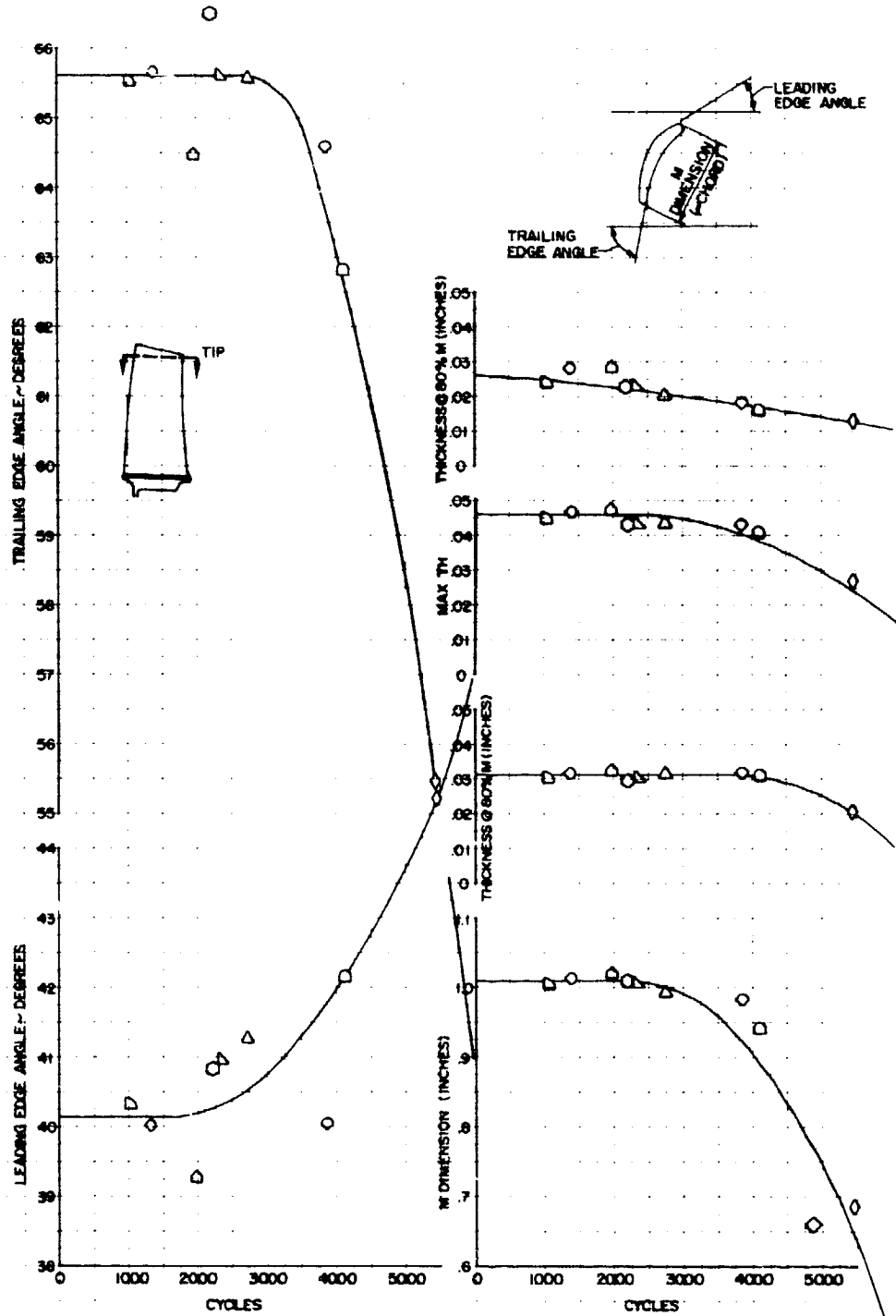


Figure 67 Airfoil Geometry Changes for Tip Section of Ninth-Stage Rotor Blade - The ninth-stage blade tips experienced large changes in leading and trailing edge angles.

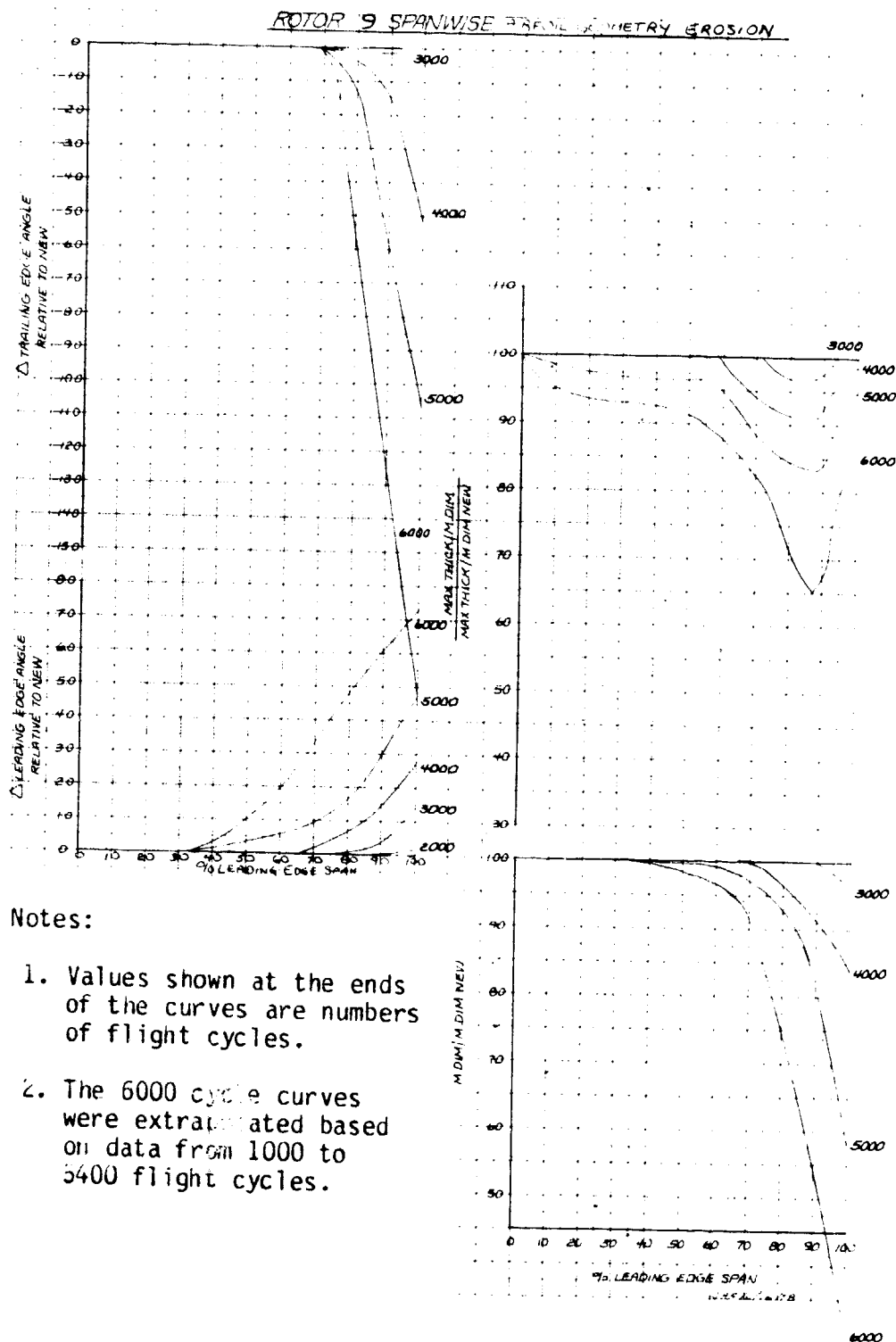


Figure 68 Airfoil Contour Changes as a Function of Leading Edge Span (Ninth-Stage Rotor Blades) - The ninth-stage blades experienced the contour changes, predominately at the tip.

The high-pressure compressor deterioration performance loss caused by contour changes versus usage is shown in Figure 69.

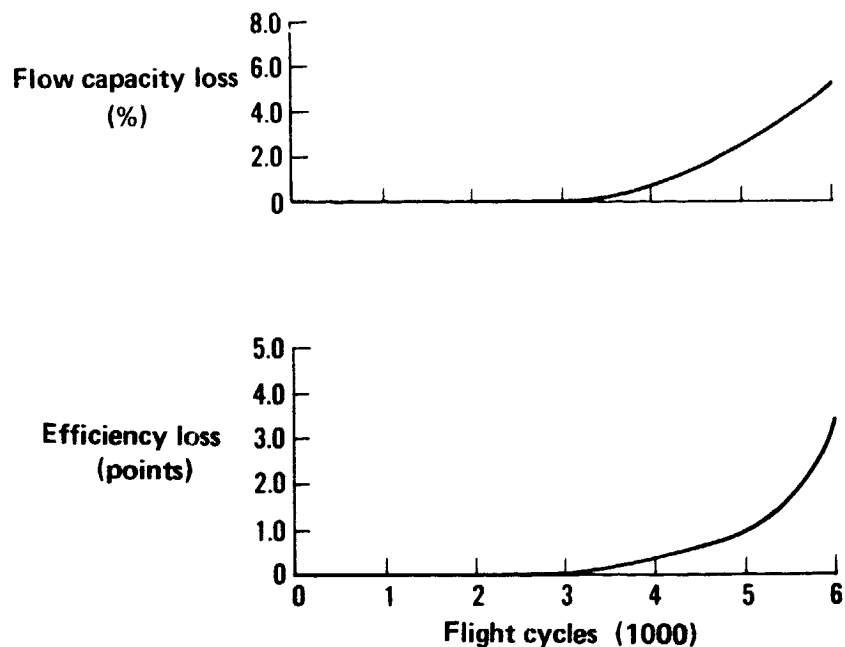


Figure 69 Estimated Effect of Airfoil Contour Changes on Performance - Contour changes produced by erosion have negligible effect on performance during the first 3000 cycles, but at 6000 cycles they produce an efficiency loss of 3.5 percentage points and an airflow loss of 5 percent.

Overall Deterioration - The combined effects of the five deterioration mechanisms on compressor performance are shown in Figure 70.

The distribution of the performance losses at low, moderate, and high flight cycles is shown in Table XVII. As shown, at low to moderate cycles, the majority of the deterioration is caused by rub-strip trenching and erosion. At high cycles, airfoil contour erosion and blade length loss become increasingly dominant.

Comparison of the overall estimated loss in high-pressure compressor performance deterioration based on used parts inspection and the levels of deterioration determined based on back-to-back service engine testing is shown in Figure 71.

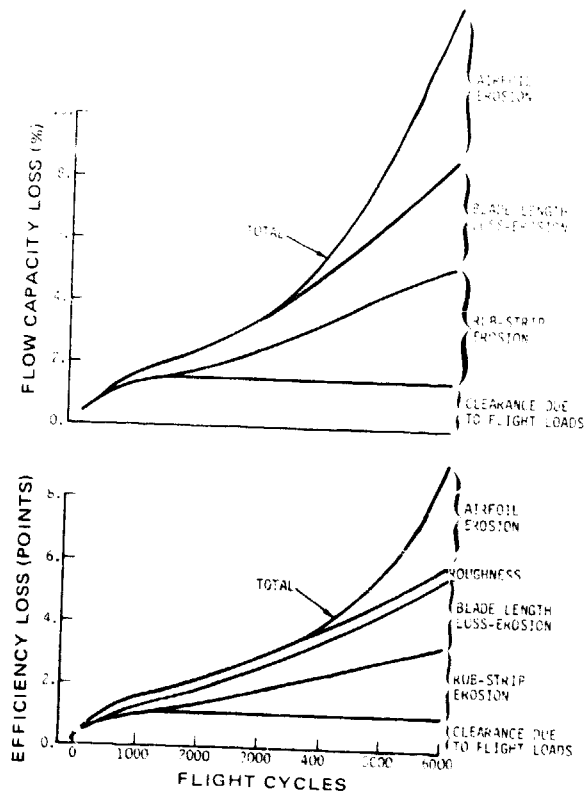


Figure 70 Total High-Pressure Compressor Performance Deterioration - At low-to-moderate age, the majority of the deterioration is caused by rub-strip wear, while at high age, airfoil contour erosion becomes increasingly dominant.

TABLE XVII

TOTAL HIGH-PRESSURE COMPRESSOR EFFICIENCY DETERIORATION

<u>Cycles</u>	<u>Total Efficiency Deterioration (Points)</u>	<u>Percent Due to Rub-Strip Trenching and Erosion</u>	<u>Percent Due to Blade Length Loss</u>	<u>Percent Due to Surface Roughness</u>	<u>Percent Due to Airfoil Contour Erosion</u>
1000	1.35	70			
3500	3.40	62	13	17	0
6000	9.40	36	28	7	3
			25	3	36

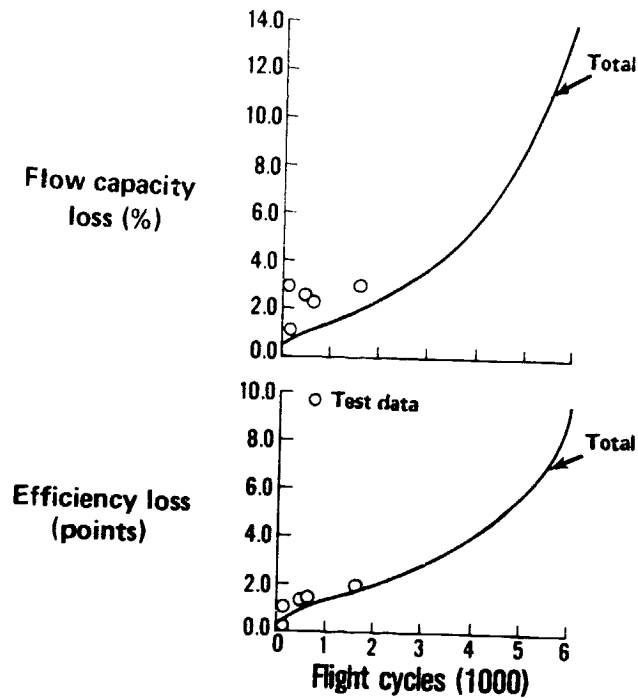


Figure 71 Predicted and Experimentally Measured High-Pressure Compressor Performance Deterioration - Good agreement is obtained between the predicted deterioration and the trends indicated by back-to-back high-pressure compressor testing.

The agreement between the efficiency data over the time frame covered by test data is reasonable and tends to support the analytically determined trends. The disagreement between the analytically predicted airflow loss and the test data could be caused by variable stator vane schedule differences and to a lesser extent by roughness, neither of which were included in the analysis. However, this lack of agreement is not of concern because losses in high-pressure compressor flow capacity have an insignificant effect on engine performance.

Performance Recovery Approach

The performance lost due to airfoil roughness is theoretically recoverable by cleaning. The roughness builds quickly, however, indicating that frequent cleaning would be required. An improved method for practical on-wing cleaning needs to be developed.

The performance increment due to tip clearance is recoverable only by replacing hardware. Figure 69 shows that above 3000 cycles, the losses from airfoil contour changes and blade length loss become increasingly significant. Rebuilding the high-pressure compressor, including rub strip and blade replacement and cleaning of stator airfoils, should be considered on any module with more than 3000 flight cycles.

4.4.4 Combustion System

Combustion system hardware deterioration involves coking of the fuel nozzles, which results in nonuniform fuel spray distribution, and changes to the critical dimensions of the combustor, in particular, the cone angle, as shown in Figure 72.

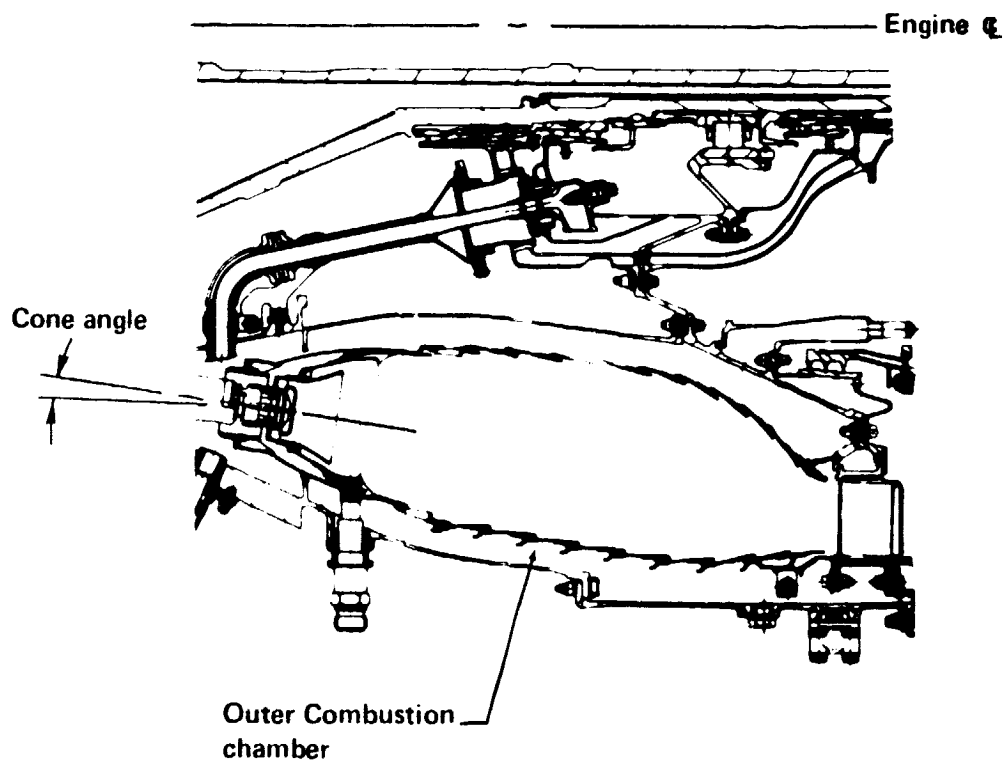


Figure 72 Definition of Combustor Cone Angle - Deviations from the optimum cone angle may result in an adverse radial temperature profile at the turbine entrance.

The two combustion system performance parameters which impact engine performance directly are burner pressure drop and combustion efficiency. However, pressure drop remains relatively constant as a function of usage level for a given combustor design, and combustion efficiency is essentially 100 percent for all power settings except idle and does not appear to be dependent on fuel nozzle or combustor conditions except in the most extreme cases of deterioration. Therefore, deterioration of the combustion system hardware does not, directly, have a significant effect on engine performance deterioration.

However, it should be noted that the engine is sensitive to the combustor exit temperature profile which is determined, in part, by the structural contours of the combustor. For example, in one back-to-back test conducted by Pratt & Whitney Aircraft on combustors with two different exit temperature profiles, the difference in combustors resulted in a 0.7 percent difference in TSFC.

The combustor does, however, have an indirect effect on the performance of the turbines, primarily as a result of changes in the combustor exit temperature profile. The temperature profile is affected by: (1) fuel nozzle coking, (2) combustor hardware dimensions as influenced by combustor repair practices, (3) compressor discharge pressure profile, and (4) changes in cone angle.

The specific turbine deterioration mechanism is dependent on the radial and circumferential distribution of the combustor discharge temperature. Three possible radial temperature distributions are sketched in Figure 73. Distribution I is weighted heavily to the midspan portion of the gas path and represents the typical distribution of a new or properly repaired combustion system. Distribution II is heavily weighted to the outer portion of the gas path and could cause the turbine cases to expand radially outward, increasing blade tip clearances with a subsequent loss in turbine efficiency. Distribution III is heavily weighted to the inner portion of the gas path and could cause blade platform curling and subsequent aerodynamic performance penalties. In addition case radial shrinkage could excessively reduce running clearances, causing blade tip and knife-edge seal wear.

Other combustor profile-related performance deterioration mechanisms are nozzle guide vane area changes, airfoil twisting, and vane soldering. These mechanisms are discussed in detail in the turbine sections (Sections 4.4.5 and 4.4.6).

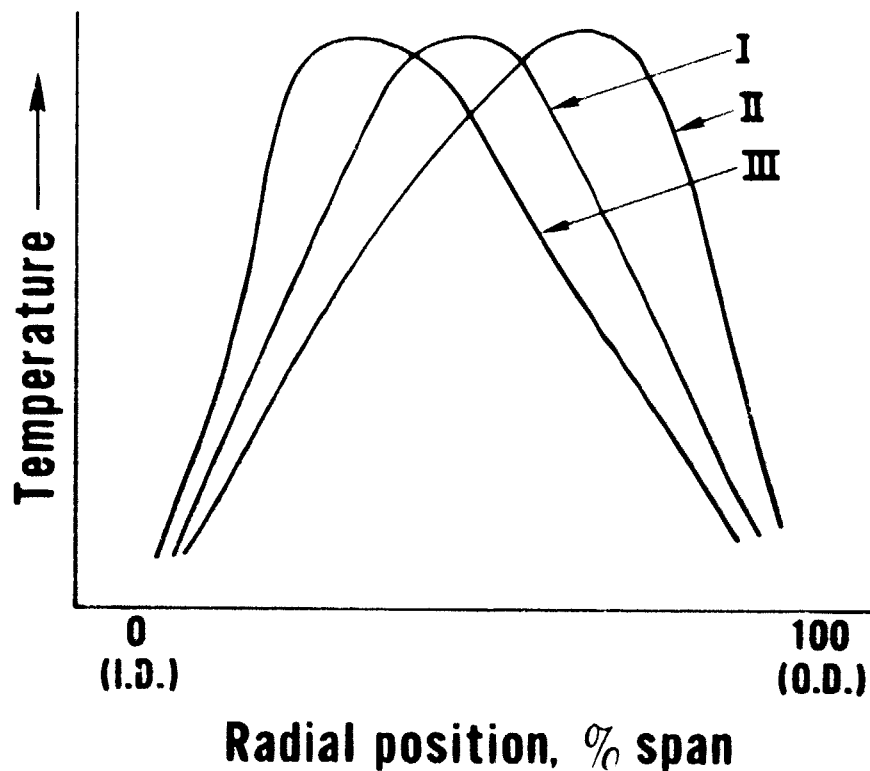


Figure 73 Combustor Radial Temperature Distributions - Distribution I is typical for a properly operating combustor, while distributions II and III may result in adverse conditions in the turbine.

It should be noted that changes in the combustor exit temperature profile may be produced by deterioration of the compressor as well as deterioration of the combustor. Compressor deterioration would tend to reduce the total pressure along the outer liner of the burner and conceivably shift the profile inward. This is because reduced blockage occurs along the inner wall due to poor penetration of the cooling flow through the outer liner secondary cooling holes, leading to a higher temperature along the inner flowpath wall of the turbine. More extensive testing is required to understand the interactions between the compressor discharge profile, combustor and fuel nozzle physical condition, and combustor discharge profile and their impact on turbine performance.

4.4.5 High-Pressure Turbine

Performance Loss Mechanisms

The performance loss mechanisms which cause high-pressure turbine performance deterioration are increased tip clearance and vane bowing and twisting. As in the compressors, the airfoil surface roughness also increases with usage, but the performance penalty is significantly lower than with the other mechanisms responsible for turbine deterioration.

Increased turbine clearance occurs as the result of engine transients and flight loads and the interaction between the blades and outer air seals. Rig test data and analysis has established the relationship between changes in tip clearance and turbine performance, and this relationship is presented in Figure 74.

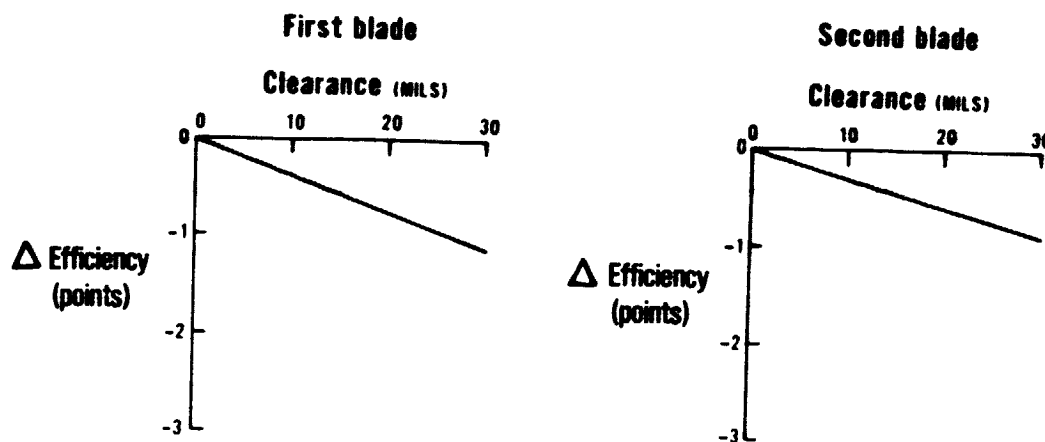


Figure 74 Effect of High-Pressure Turbine Blade Tip Clearance on Turbine Performance - Relatively small changes in tip clearance produce significant losses in turbine performance.

Vane distortion results from both aerodynamic bending loads and the temperature environment. This distortion takes the form of twisting and tilting of the inner platform relative to the vane support. The resulting mismatch of the platform creates a leakage path for cool flow into the hot main stream, resulting in reduced turbine efficiency. Figure 75 shows the first-stage vane leakage path, and Figure 76 shows the leakage path for the second-stage vane. The magnitude of the resulting leakage has been estimated analytically, and the results are shown in Figure 77.

Trailing edge bowing in a turbine vane causes the gas path flow area to change. This change results in a change in high-pressure turbine flow capacity which in turn changes the engine cycle pressure ratio and the TSFC. The magnitude of this effect is shown in Figure 78.

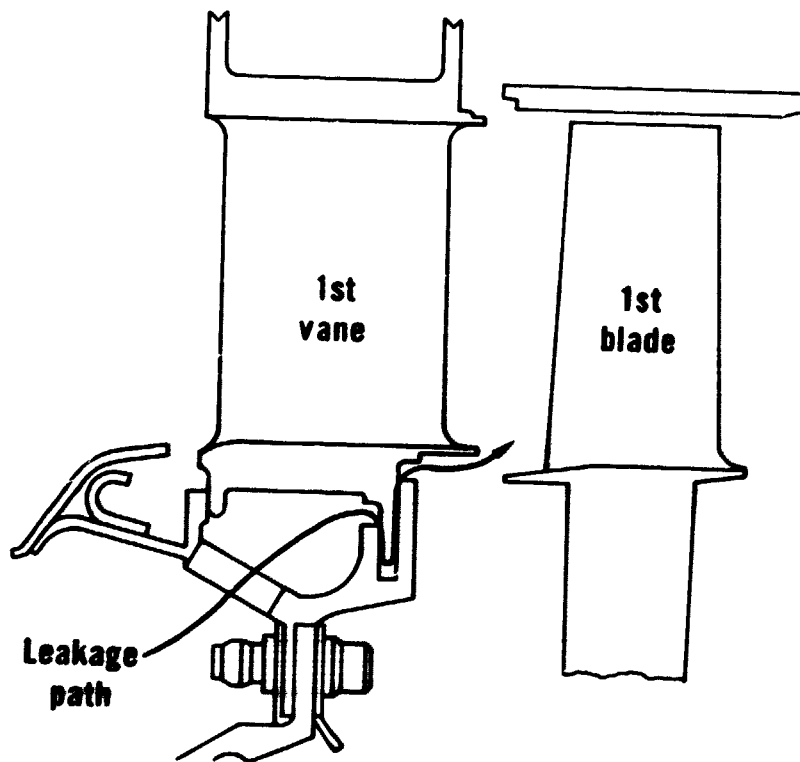


Figure 75 High-Pressure Turbine First-Stage Vane Leakage Path - Vane distortion can result in leakage under the vane platform.

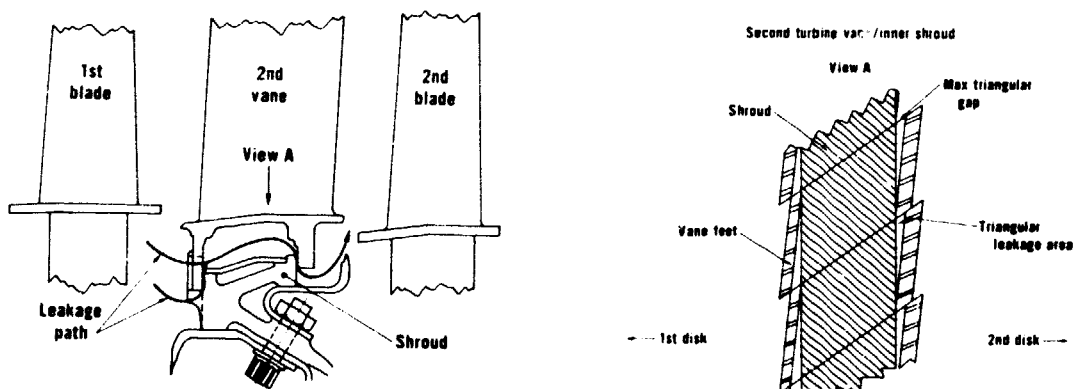


Figure 76 High-Pressure Turbine Second-Stage Vane Leakage Path - Vane twisting creates a leakage path between the vane platform and the sideplates.

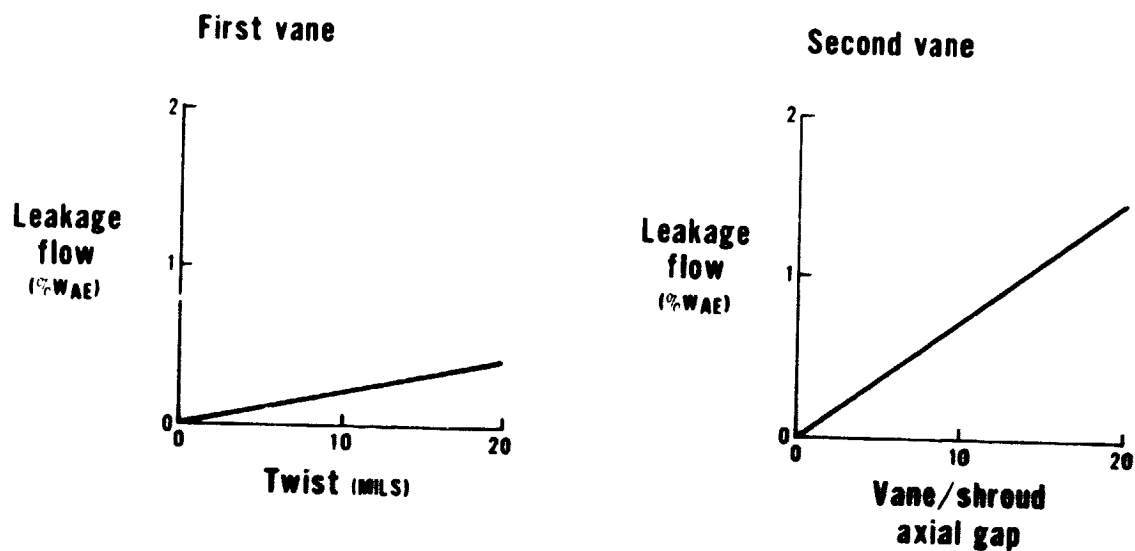


Figure 77 Analytical Estimate of High-Pressure Turbine Vane Leakage Levels as a Percent of Engine Airflow - Significant leakage flows can result from vane distortion.

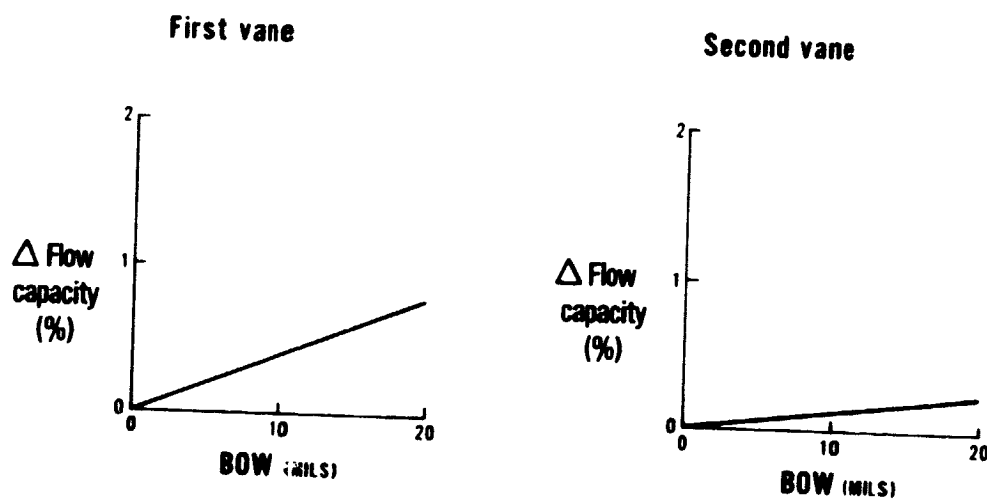


Figure 78 Analytical Estimate of High-Pressure Turbine Flow Capacity Change Produced by Vane Bowing - Vane bowing changes the turbine flow capacity which in turn changes the engine cycle pressure ratio and TSFC.

Increases in the surface roughness of airfoils is caused by particulate matter being deposited on (or roughening) the surface of the airfoils. The increase in roughness increases the friction coefficient causing an increase in boundary layer thickness and pressure loss. The net effect is decreased turbine efficiency.

Parts inspection results (see Figure 79) indicate that the concave surfaces of the airfoils have a higher average roughness than the convex surfaces. This difference occurs because the concave surface of the airfoil is subjected to impaction and scrubbing by particles in the gas stream, while the convex surface is not. The first stage has higher roughness than the second stage, perhaps because of fragmentation of the particles in the first stage.

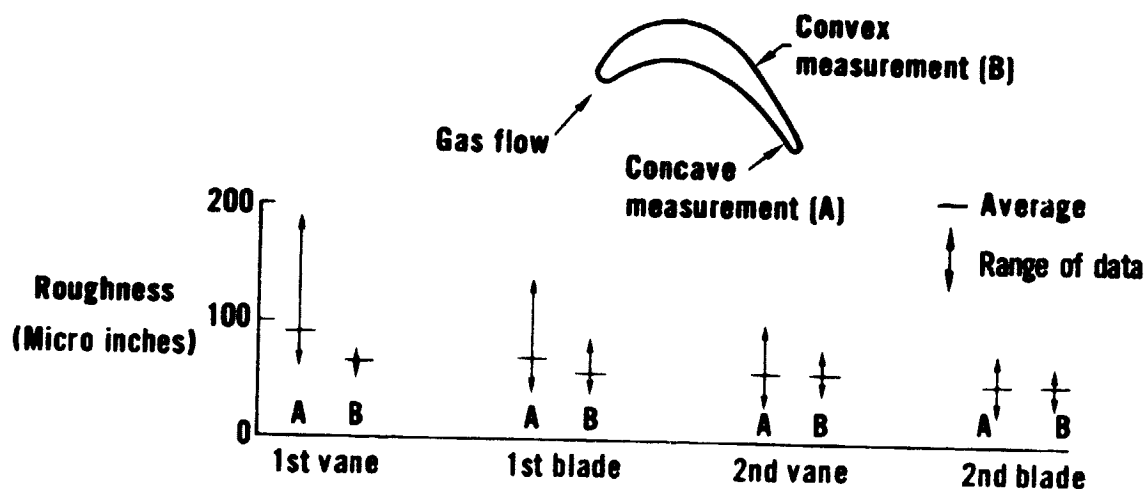


Figure 79 High-Pressure Turbine Surface Roughness Measurement Results - The greatest roughness levels occur on the concave surfaces and in the upstream stage.

Representative Performance Deterioration

Blade-Tip Clearance - Considerable effort was made to correlate tip clearance changes of the unshrouded first-stage blade with flight hours and cycles because of its performance impact. The data, however, did not imply any correlation, perhaps indicating that blade tip rubbing and clearance changes occur early in the life of the engine and that the amount of wear is related to other factors, such as rebuild standards or engine cycles utilization. Typical clearance data plotted as a function of engine cycles is shown in Figure 80.

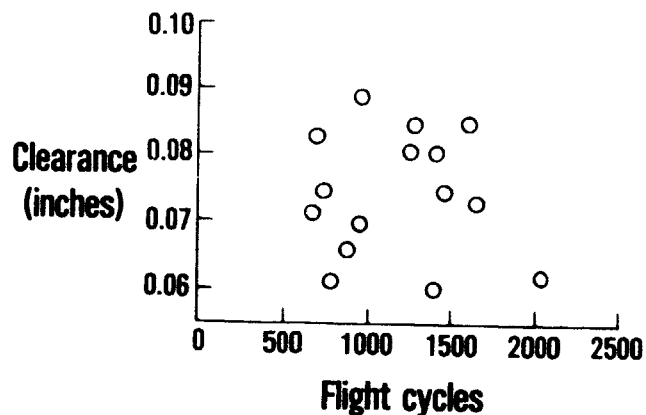


Figure 80 Teardown Clearances of High-Pressure Turbine First-Stage Outer Air Seal - Blade tip clearance data do not correlate with engine cycles.

However, the measured tip clearance data correlated when blade tip wear is plotted as a function of an inferred initial clearance, which is the measured teardown clearance minus the measured blade tip wear. This correlation is shown in Figure 81 and implies that building the turbine with an initial clearance less than 0.073 inch increases the probability of blade rubbing even though data shown for engines with smaller clearances sometimes indicate that these blades suffer very little wear. This implication is substantiated by airline first-stage blade tip build and teardown clearance data shown in Table XVIII. These data show that Airline C's rebuild clearances, which are smaller than Airline A's result in larger clearances at teardown.

The changes in first- and second-stage blade tip clearance with usage have been estimated based upon observation of airline engines and rub predictions based on analytical studies (Reference 2). These estimates were then used to predict the effect of the clearance changes on high-pressure turbine efficiency as a function of engine cycles. The results are presented in Figure 82. The band shown on this figure represents the minimum clearance change predicted from the analytical studies and the maximum clearance based on observations.

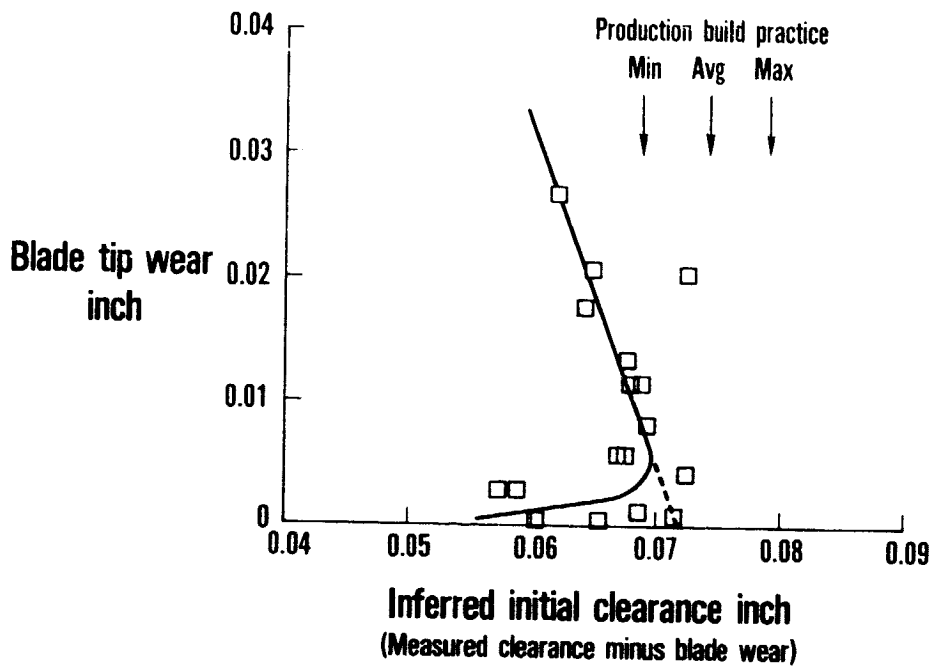


Figure 81 Correlation of High-Pressure Turbine First-Stage Blade Tip Wear With Inferred Initial Clearance - The data indicate that initial build clearances below 0.073 inch expose the turbine to rubbing and substantial tip wear.

TABLE XVIII

AVERAGE TIP CLEARANCES AT BUILD AND TEARDOWN FOR AIRLINES A AND C

	Average Tip Clearances (inch)		
	Build	Teardown	Change
Airline A (60 Engines)	0.078	0.080	0.002
Airline C (9 Engines)	0.068	0.090	0.022

Vane Twist - The distortion or twisting that occurs in the first-stage vanes was found to be very small. The estimated associated efficiency penalty is considered to be negligible.

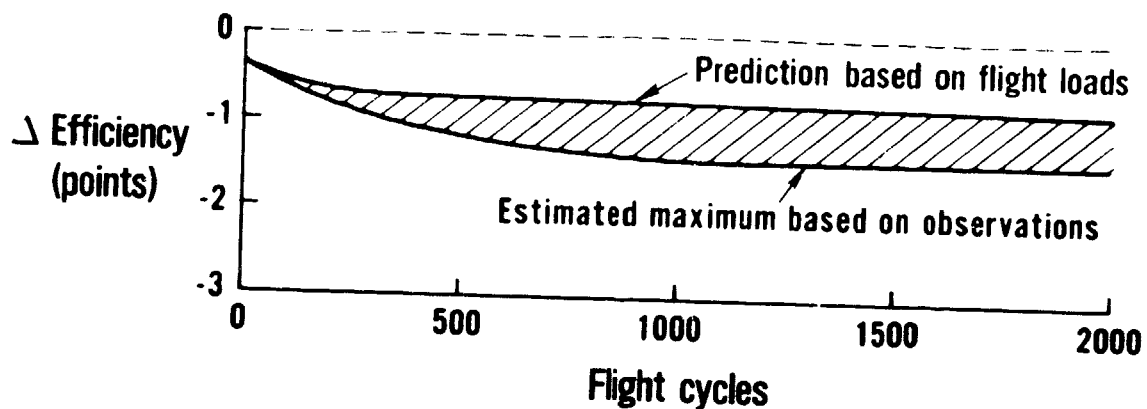


Figure 82 Predicted High-Pressure Turbine Performance Deterioration - Tip clearance changes are estimated to produce more than one percentage point deterioration in turbine efficiency.

A somewhat greater amount of twisting occurs in the second-stage vanes, although it is limited at the inner end by the front and rear inner feet. The axial distance between the feet was measured and a leakage flow was calculated using the correlation shown in Figure 77. The average efficiency penalty is estimated to be 0.55 point, as shown in Figure 83. The band shown on this figures represents data scatter in the part inspection data.

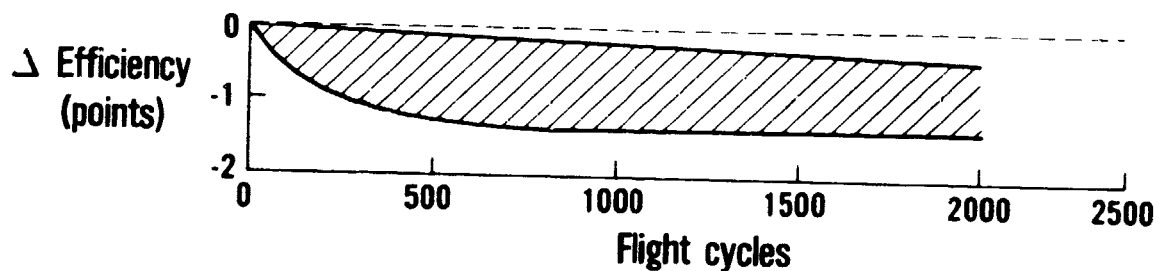


Figure 83 High-Pressure Turbine Performance Deterioration Resulting from Second-Stage Vane Twisting - The data scatter shown is based on the results of parts inspection data.

Vane Bowing - Inspection of used parts revealed a considerable range of vane bowing, which is reflected in the range of flow capacity changes shown in Figure 84. The average flow capacity increase for first-stage vane bow is estimated to be 0.2 percent, while the increase for the second stage is estimated to be 0.1 percent.

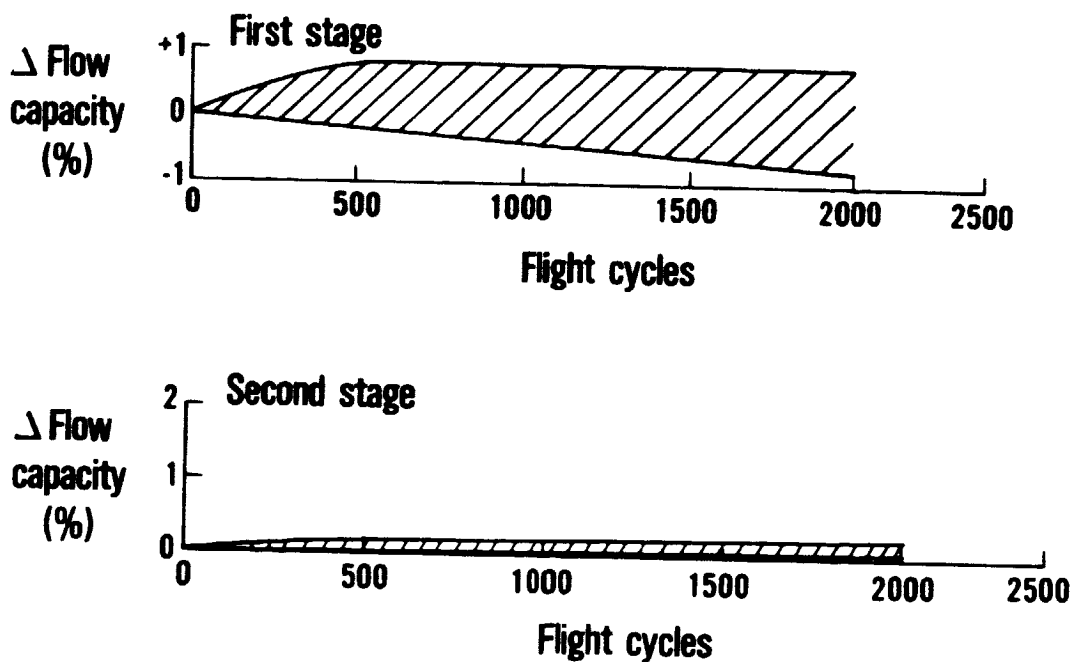


Figure 84 High-Pressure Turbine First- and Second-Stage Flow Capacity - Vane bowing results in approximately 0.2 percent increase in flow capacity in the first stage and 0.1 percent in the second stage.

Surface Roughness - The predicted effects of surface roughness levels on turbine efficiency penalties are shown in Figure 85. The surface roughness levels measured during service parts inspection were such that negligible performance loss could be assigned to this deterioration mechanism.

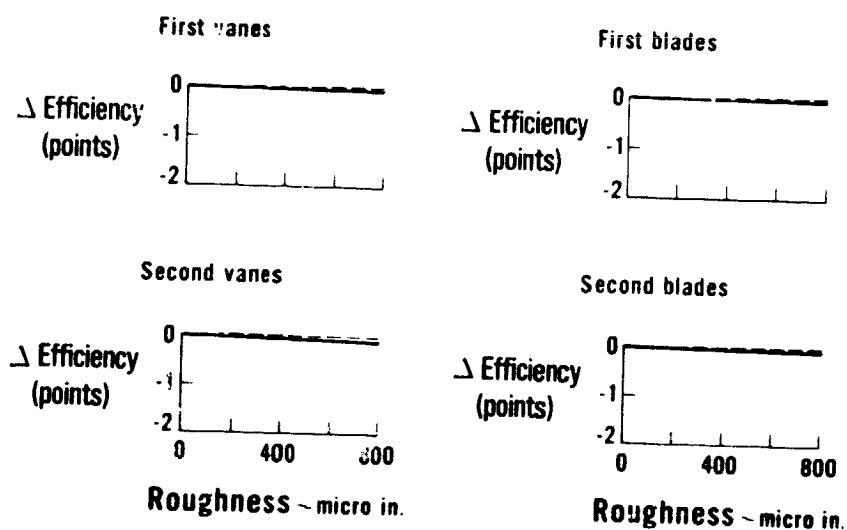


Figure 85 Estimated High-Pressure Turbine Efficiency Loss Associated With Surface Roughness - Extremely high levels of airfoil roughness would be required to produce any significant effect on high-pressure turbine performance.

Overall Deterioration - The combined effects of tip clearance changes and vane twist and bow on high pressure turbine efficiency and flow capacity are shown in Figure 86. The average effect and the range based on measured part variations are shown for each mechanism along with results of back-to-back service engine tests.

The engine data correlates well with the overall estimated efficiency loss. The data indicate that the average high-pressure turbine loses 1.45 percent in efficiency after 1000 cycles of operation. The flow capacity data, however, did not correlate with the estimated effect. The wide differences could be attributed to compressor discharge pressure profile shifts, which could introduce errors in the measurement of the compressor exit pressure (P_{S4}) which is used to calculate the turbine first stage vane area (A_5) and flow capacity.

Performance Recovery Approach

The performance loss due to blade tip clearance increases is recoverable by replacing grooved seal lands with new material, repairing damaged blade tips and knife edges, and by rebuilding the engine to recommended tolerances including those on blade length and offset grind.

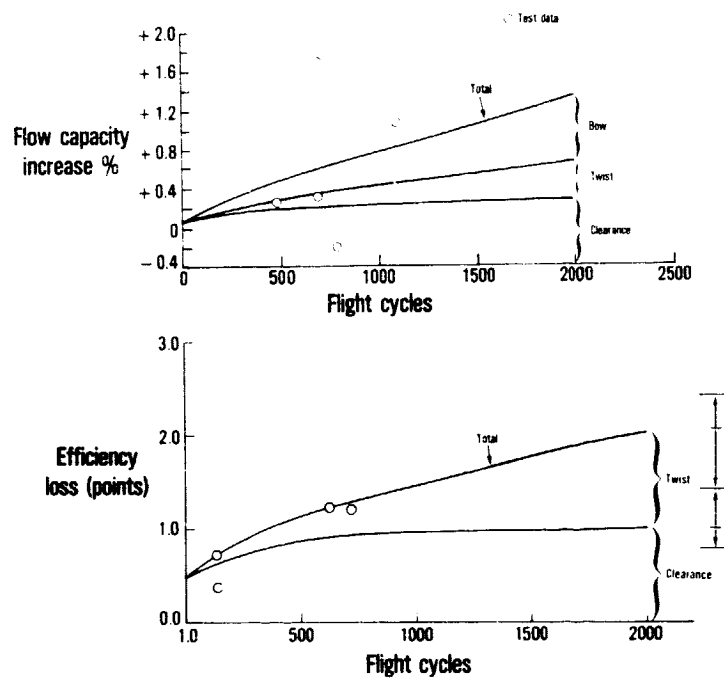


Figure 86 High-Pressure Turbine Overall Performance Deterioration - Back-to-back performance testing shows substantial variation in flow capacity, possibly because of pressure profile shifts.

The performance loss due to vane distortion is temporarily recoverable by restoring the vanes to production tolerances. If a vane is twisted upon removal from its first service run, it can be reworked to restore it to the as-new appearance. However, this repair would be effective for only a limited period of time since the vane returns to the pre-worked twist and then continues twisting as if it had never been repaired. For the first-stage vanes, twist is not a significant factor, and restoring the part to production tolerances is sufficient. For the second-stage vanes, the axial width of the inner feet should be restored by a buildup of hardfacing.

The performance loss due to bow can also be temporarily recovered by restoring the part to production tolerances. The usual way this is done is by hot restriking the airfoil.

Although the performance loss due to surface roughness is small, it is recoverable when the used airfoils are cleaned or stripped and recoated. This procedure restores the surface finish to the as-new condition.

Concerns

The inability to correlate first-stage blade rub depth or blade tip wear directly with hours or cycles suggests that other mechanisms such as combustor profile shift, rework clearance standards, case out-of-roundness, or other factors yet to be defined are involved in high pressure turbine performance deterioration.

4.4.6 Low-Pressure Turbine

Performance Loss Mechanisms

The deterioration of low-pressure turbine performance is caused by clearance changes, twisting and bowing of vanes, and vane inner diameter "soldiering". Airfoil surface roughness increases with service usage but does not significantly contribute to low-pressure turbine performance loss.

The estimated effect of low-pressure turbine clearance changes on efficiency is shown in Figure 87, based on analytical calculations.

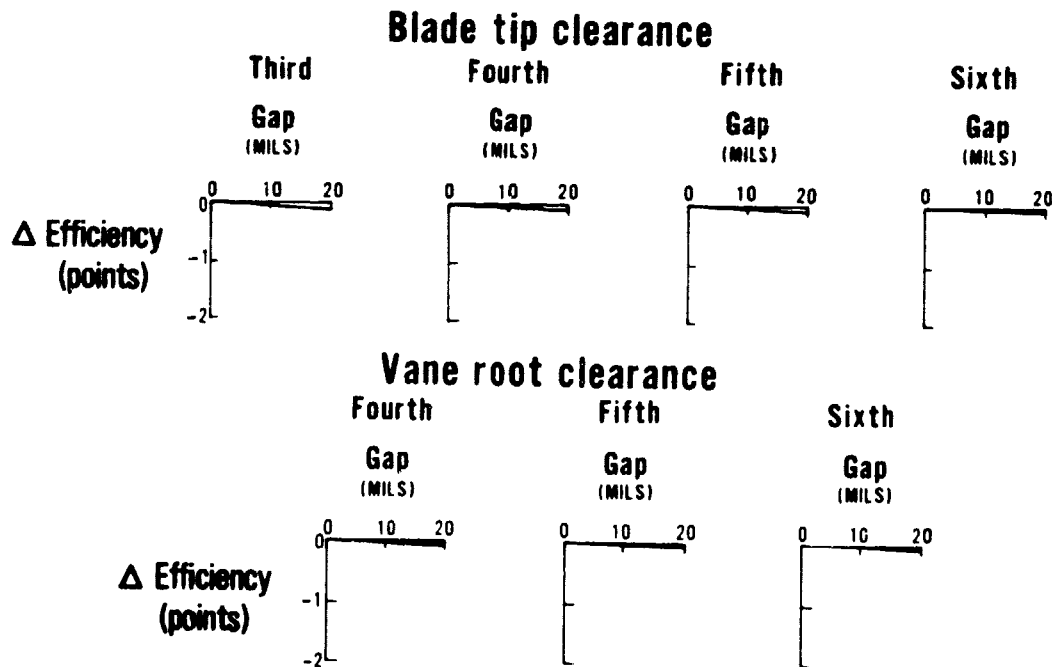


Figure 87 Effect of Blade Tip Clearance on Low-Pressure Turbine Efficiency - The combined effect of a 0.020-inch clearance change in all stages would be significant even though the effect of a clearance change in one individual stage would be very small.

Twisting and tilting of the inner platform relative to the fastened-in-place outer platform, caused by thermal loads, produces the leakage path shown in Figure 88. This thermal distortion results in low energy air mixing into the gas path, yielding a loss in turbine efficiency.

Vane trailing edge bow causes the gas path flow area to change resulting in a change in low pressure turbine flow capacity as shown in Figure 89.

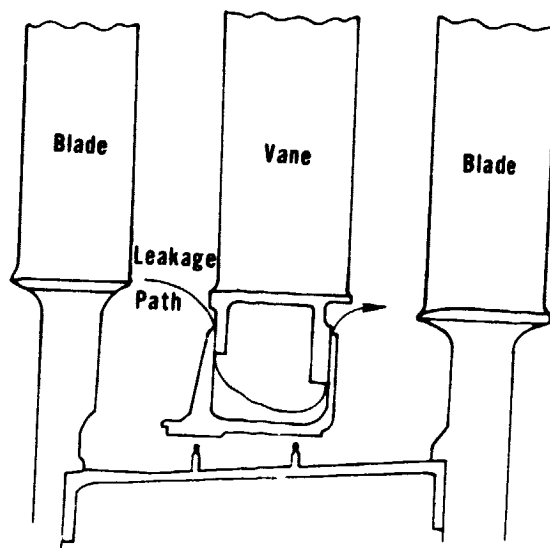


Figure 88 Low-Pressure Turbine Leakage Path Produced by Vane Twisting at Inner Platform - The leak that results causes a loss in turbine efficiency as the air mixes back into the gas path at the downstream side of the vane.

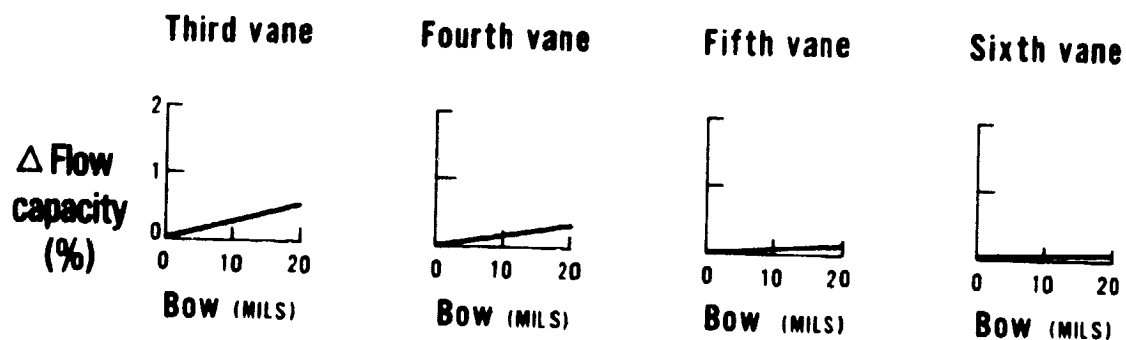


Figure 89 Estimated Effect of Vane Bow on Low-Pressure Turbine Flow Capacity - Vane bowing is estimated to increase the low-pressure turbine flow capacity by less than 1 percent.

Misalignment of vane inner platforms is termed "soldiering." It creates steps in the inner flow-path surface which cause aerodynamic losses. From visual observation of low-pressure turbine modules before teardown, the step heights were in the 0.030 to 0.050 inch range. The effect of these steps on low-pressure turbine efficiency was estimated based on analytical predictions, and the results are shown in Figure 90.

Changes in surface roughness in the low-pressure turbine are relatively small, as shown in Figure 91, and are smaller than that experienced in the high-pressure turbine. Measured roughness in this range, is estimated to cause negligible efficiency loss in the low-pressure turbine.

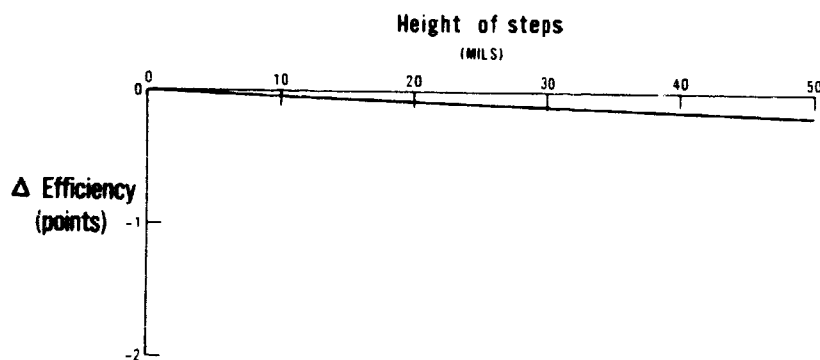


Figure 90 Effect of Vane Inner Platform Misalignment on Low-Pressure Turbine Efficiency - Misalignment, or "soldiering", typically produces steps in the gas path that range from 0.030 to 0.050 inch with a consequent efficiency penalty of about 0.2 percentage point.

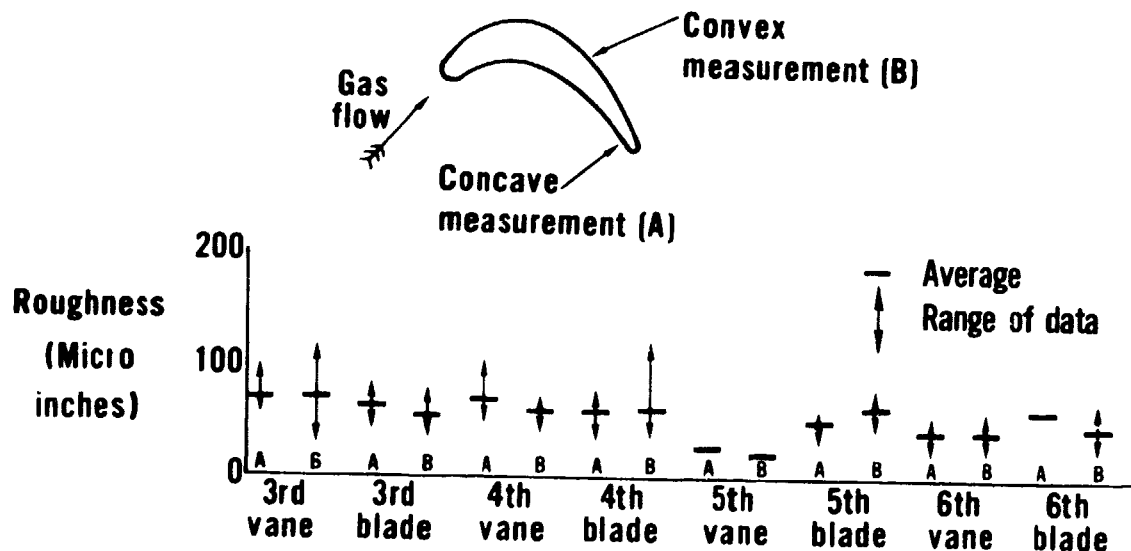


Figure 91 Low-Pressure Turbine Airfoil Surface Roughness Measurement Data - The range of roughness in the low-pressure turbine is much less than that in the high-pressure turbine.

Representative Performance Deterioration

The effect of blade tip clearance increases on low-pressure turbine efficiency with increasing flight cycles has been estimated based on observations, rub predictions based on analytical studies of the effects of flight loads (Reference 2), and airline rebuild standards. These results are shown in Figure 92 as a function of the number of flight cycles. The average efficiency loss is approximately 0.25 percentage point.

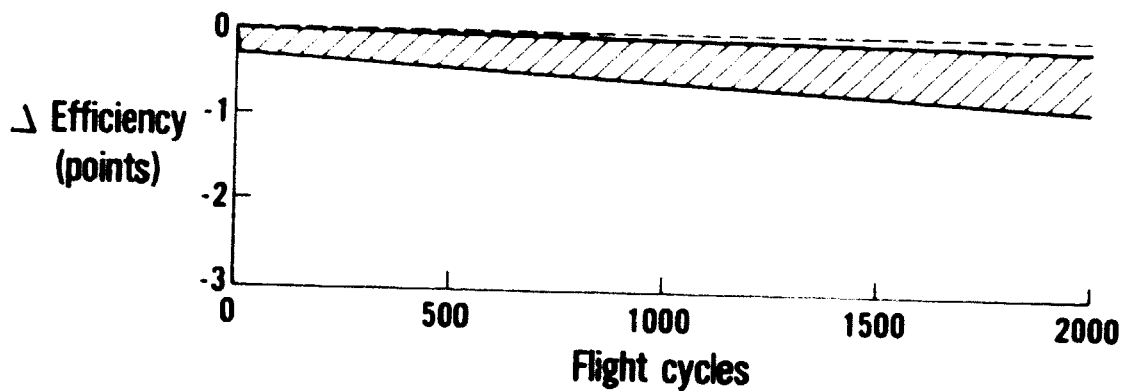


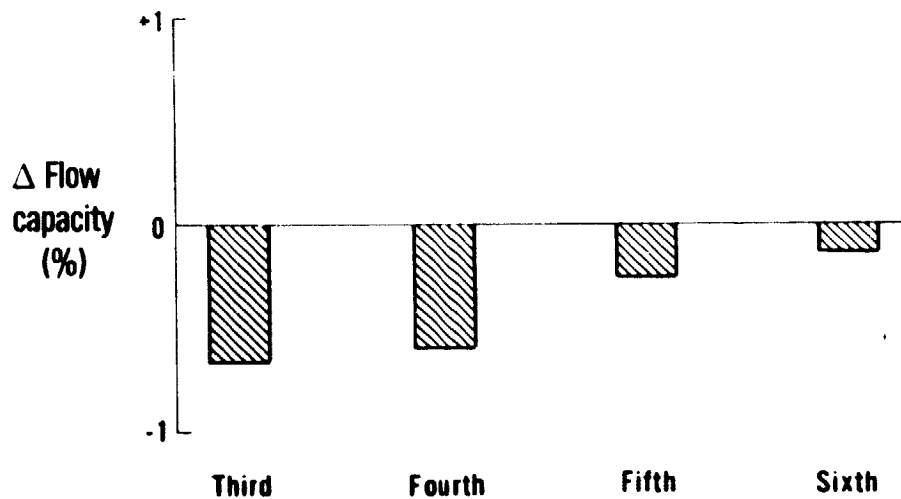
Figure 92 Effect of Blade Tip Clearance Changes on Low-Pressure Turbine Efficiency - Increases in blade tip clearances are estimated to reduce average low-pressure turbine efficiency by approximately 0.25 percentage point.

Twist was not measured in the low-pressure turbine vanes collected for inspection because analytical studies have shown that the leakage flow levels were very small (on the order of 0.06 percent of engine core airflow). Such levels of leakage would have a negligible effect on efficiency.

A decrease in flow capacity is estimated to result based on measured low-pressure turbine vane parts, as shown in Figure 93. The decrease in flow capacity is the result of vane twisting in combination with vane bowing which reduce the effective vane flow area.

Vane soldering was observed in the third- and fourth-stage vanes, with the greatest amount found in the third stage. The average efficiency penalty associated with the observed soldering was estimated to be 0.13 point.

The measured roughness for low-pressure turbine airfoils was in the range of 40 to 80 microinches. For roughness in this range, there is negligible efficiency loss in the low-pressure turbine.



Note: No time/cycle information available on LPT parts

Figure 93 Average Loss in Low-Pressure Turbine Flow Capacity Associated With Vane Bow and Twist - Average flow capacity losses ranged from 0.6 percent in the third stage to 0.2 percent in the sixth stage.

Overall Deterioration

The combined effect on low-pressure turbine performance versus flight cycles based on part inspection data, build standards, and clearance changes is shown in Figure 94. As can be seen, the overall efficiency loss due to clearance changes and vane soldering is about 0.4 percentage points after 2000 flight cycles. The effect of clearance changes on flow capacity after 2000 flight cycles is about a 0.2 percent increase.

Performance Recovery Approach

Most of the performance loss in the low-pressure turbine is due to clearance changes which are recoverable. This is achieved by:

1. Replacing grooved seal lands with new material,

2. Repairing bent or broken knife edges, and
3. Grinding the lands and knife edges to bring the clearance back to production limits.

Soldiering can be controlled by fabricating individual vanes into groups of two or three vanes. Experience has shown that this procedure will usually eliminate platform misalignment. Pratt & Whitney Aircraft experience has also shown that clustered vanes provide higher durability and provide up to a 0.2 percent TSFC improvement due to reduction in vane leakage paths between individual vanes.

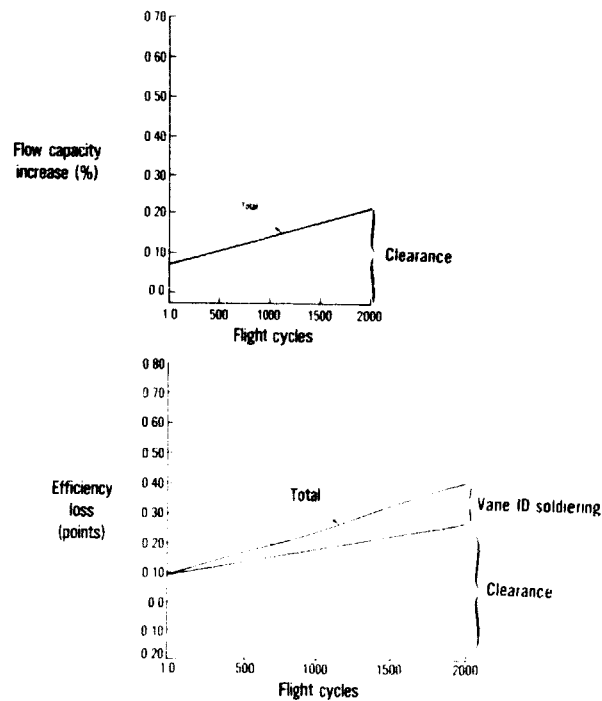


Figure 94 Estimated Average Overall Low-Pressure Turbine Performance Deterioration - The data indicate that the average low-pressure turbine loses 0.25 percent in efficiency and gains 0.15 percent in flow capacity after 1000 cycles of operation.

The performance loss caused by low-pressure turbine vane bowing can be restored by hot restriking vanes that are over the overhaul limit. The timing of all of these repairs should be keyed to an as-required disassembly of the low-pressure turbine module because the potential for performance improvement is small.

Concerns

During the data collection efforts, it was impossible to obtain sufficient low-pressure turbine parts with known usage intervals since the airlines had not maintained records of part times. The credibility of the low-pressure turbine performance loss levels is therefore suspect and no mechanisms are available at this time to improve the estimate. Airline D, however, reported that they had back-to-back tested an engine with a high time low-pressure turbine module and an all new low-pressure turbine module and were unable to detect any significant change in engine performance. This result would tend to indicate that the loss is small and support the general level of the analytical estimates.

4.5 VERIFICATION AND DATA ENHANCEMENT

As described in Section 3.3.4, the validity of the analyses were determined by conducting top-down and bottom-up analyses to define module performance deterioration and then comparing the results. This section presents the results of these analyses for Airline A to illustrate the process and then presents final results for all airlines to demonstrate the quality of agreement achieved.

4.5.1 "Top Down" Analysis Procedure

The top down analysis begins with definition of parameter deviations from a production base line. This requires correction of test data to standard conditions of temperature, pressure, and humidity; additional correction for differences in airline and engine manufacturer test cells, and any differences in engine back-to-back test configurations (such as nozzles), plus corrections for any differences in internal part configuration between the production base line and the in-service engine.

An important feature of the analytical technique mentioned previously was the use of parameter coupling to reduce the number of unknowns in the top down data sets. Table XIX illustrates the effectiveness of this technique by showing the output of the engine simulation using various possible parameter coupling techniques as well as the one finally used in the data analysis. In this table, the first column shows actual engine postrepair performance data as measured. The remaining columns show the output of the engine simulation when it iterated the module performance parameters in an attempt to match the measured overall engine performance parameters.

The first three engine simulation columns show the effect of assuming that the low-pressure spool losses occur in (1) only the fan, (2) only the low-pressure turbine, and (3) in both the fan and the low-pressure turbine with an approximately 50/50 split. Although these assumptions

permitted a reasonably close match between the predicted and measured overall engine data, the predicted module performance deterioration levels are not reasonable. They predict no loss in the low-pressure compressor, and, when all losses are assigned to the low-pressure turbine, result in an unreasonably high low-pressure turbine loss level.

TABLE XIX
 TOP DOWN ANALYSIS FOR AIRLINE B POSTREPAIR PERFORMANCE DATA
 AT 3500 CYCLES SHOWING THE EFFECTS OF
 LOW-PRESSURE ROTOR LOSS-SPLIT ASSUMPTION ON PREDICTED MODULE LOSSES

Measured Values	Predicted by Engine Simulation					
	Low-Pressure Fan Only	Low-Pressure Spool Efficiency Loss Turbine Only	Low-Pressure Spool Efficiency Loss 50/50 Split	Coupled Fan Efficiency Loss and Flow Capacity Loss	Both Fan and Low-Pressure Compressor Efficiencies and Flow Capacity Coupled	
OVERALL ENGINE PERFORMANCE						
Change In:						
Net Thrust (%)	-1.74	-1.9	-1.9	-1.8	-1.4	-1.5
Fuel Flow (%)	+1.15	+1.0	+1.0	+1.1	+1.1	+1.15
Innust Specific Fuel Consumption (%)	+2.9	+2.9	+3.0	+2.9	+2.5	+2.7
Low-Pressure Rotor Speed (%)	+1.1	+1.1	+1.1	+1.1	+1.1	+1.1
High-Pressure Rotor Speed (%)	+1.2	+1.2	+1.2	+1.2	+1.2	+1.2
Compressor Exit Total Temperature (°F)	+8	+8	+8	+8	+8	+8
Exhaust Gas Temperature (°F)	+19	+21	+21	+21	+21	+26
Fan/Low-Pressure Compressor Pressure Ratio (%)	+1.4	+1.5	+1.5	+1.4	+1.4	+1.5
Turbine Expansion Ratio (%)	-1.9	-1.7	-1.7	-1.9	-1.9	-1.9
MODULE PERFORMANCE						
Change In:						
Fan						
Efficiency (Points)	-2.6	-	-1.3	-1.4	-1.5	
Flow Capacity (%)	-2.4	-2.4	-2.4	-2.1	-2.2	
Low-Pressure Compressor						
Efficiency (Points)	-	-	-	-	-	
Flow Capacity (%)	-0.85	-0.09	-0.09	-1.0	-0.8	
High-Pressure Compressor						
Efficiency (Points)	2.1	+2.1	+2.1	+2.1	+2.0	
High-Pressure Turbine						
Efficiency (Points)	+2.6	+2.7	+2.7	+3.0	+1.4	
Inlet Area (%)	-	-	-	-	-	
Low-Pressure Turbine						
Efficiency (Points)	+1.5	+2.4	+1.1	+2.6	+2.2	
Inlet Area (%)	-	+1.4	+1.4	+1.7	+1.6	

If fan efficiency loss is coupled to fan flow capacity loss (as shown in the next column), the simulation program assigns the rest of the low-pressure spool efficiency loss to the low-pressure turbine, again with no loss in the low-pressure compressor. The last column presents the solution obtained when the low-pressure compressor efficiency loss is coupled to its own flow capacity loss in addition to the coupling of the fan loss previously discussed. This is the most likely scenario and the one used for the final data analysis. The resulting low-pressure turbine efficiency loss is very low and is consistent with observed low-pressure turbine damage which has generally been minimal based on module inspections. In addition, the high-pressure losses are predicted to be negligible, which is consistent with the condition of the high-pressure turbine in postrepair engines, since this module is usually repaired frequently.

ORIGINAL PAGE IS
 OF POOR QUALITY

It is important to note that the simulation provides good matching with the measured engine data in every case. The distribution of losses, therefore, cannot be obtained on the basis of the simulation and the engine data alone, but must depend on hardware conditions, experience, and engineering judgement. This latter assessment is made using the bottom up analysis and is discussed in the next section.

The top down analysis of Airline A's average prerepair engine at 3500 flight cycles at take-off engine pressure ratio is shown in Table XX. Here, two simulation columns are shown to the right of the test cell measured parameter column. The first column presents the simulation results with no adjustments made to the test cell data. This column indicates component shifts that appear reasonable except for the fan, which has a very low loss level. The average fan blades for this operator were known to have a high cycle time since last repair, which is inconsistent with the negligible loss level shown. Also, a thrust increase is indicated by the data for the deteriorated engine which is inconsistent with all other operator experience in general.

It was assumed, therefore, that a 1 percent thrust loss would be more reasonable and consistent with the experience of the other airlines, with the apparent increase being the result of an error in the thrust test cell correction. The results of this assumption are presented in the right hand column. As shown, the assumed 1 percent thrust loss results in a more reasonable estimate of fan loss.

4.5.2 "Bottom Up" Analysis Procedure - Long Term Deterioration

Bottom up analysis or modeling of performance deterioration requires first that module age (in flight cycles) versus engine cyclic age be determined. These trends have been developed through analysis of airline overhaul shop records on part replacement and repair. Figure 95 shows a typical plot for average part age versus engine cyclic age. The curve is typical in that it shows significant differences among the airlines studied as a results of differences in maintenance practices.

TABLE XX

TOP DOWN ANALYSIS RESULTS FOR AIRLINE A PREREPAIR
 PERFORMANCE DATA AT 3500 CYCLES SHOWING EFFECTS
 OF TEST STAND DATA ADJUSTMENTS

	Measured Values	Simulation Prediction	
		Based on Measured Values	Based on Adjusted Values
OVERALL ENGINE PERFORMANCE			
Change in:			
Net Thrust (%)	+0.35	+0.5	-1.0
Fuel Flow (%)	+3.7	+3.8	+3.7
Thrust Specific Fuel Consumption (%)	+3.4	+3.2	+4.8
Low-Pressure Rotor Speed (%)	+0.5	+0.5	+0.5
High-Pressure Rotor Speed (%)	+0.75	+0.75	+0.75
Compressor Exit Total Temperature (°F)	+7.	+7.	+6.
Exhaust Gas Temperature (°F)	+70	+70	+75
Fan/Low-Pressure Compressor Pressure Ratio (%)	+1.2	+1.3	+1.2
Turbine Expansion Ratio (%)	-1.6	-2.0	-2.6
MODULE PERFORMANCE			
Change in:			
Fan			
Efficiency (Points)		-0.1	-0.8
Flow Capacity (%)		-0.2	-1.2
Low-Pressure Compressor			
Efficiency (Points)		-0.4	-1.2
Flow Capacity (%)		-0.7	-2.0
High-Pressure Compressor			
Efficiency (Points)		-2.6	-2.5
High-Pressure Turbine			
Efficiency (Points)		-0.6	-1.2
Inlet Area (%)		+1.7	+1.7
Low-Pressure Turbine			
Efficiency (Points)		-0.9	-1.4
Inlet Area (%)		-	+0.8

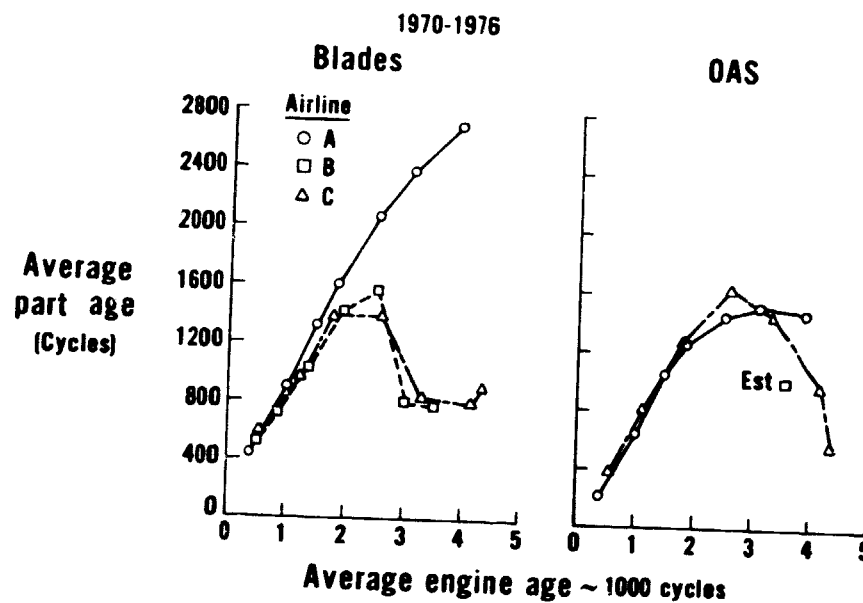


Figure 95 JT9D Fan Module Part Age - For the fan, average part age for Airline A is significantly higher than that for the other airlines studied.

From these data, an average module age was determined for each module, for each operator, at 3500 engine flight cycles, and the results are shown in Table XXI. For the fan, the module age was computed as the average of blade and rub strip age. For the low-pressure compressor, only rub strip age was used since inspection of deteriorated parts has revealed that the rub strips are by far the dominant area of deterioration. For the high-pressure compressor, an average of blade, stator vane, and outer and inner airseal age was used. For both turbines, vane age was used to predict vane bow and twist damage, and outer air-seal age for losses due to clearance increase.

The next step in the bottom up modeling approach requires definition of the performance loss of the modules at a specific age. These trends were developed from the analysis of used parts discussed previously. A typical plot is shown in Figure 96.

Using the module ages listed in Table XXI, the performance loss was read from the appropriate curves and used in the engine simulation to obtain predicted performance parameter shifts.

TABLE XXI
 MODULE AVERAGE CYCLIC AGE
 AT 3500 ENGINE FLIGHT CYCLES

	Module Age (cycles) for Airline		
	A	B	C
Fan	2030	890	1095
Low-Pressure Compressor	1850	400	1800
High-Pressure Compressor	2610	1825	2575
High-Pressure Turbine:			
Outer Air Seals	725	250	375
Blades	725	150	325
Vaness	700	100	600
Low-Pressure Turbine:			
Outer Air Seals	2750	400	1650
Vaness	2300	1200	2350

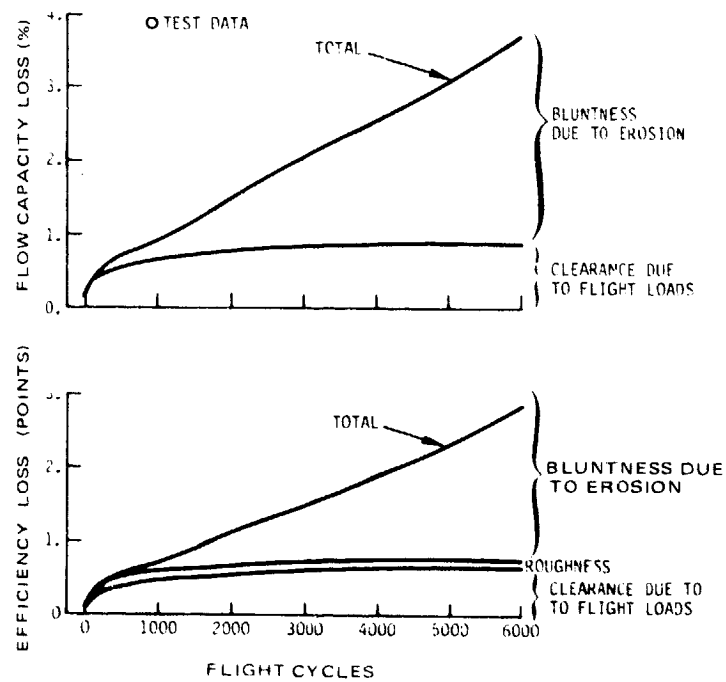


Figure 96 Fan Module Performance Vs. Module Age - Plots such as these were used to establish the relationship between module age and performance deterioration.

The results of the bottom up analysis for Airline A are shown in Table XXII. The column to the right of the observed parameter shifts shows the simulation results achieved when the engine simulator is run with component decrements obtained directly from the plots of module performance versus age, using the module ages shown in Table XXI. The simulation iteration resulted in good matching with the test data except for low-pressure rotor speed, low-pressure compressor pressure ratio, and high-pressure rotor speed. The latter difference is relatively large (-0.1 versus 0.75 percent) but is not considered to be significant for two reasons: (1) variable vane field trim alters flow capacity and high-pressure rotor speed independent of deterioration, and (2) a change in high-pressure compressor flow capacity does not significantly affect any gas generator parameter other than the high-pressure rotor speed.

TABLE XXII
 BOTTOM UP ANALYSIS RESULTS FOR AIRLINE A PREREPAIR
 PERFORMANCE DATA AT 3500 CYCLES

	Measured Values	Simulation Prediction	
		Initial Prediction	With Build Standard Adjustments
OVERALL ENGINE PERFORMANCE			
Change in:			
Net Thrust (%)	+0.35	+0.2	-1.0
Fuel Flow (%)	+3.7	+3.8	+3.5
Thrust Specific Fuel Consumption (%)	+3.4	+3.6	+4.6
Low-Pressure Rotor Speed (%)	+0.5	+1.5	+0.7
High-Pressure Rotor Speed (%)	+0.75	-0.1	+0.04
Compressor Exit Total Temperature (°F)	+7	+9	+11
Exhaust Gas Temperature (°F)	+70	+72	+69
Fan/Low-Pressure Compressor Pressure Ratio (%)	+1.2	+3.5	+1.6
Turbine Expansion Ratio (%)	-1.6	-1.1	-1.4
MODULE PERFORMANCE			
Change in:			
Fan			
Efficiency (Points)		-1.1	-1.1
Flow Capacity (%)		-1.4	-1.4
Low-Pressure Compressor			
Efficiency (Points)		-0.9	-0.9
Flow Capacity (%)		-1.9	-1.9
High-Pressure Compressor			
Efficiency (Points)		-2.6	-2.6
High-Pressure Turbine			
Efficiency (Points)		-1.3	-1.3
Inlet Area (%)		+0.6	+0.6
Low-Pressure Turbine			
Efficiency (Points)		-0.2	-0.7
Effect of 0.02 Inch			
Inlet Area (%)		+0.02	+0.3*
Clearance Increase			

*Includes 0.5 percent low-pressure turbine leakage

Although relatively good matching was obtained, a further modification was made to the simulation input because the documented rebuild standards discussed previously show that Airline A builds the low-pressure turbine 0.020 inch open in tip clearance relative to the nominal clearance. Also, the comparable top down analysis for this airline operator showed an effective low-pressure turbine inlet area increase relative to production due either to vane bow or leakage. Since the used part analysis did not show significant vane bow, a low-pressure turbine leak was assumed. The final simulation, which includes both these changes, is shown in the last column of Table XXII.

4.5.3 Comparison of Top Down and Bottom Up Analysis Results

The final step in the verification and data enhancement portion of the analysis was comparison of the top down and bottom up analysis results and adjustment of the data where indicated. Tables XXIII, XXIV, and XXV show final side-by-side results of the top down and bottom up models for each of the airlines investigated. In general, it will be noted that good agreement is obtained between the results of the two analyses with the exception of the high-pressure rotor speed and the turbine flow areas, and these differences are not of great concern since they typically are related to field trim adjustments rather than deterioration.

TABLE XXIII
RESULTS OF TOP DOWN AND BOTTOM UP ANALYSIS RESULTS FOR AIRLINE A
PREREPAIR PERFORMANCE DATA AT 3500 CYCLES
AFTER APPROPRIATE DATA ADJUSTMENTS

	Measured Values	Simulation Prediction	
		Top Down Prediction	Bottom Up Prediction
OVERALL ENGINE PERFORMANCE			
Change in:			
Net Thrust (%)	+0.35	-1.0	-1.0
Fuel Flow (%)	+3.7	+3.7	+3.5
Thrust Specific Fuel Consumption (%)	-3.4	-4.8	-4.6
Low-Pressure Rotor Speed (%)	+0.5	+0.48	+0.7
High-Pressure Rotor Speed (%)	+0.75	+0.75	+0.04
Compressor Exit Total Temperature (°F)	+7	+6	+11
Exhaust Gas Temperature (°F)	+70	+75	+69
Fan/Low-Pressure Compressor Pressure Ratio (%)	+1.2	+1.2	+1.6
Turbine Expansion Ratio (%)	-1.6	-2.6	-1.4
MODULE PERFORMANCE			
Change in:			
Fan			
Efficiency (Points)		-0.8	-1.1
Flow Capacity (%)		-1.2	-1.4
Low-Pressure Compressor			
Efficiency (Points)		-1.2	-0.9
Flow Capacity (%)		-2.	-1.9
High-Pressure Compressor			
Efficiency (Points)		-2.5	-2.6
High-Pressure Turbine			
Efficiency (Points)		-1.2	-1.3
Inlet Area (%)		+1.7	+0.6
Low-Pressure Turbine			
Efficiency (Points)		-1.4	-0.7
Inlet Area (%)		+0.8	+0.3 (+ Leakage)

The results for Airline B included additional differences in measured thrust and fuel flow (although predicted thrust specific fuel consumption was close to the measured value). In addition, the predicted exhaust gas temperature was higher than measured. However, the component shifts predicted by the two analyses for this airline are similar with the exception of the turbine areas. This airline has had significant problems with turbine vane distress and it is possible that the average trend of vane area change with usage from part inspection data understates the problem with respect to this airline or that historical vane area rework and area classing problems existed.

TABLE XXIV
RESULTS OF TOP DOWN AND BOTTOM UP ANALYSIS RESULTS FOR AIRLINE B
PREREPAIR PERFORMANCE DATA AT 3500 CYCLES
AFTER APPROPRIATE DATA ADJUSTMENTS

	Measured Values	Simulation Prediction	
		Top Down Prediction	Bottom Up Prediction
OVERALL ENGINE PERFORMANCE			
Change in:			
Net Thrust (%)	-1.7	-1.5	-0.7
Fuel Flow (%)	+1.0	+0.95	+2.1
Thrust Specific Fuel Consumption (%)	+2.8	+2.5	+2.9
Low-Pressure Rotor Speed (%)	+1.1	+1.1	+0.9
High-Pressure Rotor Speed (%)	+1.1	+1.2	+0.1
Compressor Exit Total Temperature (°F)	+7	+9	+11
Exhaust Gas Temperature (°F)	+18	+20	+43
Fan/Low-Pressure Compressor Pressure Ratio (%)	+1.4	+1.4	+1.7
Turbine Expansion Ratio (%)	-2.0	-1.8	-0.6
MODULE PERFORMANCE			
Change in:			
Fan			
Efficiency (Points)		-1.5	-1.1
Flow Capacity (%)		-2.2	-1.4
Low-Pressure Compressor			
Efficiency (Points)		-0.6	-0.8
Flow Capacity (%)		-1.0	-1.4
High-Pressure Compressor			
Efficiency (Points)		-2.0	-2.1
High-Pressure Turbine			
Efficiency (Points)		-	-0.6
Inlet Area (%)		+2.8	+0.3
Low-Pressure Turbine			
Efficiency (Points)		-0.1	-0.3
Inlet Area (%)		+1.7	+0.1 (+ Leakage)

Results for Airline C are shown in Table XXV. The excellent agreement between the top down and bottom up predictions of module performance and overall agreement of the predicted engine performance parameter changes with the measured values indicate that the losses assessed for the module are credible.

TABLE XXV
RESULTS OF TOP DOWN AND BOTTOM UP ANALYSIS RESULTS FOR AIRLINE C
PREREPAIR PERFORMANCE DATA AT 3500 CYCLES
AFTER APPROPRIATE DATA ADJUSTMENTS

	Measured Values	Simulation Prediction	
		Top Down Prediction	Bottom Up Prediction
OVERALL ENGINE PERFORMANCE			
Change in:			
Net Thrust (%)	-0.6	-0.5	-0.6
Fuel Flow (%)	+4.4	+4.1	+4.5
Thrust Specific Fuel Consumption (%)	+4.9	+4.7	+5.2
Low-Pressure Rotor Speed (%)	+0.9	+0.8	+0.4
High-Pressure Rotor Speed (%)	+1.2	+1.1	-
Compressor Exit Total Temperature (°F)	-	+11	+6
Exhaust Gas Temperature (°F)	+79	+83	+89
Fan/Low-Pressure Compressor Pressure Ratio (%)	+2.7	+2.6	+1.7
Turbine Expansion Ratio (%)	-0.9	-1.2	-2.1
MODULE PERFORMANCE			
Change in:			
Fan			
Efficiency (Points)		-0.8	-0.6
Flow Capacity (%)		-1.2	-0.8
Low-Pressure Compressor			
Efficiency (Points)		-1.1	-1.2
Flow Capacity (%)		-1.8	-1.8
High-Pressure Compressor			
Efficiency (Points)		-2.6	-2.4
High-Pressure Turbine			
Efficiency (Points)		-2.5	-2.2
Inlet Area (%)		+0.9	+1.0
Low-Pressure Turbine			
Efficiency (Points)		-0.1	-0.7
Inlet Area (%)		+1.7	+0.3 (+ Leakage)

*With baseline adjustments and additional test cell corrections.

Overall, the two approaches provide credible agreement with the airline test cell data and agree reasonably well with each other. The bottom up analysis, therefore, supports the level of module deterioration determined from the top down approach, and suggests that the "real level" of module deterioration is close to the values estimated to exist.

SECTION 5.0

PRELIMINARY MODELS OF JT9D ENGINE PERFORMANCE DETERIORATION

This section presents the preliminary models of JT9D module and engine deterioration. It should be noted that these models are preliminary, being based on the data analyzed to date, and that they will be refined during the course of the program.

5.1 MODULE DETERIORATION MODELS

The preliminary performance deterioration models for the JT9D engine modules are presented in Figures 97 through 101. Shown are the estimated overall losses in efficiency and flow capacity as a function of module part age in flight cycles for each module. These curves are based on the data presented in Section 4.0.

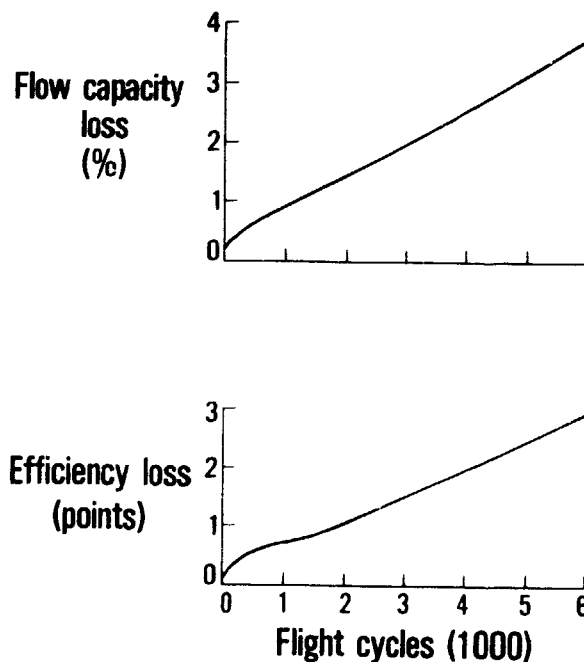


Figure 97 Preliminary Model of JT9D Fan Performance Deterioration - The model was developed from part inspection results with the deterioration level corroborated by back-to-back test data and analysis of prerepair test data.

PRECEDING PAGE BLANK NOT FILMED

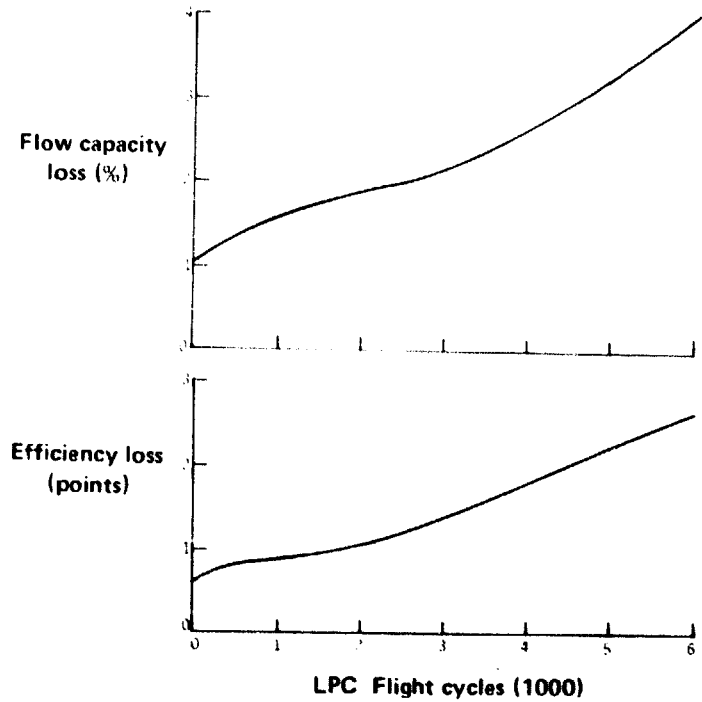


Figure 98 Preliminary Model of JT9D Low-Pressure Compressor Performance Deterioration - The model was developed from part inspection results with the deterioration level corroborated by back-to-back test data and analysis of prerepair test data.

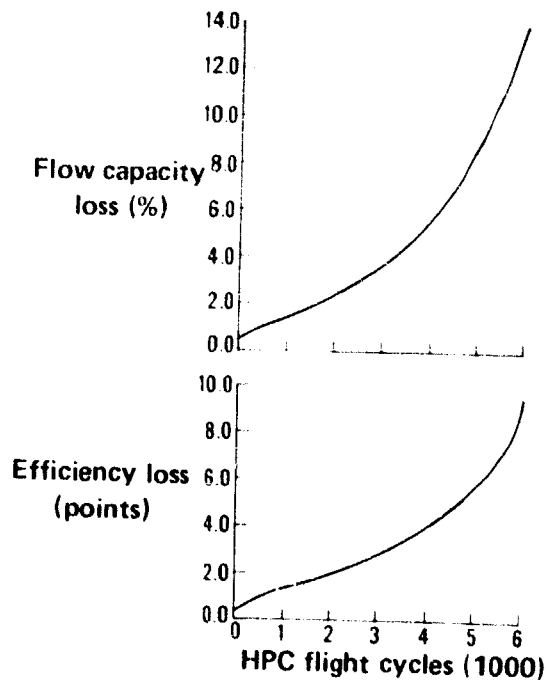


Figure 99 Preliminary Model of JT9D High-Pressure Compressor Performance Deterioration - The model was developed from part inspection results with the deterioration level corroborated by back-to-back test data and analysis of prerepair test data.

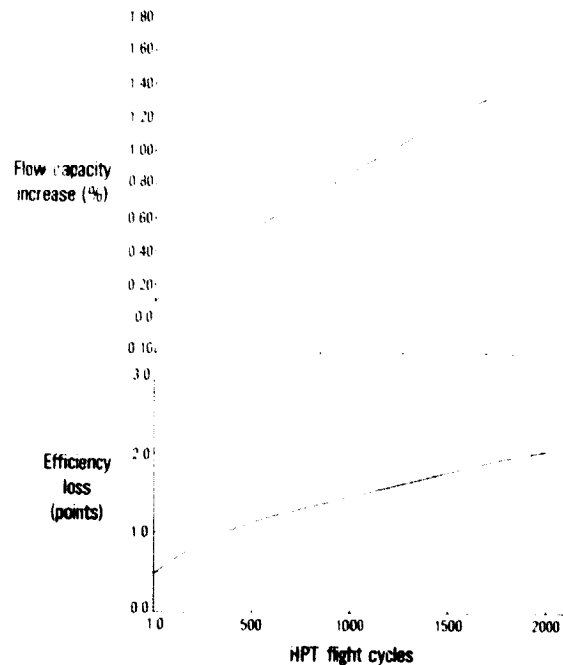


Figure 100 Preliminary Model of JT9D High-Pressure Turbine Performance Deterioration - The model was developed from part inspection results with the deterioration level corroborated by back-to-back test data and analysis of prerepair test data.

Figure 102 shows the distribution, by module, of TSFC loss and relative contribution of each damage mechanism as synthesized from the module deterioration models. The time frames covered are the 1st, 500th, 1000th, 2000th, and 3000th flights since the average engine was new. All time frames are estimates of prerepair performance levels. In synthesizing the 2000th and 3000th-flight engine performance loss level, it was assumed that the high pressure turbine had been repaired every 1000 flight cycles, and the low pressure turbine every 2000 flight cycles. However, the effect of increasing flight cycles is clearly evident.

5.2 ENGINE DETERIORATION MODEL

Figure 103 shows the preliminary estimated prerepair engine deterioration model of TSFC versus engine flight cycles synthesized to show the portion of deterioration related to each major cause.

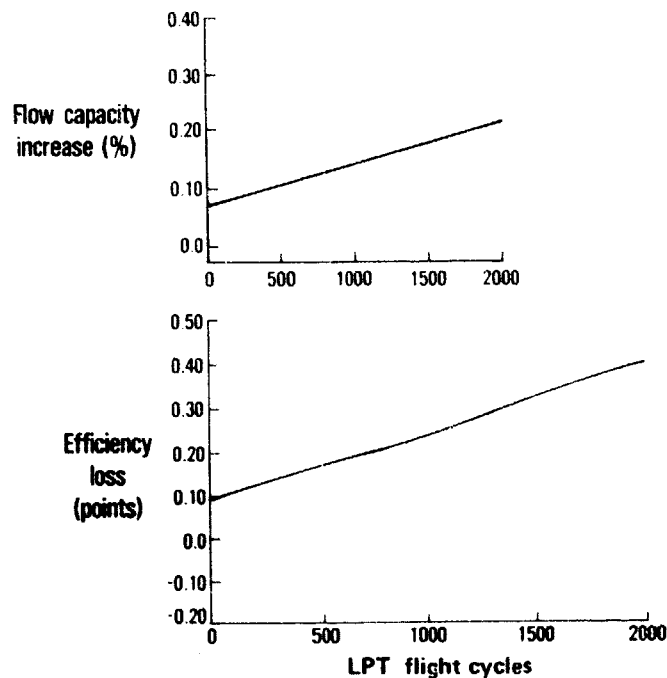


Figure 101 Preliminary Model of JT9D Low-Pressure Turbine Performance Deterioration - The model was developed from part inspection results with the deterioration level corroborated by back-to-back test data and analysis of prerepair test data.

These causes are divided into three categories: (1) clearance changes which appear to be caused by flight loads and engine in-flight transients; (2) erosion damage to airfoils and seals; and (3) thermal distortion. Individual operator experience will be above or below this line as a result of such factors as maintenance practices. The anticipated range of this variation is shown as a band on Figure 103.

Figure 104 shows a comparison of the preliminary model of prerepair performance deterioration versus the average level determined from the analysis of historical data and indicates reasonable agreement as to the overall level of deterioration for both short- and long-term deterioration. The divergence occurring above 3000 cycles reflects refurbishment of the cold section of the engine by the airlines which results in a lower level of erosion losses than are included in the average engine model.

As noted earlier, these preliminary models of module and engine performance deterioration will be refined during the course of the program.

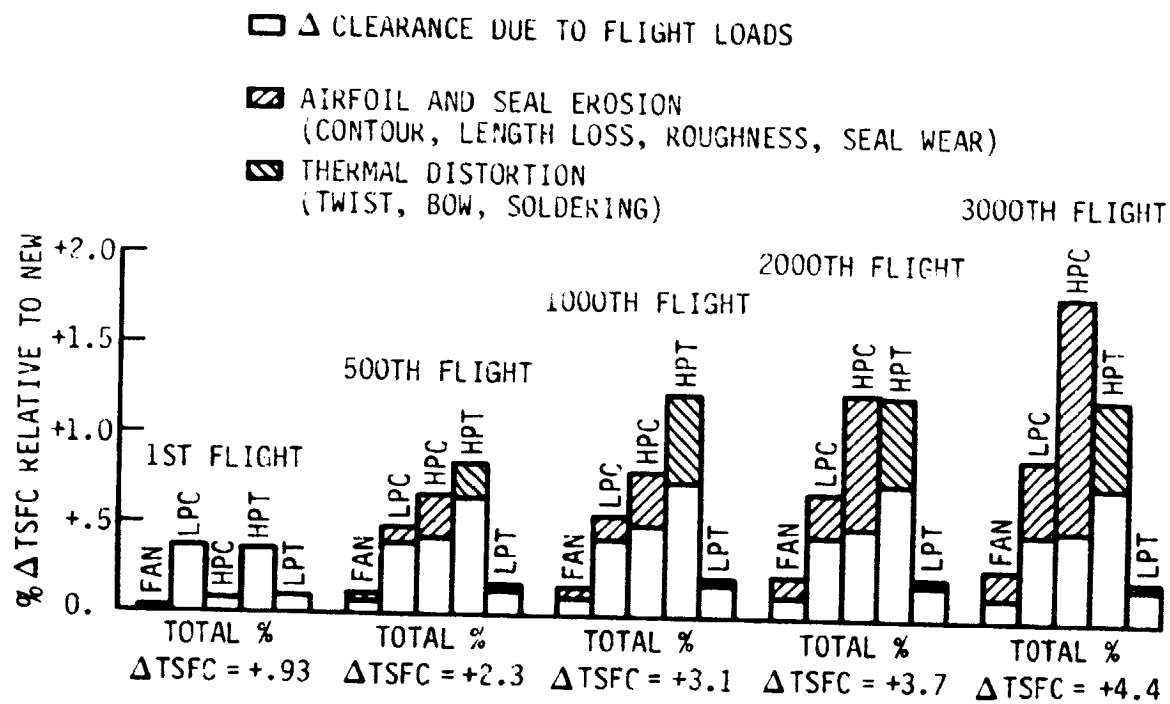


Figure 102 Preliminary Model of JT9D Prerepair Average Engine and Module Performance Deterioration - Deterioration levels are shown at sea level static take-off conditions.

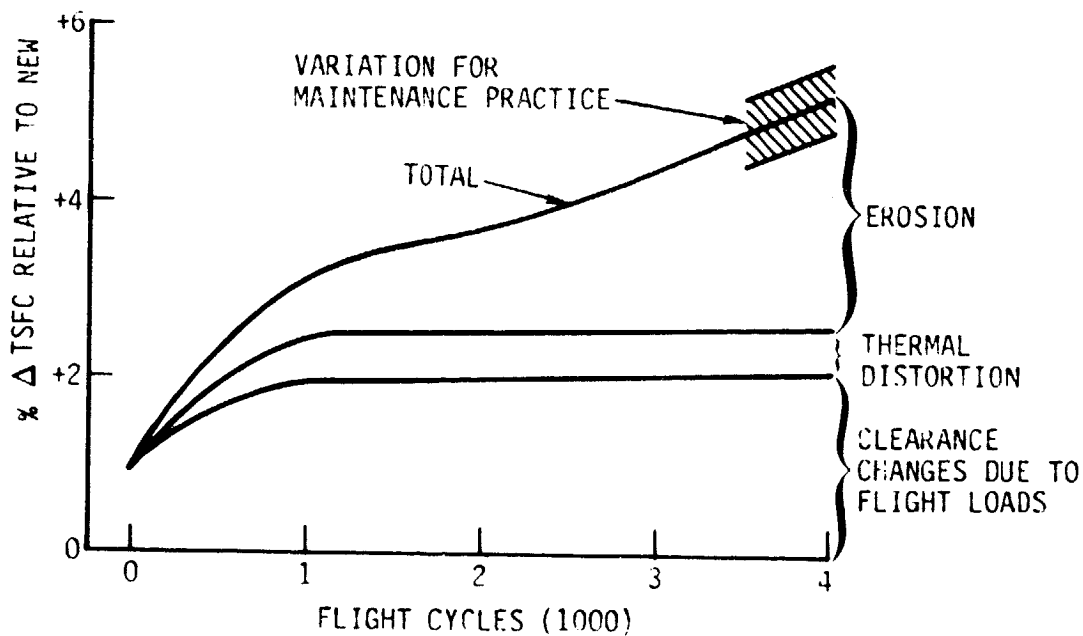


Figure 103 Preliminary Model of JT9D Prerepair Average Engine Performance Deterioration - The contributions of each major cause of deterioration are compared at sea level static take-off conditions.

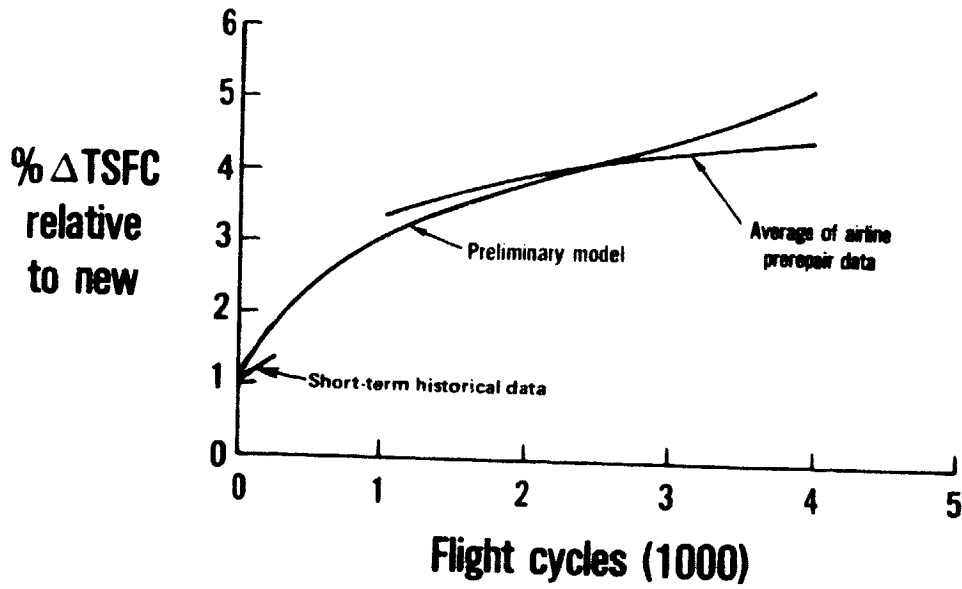


Figure 104 Comparison of Preliminary Model of JT9D Prerepair Average Engine Performance Deterioration and Observed Deterioration - The comparison shows reasonable agreement in overall performance deterioration level.

SECTION 6.0

PRELIMINARY RECOMMENDATIONS

Based on observations of airline procedures and practices and historical information collected as part of the NASA JT9D Engine Diagnostics Program, this section presents preliminary recommendations to reduce performance deterioration on-the-wing and improve performance recovery in the shop. The areas of engine operating procedures, performance monitoring, maintenance practices and design criteria are addressed. In addition, examples of repair interval optimization for some of the performance recovery recommendations are included to provide a basis for an individual airline cost benefit analysis.

6.1 ENGINE OPERATING PROCEDURES

Production acceptance testing of new engines at Pratt & Whitney Aircraft has shown very little deterioration (0.2 percent TSFC maximum) from the initial data point to the final calibration. This running includes all of the various types of operation (including snap acceleration and deceleration transients) that are required in customer test stands or during ground test operation in the aircraft. The following guidelines have been developed to minimize deterioration during this type of running during post-production engine operation :

1. Operate at idle power for a minimum of 5 minutes after start before accelerating above idle.
2. The initial acceleration from idle on a repaired engine should consist of gradual incremental power increases.
3. Unnecessary hot, fast accelerations or decelerations should be avoided:
 - a. Whenever possible, accelerations or decelerations should be slow, that is, at a rate equivalent to a minimum of 60 seconds for a full power-lever excursion between idle and take-off power.
 - b. Following more than one minute of operation at or above bleeds closed power, the engine should be operated at idle for:
 - (1) 7 minutes prior to a slow acceleration (that is, 60 seconds minimum, idle to take-off);

- (2) 15 minutes prior to a snap acceleration, which is defined as a power lever movement of one second or less for a full excursion.
- c. When snap decelerations are required, they should be performed as soon as possible after reaching high power (0 to 10 seconds preferred, 30 seconds maximum).
- d. Engine calibrations should be performed in a decreasing power direction so that the engine will be "cool" at the end of the calibration prior to shutdown or other operation.
- e. Run at idle for a minimum of 5 minutes before shutting down.

Adherence to these procedures will minimize blade to rub-strip contact by producing a more gradual contact. Abrupt contact in high-pressure turbine stages can cause localized metal transfer and build up on the rub strip which would result in excessive blade tip wear.

Sufficient "cool down" time at idle after being at high power and prior to an acceleration up to high power (as prescribed in 3.b above) is required to prevent excessive blade to rub-strip contact resulting from a hot rotor accelerating in a relatively cool case. Similarly, if snap decelerations are to be made, they should be performed as soon as possible after reaching high power (3.c above) to minimize the amount of thermal growth of the rotor disk which can potentially rub the "cool" case after the deceleration is made. Figure 105 graphically presents the interaction of a typical hot rotor and rub strip (i.e., tip clearance) during an acceleration/deceleration cycle.

Use of the above procedures may result in a slightly longer time to complete a particular test, however, prevention of unnecessary engine deterioration will result.

6.2 PERFORMANCE MONITORING

6.2.1 Performance Trending and Management

Data gathering activity during the historical data collection has highlighted the need for improved management information concerning engine and fleet deterioration. It has been clearly identified that large variations exist between operator practices that have an impact on deterioration. An airline operator's fleet-fuel consumption level is dependent on two factors, performance retention while on-the-wing, and performance recovery while in the shop. To effectively manage these factors, complete records of individual engine performance histories and repairs are required.

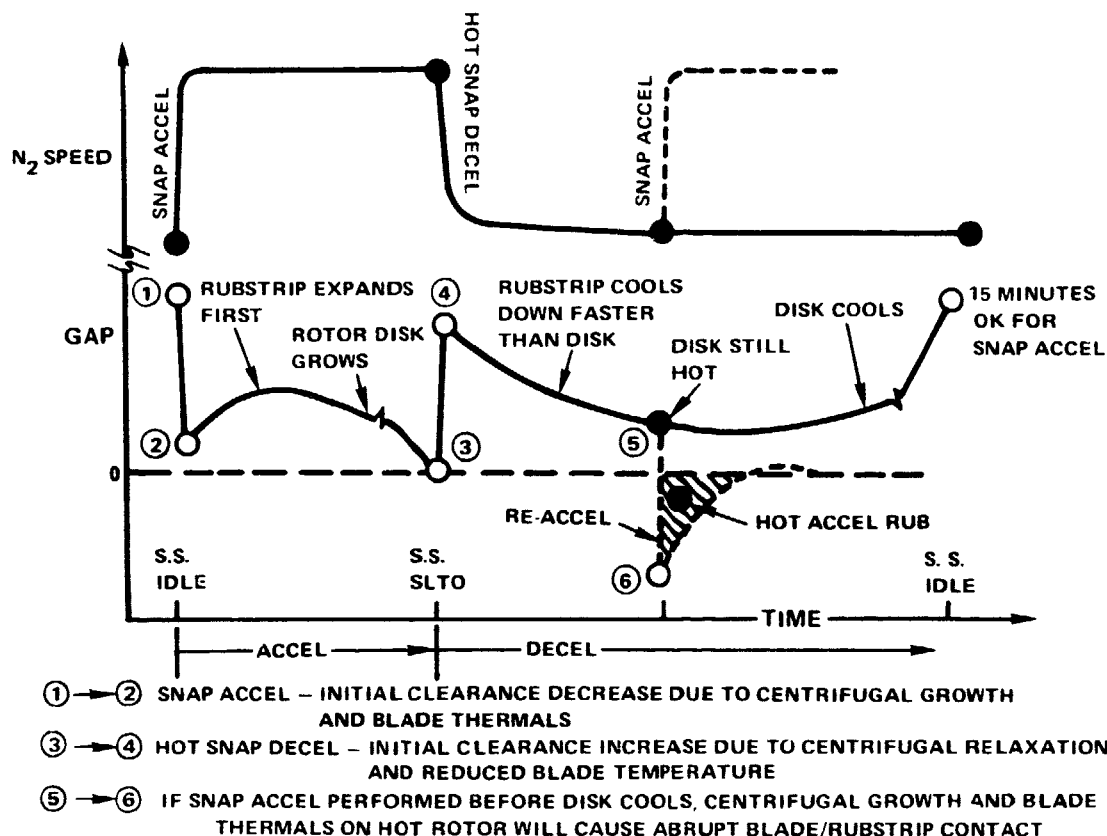


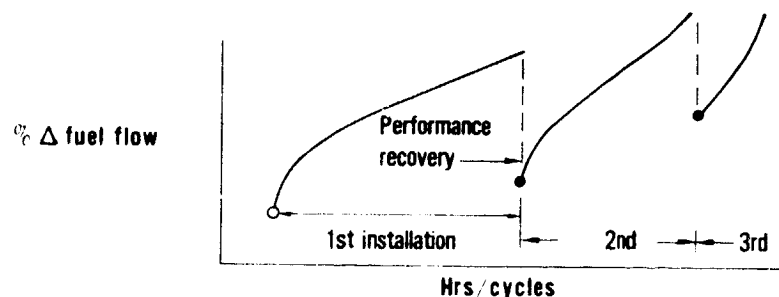
Figure 105 Hot Rotor/Rub Strip Interaction - Because the thermal expansion and contraction rate of the case (and the rub strip) is faster than that of the rotor disk, an abrupt blade/rub strip contact will occur if a snap acceleration is performed before the disk cools.

It is customary to discard definitions of operating procedures when they are superseded. For purposes of safety and uniformity, this is a reasonable approach; however, this information is essential in the documentation of engine trends. (It was fortunate for this study that each of the three airlines, in their own way, retained information permitting historical documentation of performance deterioration trends.)

Since each airline operator differs in maintenance practices and engine deterioration experience, it is necessary to establish a means to identify each airlines' fleet deterioration characteristics and to correlate shop practices with performance recovery. To accomplish this, an integration of existing information is necessary.

This basic information exists in various forms at all airline operators. It would be desirable to develop a uniform program with the capability of comparison of operator characteristics. Such a common program would permit identification of relative deterioration rates for operators in adverse operating environments such as mid-East deserts with operators in cold clean climates. A program of this nature provides the tool each operator needs to assess their own performance retention and restoration.

Figure 106 illustrates the type of information that could be available from an individual engine history. Comparisons could be made of deterioration rates on-the-wing for the initial installation (run) and for subsequent installations after repair or maintenance relative to the shop activities performed. Graphic display records of this type could identify the nature of an airline operator's problem. The effectiveness of refurbishment and new performance-improvement hardware can be evaluated. Deterioration rates can be monitored to determine how they respond to operational practices such as reduction of water usage, modifications in derated operation, or variations in route structure.



Shop activity information	1st run - hrs/cycles, date, removal cause, shop action, perf. recovery 2nd run " 3rd run " 4th run etc.
Management analysis	Shop visit rate, deterioration rate, maintenance cost, shop effectiveness, performance margin, projected removal date, etc.

Figure 106 Management Tool Required - A computerized management tool is required which "integrates" existing information and correlates actual individual engine histories with shop activity.

A computerized management tool would be required to integrate existing information and correlate actual individual engine histories with shop activity. This could provide management a means to evaluate effectiveness of shop visits and assist in controlling those factors that increase fuel consumed.

To achieve such a management tool several steps are necessary.

- 1) Engine condition monitoring programs must be completely rewritten and expanded in scope to provide history retention and computer graphic displays.
- 2) Shop activity must be recorded in computer format for storage.
- 3) Computerized data (performance and shop records) must be retained for the life of the engine.

6.2.2 Test Stand Instrumentation

Based on the observations of the airlines' tests facilities, several areas were noted where improvements could be made in the instrument calibration procedures. The recommendations fall in five categories as shown below:

- o Data retention
- o Calibration standards
- o Written calibration procedures
- o Calibration techniques
- o Calibration analysis

Data Retention

One of the major difficulties in correlating observed engine performance changes to possible instrumentation problems is the lack of calibration data. The majority of the airlines require only that the instruments be calibrated and adjusted to the necessary tolerances and do not provide a data retention procedure for the calibration results.

By developing calibration forms for each instrument and retaining the forms within their respective standards departments, any questions concerning the validity of performance data could be checked against the calibration results. It would also provide a method to identify instruments which exhibit consistent problems and should be replaced. The information on the calibration forms should include:

- o Working instrument identification (serial number, range, engine parameter);
- o Calibration instrument identification;

- o Calibration date;
- o Calibration set points, working instrument outputs, deviations from calibration instrument;
- o Whether the working instrument was within tolerance or not, and if not, what action was taken.

This would mean additional bookkeeping work, but would yield better information concerning the accuracy of the test stand instrumentation and its effect on engine performance measurements.

Calibration Standards

The majority of the instrument calibrations are conducted by personnel within each airline utilizing equipment maintained in-house. A few instruments are transferred to the vendors or to an outside firm for calibration.

For those instruments calibrated by the airlines, the general rule is to use instruments of similar types but retained as standards in their calibration laboratory. In this case, the errors associated with the standard are equal to that of the working instrument. When the accuracy of the working instrument is near the tolerance specified by the Pratt & Whitney Aircraft Test Instruction Sheet (T.I.S.), the actual error contributed by the calibration process can exceed the limits since the error of the standard can enter in as a bias term. To avoid this bias, the error attributed to the primary standard should be much less than that of the working instrument. This is a function of the T.I.S. limits involved and the error of the working instrument and will thus vary from facility to facility.

Some airlines may also employ transfer standards, that is, calibration instruments located on the test stand and periodically calibrated against primary standards in a separate laboratory. The resultant error contributed to the working instrument is then a function of both calibration instrument errors which enter in as bias terms.

Working instruments calibrated by vendors or other outside firms have a similar calibration hierarchy, but the error contributions may not be available. This may apply to calibration instruments as well.

Therefore, the individual airlines should re-examine their calibration processes to minimize the error contributions to the final measurement error. This may require the replacement of calibration instruments with those more suited to the particular working instruments.

Written Calibration Procedures

Calibration procedures, for two of the three airlines studied, were primarily from manufacturer-supplied manuals. A more desirable approach, practiced by the third airline studied, is to develop a calibration procedure for all test stand instrumentation that includes calibration-instrument calibration data sheets, tolerance check-out procedures and disposition of out-of-tolerance instruments. This approach condenses manufacturers' information into a form applicable to the airlines test cell and provides a step-by-step process for checking, calibrating, and recording instrument data. A procedure of this nature would be of benefit to all airlines since it would put into a single manual all the information necessary for the instrument calibration procedures.

Calibration Techniques

An additional step in the calibration process concerns the acquisition of preadjustment instrument calibrations. This is the calibration of any instrument before adjustment to zero, span, etc. Since the calibration intervals for certain instruments can reach six months to a year, the instrument will drift to some degree within that interval. By performing an preadjusted calibration, the amount of the drift can be quantified and its affect on performance measurements analyzed. After this step, required adjustments should be performed and the calibration repeated. Both the preadjusted and adjusted calibration records would be retained.

Calibration Analysis

By developing a process for calibrating the test stand instrumentation and retention of the resultant data on a long-term basis, an analysis program can be initiated to evaluate the individual instruments. This would include the identification of problem instruments which exhibit consistently high errors, as well as verifying the accuracies of instruments that are functioning properly. Also, by examination of the calibration errors versus time, it would be possible to determine if certain instruments require calibration and adjustment on a more frequent basis.

6.2.3 Test Stand Correlation

One of the primary functions of postrepair and postoverhaul testing of JT9D engines is to ensure that the engine will meet all applicable performance requirements, especially thrust and exhaust gas temperature guidelines and limits. It is therefore necessary to establish test stand performance parameter correction curves to relate parameters measured in an airline's test stand to those levels upon which limits are based.

Test stand correlation testing generally involves back-to-back testing between the Pratt & Whitney Aircraft Middletown test facility and the airline's test stand. During testing in the airline's test stand, an engine should be run in the exact same nacelle configuration (that is, QEC or bifurcated fan ducts) as the engine which will later use these corrections. Corrections generated will be valid only for the configuration(s) tested during the test stand correlation testing.

Accurate test stand corrections are extremely important when analyzing engine performance changes in an airline's test stand relative to a base line established elsewhere. For example, if one wishes to analyze engine test performance levels relative to Pratt & Whitney Aircraft new engine performance levels, accurate test stand corrections are required.

Following the completion of a test stand correlation program, a procedure should be established for continuing surveillance of changes made to the test stand which might invalidate the test stand correction results. Listed below are examples of changes which Pratt & Whitney Aircraft feels would require recorrelation of the test stand:

- o Any major changes to test stand inlet and exhaust areas.
- o Change in the location of the exhaust augmentor tube relative to engine exhaust.
- o Any change in the test stand which would affect the airflow through the stand.

Similarly, if changes are made in an engine's installed configuration (whether bare engine, partial or full QEC) compared to its configuration during the test stand correlation, which affects its installed performance, the test stand will have to be recorrelated. Listed below are examples of engine installation changes which will necessitate test stand recorrelation:

- o New or revised airframe supplied production inlet.
- o New or revised airframe supplied exhaust system components (including primary nozzle, fan duct (where applicable), thrust reversers, etc.)

- o Use of air bleed, power extraction, etc., which is not turned off during testing.

6.3 MAINTENANCE PRACTICES

This section presents preliminary recommendations for the retention of engine performance. Detailed data on the causes of deterioration were presented for each module in Section 4.4, and the results are summarized in the following discussion.

The following preliminary recommendations cover the work that could be done to recover the performance lost with usage and an estimate of when these actions should be undertaken. The recommendations are presented on an individual module basis, and refinements will be developed and based on new data from the on-going activities.

6.3.1 Fan

Fan performance deterioration is caused by increases in tip clearances, surface roughness, and blade leading edge bluntness. Increased tip clearances result from flight loads and appear to stabilize after 1000 flight cycles. Surface roughness increases with usage and also appears to stabilize. However, blade leading edge bluntness continues to increase with age resulting in an increasing performance penalty.

Based on these causes, periodic hand cleaning of the fan when the engine is in the shop, and restoration of the leading edge between 2000 and 3000 cycles are the two recommended maintenance actions. As long as the fan rub strip is mechanically sound and the tip clearances are within Overhaul Manual limits, no restoration of fan blade clearance is recommended due to the short-term rub-out from the effect of flight loads.

6.3.2 Low-Pressure Compressor

The causes of reduced performance in the low-pressure compressor are tip clearance, roughness, and airfoil leading edge shape. Surface roughness increases and then appears to stabilize. Tip clearances, however, continue to increase from the effects of erosion on the rubber outer air seals. Airfoil leading edge shape or bluntness is not judged to be significant at this time up to the current level of usage (4000 to 5000 cycles).

The low-pressure compressor should be chemically cleaned at every exposure and the rub strips replaced between 2000 and 3000 cycles when the engine is in the shop. The effect of airflow losses particularly on EGT, as well as TSFC, suggest more attention be placed on this module. The airfoils are beginning to show signs of thinning from the samples inspected with 5000 cycles usage. Consideration should be given to replacing these airfoils between 5500 and 6500 cycles depending on their condition at that time.

6.3.3 High-Pressure Compressor

The performance losses in the high-pressure compressor are caused by changes in blade tip clearance, airfoil surface roughness, and airfoil contour. Tip clearance changes are caused by both erosion of the outer air seal material and blade length reduction and these are significant through all levels of usage. Roughness appears to increase rapidly during the first 1000 cycles and then stabilize. Based on analysis, the effects of airfoil contour change become important at usage levels beyond 3000 cycles in the blades.

The fuel consumption and exhaust gas temperature performance losses caused by the high-pressure compressor are such that the compressor should be completely refurbished between 2500 and 3500 cycles with long blades and new/refurbished rub strips in all stages. The stators should also be chemically cleaned at this time. Based on stator thinning, the stators, as well as the blades and outer air seals should be replaced at the next interval or 5000 to 7000 cycles.

There is a strong correlation between exhaust gas temperature recovery and compressor blade length. The sensitivity of exhaust gas temperature recovery to average blade length suggests that small changes in compressor clearance effect the combustor temperature profiles, rather than causing a real exhaust gas temperature recovery. This correlation further suggests that maintenance of clearance standards are very important.

6.3.4 Combustion System

While the direct effect of combustor deterioration on performance is insignificant, the indirect effects are major. Changes in radial and circumferential temperature patterns affect clearances, and a host of other mechanical shape changes in the turbine, as well as durability.

When the burner is repaired, the dimensions, and particularly the cone angle, should be restored. The fuel nozzles should also be removed and cleaned. The potential for cumulative damage and reduced structural stability of the front end suggest that the burner not be used beyond the third installation. Turbine durability and performance losses can be traced to variations in combustor repair practices.

6.3.5 High-Pressure Turbine

The performance deterioration of the high-pressure turbine appears to be dominated by tip clearance changes and the second-stage vane inner shroud leakage. It has been impossible to correlate tip clearance changes with usage from measurement data. However, blade tip wear of first-stage turbine blades does correlate with initial build clearances and build standards with respect to blade length. Analytical studies suggest that even with controlled build clearances, tip clearance is affected by flight loads. Based on these factors, control of first-stage blade length by hand selection or drum grinding to a constant diameter is recommended. The outer air seals should be offset ground to the requirement set forth in the Overhaul Manual. The tip clearance should be set to 0.073 ± 0.002 inch. The second-stage blade clearances should be set to the nominal dimension, and the second-stage vane inner foot dimensions should be set to the tight side of the tolerance band.

6.3.6 Low-Pressure Turbine

The low-pressure turbine performance deterioration does not appear to be significant, and the losses that do occur are caused by blade tip clearance changes and vane platform soldiering. Rebuild standards which open all tip clearances are, however, causing an increase in performance deterioration as a result of the rebuild process. The ring seals of the low-pressure turbine are very responsive to temperature changes, and hot shutdowns will cause rubbing and performance loss due to the rapid contraction of these seals.

The performance penalties for increased tip clearance are larger in the third stage (first low-pressure turbine stage) than in the sixth stage. The tip clearances should be kept to nominal dimensions, particularly in the third and fourth stages during rebuild, and platform soldiering should be eliminated by vane repair when the low-pressure turbine is opened for other reasons.

6.3.7 Summary

The performance restoration achieved as a result of the refurbishments discussed above is shown in Table XXVI. The effects on TSFC and exhaust gas temperature are given for cruise and takeoff conditions, respectively, since these are the areas of prime concern to airline operators. It should be noted that the combined effect of the module refurbishments on overall engine performance is not the simple addition of the individual module improvements because of engine rematching. The proper combined effect is shown at the bottom of the table. Not all of the performance recovered will be kept because the short term deterioration mechanisms will increase the level of thrust specific fuel consumption as with new engines.

TABLE XXVI
EFFECT OF RECOMMENDED REFURBISHMENTS

Module	Cycles	Efficiency Change (points)	Component Effects		
			Flow Capacity Change (%)	TSFC Change (%) at Cruise	EGT Change (°F) at Take-Off
Fan	3000	+1.22	+0.78	-0.7	+1
Low-Pressure Compressor	3000	+1.4	+2.3	-1.2	-22
High-Pressure Compressor	3000	+2.8	N/A	-1.0	-32
High-Pressure Turbine	1000	+1.5	-1.1	-0.8	-29
Low-Pressure Turbine	2000	+0.4	Neg	-0.3	-4
Combined Effect on Engine				-3.6	-81

6.4 DESIGN CRITERIA

The results of the analysis of the historical data and, in particular, the results of the parts inspections, have provided detailed information from which recommendations can be formulated to improve performance retention over both the short and long terms. These recommendations include a definition of the need and objectives for additional research, specific design and development actions, and improved maintenance practices.

The major causes of performance deterioration are the effect of flight loads on engine clearances, erosion, thermal distortion, and variances in rebuild standards. The following paragraphs discuss each cause and the related recommendations.

6.4.1 Flight Loads

The effect of flight loads have been examined both in this historical study and under the short-term deterioration analysis efforts, and the results to date have been reported in References 2 and 3. Although a continuing effort is planned to validate and refine the preliminary models of short-term performance deterioration and the effects of flight loads, sufficient data is currently available on which to base preliminary recommendations for flight-load related design criteria.

The losses in performance are caused by the combined effects of flight loads and the thrust bending moment. To reduce the performance loss due to thrust and air loads effects, increases in engine case stiffness, relocation of the thrust mounts to the horizontal centerline of the engine, isolation of the engine such that the aerodynamically induced loads are not carried by the engine, structurally stiffening of the engine through use of nacelle structure to carry all or part of the bending loads, or a combination of several of these approaches is required. As part of the NASA JT9D Engine Diagnostics Program, a test program will be conducted to validate the currently estimated impact of aerodynamic loads on engine clearances and to provide detailed information from which the most appropriate corrective action can be defined.

Reduction of the effects of clearance changes caused by gravitational and gyroscopic loads will require increasing the number of bearings and frames in the engine. The corrective action outlined above would require complete redesign and certification of the engine and is not a realistic approach with respect to the JT9D engine but is being considered for future engines.

6.4.2 Erosion

The documented effects of erosion on compressor airfoils and seals support the need to improve the erosion resistance of these parts. The rubber outer air seals should be replaced with a more erosion resistant material. In the long term, either airfoil material changes or the development of erosion resistant coatings for application to both static and rotating airfoils are required. The development of suitable erosion resistant coatings is estimated to have the most likelihood of early success within reasonable levels of cost. Based on the damage rates and estimated performance losses, coatings for the high-pressure compressor airfoils are the most critical need, followed by application in the fan and low-pressure compressor.

The selection and screening of candidate coatings will take some period of time, and service evaluation testing is required prior to wide spread use of airfoil coatings for performance retention. Active programs currently exist in both areas on other Pratt & Whitney Aircraft engines (JT3D and JT8D) and have been initiated on the JT9D. These coatings will not eliminate the need to periodically refurbish, replace, or recoat airfoils and seal materials. Performance life improvements between 50 and 100 percent are anticipated from the use of these coatings and new seal materials.

The control of the quantity of erosive material that enters the compressor through the use of passage shaping is a possibility for foreign object damage control. The size of the particles that cause the bulk of the erosion damage are estimated to be such that passage shaping may have little effect. The use of boundary layer bleeds to

remove the erosive material at positions where it tends to concentrate may have a somewhat higher probability of success. These areas will require extensive research and should be investigated.

6.4.3 Thermal Distortion

Thermal distortion results from the basic temperature and stress environment of the turbines and changes to that environment. Based on observations and the mechanical condition of turbine parts analyzed during the program, compressor and combustor deterioration appear to cause radial and circumferential changes in the turbine inlet temperature profiles. These changes elevate metal temperatures above design levels and result in thermal distortion of the turbine parts. Turbine vane bow results in flow area changes which control the operating lines of the compression system. Platform curl and vane twist increase the secondary flow losses and reduce efficiency. Higher temperatures near the annulus walls increase running clearances due to differential thermal growth of the cases and seals relative to the rotors.

Fundamental to corrective action is the development of an understanding of the causal factors that produce combustor temperature profile shifts. Component and engine testing is required to quantify the relative importance of these variables prior to making definitive recommendations for design criteria changes.

6.4.4 Rebuild Standards

The Pratt & Whitney Aircraft JT9D Overhaul and Repair Manuals were originally developed with the objective of prolonging the useful life of parts to reduce maintenance costs on the basis of structural and safety criteria. Permissive variations are provided in the Overhaul Manual for clearance, part repair, or blending to permit airline maintenance shop flexibility. As was expected, the result is that each airline customizes the Overhaul Manual and Repair/Modification Standards to fit its unique requirements and experience with the engine.

However, this approach has had a significant effect on fuel consumption. Data obtained in this study indicates that variations in rebuild standards produce variations in fuel consumption amounting to as much as +0.5 percent. The size of this variation coupled with the realities of higher fuel costs suggest the need to revise the manuals to provide service information beyond that required to meet structural and safety requirements. This new information should provide data on repair practices affecting fuel consumption so that each airline can determine the trade-offs between fuel consumption increases and maintenance cost increases.

6.4.5 Summary

Future engine design should address the basic causes of performance deterioration discussed above. The potential impact of flight loads should be analyzed to assist in defining bearing configurations, case stiffness requirements, and engine installation structural integration. Consideration should be given to the effects of erosion in selection of airfoil geometric properties, materials, and coatings. The design of turbines should consider closely the potential effects of adverse temperature pattern changes. Maintenance manuals should provide additional information as to the effects of increased clearance and part repair practices on engine and module performance.

6.5 PERFORMANCE DETERIORATION CONTROL AND MANAGEMENT

Fleet average engine performance levels are established by the deterioration characteristics of the JT9D engine and, through the engine repair process, by airline maintenance practices. These practices include clearance levels, repair procedures, and scrappage criteria which establish the average performance age of gas-path parts. The preceding sections of this report have presented the results of studies utilizing historical data in analyzing the deterioration process and the damage mechanisms that cause performance losses with respect to usage. The variations in prerepair and postrepair performance levels, and hence average fleet performance, are traceable in the majority of cases to either average gas-path part ages or airline rebuild standard variations.

The management of fleet performance levels must ultimately be approached on an individual engine basis during engine repair. However, the fundamental process is more readily understandable if presented in terms of part age control and module refurbishment intervals. The concept of part age control is related to the aging process of parts as engine nameplate age increases. Figure 107 shows the estimated average high-pressure compressor blade part age determined from part usage and repair rates for the three subcontractor airlines in this study. A correlation line drawn from the origin through part and engine age equalities is helpful in understanding the part age trends shown. Typically, during early service, the part age is very close to engine age. Part age tends to stabilize at a relatively constant level as engine age increases through normal repair, scrappage, modifications, and conversion events.

The maintenance recommendations presented in Section 6.4 are directed toward establishing an upper boundary of part age on an individual engine basis where appropriate part repair or replacement should be considered. When parts are repaired or replaced as they reach, for example, 3000 cycles, the age of parts in a fleet of engines will

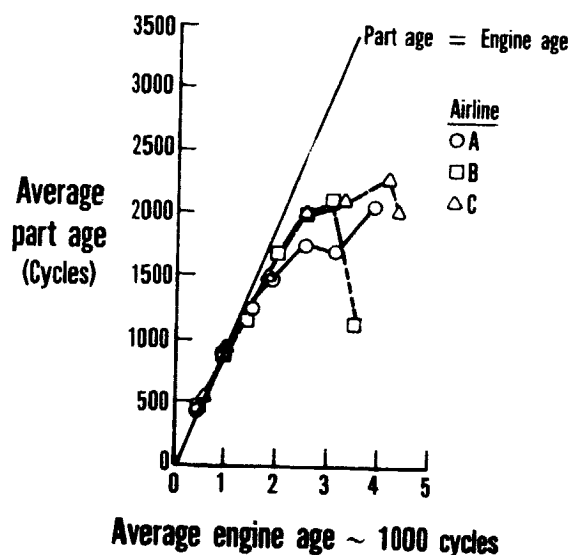


Figure 107 JT9D High-Pressure Compressor Blade Age (Stages 5 through 15) - As engine age increases, part age tends to stabilize.

become statistically distributed between essentially zero and 3000 cycles, and the long-term fleet average part age will be one-half the repair interval or 1500 cycles. It is this value of average part age that should be considered for management control because it establishes the average performance level of each module and, in combination with all of the modules, the average engine performance levels exhibited by the fleet.

Table XXVII shows the recommended repair/replacement intervals set forth in Section 6.3, the associated average part age targets, and the average part ages of the three airline subcontractors. This table shows that for these three airlines, the average part ages were already very close to the average part age targets. These data indicate the need for small refinements in cold section repair frequency and part replacement rates.

Cost-benefit studies are needed to evaluate the merits of changing long standing airline maintenance policies and philosophies. The individual airlines are best equipped to make these types of studies and to include all of the factors important in their own decision making process. However, to show the effect of selecting different repair intervals from those recommended in Section 6.3, cost optimization studies were carried out for the cold section modules.

The cost benefit study process consists of three steps:

1. Determination of the performance that could be recovered as a function of part age;

TABLE XXVII

COMPARISONS OF RECOMMENDED REPAIR/REPLACEMENT INTERVALS
AND ASSOCIATED AVERAGE PART AGES WITH
AVERAGE PART AGES FOR AIRLINES

Module	Recommended Repair Interval (Cycles)	Average Part Age Target (Cycles)	Estimated Average Part Ages (Cycles) at End of 1976 for Airlines		
			A	B	C
Fan:					
Blades	3000	1500	2700*	800	800
Outer Air Seals	3000	1500	1500	N/A**	600
Low-Pressure Compressor:					
Blades	6000	3000	3100	1200	2900
Outer Air Seals	3000	1500	1500	400	1600
Vanes	6000***	3000 est.	3300	900	2000
High-Pressure Compressor:					
Blades	3000	1500	2000	1100	2000
Outer Air Seals	3000	1500	1800	350	2900
Vanes (8-15)	6000***	3000	2700	2100	2800

* 1200 cycles if Airline A shop fan blade rework is counted due to quality of leading edge after repair.

** Not Available.

*** Estimated, as parts inspected were just beginning to show levels of distress which would have a significant performance impact.

2. Determination of the fuel cost per flight hour that could be recovered as a function of part age;

3. Determination of the cost of repair per flight cycle;

The data resulting from steps 2 and 3 are then plotted and summed, with the result indicating the total cost of recoverable fuel and repair as a function of repair time. The minimum of this curve indicates the most cost effective time for repair.

The following ground rules were selected for these studies for application to all modules:

- 1) Labor costs were excluded since the repair recommendations presented in Section 6.3 can be accomplished when the individual engine modules are disassembled for other reasons;
- 2) Part repair or replacement costs were included and determined based on 1978 part repair prices;
- 3) The repair dollar per flight hour costs were determined by using the repair intervals in flight cycles times an average of 3.5 flight hours per flight cycle; and
- 4) Fuel costs were based on an average cruise fuel consumption of 950 gallons per hour, a fuel-to-carry-fuel factor of 1.1, and a cost of 40 cents per gallon. Therefore, the fuel cost per flight hour is estimated to be \$418 per hour. Hence, a one percent change in TSFC at cruise equates to \$4.18 per hour.

For the fan, the recommended maintenance was airfoil cleaning, blade leading edge restoration through leading edge insert repair of damaged blades and chamfer cut of other blades. Repair of these items provides the performance recovery shown in Figure 108. The estimated cost for these repairs was \$5000 per set for leading edge restoration and an additional one-cent-per-hour cost for periodic cleaning of the fan blades.

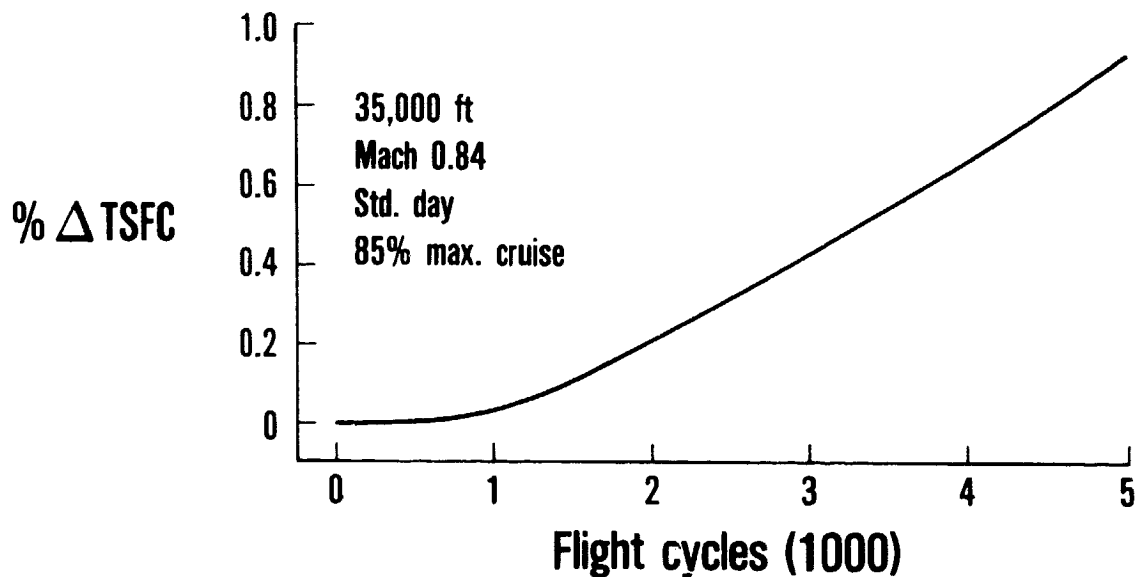


Figure 108 JT9D Fan Performance Recovery Potential - It is estimated that 0.43 percent TSFC can be recovered by refurbishment of the fan at 3000 cycles.

These costs resulted in the optimization curve shown in Figure 109 and indicate an optimum repair interval of 2500 cycles. However, the recommended repair interval is 3000 cycles because it is believed that the chamfer cut leading edge incorporated in the repair may deteriorate more rapidly than a new blade leading edge. Hence, the recommended repair interval should be extended by 500 cycles to favor reduced maintenance cost.

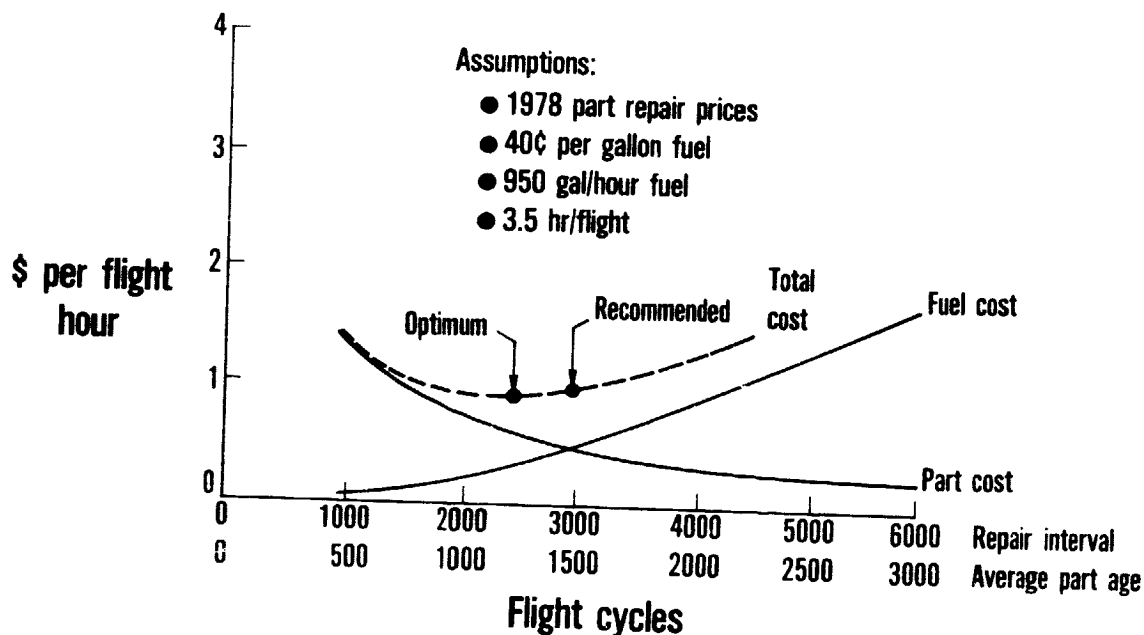


Figure 109 Cost Optimization of Fan Repair Interval - The recommended repair interval of 3000 flights is only slightly beyond the optimum cost point.

For the low-pressure compressor, the recommended maintenance was replacement of the outer air seals and cleaning. Replacement of these seals and cleaning provides the performance recovery shown in Figure 110. The estimated cost for these repairs was \$1260 for replacement of outer air seals and an additional one cent per hour cost for periodic cleaning.

These costs resulted in the optimization curve shown in Figure 111 and indicate an optimum repair interval of 2000 cycles. However, since the total cost does not change significantly with cycles, it is recommended that airfoil cleaning and outer air seal replacement be considered whenever the module is opened for other reasons.

For the high-pressure compressor, the recommended maintenance was replacement of the blades in all rows and outer air seals. Replacement of these blades and seals provides the performance recovery shown in Figure 112. The estimated cost for these repairs is \$36,540.

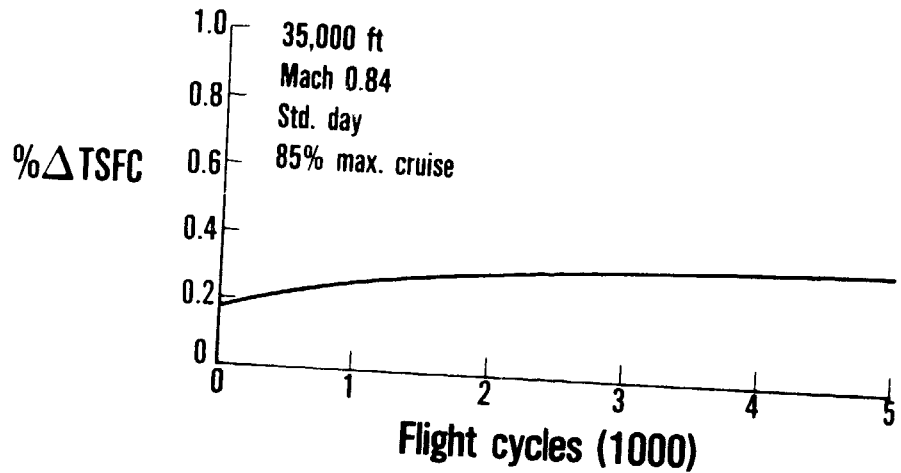


Figure 110 JT9D Low-Pressure Compressor Performance Recovery Potential - It is estimated that 0.31 percent TSFC can be recovered by refurbishment of the low-pressure compressor at 3000 cycles.

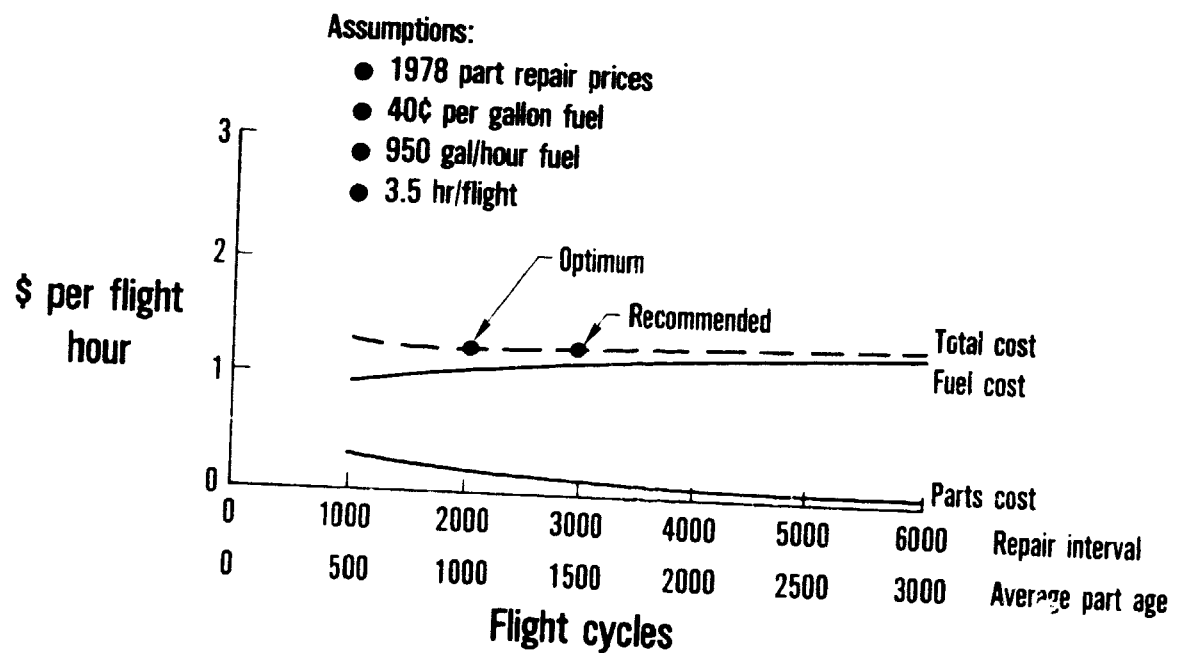


Figure 111 Cost Optimization of Low-Pressure Compressor Repair Interval - The optimum cost point is at about 2000 cycles, indicating that the compressor should be refurbished whenever the module is opened for other reasons.

These costs resulted in the optimization curve shown in Figure 113 and indicate an optimum repair interval of 4000 cycles. However, the high-pressure compressor deterioration has a significant impact on the turbine inlet temperature level and profile which, in turn, has a

significant impact on turbine durability. This suggests use of a repair interval of 3000 cycles. As shown in the figure, this recommended interval increases the cost by \$0.45 per hour, but this cost is offset by savings in the turbine.

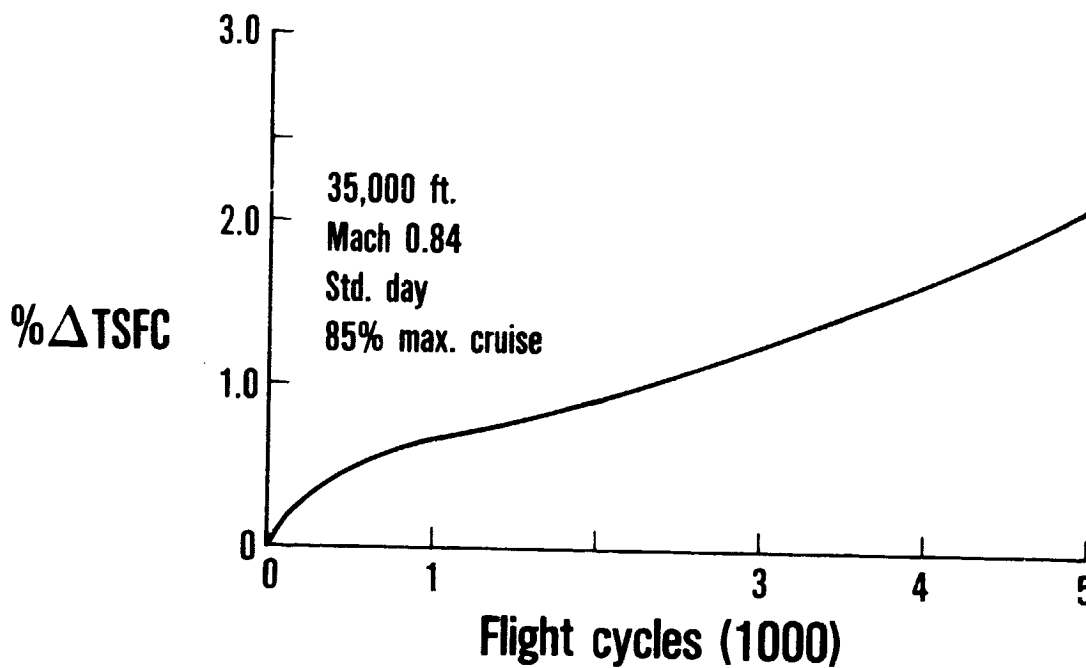


Figure 112 JT9D High-Pressure Compressor Performance Recovery Potential - It is estimated that 1.27 percent TSFC can be recovered by refurbishment of the compressor at 3000 cycles.

These examples of repair interval optimization studies provide a framework for individual airlines to accomplish their own comprehensive cost benefit studies based on their individual operating environment and economic circumstances.

The cost effectiveness studies were based on a \$0.40 per gallon fuel cost. As fuel costs rise, the motivation for incorporating these recommendations will become greater.

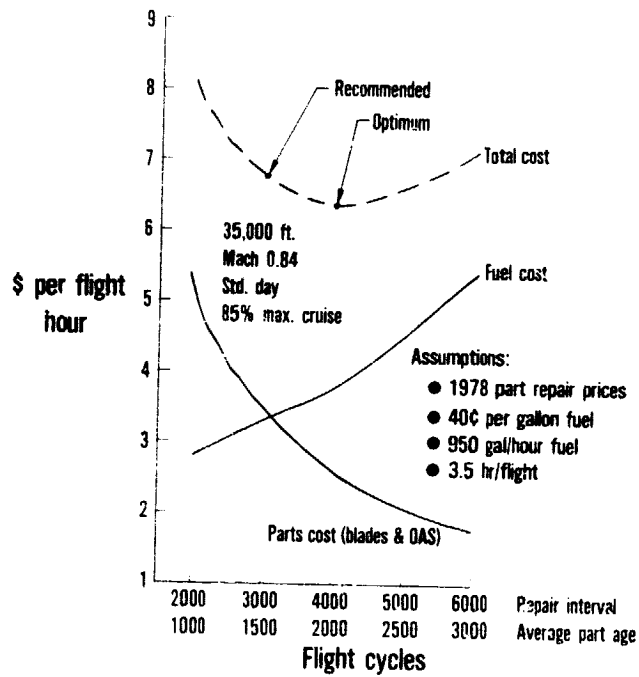


Figure 113 Cost Optimization of High-Pressure Compressor Repair Interval - The optimum cost point is beyond the recommended 3000-cycle interval, but it is expected that the added increment in parts cost would be more than offset by reduced turbine maintenance cost and longer time between shop visits.

SECTION 7.0

CONCLUSIONS

The conclusions that can be drawn from the results of these studies of historical data are not final because the NASA JT9D Engine Diagnostics Program is continuing, and analyses of additional, more carefully documented engine test data and experience may suggest revisions to one or more of the results and preliminary deterioration models presented previously.

Furthermore, there are a number of major points that could not be resolved from available historical data or within the time frame permitted by this study.

First - The adequacy of the current techniques to define the detailed performance effects of specific types of damage to parts. The techniques used were based on analyses developed to predict the performance effects of geometric changes to new parts. While these analyses are well substantiated by testing over a range of geometries appropriate for new parts, the geometries in used parts often exceeded those for which test data were available. As a result, considerable extrapolation was required.

Second - Historical airline engine test stand correlations and instrumentation calibrations were in many instances suspect due to the lack of records or the infrequency with which such correlation testing and calibrations had been accomplished. An attempt was made to correct for these deficiencies through the top-down, bottom up data enhancement technique. However, a degree of uncertainty still necessarily remains in the resulting analytical model particularly with respect to fleet average trends and specific airline results.

Third - The role that the condition of the engine cases play in short- or long-term deterioration. It is known that leakage occurs between cases and that distortion of the cases occurs. However, in this analysis of historical engine performance test data all of the performance losses were assigned to specific damage mechanisms in the

Note: In reviewing the data presented in this document, it should be recognized that a comparison of the airlines on the basis of the data presented in this report is inappropriate. The reason for this is that the historical studies have covered the time period prior to December 31, 1976, and since this time, each of the airlines studied has undergone numerous maintenance program changes which have effected their overall engine deterioration picture concerning prerepair and postrepair performance levels and performance deterioration problems.

modules of the engine. With respect to distortion, there is some evidence that distortion of the JT9D engine major cases will force other intervening cases out-of-round and lead to significant rub problems and losses in performance. The variation in high-pressure turbine circumferential rub patterns and rub depths observed in historical data could be caused by variations in the roundness and flatness of the diffuser and/or combustor outer case beyond the recommended limits in the Overhaul Manual. Quantification of this potentially important deterioration mechanism must await additional field data which was not available from historical records.

7.1 OVERALL ENGINE PERFORMANCE DETERIORATION

Engine performance deterioration results from the gradual degradation of the mechanical condition of engine parts. Four causes of this degradation have been identified: (1) the effects of flight loads that distort the shape of engine cases, produce rubbing, and result in increased clearances; (2) erosion of airfoils and outer air seals resulting in increased roughness and bluntness, loss of camber, loss of blade length, and increased operating clearances; (3) thermal distortion produced by changing turbine inlet temperature patterns resulting in area changes, increased leakages, and changed clearances; and (4) operator repair practices and rebuild standards that have an impact on the cumulative levels of part mechanical damage versus time and the levels of prerepair and postrepair performance. The probable role of each cause of performance deterioration has been identified and quantified versus usage at both the whole engine and module levels from analysis of historical performance, maintenance, and part inspection data.

7.1.1 Short-Term Performance Deterioration

The analysis of historical short-term data indicated that the average engine of the JT9D-3A/7/20 family loses 1 percent in thrust specific fuel consumption (TSFC) on the first flight relative to the level of measured performance at sea-level static take-off conditions of the engine when new. This loss in performance grows to 1.5 percent by the 200th flight. Analysis of these data indicate that 55 percent of the TSFC loss is associated with the performance losses of the low-pressure spool (fan, low-pressure compressor, and low-pressure turbine) and 45 percent with the performance losses of the high-pressure spool (high-pressure compressor and high-pressure turbine). This short-term performance loss appears to result from clearance increases caused by rubbing between stationary and rotating parts. This rubbing is caused by deflections of engine cases and rotors produced by aircraft induced flight loads. However, with continuing in-service exposure, the probability of more severe loads causing additional damage increases, but at a much slower rate.

7.1.2 Long-Term Performance Deterioration

The long-term performance loss of the engine gradually increases with increased usage. Analyses of prerepair test stand data indicate that the average TSFC performance deterioration of the fleet of JT9D-3A/7/20 family of engines prior to repair is 4.4 ± 0.5 percent at 3500 flights or approximately 12,000 hours of operation relative to new production engine performance levels. The performance losses at this time frame are dominated by the high-pressure spool rather than the low-pressure spool.

The estimated distribution of the prerepair performance loss at 3500 flights by major causes are 40 percent due to flight loads, 40 percent due to erosion, 20 percent due to thermal distortion, with the total level varying by ± 13 percent as a result of differences in maintenance practices.

The analyses of postrepair test stand data indicate that the fleet average postrepair level of TSFC deterioration is 3.5 ± 0.7 percent at 3500 flights, representing an average recovery of 0.9 percent. The majority of the TSFC recovery results from high-pressure turbine restoration. Historical data indicates that an additional 1.9 percent in TSFC recovery can be realized by refurbishment of the engine cold section (fan, low- and high-pressure compressor). The balance of average unrecovered performance, approximately 1.6 percent in TSFC, is caused by mechanical conditions distributed among all the modules that are not typically refurbished.

7.2 ENGINE PERFORMANCE RECOVERABILITY

Synthesis of the best postrepair module performance loss levels analyzed from historical postrepair data indicate that a +2.0 percent TSFC deterioration level, at sea level static take-off power conditions, with respect to new engine performance is achievable on a fleet average engine basis.

This level of postrepair performance can be achieved by periodic cold-section restoration and attention to turbine nozzle vane area classification and rework standards, turbine clearance and rebuild standards, and fan leading edge refurbishment. The ability to achieve and sustain for a reasonable time a postrepair average TSFC deterioration level lower than + 2.0 percent is believed to be limited by the short-term effects of flight loads. These cause localized increases in seal clearance which build up rapidly.

7.3 DETERIORATION MODELS

7.3.1 Engine Deterioration

The preliminary deterioration model developed for the average JT9D engine and presented in Section 5.0 of this report agrees well with the level of deterioration observed for the fleet of JT9D engines. Considerable variance from this model should be expected when compared to individual airline trends. This average engine model, as well as the module deterioration models, are preliminary and may be revised on the basis of new data currently being collected and analyzed.

7.3.2 Module Deterioration

Significant progress has been achieved in understanding and documenting the mechanisms that cause performance deterioration and the role that each mechanism plays as engine operating usage increases. These mechanisms are presented in detail in Section 4.0. The following paragraphs summarize the major conclusions.

Fan

The major performance loss mechanism in the fan is estimated to be leading edge bluntness, with airfoil roughness and increased tip clearance making significant, but less important, contributions to the total loss in fan performance. The documentation of damages to fan blades versus usage is continuing.

Low- and High-Pressure Compressors

The performance loss mechanism of most importance in the low-pressure compressor is estimated to be tip clearance increases due to erosion of outer air seal material, with airfoil roughness being of secondary importance. The high-pressure compressor performance loss is dominated by the effects of erosion, with the major mechanisms being clearance increase, increased roughness, and airfoil camber loss (with camber loss being the cause of accelerating performance deterioration beyond approximately 3000 flight cycles). The estimated high-pressure compressor performance losses become very large by 5000 flight cycles.

Combustion System

The combustor and fuel nozzles have important indirect effects on turbine performance loss as the result of changes in turbine inlet temperature profile. These temperature profile changes have been inferred to have occurred on the basis of significant variances in part condition and rub experience between airline operators. These variances result in operating clearance changes and thermal distortion of turbine parts. The magnitude of turbine and engine performance loss resulting from temperature profile shifts can not be quantified from available historical data.

High- and Low-Pressure Turbines

The major cause of high-pressure turbine performance deterioration is increase in blade tip clearance, with vane bow and second-stage vane twisting being of major but somewhat less importance. Low-pressure turbine performance deterioration is caused by tip clearance increases, with all other mechanisms being of minor significance. Airline rebuild standards appear to cause significant variations in levels of both prerepair and postrepair performance loss in the turbines.

APPENDIX A

AIRLINE VARIATIONS IN
OPERATING PROCEDURES AND THRUST USAGE

VARIATIONS IN PAN AMERICAN OPERATING PROCEDURES AND THRUST USAGE

1. Take-Off

March 1970

Initiated water usage for take-off power EGT reduction and increased thrust (Fn).

May 1971

Started use of reduced take-off thrust from JT9D-3 dry ratings.

October 1971

Initiated JT9D-3A dry ratings for performance but discontinued due to insufficient EGT margins.

January 1972

Policy: JT9D-3A dry for normal operation;

JT9D-3 wet for EGT margin increase;

JT9D-3A wet for performance, as required.

December 1973

Terminated use of water and started removal of all water systems (Latter stage of conversion to JT9D-7/7A configuration).

1977

Using JT9D-3A dry ratings and Assumed Temperature Method (ATM) of thrust derate up to -0.06 EPR.

2. Climb

Prior to April 1971 - used full JT9D-3 climb rating.

April 1971

Introduced reduced thrust using circular calculator; reduced to 2,000 foot-per-minute climb at sea-level to 500 feet per minute at 25,000 feet altitude, and hold at 500 feet per minute to cruise altitude.

November 1972

Established 774°C EGT climb limit.

Early 1973

Eliminated any climb derate and used JT9D-3A full rating when JT9D-7 and JT9D-7A conversions were introduced.

3. Cruise

Standard cruise is Mach 0.85.

VARIATIONS IN TWA OPERATING PROCEDURES AND THRUST USAGE

1. Take-Off

TWA historically used full wet JT9D-3A take-off thrust on all flights from 1971 through October 5, 1976 except for short periods of dry usage during the winter of 1972 and 1973. After October 5, 1976, all take-offs were dry except the Los Angeles to London flight.

2. Climb

Prior to July 18, 1972, full JT9D-3A climb power was used along a 340 knots/Mach 0.82 profile.

After July 18, 1972, a thrust derate of 0.04 EPR was applied above flight level 250 (25,000 feet) if aircraft weight was below 600,000 pounds.

3. Cruise

Prior to October 1972, cruise at Mach 0.84 was standard.

After October 1972, cruise was increased to Mach 0.85.

VARIATIONS IN NORTHWEST OPERATING PROCEDURES AND THRUST USAGE

1. Take-Off

Dry take-offs are performed for all flights. The JT9D-7 and JT9D-7CN engines used JT9D-3A ratings and derate up to 0.06 EPR if take-off gross weight (TOGW) is less than the limiting TOGW for 100°F inlet.

2. Climb

Full JT9D-3A climb power is used if 747 TOGW is greater than 625,000 pounds. If TOGW is below 625,000 pounds, JT9D-3A maximum cruise is used below flight level 300 (30,000 feet) and JT9D-3A climb above flight level 300.

3. Cruise

Standard cruise is Mach 0.85.

APPENDIX B

USED PARTS CONDITION AND PHOTOGRAPHIC DOCUMENTATION

INTRODUCTION

Approximately 750 used airfoils were collected from the subcontractor airlines and other sources at Pratt & Whitney Aircraft and inspected to determine parts condition as a function of usage levels. The results of the analytical inspections were presented in Section 4.0. Visual observations regarding parts condition were also made for qualitative comparison with the analytical results. Photographs of these visual observations and supporting data are presented in this section. The photographs were taken where a substantial number of parts with known time and cycles were collected, including low- and high-pressure compressor blades, and high-pressure turbine vanes and blades.

Fan

Very few fan blades were collected for inspection during this phase of the Diagnostics Program and no photographs were taken.

Low-Pressure Compressor

No variation in physical condition of low-pressure compressor blades was observed either as a function of usage level, as shown in Figures B-1 through B-3, or as a function of the axial position in the engine, as shown in Figures B-4 and B-5.

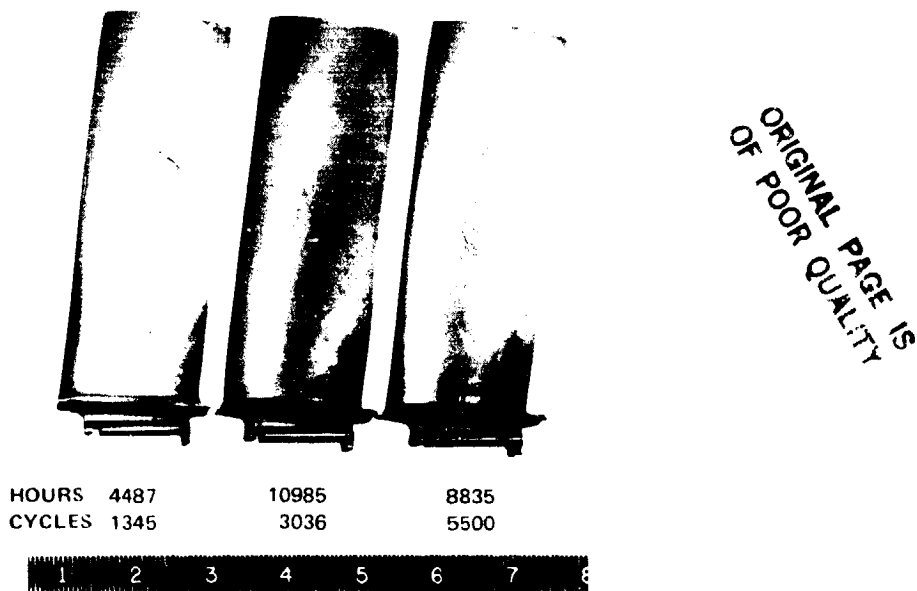


Figure B-1 JT9D Second-Stage Low-Pressure Compressor Blades.

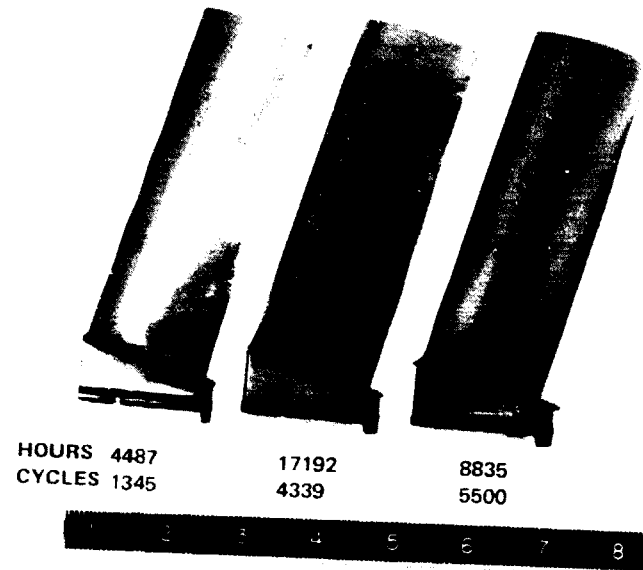


Figure B-2 JT9D Third-Stage Low-Pressure Compressor Blades.

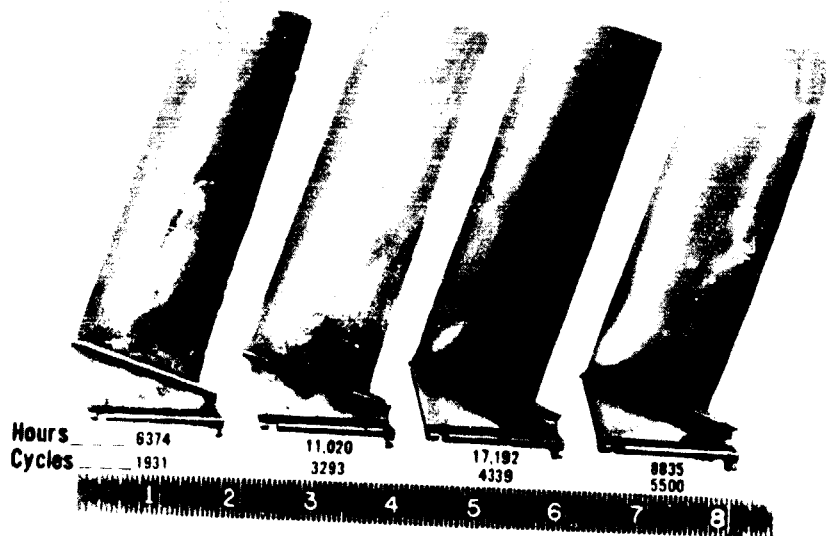


Figure B-3 JT9D Fourth-Stage Low-Pressure Compressor Blades

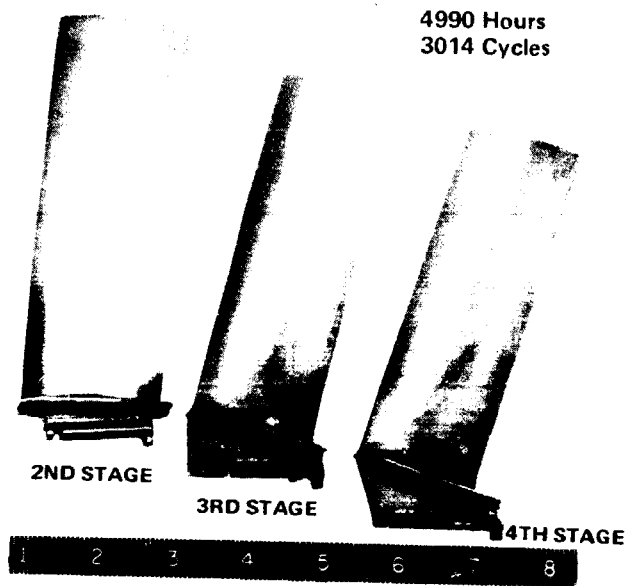


Figure B-4 JT9D Low-Pressure Compressor Blades.

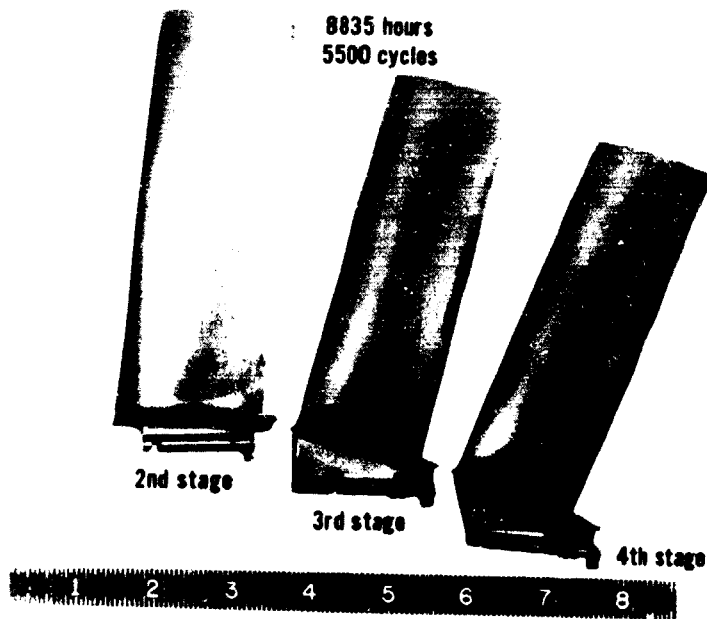


Figure B-5 JT9D Low-Pressure Compressor Blades.

OF 5 INCL PAGE IS
OF POOR QUALITY

This lack of variation in physical condition is further shown in Figure B-6 through B-8 where the results of measurements taken on service parts show negligible loss in blade length with respect to increasing usage. The data for airfoil profile changes versus cycles are shown in Figure B-9 through B-14. As can be seen from these data, there were no significant changes in the airfoil properties with increasing cyclic age.

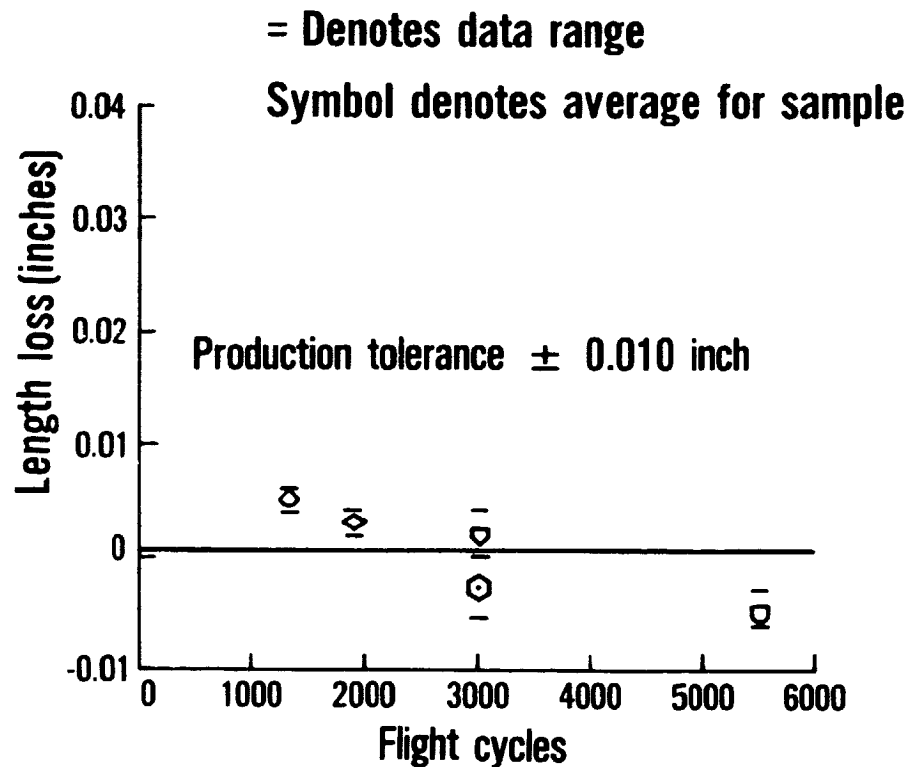


Figure B-6 Low-Pressure Compressor Blade Length Loss Data for Rotor 2.

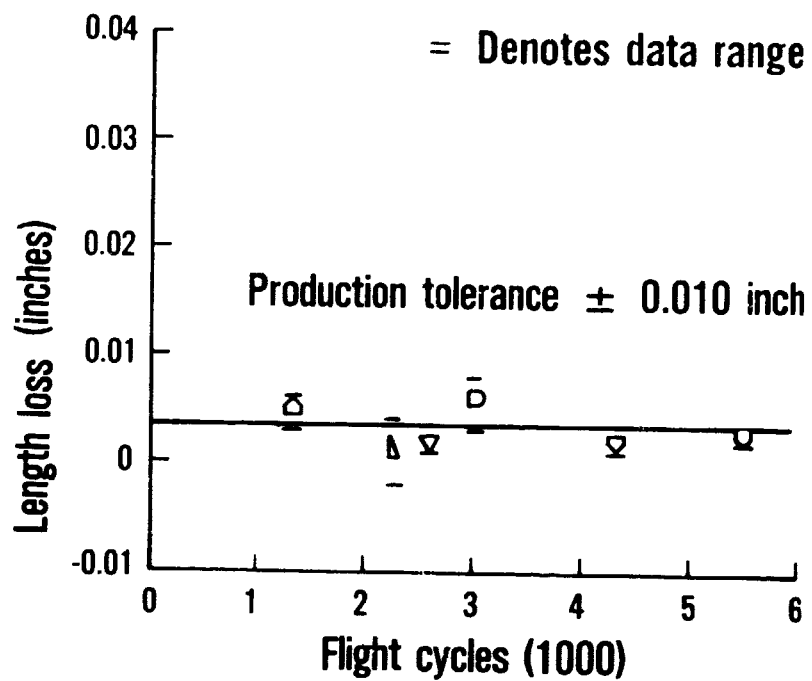


Figure B-7 Low-Pressure Compressor Blade Length Loss Data for Rotor 3.

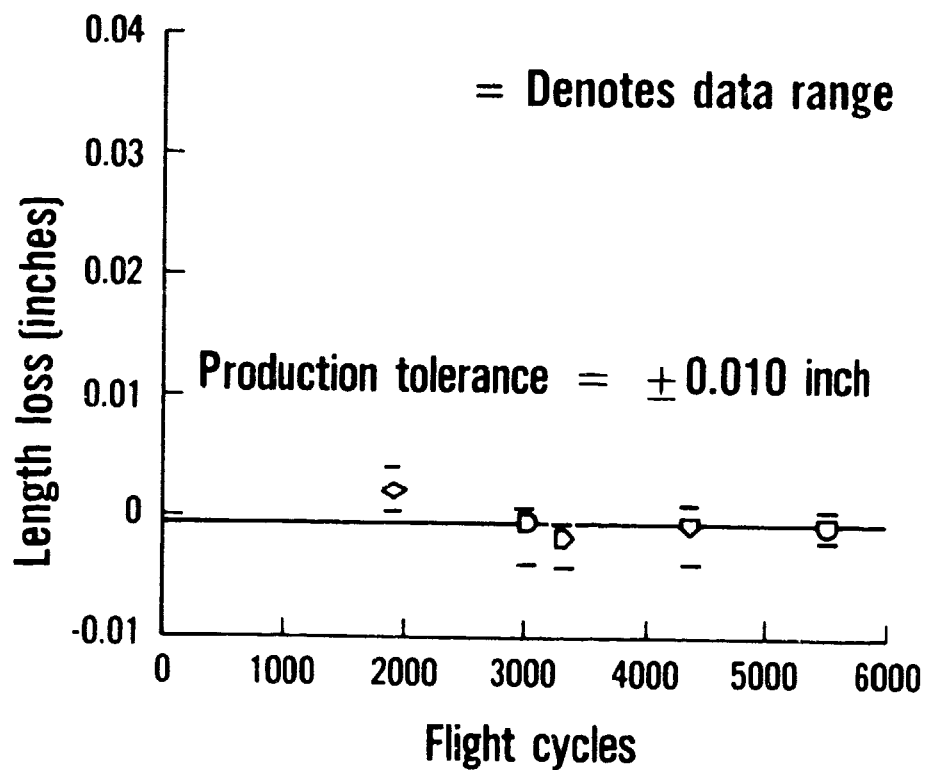


Figure B-8 Low-Pressure Compressor Blade Length Loss Data for Rotor 4.

GEOMETRY CHANGES OF AIRFOIL PROPERTIES DUE TO EROSION NEAR TIP OF ROTOR 2

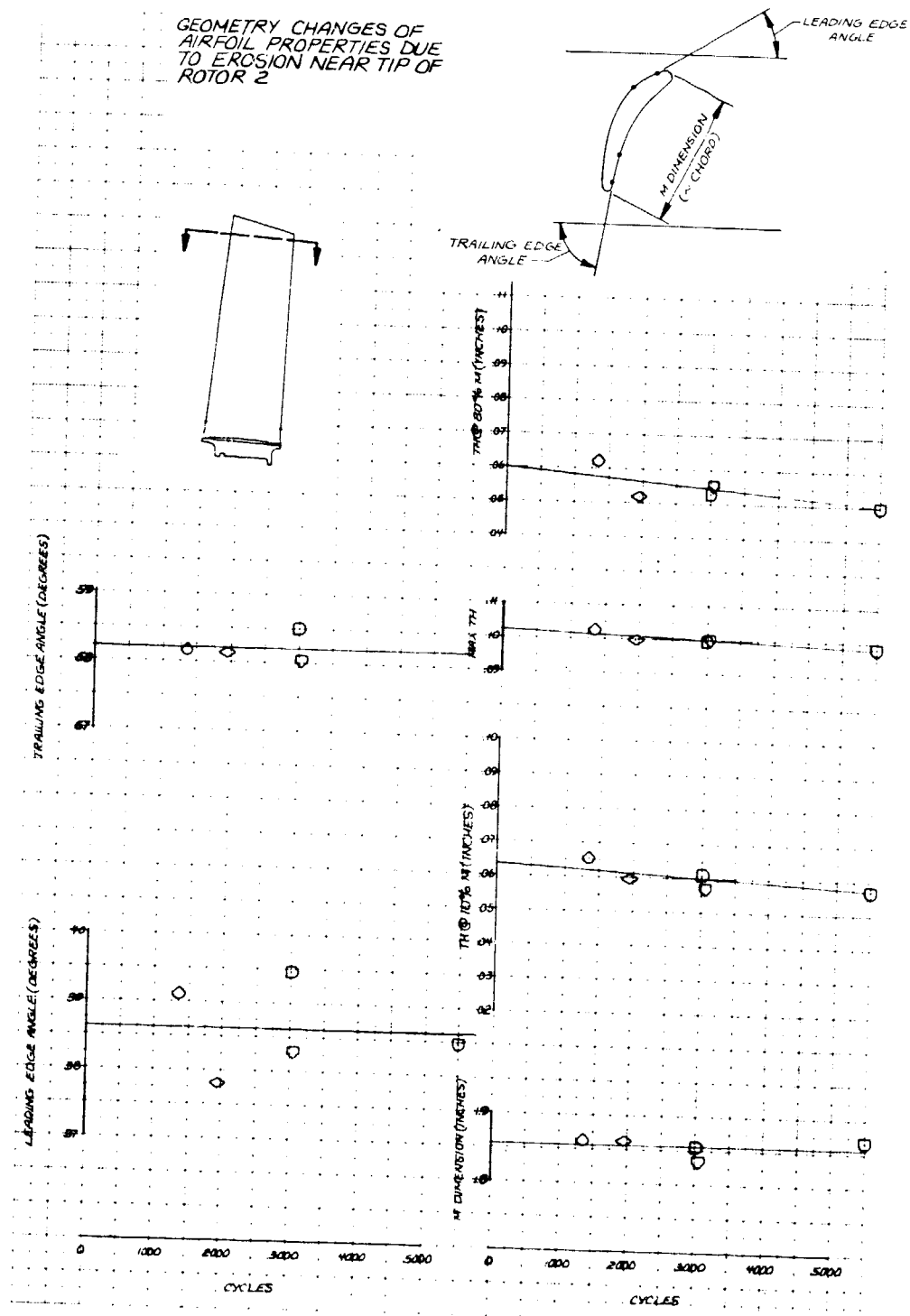


Figure B-9 Second-Stage Rotor Tip Profile Data

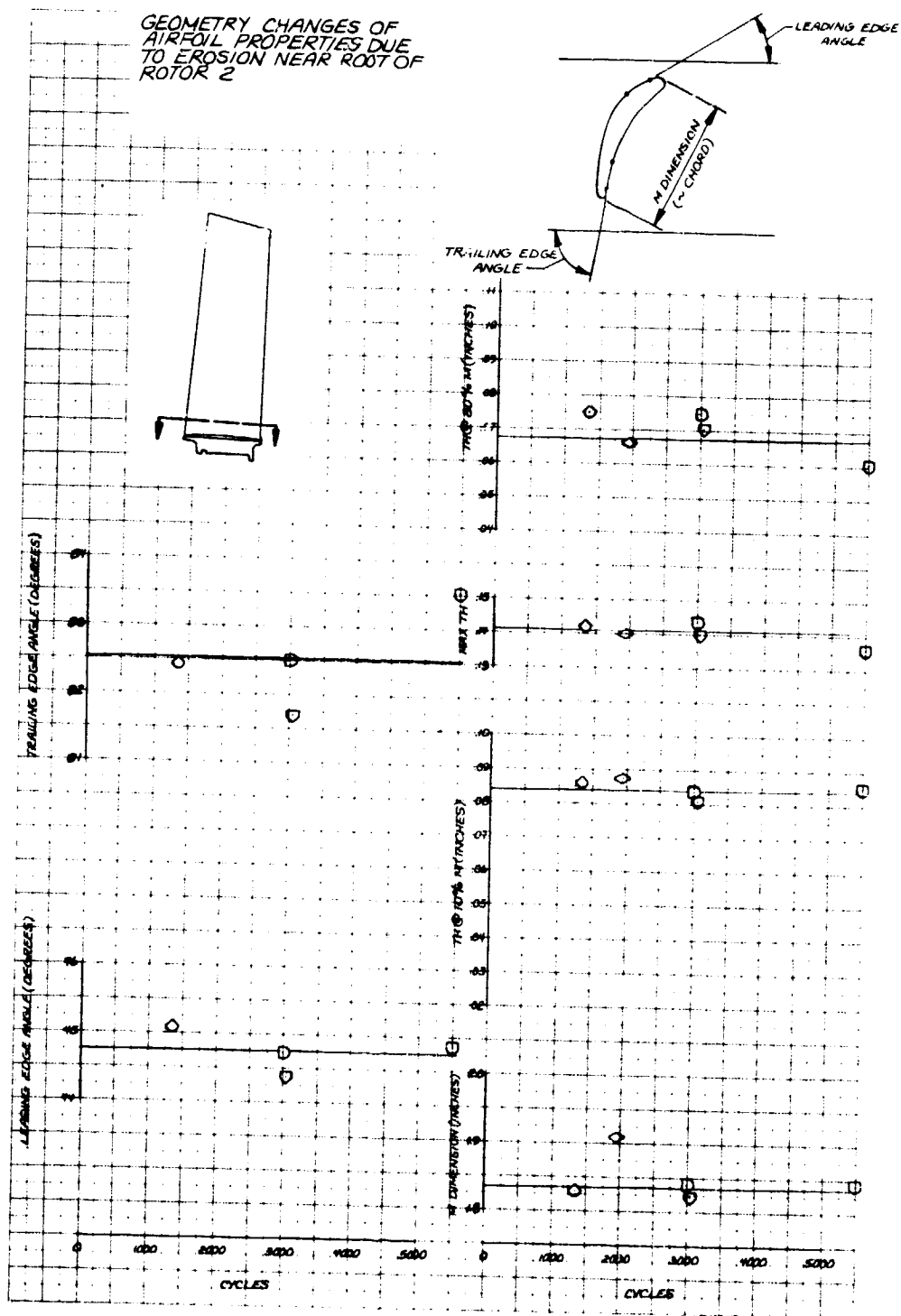


Figure B-10 Second-Stage Rotor Root Profile Data.

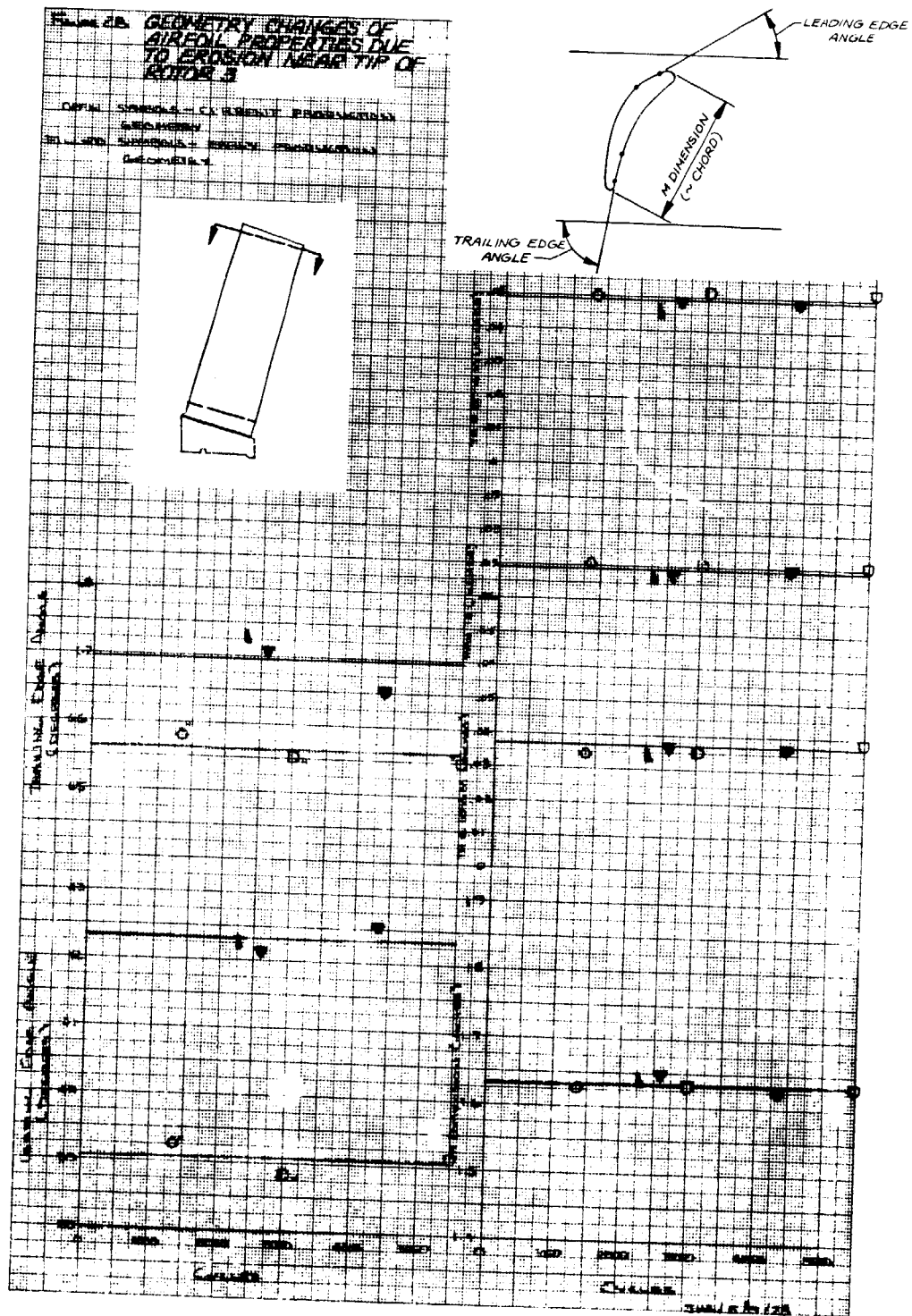


Figure B-11 Third-Stage Rotor Tip Profile Data.

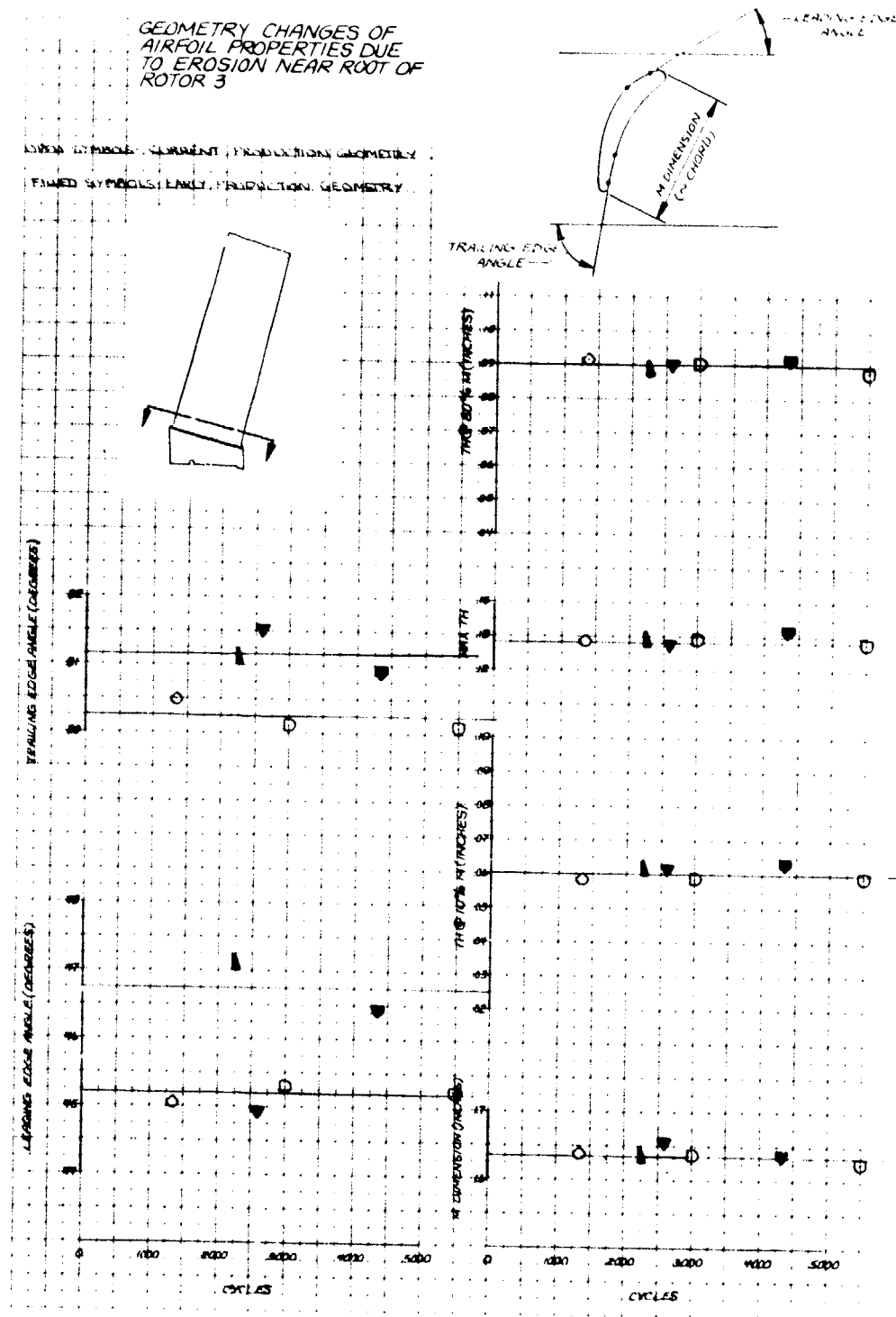


Figure B-12 Third-Stage Rotor Root Profile Data.

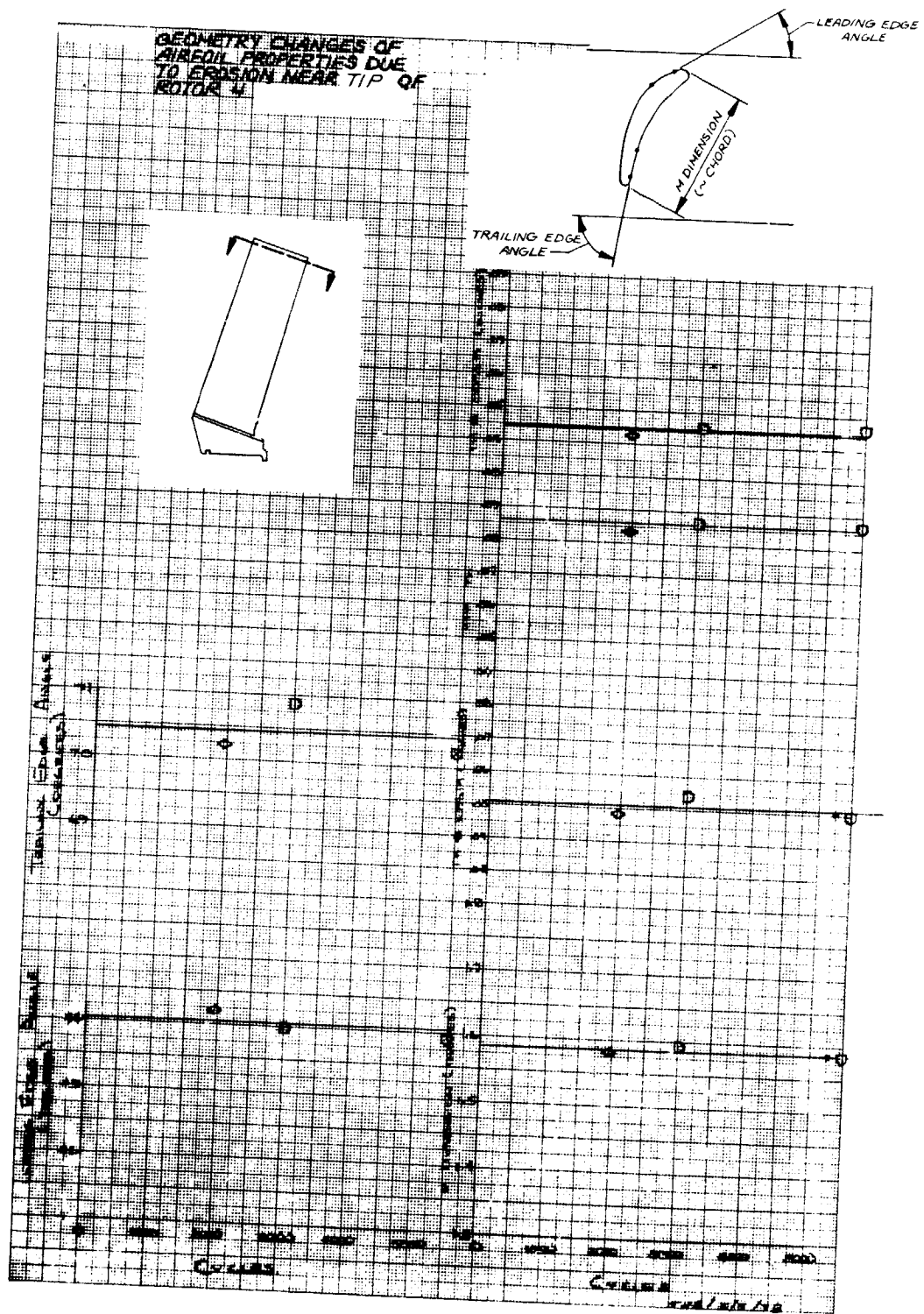


Figure B-13 Fourth-Stage Rotor Tip Profile Data.

GEOMETRY CHANGES OF AIRFOIL PROPERTIES DUE TO EROSION NEAR ROOT OF ROTOR 4

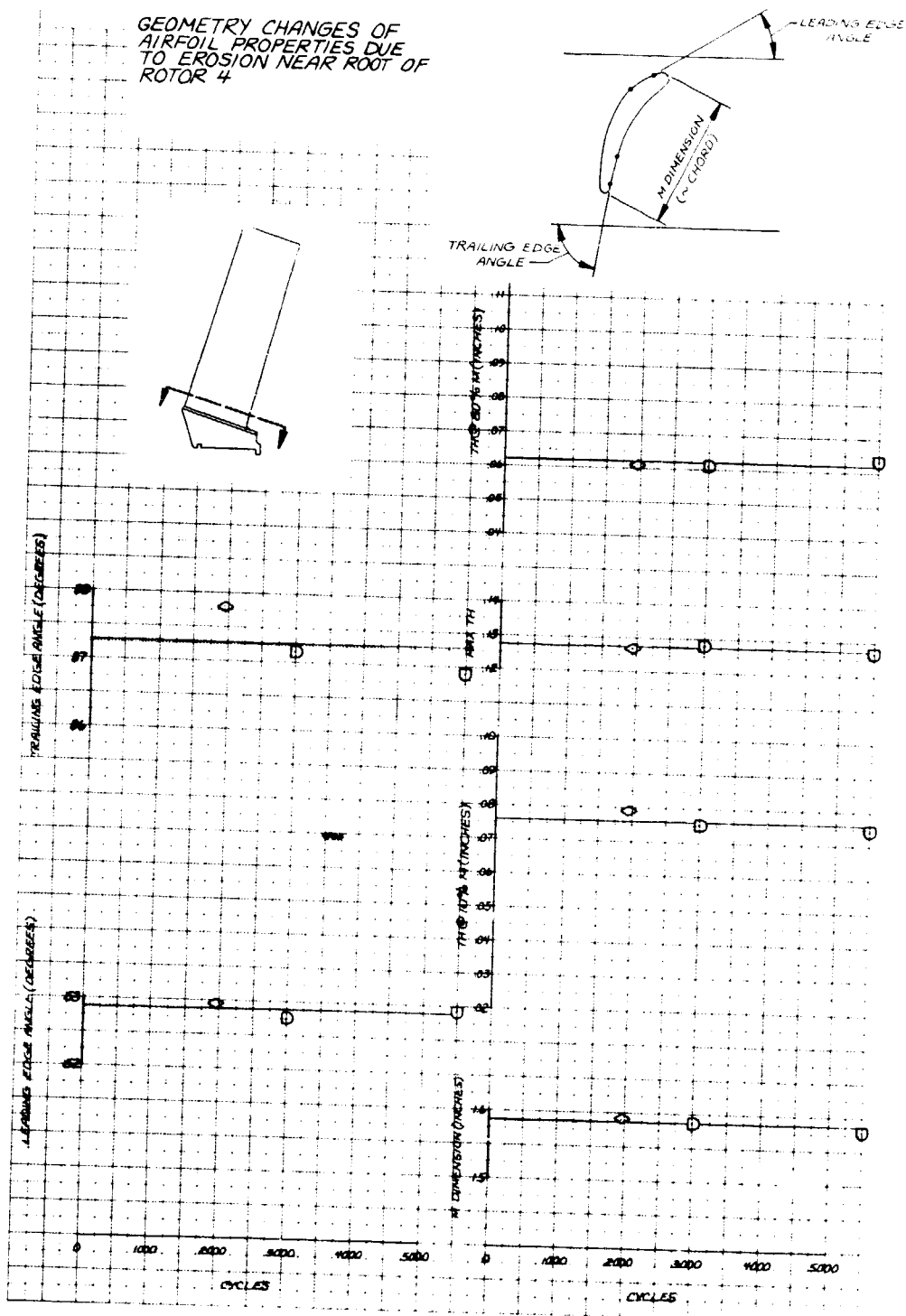


Figure B-14 Fourth-Stage Rotor Root Profile Data.

High-Pressure Compressor

The physical condition of the high-pressure compressor blades is shown in Figures B-15 through B-20. Deterioration in the high-pressure compressor is related to the cyclic usage level and accelerates beyond 3000 cycles as shown in Figure B-16. Deterioration at a given usage level is a function of the position within the compressor as shown in Figure B-19. Variation from stage to stage may be caused by:

1. The transition in the abradable rub-strip material from rubber to feltmetal at stage 8.
2. The transition in blade material from titanium to steel at stage 14.
3. The location of a bleed aft of stage 9 which is used extensively during ground operations.

Figure B-20 shows the impact of the "squealer cut" on the tip of the sixth-stage blade which is employed to control the structural dynamic properties of the airfoil. This "pre-thinning" of the airfoil tip accelerates the erosion and loss of airfoil contour of this stage blade.

Based on the inspection of used high-pressure compressor rotor blades, Figures B-21 through B-26 show the changes to the airfoil properties caused by erosion at a root and a tip section for Rotors 6, 9, and 14. This airfoil geometry change was crossplotted against diameter to give a radial representation of the changes, and the results are shown in Figures B-27 through B-29.

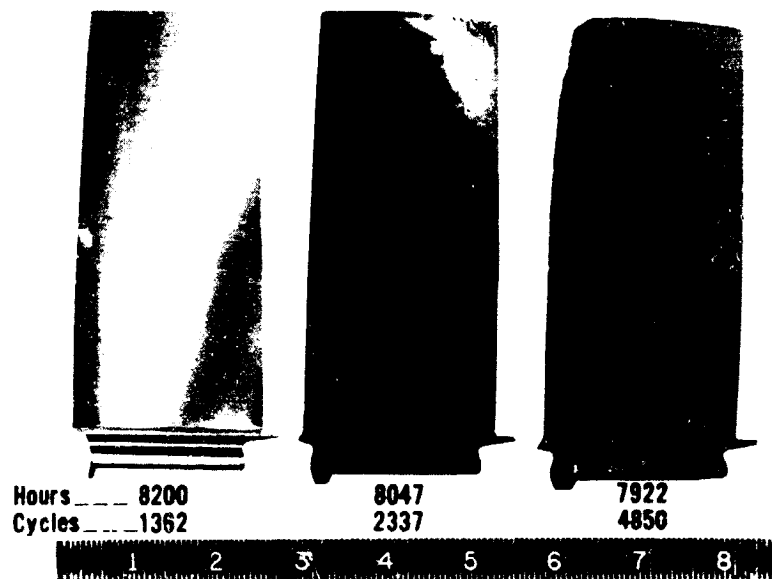


Figure B-15 JT9D Fifth-Stage High-Pressure Compressor Blades.

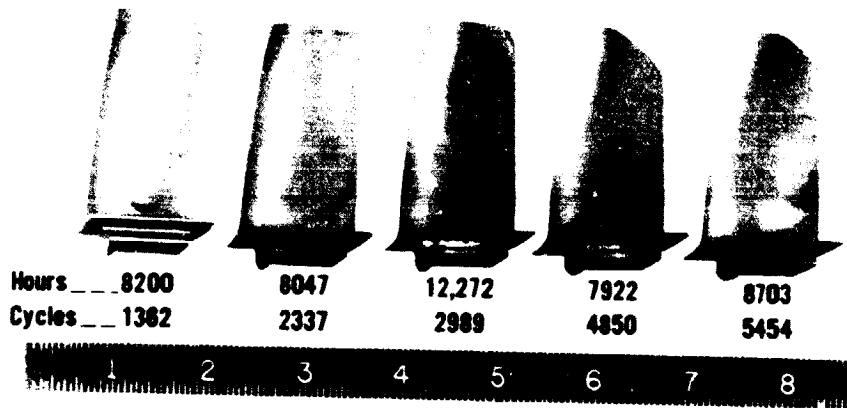


Figure B-16 JT9D Ninth-Stage High-Pressure Compressor Blades.

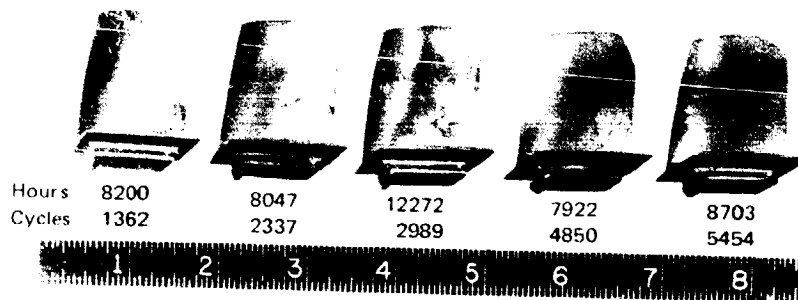


Figure B-17 JT9D Twelfth-Stage High-Pressure Compressor Blades.

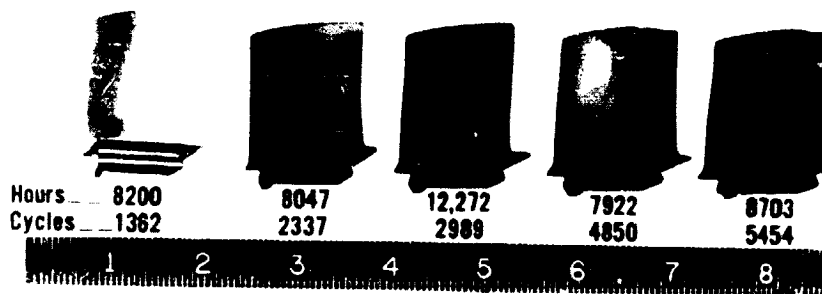


Figure B-18 JT9D Fifteenth-Stage High-Pressure Compressor Blades.

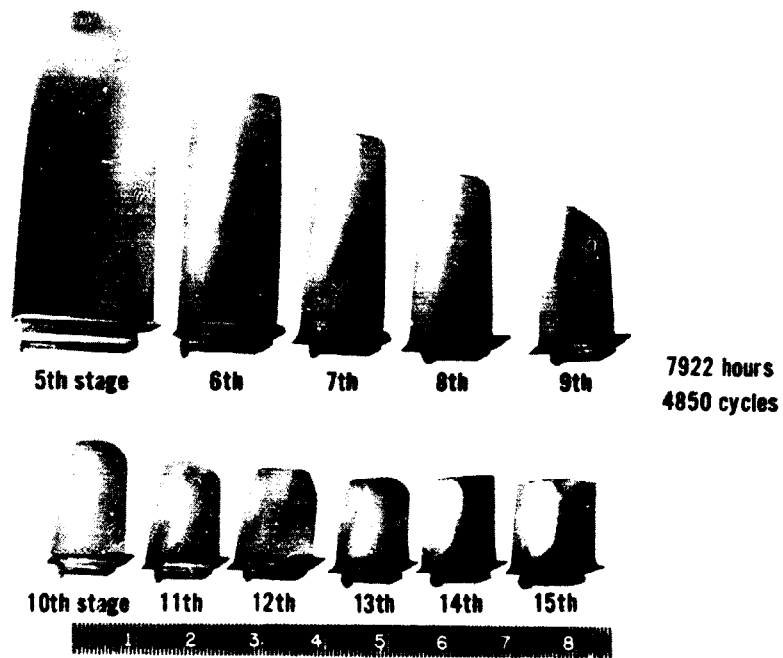
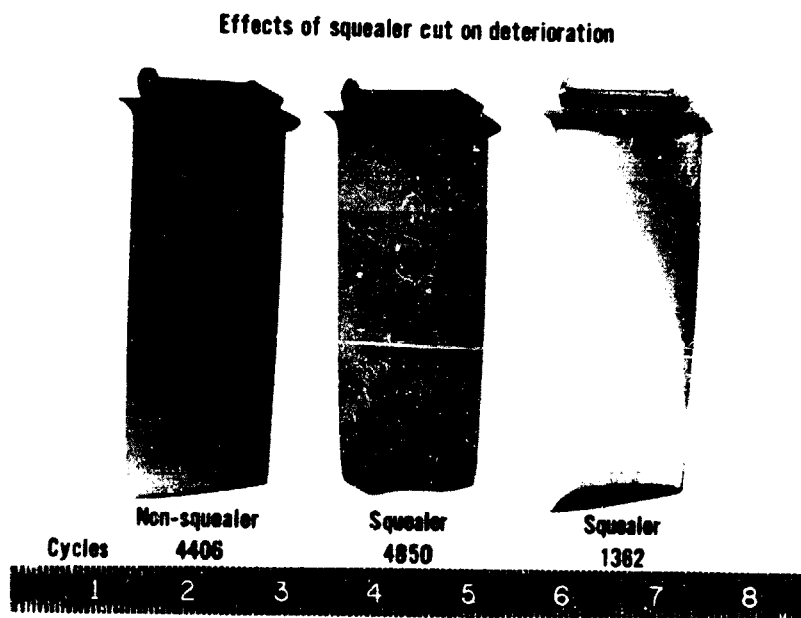


Figure B-19 JT9D High-Pressure Compressor Blades.



ORIGINAL PAGE IS
OF POOR QUALITY

Figure B-20 JT9D Sixth-Stage High-Pressure Compressor Blades.

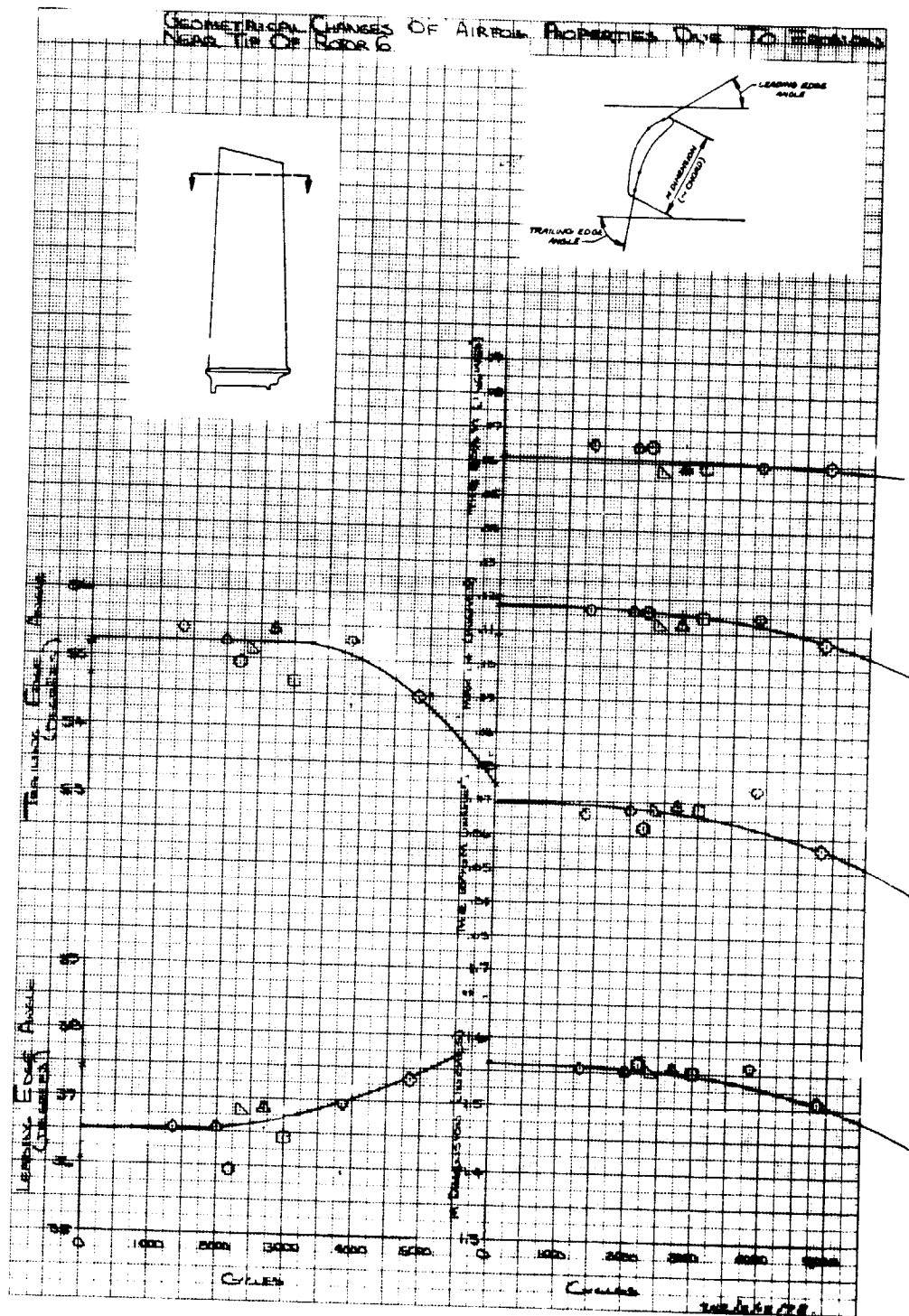


Figure B-21 Geometry Changes for Tip Section of Sixth-Stage Rotor Blade.

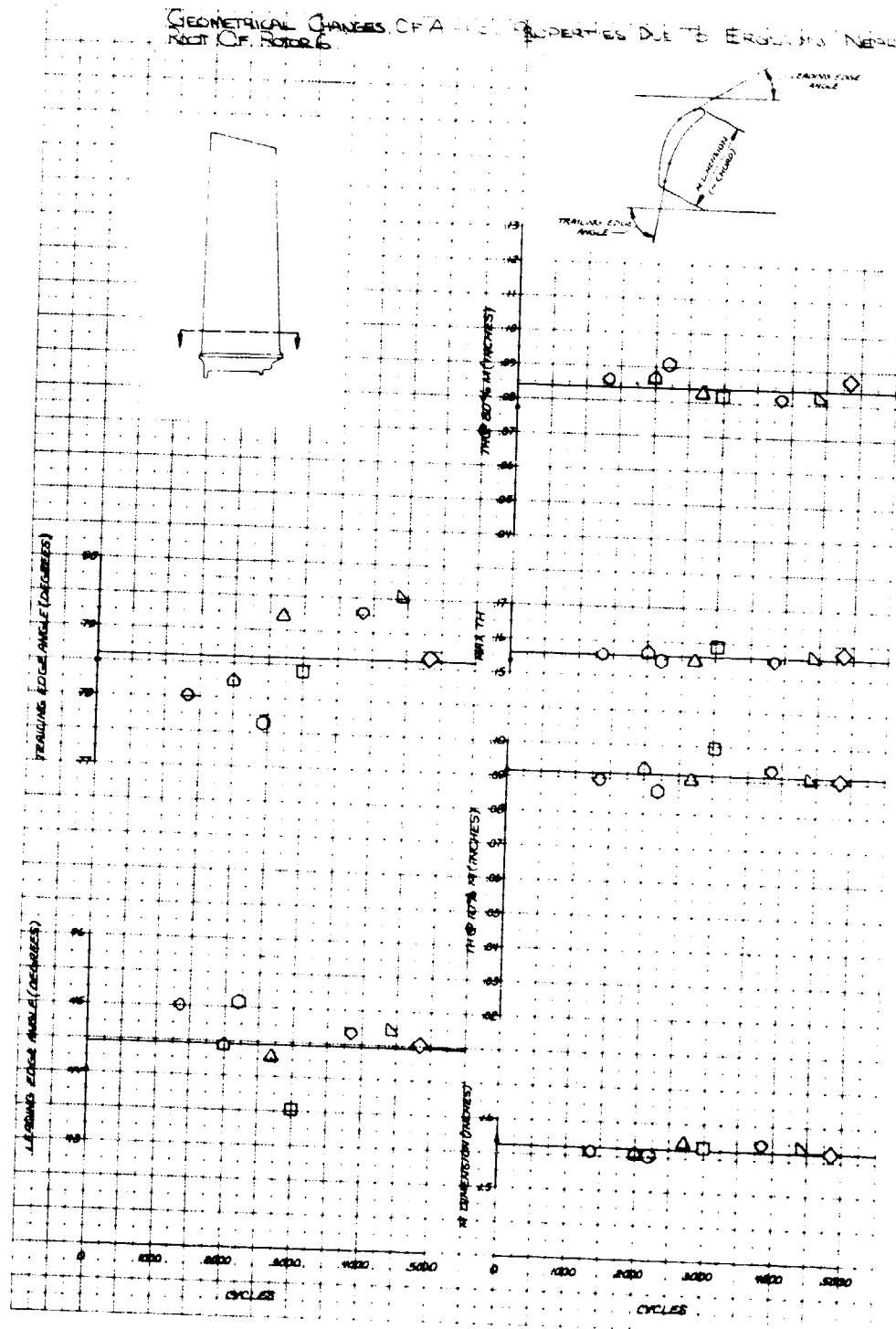


Figure B-22 Airfoil Geometry Changes for Root Section of Sixth-Stage Rotor Blade.

GEOMETRICAL CHANGES OF AIRFOIL PROPERTIES DUE TO EROSION NEAR TIP OF ROTOR 9

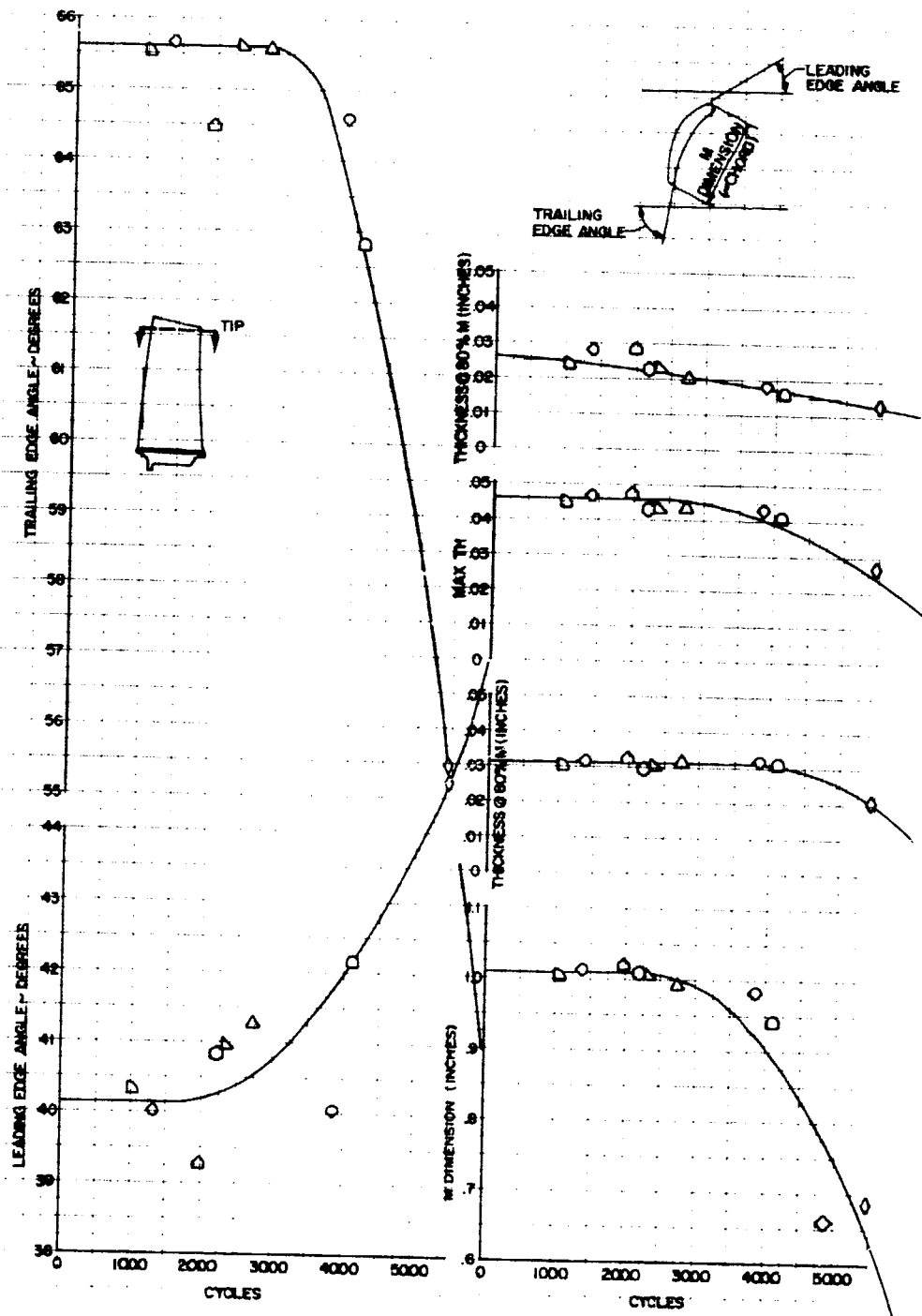


Figure B-23 Airfoil Geometry Changes for Tip Section of Ninth-Stage Rotor Blade.

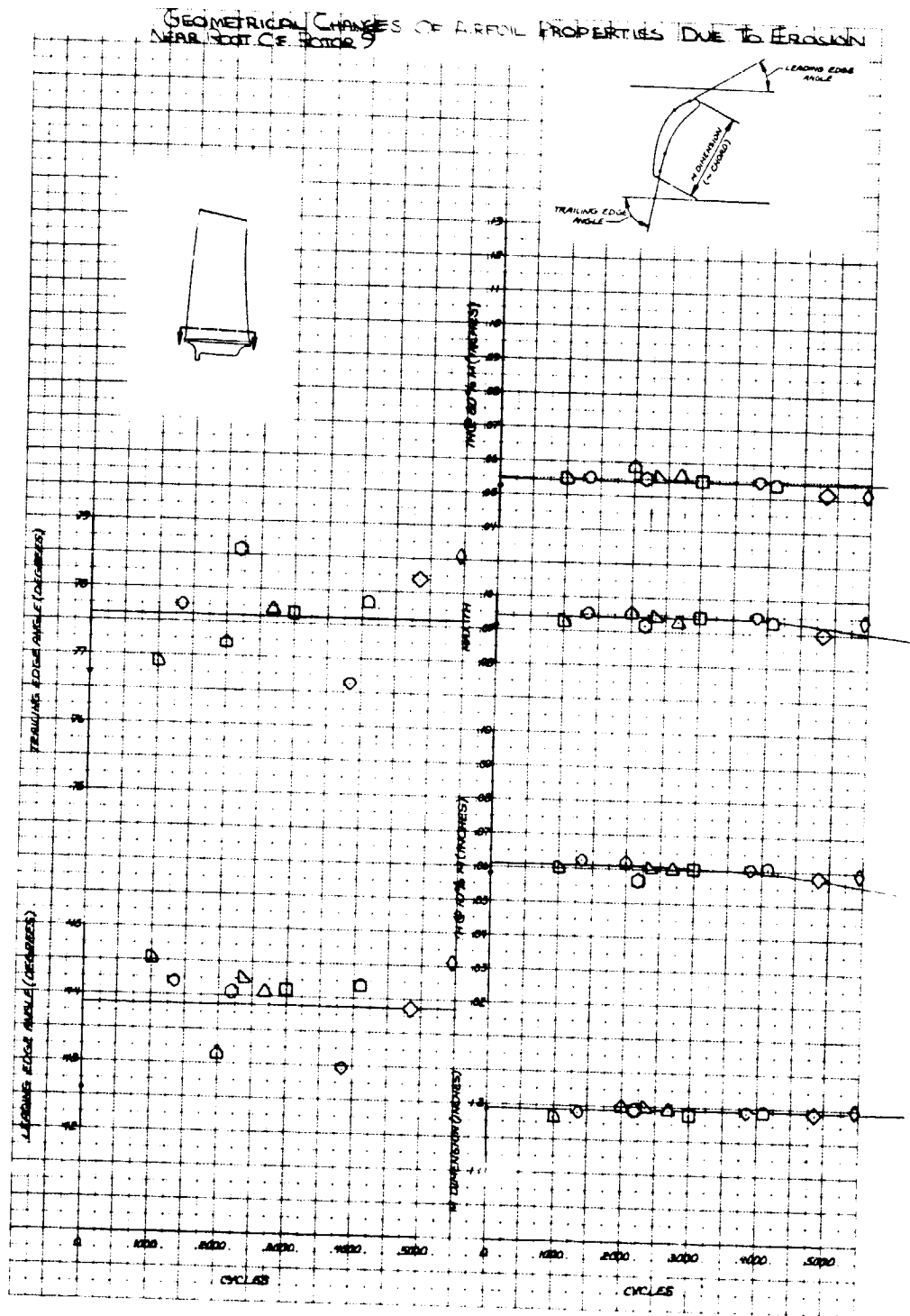


Figure B-24 Airfoil Geometry Changes for Root Section of Ninth-Stage Rotor Blade.

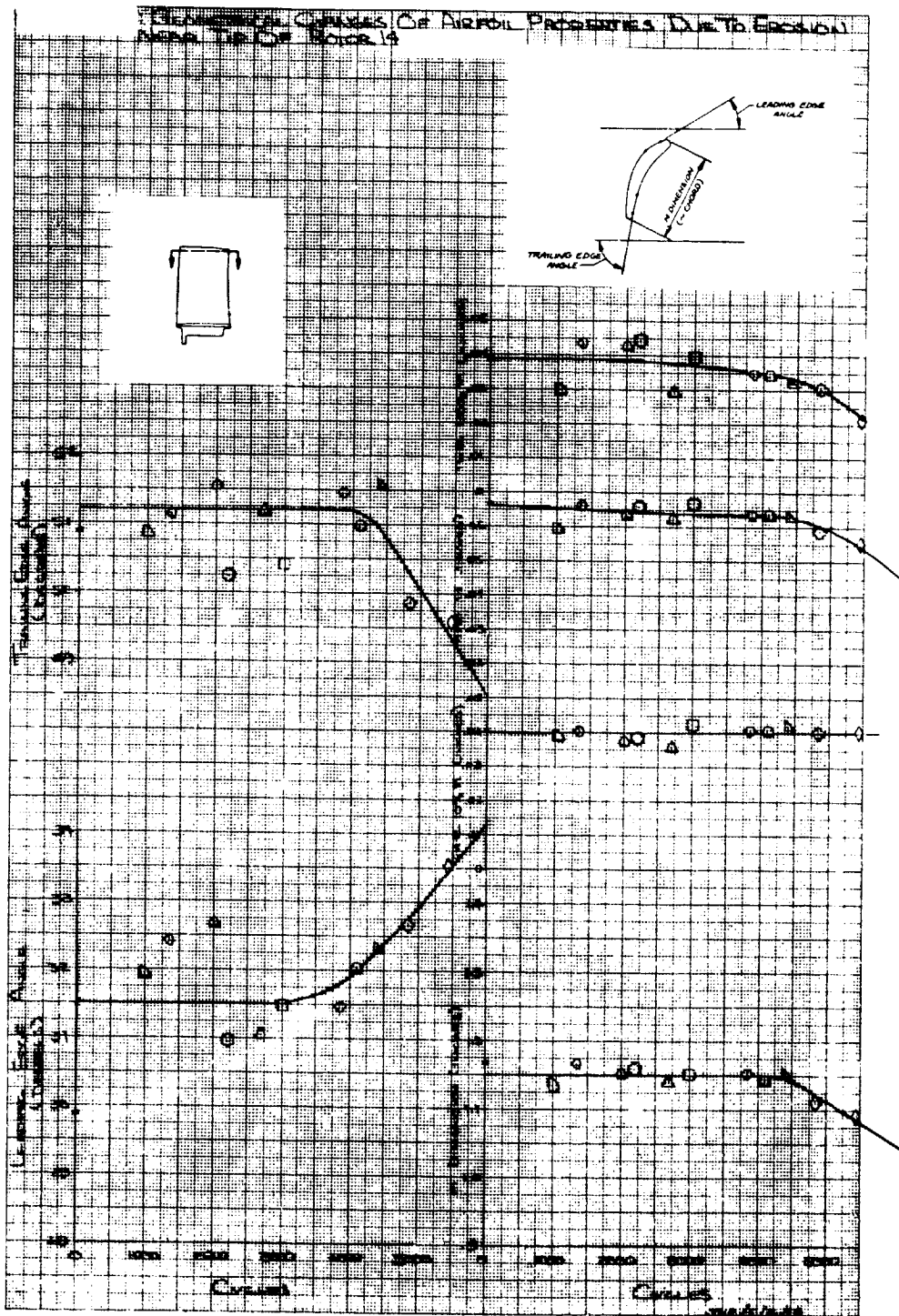


Figure B-25 Airfoil Geometry Changes for Tip Section of Fourteenth-Stage Rotor Blade.

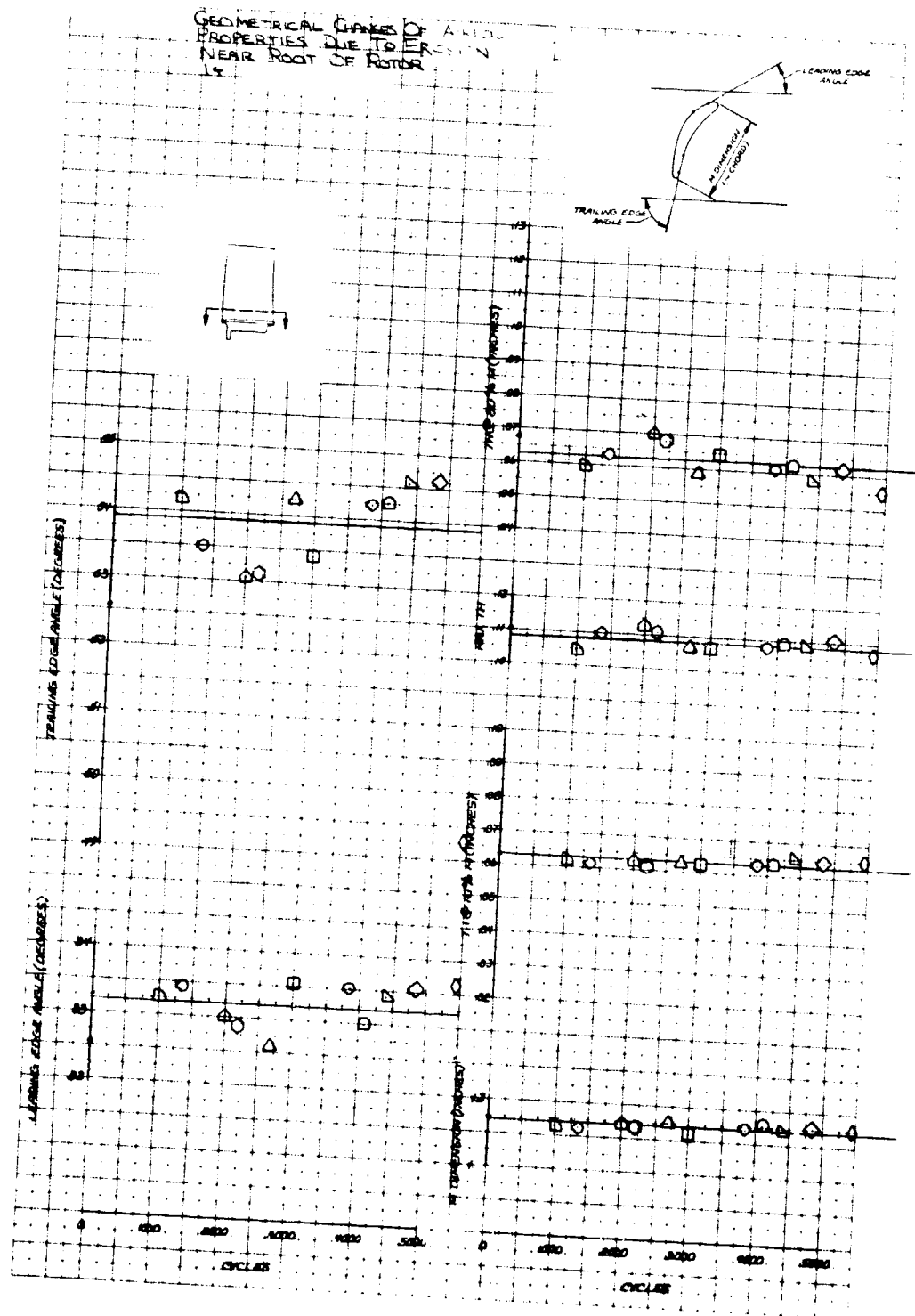


Figure B-26 Airfoil Geometry Changes for Root Section of Fourteenth-Stage Rotor Blade.

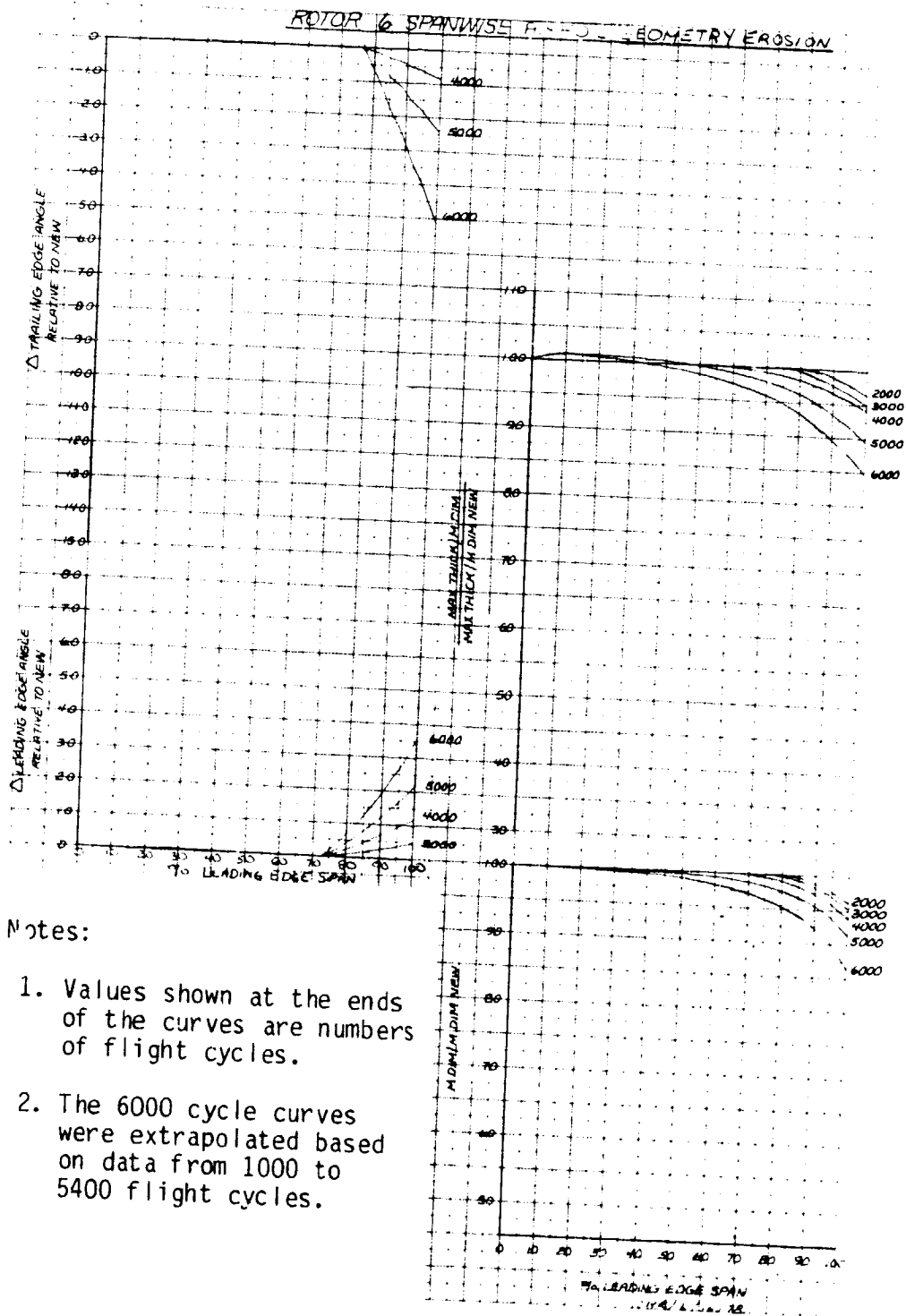


Figure B-27 Airfoil Geometry Changes for Span of Sixth-Stage Rotor Blades.

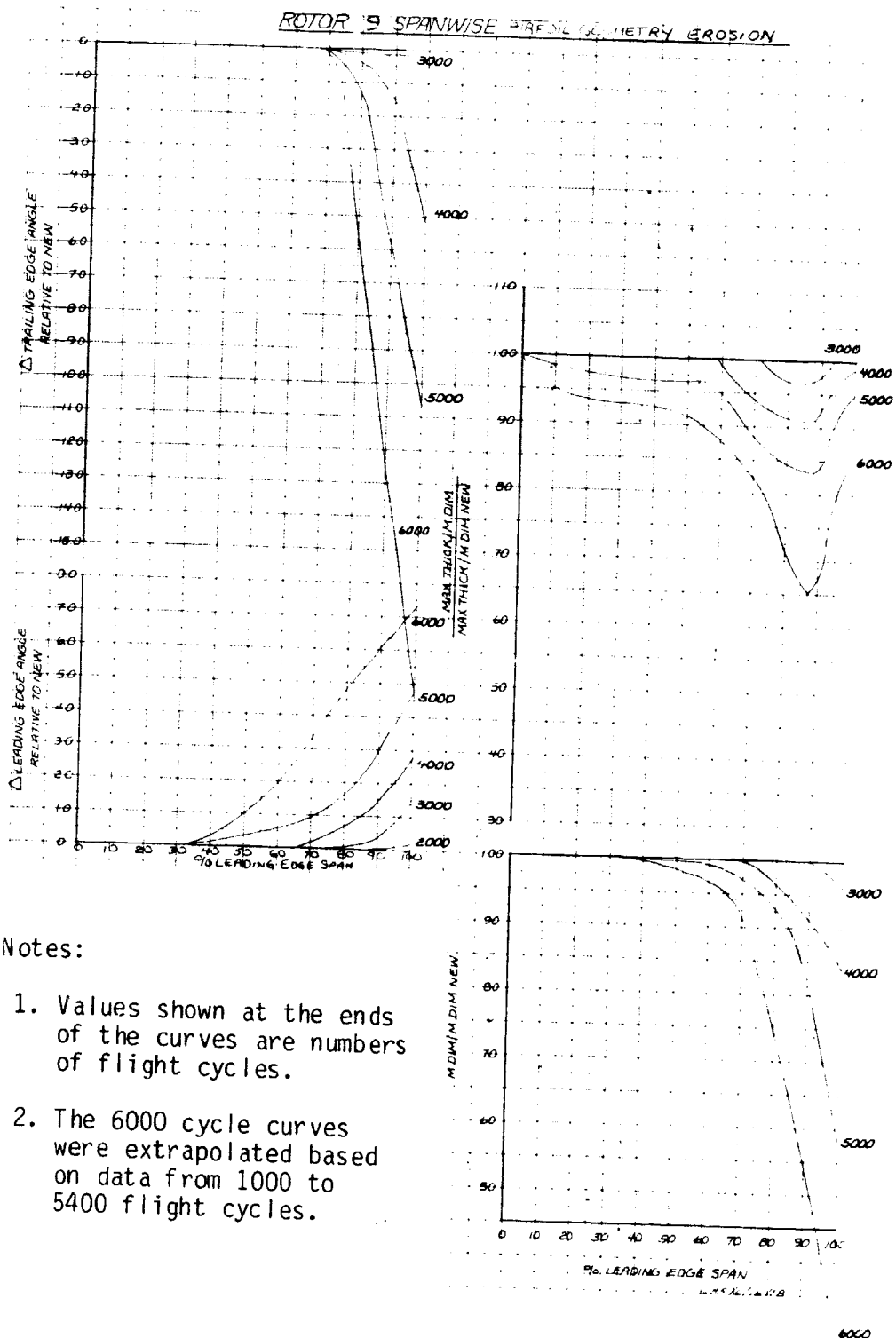
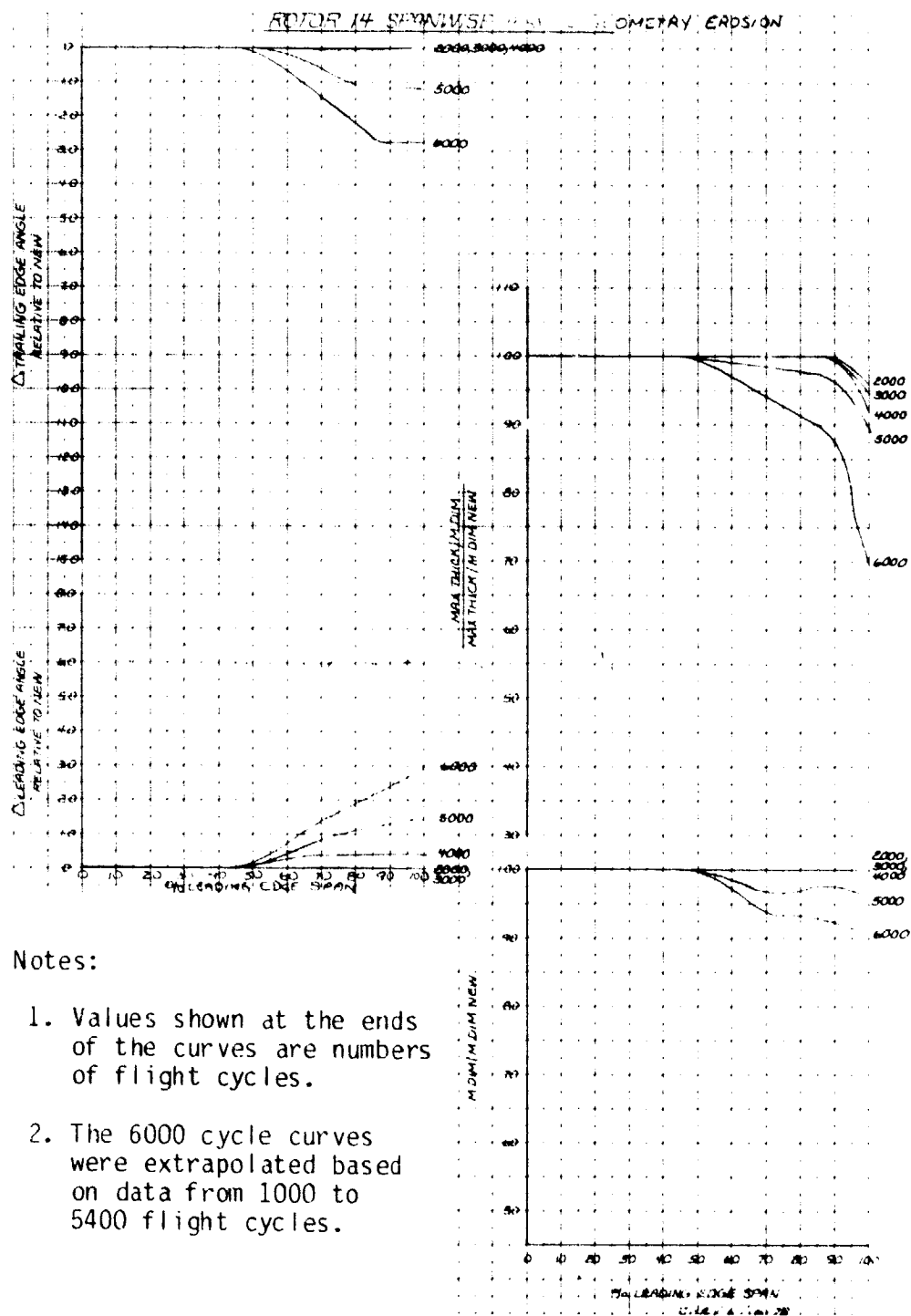


Figure B-28 Airfoil Geometry Changes for Span of Ninth-Stage Rotor Blades.



Notes:

1. Values shown at the ends of the curves are numbers of flight cycles.
2. The 6000 cycle curves were extrapolated based on data from 1000 to 5400 flight cycles.

Figure B-29 Airfoil Geometry Changes for Span of Fourteenth-Stage Rotor Blades.

High-Pressure Turbine

Figures B-30 through B-37 show the physical condition of high-pressure turbine airfoils collected for detailed inspection. The photographs show little visible deterioration of these airfoils. More rigorous inspection techniques were required to document parts condition (such as bow, twist, and tip wear which exist but are not visible from photographs) as a function of parts age. The high time first-stage turbine blades would have been repaired at least once.

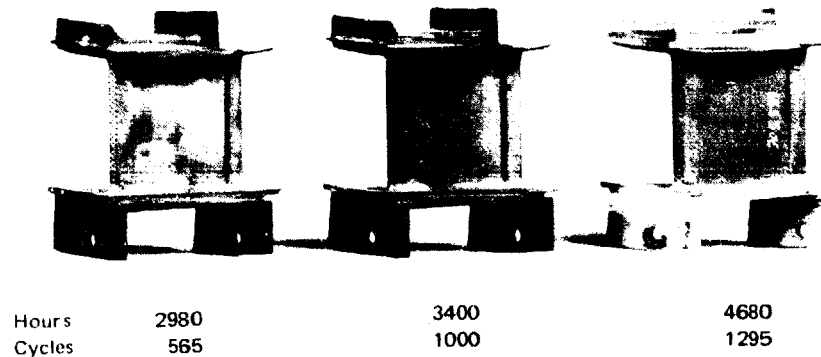


Figure B-30 JT9D First-Stage High-Pressure Turbine Vanes.

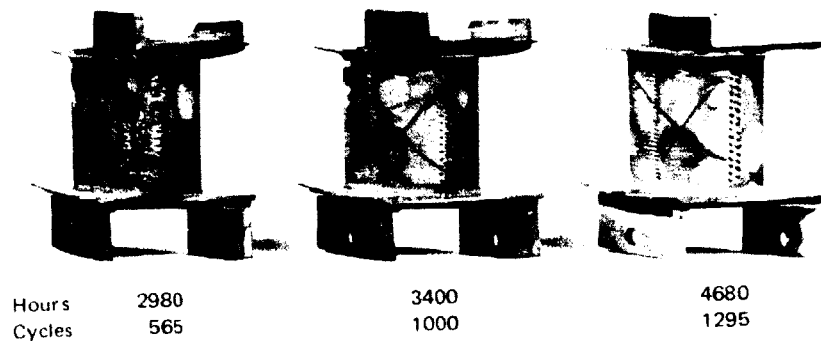
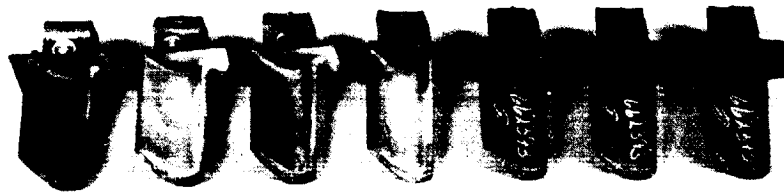


Figure B-31 JT9D First-Stage High-Pressure Turbine Vanes.



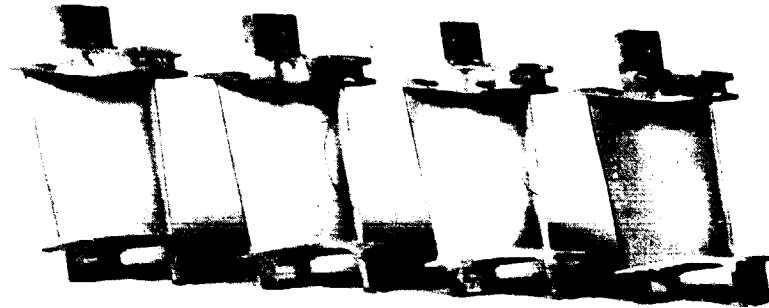
Hours	1450	2980	3235	6495	7900 est	10,500 est	11,300 est
Cycles	880 est	565	610	1900 est	2000 est	2,800 est	3,000 est

Figure B-32 JT9D First-Stage High-Pressure Turbine Blades.



Hours	1450	2980	3235	6495	7900 est	10,500 est	11,300 est
Cycles	880 est	565	610	1900 est	2000 est	2,800 est	3,000 est

Figure B-33 JT9D First-Stage High-Pressure Turbine Blades.



Hours	2900	3500	5600	6500
Cycles	580	785	1640	1935

Figure B-34 J9D Second-Stage High-Pressure Turbine Vanes.



Hours	2900	3500	5600	6500
Cycles	580	785	1640	1935

Figure B-35 JT9D Second-Stage High-Pressure Turbine Vanes.



Hours	3000	3615	4400	6835	7870	9,655	12,200	13,500
Cycles	565	1000 est	1330	1800 est	2000 est	2,500 est	3,200 est	3,500 est

Figure B-36 JT9D Second-Stage High-Pressure Turbine Blades.



Hours	3000	3615	4400	6835	7870	9,655	12,200	13,500
Cycles	565	1000 est	1330	1800 est	2000 est	2,500 est	3,200 est	3,500 est

Figure B-37 JT9D Second-Stage High-Pressure Turbine Blades.

Low-Pressure Turbine

Photographs of the low-pressure turbine airfoils collected were not made because of the lack of signs of deterioration which could be adequately photographed such as bow, twist, and light rub.

APPENDIX C

PARTS USAGE AND REPAIR RATE ANALYSIS

INTRODUCTION AND SUMMARY

This appendix summarizes the results of the analysis of the parts replacement/repair rates of each of the three airlines participating in the NASA JT9D Jet Engine Diagnostics Program. Necessary data were gathered to identify parts usage of all gas path parts which could be significant contributors to engine performance deterioration. The source documents and years of availability of the data at each airline have been described in detail in Trip Reports to NASA dated during March, April, and May of 1977.

Data were acquired from the airlines for all types of maintenance actions which could have an impact on engine performance. These data included the quantity of parts scrapped, repaired, or used in conversion from one model to another. Since some repair actions are made strictly for mechanical reasons and have no impact on part performance, it was necessary to review the types of repairs performed on each part and the repair practices at each airline to determine which repair actions should be counted as restoring performance and which should not. The parts usage rate, for actions which restored part performance, was then calculated. This parameter is expressed as percent of parts replaced per 1000 engine flight hours (EFH), as discussed in Section 3.0.

Knowing the parts usage rates, the aircraft introduction rate, and flight hours and cycles per year for each airline, a computer model was constructed to estimate the average time/age since performance restoration, by year, for each of the gas-path parts of interest. This is the primary output of the Parts Usage Rate Analysis.

These data were also analyzed as a part of the "bottom-up" performance analysis method to determine the average module part age (flight cycles) as a function of engine age. These part times/ages were then used in conjunction with the results of the mechanical inspection of parts versus part time/age to determine the contribution of each type of part to the loss in efficiency and flow capacity of each module.

Since the parts usage data at each of the airlines is considered proprietary, the airlines are identified in this report as Airlines A, B, and C.

RESULTS

Figures C-1 through C-6 present the trends of the average age of parts in each module versus engine cyclic age for Airlines A, B, and C. The

variations in part age between airlines can be seen and would be expected to contribute to differences in engine performance deterioration levels.

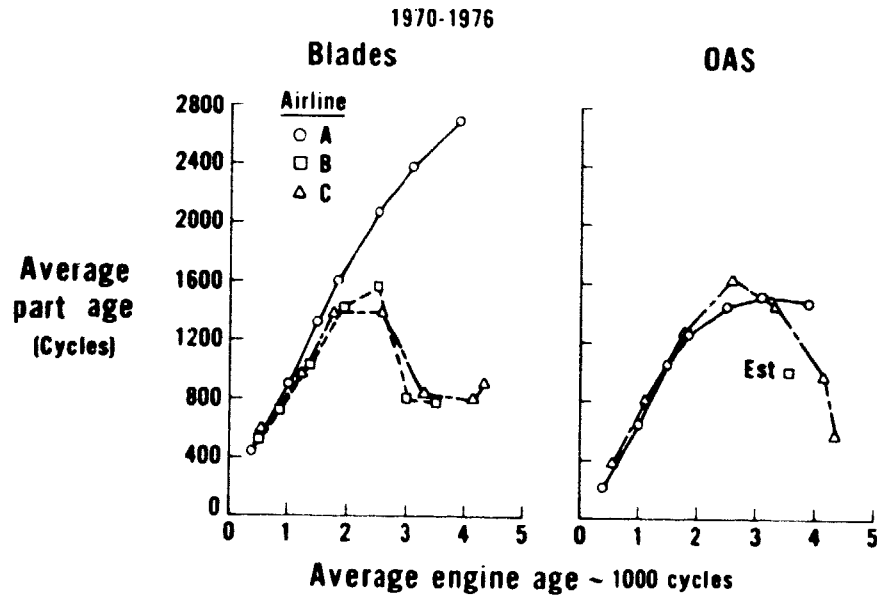


Figure C-1 JT9D Fan Module Part Age.

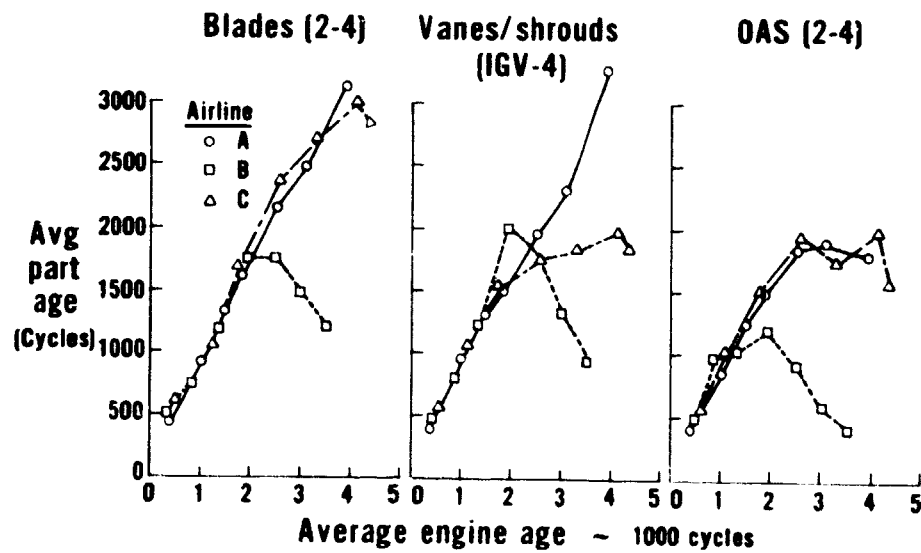


Figure C-2 JT9D Low-Pressure Compressor Module Part Age.

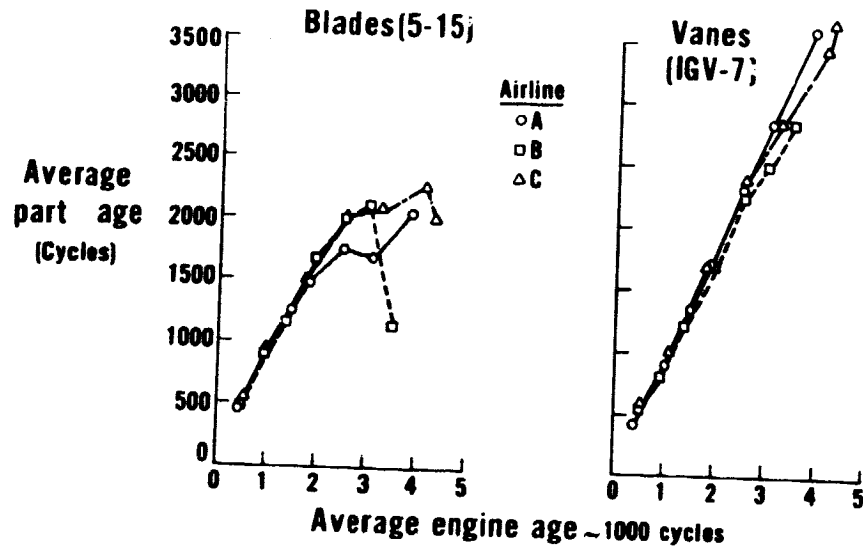


Figure C-3 JT9D High-Pressure Compressor Blade and Vane Part Age.

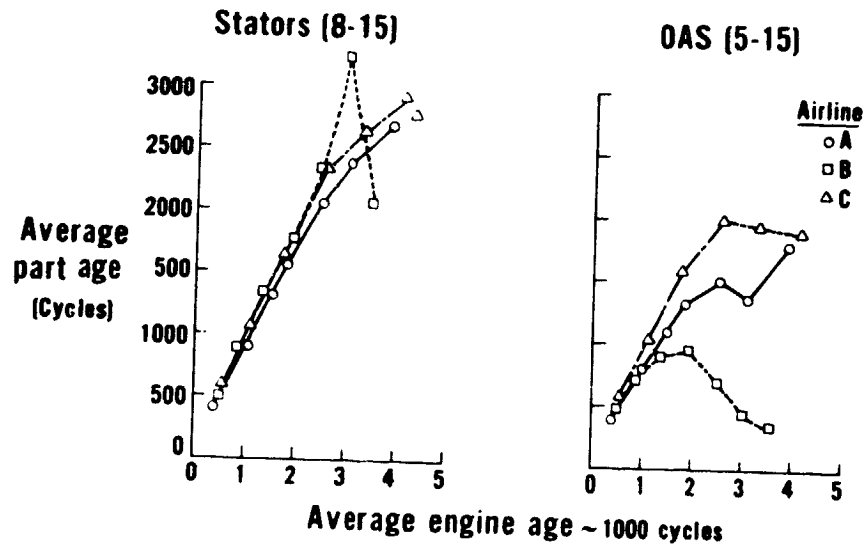


Figure C-4 JT9D High-Pressure Compressor Stator and Outer Air Seal Part Age.

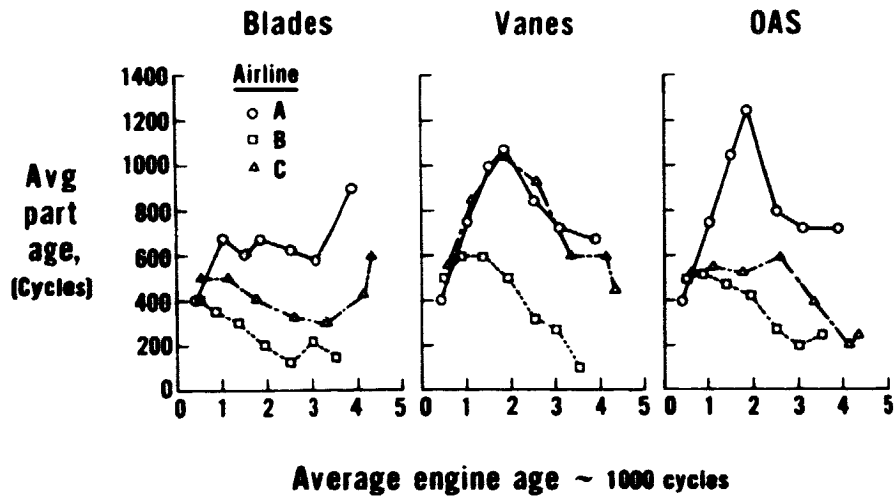


Figure C-5 JT9D High-Pressure Turbine Module Part Age.

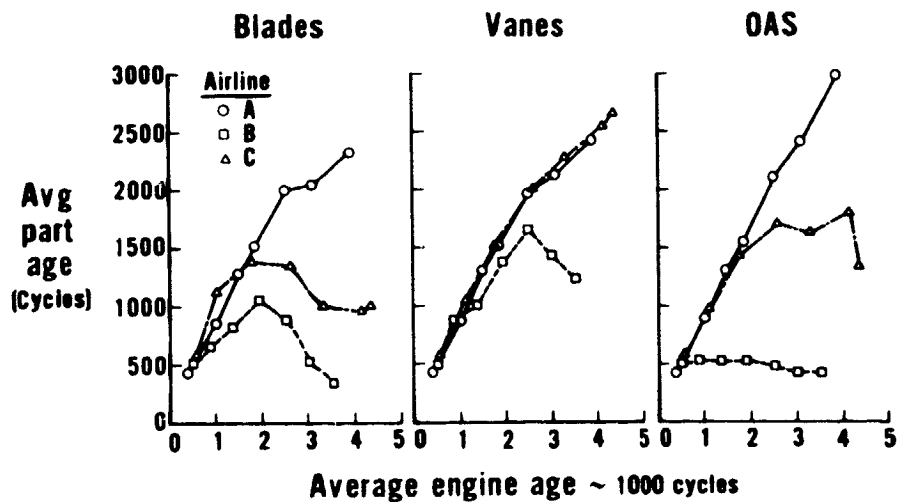


Figure C-6 JT9D Low-Pressure Turbine Module Part Age.

APPENDIX D
REBUILD STANDARDS VARIATIONS

TABLE D-1

VARIATIONS IN COLD SECTION REBUILD STANDARDS

(page 1 of 8)

Part	Item	I&C Ref No	PAWA Standard Min Max	Airline Standard Min Max	P&W Engine Manual Reference	Airline Engine Manual Reference
1 Fan blade	Blend depth limits		0.250 in tip 0.250 on I.F. & TE	0.750 in tip 0.500 on I.F. & TE	72-31-05 Insp-01 pg 805	1-1-302 pg 3
	Rub depth limits		Above horizontal ϕ , depth of rub not to exceed 0.100 Below horizontal ϕ , depth of rub not to exceed 0.215 for 120° and not to exceed 0.155 for remainder.	Depth of rub not to exceed 0.160 max for not more than 120° and not more than 0.120 for remainder	72-31-01 Insp-01 pg 804	1-4-301 pg 5
2 Fan hubstrip (ASC)	Tip clearances (0.085 vertical offset, P/N 710061) (no vertical offset, P/N 674979) (0.085 vertical offset, P/N 727155) (0.115 vertical offset, P/N 732768) (0.085 vertical offset, P/N 727094)	200R	0.110 0.130	0.130 0.150	72-100-00 Inst-03 pg 413	5-8-501 pg 3
			0.150 0.170	0.150 0.170		
			0.110 0.130	0.110 0.130		
			0.095 0.115	0.110 0.130		
3 Fan exit guide vane	Blend depth limits		Maximum reduction to vane chord length is 0.500	Maximum reduction to vane chord length is 0.500 on vID portion and 0.375 on ID portion	72-33-02 Insp-01 pg 801	1-4-304 pg 1
	Wear limits		No stated limits. Recommend complete replacement at total disassembly.	Vane wake erosion allowable to depth of 0.070. Rub allowable to depth of 0.050	72-32-06 Insp-01 pg 812	1-2-308 pg 4
4 2nd LPC blade rib strip	Wear limits		No stated limits. Recommend complete replacement at total disassembly.	Rub allowable to depth of 0.030	72-32-06 Insp-01 pg 812	1-2-308 pg 4
			0.056 0.085	Measured, no RID limits indicated in manual. Assume full restoration used (denoted with F)	72-32-00 Insp-02 pg 807 72-32-00 Insp-02 pg 808	1-2-506 pg 4 1-2-505 pg 5
			0.016 0.043	After reconditioning and removal of sharp edges, vane can have 0.035 erosion under min chord.	72-34-11 Insp-01 pg 801	1-4-315 pg 3
5 3rd LPC blade ribstrip	Wear limits		No stated limits. Recommend complete replacement at total disassembly.	Rub allowable to depth of 0.030	72-32-06 Insp-01 pg 812	1-2-308 pg 4
			0.056 0.085	Measured, no RID limits indicated in manual. Assume full restoration used (denoted with F)	72-32-00 Insp-02 pg 807 72-32-00 Insp-02 pg 808	1-2-506 pg 4 1-2-505 pg 5
			0.016 0.043	After reconditioning and removal of sharp edges, vane can have 0.035 erosion under min chord.	72-34-11 Insp-01 pg 801	1-4-315 pg 3
6 LPC blade	Tip clearances	36	0.056 0.085	Measured, no RID limits indicated in manual. Assume full restoration used (denoted with F)	72-32-00 Insp-02 pg 807 72-32-00 Insp-02 pg 808	1-2-506 pg 4 1-2-505 pg 5
			0.016 0.043	After reconditioning and removal of sharp edges, vane can have 0.035 erosion under min chord.	72-34-11 Insp-01 pg 801	1-4-315 pg 3
			0.038 0.062F	After reconditioning and removal of sharp edges, vane can have 0.035 erosion under min chord.	72-34-11 Insp-01 pg 801	1-4-315 pg 3
7 LPC blade	Tip clearances	37	0.016 0.043	After reconditioning and removal of sharp edges, vane can have 0.035 erosion under min chord.	72-34-11 Insp-01 pg 801	1-4-315 pg 3
			0.038 0.062F	After reconditioning and removal of sharp edges, vane can have 0.035 erosion under min chord.	72-34-11 Insp-01 pg 801	1-4-315 pg 3
			0.038 0.062F	After reconditioning and removal of sharp edges, vane can have 0.035 erosion under min chord.	72-34-11 Insp-01 pg 801	1-4-315 pg 3
8 HCV	Erosion limits		No stated limit, min chord dimension apply.	After reconditioning and removal of sharp edges, vane can have 0.035 erosion under min chord.	72-34-11 Insp-01 pg 801	1-4-315 pg 3
			0.0002 0.0027	0.0002 0.0027	72-34-00 Insp-03 pg 814	1-4-319 pg 1
			0.0002 0.0027	0.0002 0.0027	72-34-00 Insp-03 pg 814	1-4-319 pg 1
9 HCV unison ring to shoulder pin clearance	Erosion limits		No stated limit, min chord dimension apply.	After reconditioning and removal of sharp edges, vane can have 0.035 erosion under min chord.	72-34-11 Insp-01 pg 801	1-4-315 pg 3
			0.0002 0.0027	0.0002 0.0027	72-34-00 Insp-03 pg 814	1-4-319 pg 1
			0.0002 0.0027	0.0002 0.0027	72-34-00 Insp-03 pg 814	1-4-319 pg 1

TABLE D-I (Cont'd.)

VARIATIONS IN COLD SECTION REBUILD STANDARDS

(page 2 of 8)

Part	Item	FACT Ref No.	FAWA Standard		Airline Standard		PAWA Engine Manual Reference	Airline Engine Manual Reference					
			Min	Max	Min	Max							
10. HPC Blade	Minimum length if HPC duct at minimum diameter or disk at maximum diameter		5.048		5.043		72-305-05 Insp-01 pg 810	2-5-312 pg 4					
			4.087		4.082								
			3.380		3.375								
			2.805		2.800								
			2.343		2.338								
			2.006		2.001								
			1.808		1.803								
			1.633		1.628								
			1.535		1.530								
			1.543		1.538								
			1.539		1.534								
			11. 8th - 15th HPC ducts	Rush depth		Abrasion limited in an arc of 120° acceptable to a max depth of 0.044 (0.049 P.S.)				72-35-06 Insp-01 pg 830 for stages 9 & 10 and 72-35-12 Insp-01 pg 802 for stages 8 & 11-15	2-5-317 pg 7 for stages 9 & 10 and 2-5-340 through 344 for stages 8 & 11-14 and 2-5-322 for stage 15		
						Abrasion which extends more than 120° acceptable to a depth of 0.017.							
			12. 5th-15th HPC ducts	Erosion		Axial erosion limited to				72-35-06 Insp-01 pg 830	2-5-317 stages 9 & 10 2-5-340-344 stages 11-14 & 8 2-5-322 stage 15		
						0.150 for stage 5							
0.190 for stage 6													
0.125 for stage 7													
0.155 for stage 8													
0.120 for stage 9													
0.130 for stage 10													
0.170 for stage 11													
0.145 for stage 12													
0.180 for stage 13													
13. 5th - 14th HPC IAS	Knife edge wear		Conserve RFO limit on each K/F of each IAS				72-35-07 Insp-01 pg 801	2-5-324 pg 1 through 2-5-333 pg 1					
			For all 3 K/F IAS config. 1)										
			One K/F may exceed RIO limit by 0.025 on diameter if the other 2 K/F's are within RIO.										
			2) Any 2 K/F's may exceed RIO limit, 1 by 0.015 and the other by 0.007 on the diameter if the third K/F is within RIO.										
			Use no more than 2 of the above IAS per HPC.										

TABLE D-I (Cont'd.)
 VARIATIONS IN COLD SECTION REBUILD STANDARDS

(page 3 of 8)

Part	Item	FACI Ref. No.	P&WA Standard		Airline Standard		P&WA Engine Manual Reference	Airline Engine Manual Reference
			Min	Max	Min	Max		
14. 5th - 15th HPC blades	Tip clearances	38R through 39R	P&WA full restoration or partial restoration clearances may be used. Maximum allowable clearance for full restoration generally is 0.003 larger than blueprint maximum. Maximum allowable clearance for partial restoration is generally 0.013 larger than blueprint maximum.		P&WA full restoration clearances used.		72-35-00 Imp-00	2-5-508 through 2-5-515
15. 5th - 15th HPC blades	Root sealing				Blade roots not sealed.		72-35-03 Assy	2-5-501

TABLE D-1 (Cont'd.)

VARIATIONS IN COLD SECTION REBUILD STANDARDS

(page 4 of 8)

Part	Item	F&CI Part No.	PAWA Standard		Airline Standard		PAWA Engine Manual Reference	Airline Engine Manual Reference	
			Min	Max	Min	Max			
1 Fan blade AIRLINE B	Blend limits		Leading edge damage on inner half of airfoil acceptable to a depth of 0.005		Leading or trailing edge damage on inner half of airfoil acceptable to a depth of 0.005		72-31-05 Imp 01 pg 803	72-31-05 O/H Imp 00 pg 303	
			Blend 0.040 beyond damage if crack is indicated, blend 0.006 beyond crack bottom		Blend 0.020 beyond damage if crack is indicated, blend 0.010 beyond crack bottom				
			Min chord maintained with in 2.000 of TE platform		Min chord maintained with in 1.000 of TE platform				
			No recommendation		Limit the number of blends to the max blend limit to 2 per blade.				
2 Fan blade (after honeycomb case)	Tip clearances	2008	0.110	0.130	0.130	0.150	72-00-00 Insall 03 pg 415	72-00-00 H/M Rem./ Insall 05 pg 414 Supplement	
	Blend limits		Limit the number of blended airfoils in each disk or vator assembly to 20% of total		Same as PAWA, except certain blends are not counted in calculating the 20% limit		72-35-05 & 06	72-35-05 & 06	
4 LPV rotating	Erosion limits		No recommendation on erosion. Recommend total refurbishment at each complete disassembly.		For 2nd stage reentry, severe erosion is allowable to a depth of 0.070 and blade rub to a depth of 0.050. For 3rd stage blade rub to a depth of 0.030 is acceptable.		72-32-06 Imp 02 pg 804	72-32-06 O/H Imp 00 pg 312	
			2nd	0.056	0.085	0.088F			0.091F
5 LPV blades	Tip clearances		3rd	0.016	0.043	0.046F	0.056F	72-32-00 Imp-02 pg 807	72-32-00 Clear 00 pg 606 Supplement
			4th	0.013	0.062F	0.072F	0.072F		
7 LPV vanes	Blend limits		No limit		1/32" max tip radius on LE and TE		72-35-05 Imp 01 pg 802	72-35-05 O/H Imp 00 pg 302 Supplement	
			Limit the number of blended vanes in each assembly to less than 20% of total		Same as PAWA except certain blends are not counted in calculating the 20% limit				

TABLE D-1 (Cont'd.)
 VARIATIONS IN GOLD SECTION REBUILD STANDARDS

Part	Tooth	FACI Part No.	P&WA Standard		Airline Standard		P&WA Engine Manual Reference	Airline Engine Manual Reference
			Min	Max	Min	Max		
8. HPC vanes	Blend limits							
9. HPC vanes (stages 8, 9, 10)	Selected vane replacement		Replace up to 100% vanes per assembly		Not checked due to lack of leveling		72-35-06 O/H Insp pg 305 Temporary revision	
10. HPC ducts (stages 8, 11, 15)	Wear limits		Abrasion limited to an arc of 120° acceptable to a max depth of 0.034. Abrasion which extends more than 120° acceptable in a depth of 0.017		Replace on more than 16 vanes per assembly	72-35-06 Repair 24 Supplement 24B pg 1	72-35-06 Repair 24	
11. HPC 7-14 stage IAS	Groove limits		Grooves to a maximum depth of 0.030 allowed in a maximum arc of 120°. Grooves beyond 120° arc are acceptable to a depth of 0.015		Allows abrasions 0.010 or 0.015 deeper than P&WA limits	72-35-12 Insp 01 pg 802	72-35-12 O/H Insp pg 302 Temporary revision and 72-35-00 Insp para 78(h)	
12. HPC blade	Tip clearances	348 through top	P&WA full restoration or partial restoration clearances may be used. Maximum allowable clearance for full restoration generally is 0.003 larger than blueprint maximum. Maximum allowable clearance for partial restoration is generally 0.013 larger than blueprint maximum		Grooves to a maximum depth of 0.030 allowed over an arc of 160°	72-35-06 Insp 01 pg 834	72-35-06 O/H Insp	72-35-00 O/H Clear

(page 5 of 8)

TABLE D-I (Cont'd.)

VARIATIONS IN COLD SECTION REBUILD STANDARDS

(page 1 of 8)

Part	Item	F&G Ref. No.	P&WA Standard		Airline Standard		P&WA Engine Manual Reference	Airline Engine Manual Reference	
			Min	Max	Min	Max			
AIRLINE C 1. Fan blades (CN eng's only)	Part span shroud radius damage limits	-	Damage must not extend in- to airfoil. Blend to 0.250 min radius.		No limit.		72-31-05 Insp 01 pg 820	72-31-05 O/H Insp pg 318	
	Rubdepth	-	Depth of rub is 0.140 max for not more than 120° and not more than 0.120 for re- mainder.		Depth of rub is 0.150 max for not more than 120° and not more than 0.120 for re- mainder.		72-33-01 Insp 01 pg 801	72-33-01 O/H Insp pg 301	
	Number missing	-	No recommendations.		Continue in service with one missing.		-	72-33-03 H/M Insp pg 603	
4. Fan exit liner segment	Damage limits	-	Continue in service with any number of tears less than 4.0".		Continue in service without the mesh		72-33-05 Insp 01 pg 801	72-33-50 O/H Insp pg 301	
5. 2nd - 4th LPC blade (CN engines only)	Length	-	No recommendations		5.361 5.373 for 2nd 5.039 5.051 for 3rd 5.006 5.018 for 4th		-	72-32-05 O/H Insp pg 303	
	Grooving limit	-	No recommendations.		Grooves acceptable to a depth of 0.050 if blended.		-	72-32-06 O/H Insp pg 309	
7. 1st LPC IAS	Rub depth	-	Rubs to a depth of 0.060 and in a width of 0.125 are ac- ceptable.		Rubs to a width of 0.125 for 360° or 0.250 for 180° are ac- ceptable. No limit on depth if not into metal.		72-32-06 Insp 01 pg 812	72-32-06 O/H Insp pg 311	
	Tip clearances	36	0.016	0.085	0.088	0.098P	72-32-00 Insp 02 pg 807	9252 * 3008 & 9230 * 3002	
8. LPC blade	Clearance	2nd	0.016	0.043	0.046	0.056P	-	-	
		3rd	0.038	0.062	0.072P	-	-	-	
		4th	0.154	0.174	0.194	0.219	72-32-00 Insp 02 pg 813	9230 * 3002	
10. IGV	Blend limits	-	Trailing edge nicks must be repaired and may not ex- ceed a depth of 0.0937.		Trailing edge nicks to a depth of 0.020 acceptable if Ni-Cod coating intact.		72-34-11 Insp 01 pg 801	72-34-11 O/H Insp pg 301	
	Clearance	206R	0.020	0.055	0.075	0.020	0.065	0.065	72-34-00 Insp 03 pg 808

TABLE D-I (Cont'd.)
 VARIATIONS IN COLD SECTION REBUILD STANDARDS

(page 7 of 8)

Part	Item	F&CI Ref. No.	PAWA Standard Min	PAWA Standard Max	RIO	Airline Standard Min	Airline Standard Max	RIO	PAWA Engine Manual Reference	Airline Engine Manual Reference
12. HPC vanes (CN eng's only)	Blend limits		Repair nicks and round bottom dents.			Nicks and round bottom dents allowable if Ni-Cad plating intact to following limits: 1) Idents - 1/16 in. dia., opposite side related no more than 0.010. 2) TE nicks - acceptable to a depth of 0.020. 3) LE nicks - acceptable up to 0.010 deep over 25% LE.			72-35-06 Insp 01 PG 801	72-35-06 O/H Insp PG 305
13. 5th and 6th HPC vane (CN eng's only)	Contour		Not inspected			Inspected with PA fixture.				72-35-06 O/H Insp PG 342
14. 5th, 6th, 7th HPC vane (CN eng's only)	Blend limits		Limit number of blended vanes to 20% per stage.			No limit			72-35-06 Insp 01 PG 801	72-35-06 O/H Insp PG 301
15. 5th, 6th HPC IAS (CN eng's only)	Groove limits		Grooving acceptable to a maximum depth of 0.035 for 120° or to a maximum depth of 0.018 if over 120°.			No limit if groove is not in to metal.			72-35-06 Insp 01 PG 834	72-35-06 O/H Insp PG 333
16. 7th, 14th HPC IAS (CN eng's only)	Groove limits		Groove width must be less than 0.145. Circumferentially adjacent grooves not permitted on all lands.			Groove width must be less than 0.075. Circumferentially adjacent grooves permitted on all lands if one groove is less than 0.10 deep.			72-35-06 Insp 01 PG 834	72-35-06 O/H Insp PG 334
17. 5th, 6th, 7th HPC vane OD Bushing	Wear limits	343 350 355	Do not inspect using normal shop inspection techniques. Use special technique in 72-35-06 Rep 27.			Inspect using normal techniques			72-35-00 Insp 02 PG 827 72-35-06 Insp 01 PG 805	72-35-00 O/H Clear PG 621
18. 5th, 6th, 7th HPC vane ID Bushing to vane (CN engines only)	Clearance	378 401 402	0.020 0.020 0.020	0.050 0.050 0.055	0.075 0.075 0.075	RIO limit 0.010 tighter than P&WA limit for CN engines.			72-35-00 Insp 02	72-35-00 O/H Clear.
19. HPC blade	Tip clearances	388 through 398	PAWA full restoration or partial restoration clearances may be used. Maximum allowable clearance for full restoration generally is 0.003; larger than blueprint maximum. Maximum allowable clearance for partial restoration is generally 0.013; larger than blueprint maximum.			Checked at assembly but no RIO limit given. Now use full restoration clearances.			72-35-00 Insp 02	9252 • 3516

ORIGINAL PAGE IS
 OF POOR QUALITY.

TABLE D-1 (Cont'd.)

VARIATIONS IN COLD SECTION REBUILD STANDARDS

(page 8 of 8)

Part	Item	F&CT Ref No.	PAWA Standard		Airline Standard		PAWA Engine Manual Reference	Airline Engine Manual Reference
			Min	Max	Min	Max		
20 HPC IAS	Clearances	Various					72-35-00 Insp 02	9252 * 3616
21 Vari Vane rigging system (TN engines only)	General condition						72-35-24 Insp 01 pg 801	72-34-11 O/H Insp pg 307 72-35-06 O/H Insp pg 342 72-35-24 O/H Insp pg 301

Checked at assembly but no RIO limit given. Now use full restoration clearances.

Rig pin hole wear allowable to 0.015 over B/P. For assembled rotor assemblies, no movement is allowed between vane and vane arm. Movement between vane arm and unlock ring must be less than 0.015. With K/V's in open position, total movement between vane and IT throat may be up to 0.055 for 11 vanes but must not exceed 0.040 for remaining 53. With 5th, 6th, and 7th vanes in open position, total movement between vane and ID throat must be less than 0.040 for all vanes.

No OIM recommendations comparable to Airline C's OIM except for rig pin hole. No rig pin hole wear over B/P allowable.

TABLE D-II
 VARIATIONS IN HOT SECTION REBUILD STANDARDS

(page 1 of 2)

Part	Item	F&CT Ref. No.	P&WA Standard		Airline Deviation		Build Sheet	Engine Manual	
			Min	Max	Min	Max			
AIRLINE A 1 Low-pressure turbine blade KE seals	3rd	1098/1099	0.007	0.023	0.039	0.007	0.043	41967 7/23/76 72-52-03 p. 3108	
	4th	1100/1101	0.017	0.033	0.049	0.017	0.053		
	5th	1051/1052	0.060	0.084	0.114	0.060	0.104		
	6th	1067/1068	0.0470	0.071	0.114	0.047	0.091		
2 1st turbine blade	Tip clearances	1590	0.067	0.079	0.095	0.067	0.080	72-51-12 Rep 03 p 403 FP 76 686 7/2/76 Item 11 and 12 72-51-12 Rep 12 p 403 FP 76 696 7/2/76 Item 17 72-51-13 Insp 00 p 307 FP 76 713 9/17/76 72-51-13 HM insp/ck 00 p 604/ 605 FP 76 632/633/634 8/19/76	
	Tip clearances	1590	0.067	0.079	0.095	0.077	0.089		
AIRLINE B 1 1st turbine OAS	Offset grind	1566 1567	0.0045 X 0.0145		0.0045 X 0.0195				
	Offset grind	1566 1567	0.0045 X 0.0145		0.0045 X 0.0195				
3 1st stage turb. airseal	Clearances	2130	0.076	0.084	0.094	0.076	0.084	0.121	max incl blends
		2131	0.076	0.084	0.094	0.076	0.084	0.121	max incl blends
		2132	0.076	0.084	0.094	0.076	0.084	0.121	max incl blends
4 1st stage turbine airseal	Clearances		incr radial clearance to 0.057 (+0.010) (individual - no blends)		incr radial to 0.070 w/formula incl. blends.		+0.020 clearance		
			incr radial to 0.070 w/formula incl. blends.						

TABLE D-II (Cont'd.)
 VARIATIONS IN HOT SECTION REBUILD STANDARDS

(page 2 of 2)

Part	Item	F&C Ref No.	P&WA Standard		Airline Deviation		Build Sheet	Engine Manual		
			Min	Max	Min	Max				
AIRLINE: C	1. F. nozzle flow check									
	Airflow		Fuel Flow		Airflow not valid		9250 • 3824			
2. No. 1-2 turbine blades	TE blend		0.005 max depth		Blend to 1st row pellets 1 per build			TR 72-1236 10/15/75		
3. 3rd turbine blade	Radial tip clearance front KE Ring 729959 (honeycomb)	1098	0.007	0.023	0.039	0.010	0.028	0.039	Incr.	9230 • 5202 P2
	Radial tip clearance rear KE Ring 729959 (honeycomb)	1099	0.007	0.023	0.039	0.010	0.028	0.039	Incr.	9230 • 5202 P3
4. 4th turbine inner airseal	Seal clearance front seal 677867 Shroud 693174, 693184, 693194	1029	0.146	0.154	0.214	0.146	0.154	0.174	Decr	9230 • 5202 P4
	Seal clearance rear seal 677867 Shroud 694174, 693184, 693194	1030	0.146	0.154	0.214	0.146	0.154	0.174	Decr	9230 • 5202 P5
5. 4th turbine blade	Radial tip clearance front KE Ring 706943	1100	0.020	0.036	0.052	0.030	0.046	0.062	Incr.	9230 • 5202 P6
	Radial tip clearance rear KE	1101	0.020	0.036	0.052	0.030	0.046	0.062	Incr	9230 • 5202 P6
6. 1st turbine blade	Radial tip clearance	1590	0.067	0.079	0.095	0.066	0.085	0.095		

TABLE D-III
 BLADE TIP CLEARANCE VARIATION SUMMARY

AIRLINE A

Module	Stage	Clearance Differences from P&WA Nominal (inch)	
		Airline Nominal	Airline RIO
Fan (offset honeycomb) (0.115 in. offset ASG)	1	+0.020	+0.030
	1	+0.015	+0.025
LPC (assume full restoration clearances used)	2	+0.002	+0.018
	3	+0.002	+0.017
	4	+0.000	+0.017
HPC	5	+0.002	+0.011
	6	+0.002	+0.011
	7	+0.002	+0.011
	8	+0.002	+0.010
	9	+0.002	+0.009
	10	+0.004	+0.014
	11	+0.002	+0.009
	12	+0.003	+0.011
	13	+0.002	+0.009
	14	+0.002	+0.009
	15	+0.002	+0.008
HPT	1	+0.000	+0.007
	2	+0.000	+0.014 F&R*
LPT	3	+0.010	+0.028 F&R
	4	+0.010	+0.028 F&R
	5	+0.010	+0.042 F&R
	6	+0.010	+0.055 F&R

*F&R – Front and Rear

TABLE D-IV

(page 1 of 2)

BLADE TIP CLEARANCE VARIATION SUMMARY

AIRLINE B

OVERHAUL ENGINES

Module	Stage	Clearance Differences from P&WA Nominal (inch)		
		Airline Nominal	Airline RIO	
Fan (offset honeycomb)	1	+0.020	+0.030	
LPC	2	+0.002	+0.018	
	3	+0.002	+0.017	
	4	+0.000	+0.017	
	HPC	5	+0.002	+0.011
6		+0.002	+0.011	
7		+0.002	+0.011	
8		+0.002	+0.010	
9		+0.002	+0.009	
10		+0.004	+0.014	
11		+0.002	+0.009	
12		+0.003	+0.011	
13		+0.002	+0.009	
14		+0.002	+0.009	
15		+0.002	+0.008	
HPT		1	+0.010	+0.022
		2	+0.000	+0.014 F&R*
LPT		3	+0.000	+0.028 F&R
		4	+0.000	+0.028 F&R
	5	+0.000	+0.042 F&R	
	6	+0.000	+0.055 F&R	

*F&R - Front and Rear

ORIGINAL FILE IS
OF POOR QUALITY

TABLE D-IV (Cont'd)

(page 2 of 2)

BLADE TIP CLEARANCE VARIATION SUMMARY

AIRLINE B

HEAVY MAINTENANCE ENGINES

Module	Stage	Clearance Differences from P&WA Nominal (inch)		
		Airline Nominal	Airline RIO	
Fan (offset honeycomb)	1	+0.020	+0.030	
LPC	2	+0.007	+0.028	
	3	+0.007	+0.027	
	4	+0.005	+0.022	
HPC	5	+0.007	+0.021	
	6	+0.007	+0.021	
	7	+0.007	+0.021	
	8	+0.007	+0.020	
	9	+0.007	+0.019	
	10	+0.007	+0.019	
	11	+0.007	+0.019	
	12	+0.007	+0.019	
	13	+0.007	+0.019	
	14	+0.007	+0.019	
	15	+0.007	+0.019	
	HPT	1	+0.010	+0.022
		2	+0.000	+0.014 F&R*
	LPT	3	+0.000	+0.028 F&R
		4	+0.000	+0.028 F&R
5		+0.000	+0.042 F&R	
6		+0.000	+0.055 F&R	

*F&R – Front and Rear

TABLE D-V
 BLADE TIP CLEARANCE VARIATION SUMMARY
 AIRLINE C

Module	Stage	Clearance Differences from P&WA Nominal (inch)	
		Airline Nominal	Airline RIO
Fan	1	+0.000	+0.010
LPC (Assume full restoration clearances used)	2	+0.002	+0.018
	3	+0.002	+0.017
	4	+0.000	+0.017
HPC (Assume full restoration clearances used)	5	+0.002	+0.011
	6	+0.002	+0.011
	7	+0.002	+0.011
	8	+0.002	+0.010
	9	+0.002	+0.009
	10	+0.004	+0.014
	11	+0.002	+0.009
	12	+0.003	+0.011
	13	+0.002	+0.009
	14	+0.002	+0.009
	15	+0.002	+0.008
HPT	1	+0.003	+0.022
	2	+0.000	+0.014 F&R*
LPT	3	+0.004	+0.028 F&R
	4	+0.005	+0.028 F&R
	5	+0.000	+0.042 F&R
	6	+0.000	+0.055 F&R

*F&R – Front and Rear

APPENDIX E

QUALITY ASSURANCE

The P&WA quality assurance program provided the general policy for 1) directing the inspection of used parts collected and 2) establishing the adequacy of the airline test cell facility performance data collected in the data collection effort of the NASA JT9D Jet Engine Diagnostics Program. Specifically: hardware traceability procedures were established; existing inspection procedures and equipment calibrations were reviewed and followed; and available performance test instrumentation calibration records for each airline were analyzed to ensure the accuracy of all data collected.

Hardware selected for detailed inspection was identified and marked at the time of selection at the airline facilities as to engine and module serial number from which it was obtained. From the airline engine and module repair records, the usage level of the parts was then determined and recorded. The parts were marked with the identifying codes shown in Figures E-1 and E-2 for compressor parts and turbine parts, respectively, and returned to P&WA for inspection.

These codes were marked on each part and on all corresponding inspection sheets so that correlation of recorded data with part time and cycles was ensured.

INSPECTION EQUIPMENT CALIBRATIONS

All tools, fixtures, and machines used to perform the required inspections were calibrated using measurement standards which are traceable to an appropriate ultimate reference such as the National Bureau of Standards. These calibrations are performed at established intervals in facilities where environmental controls have been established to ensure adequate results. The calibrations are conducted according to written procedures to ensure consistency. The recalibration intervals for the equipment, including standards, are established with judgements based on degree of use, environment of use, required accuracy, and stability. Calibration records are maintained for each measuring device in order to assess accuracy and stability and to facilitate recall of the equipment. Measuring and test equipment are labeled to establish the calibration status for the user.

INSTRUMENTATION CALIBRATIONS

The calibration records of test equipment used by the airlines to measure the performance related parameters of JT9D engines were analyzed and compared with the P&WA JT9D Test Instruction Sheet (TIS) manual.

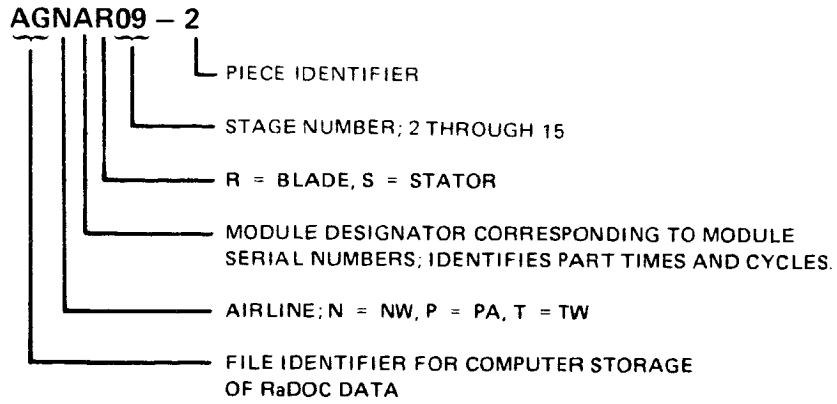


Figure E-1 Identifying Codes for Compressor Parts.

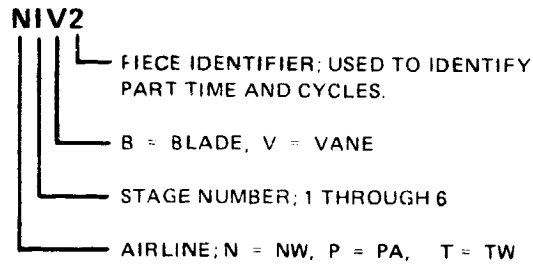


Figure E-2 Identifying Codes for Turbine Parts.

APPENDIX F

ACRONYMS AND SYMBOLS

ACRONYMS (Organizations)

AA	American Airlines
BCAC	Boeing Commercial Airplane Company
DAC	Douglas Aircraft Company
NASA	National Aeronautics and Space Administration
NW	Northwest Airlines
PA	Pan American World Airways
P&WA	Pratt & Whitney Aircraft
TBC	The Boeing Company
TWA	Trans World Airlines
UA	United Air Lines

SYMBOLS AND ACRONYMS

A	Area (feet ²)
A/C	Aircraft
ASG	Axial-skewed grooved
ATM	Assumed temperature method
B/P	Blueprint
BPR	Bypass ratio
CG	Circumferential grooved
(CN)	Conversion
ECM	Engine condition monitoring
Eff	Efficiency (percent)
EFH	Engine flight hours
EGT	Exhaust gas temperature (°F)(°C); measured at HPT discharge
EPR	Engine pressure ratio
F	Engine thrust (pounds)
FC	Flow capacity
H/M	Heavy maintenance
HP	High pressure
HPC	High-pressure compressor
HPT	High-pressure turbine
Hz	Hertz
IAS	Inner air seal
ID	Inside diameter
IGV	Inlet guide vanes
K	Kilo (10 ³)
KE	Knife edge

le	Leading edge
LP	Low pressure
LPC	Low-pressure compressor
LPT	Low-pressure turbine
M	Mach number
Mod	Modification
N	Rotor speed (rpm)
NASTRAN	NAsa STRuctural ANalysis computer program
OAS	Outer air seal
OD	Outside diameter
O&R	Overhaul & repair
O/H	Overhaul
OHM	Overhaul Manual
P	Absolute pressure (lb/in ²)(psia)
p	Gage pressure (lb/in ²)(psig)
P/N	Part Number
PR	Pressure ratio
QEC	Quick Engine Change
RIO	Repair if over
SLS	Sea level static
S/N	Serial Number
(SP)	Special Performance
S.S.	Steady state
Std	Standard
T	Absolute temperature (°R)
t	Temperature (°F)(°C)
te	Trailing edge
T/O	Take-off
TOBI	Tangential onboard injection system
TSFC	Thrust specific fuel consumption (lb/hr-lb)
w	Mass flow (lbm/sec)
β	Vane angle (degrees)
Δ	Change
δ	Pressure correction (in. Hg/29.92)
η	Efficiency (percent)
θ	Temperature correction (°R/519)
μ	Micro (10 ⁻⁶)

SUBSCRIPTS

1	Undisturbed inlet (pressure and temperatures)
1	Low-pressure rotor (rotor speeds)
2	Fan inlet (pressures and temperatures)
2	High-pressure rotor (rotor speeds)
2.4	Fan blade discharge
2.6	Fan exit guide vane discharge
3	LPC discharge
4	HPC discharge
5	HPT inlet
6	HPT discharge
7	LPT discharge
a	Absolute
am, a	Ambient
b	Burner
c	Compressor
cell	test cell
est.	Estimated
f	Fuel
g	Gage
i	innerwall
max.	maximum
n	Net
s	Static
t	Stagnation (total)
t	Time

REFERENCES

1. Bouchard, R. J., Beyerly, W. R., and Sallee, G. P.: Short-Term Performance Deterioration in JT9D-7A(SP) Engine 695743. NASA CR-135431, 1978.
2. Jay, A. and Todd, E. S.: Effect of Steady Flight Loads on JT9D-7 Performance Deterioration. NASA CR-135407, 1978.
3. Jay, A. and Lewis, B. L.: Effect of Time-Dependent Flight Loads on JT9D-7 Performance Deterioration. NASA CR-159681, 1979.

Page 216 INTENTIONALLY BLANK